ESD-TDR-63-354, VOL 5

FINAL REPORT
ON
RANGE INSTRUMENTATION PLANNING STUDY
TECHNICAL DOCUMENTARY REPORT NO. ESD-TDR-63-354

VOLUME 5: TRACKING, TELEMETRY, AND COMMAND (TTC)

OCTOBER 1963

DIRECTORATE OF AEROSPACE INSTRUMENTATION
DEPUTY FOR ENGINEERING AND TECHNOLOGY
ELECTRONIC SYSTEMS DIVISION
AIR FORCE SYSTEMS COMMAND
UNITED STATES AIR FORCE
L. G. Hanscom Field, Bedford, Mass.

Prepared under Contract No. AF 19(628)-2356

by
TRW Space Technology Laboratories
One Space Park
Redondo Beach, California

(18) (19)

ESD-TDR-63-354-VOL-5

(7) FINAL REP[redacted]T.

[redacted]

(6) RANGE INSTRUMENTATION PLANNING STUDY.

[redacted]

VOLUME 5: TRACKING, TELEMETRY, AND COMMAND (TTC),

(11) OCT[redacted] [redacted]63,

(12) 1v.

(14) Rept. no. 8691-6098-RU000-Vol. 15

DIRECTORATE OF AEROSPACE INSTRUMENTATION
DEPUTY FOR ENGINEERING AND TECHNOLOGY
ELECTRONIC SYSTEMS DIVISION
AIR FORCE SYSTEMS COMMAND
UNITED STATES AIR FORCE
L. G. Hanscom Field, Bedford, Mass.

(15)

[redacted] Contract [redacted] AF 19(628)-2356

[redacted]

(5) TRW Space Technology Lab[redacted]s.,

[redacted]

Redondo Beach, Calif[redacted]

FOREWORD

This volume consists of Appendices VI through XIX, which deal with tracking, telemetry, command, and related topics. Thus, for example, both time synchronization and geophysical considerations are included in this volume because of their relevance to the metric data problem, even though they do not concern metric instrumentation in the strict sense. Additional information (classified) pertaining to tracking, telemetry, and command may be found in Volume 8. In addition, information pertinent to the subject of this volume but broader in scope may be found in Volume 6.

The numbering of the figures, tables, references, and equations is consecutive for the appendices in this volume. For the convenience of the reader, however, the pagination of each appendix reflects the appendix designator; for example, Appendix VI has its pages numbered 6-1, 6-2, 6-3, etc.

This volume and the other seven volumes making up this report have a standard table of contents immediately following the abstract page. Additionally, a major-heading table of contents for each of the other volumes is shown in reduced size immediately following the standard table of contents. The list of abbreviations and symbols used in the report has been included in each volume.

The STL Document Control Number for Volume 5 is 8691-6098-RU000.

This abstract is UNCLASSIFIED

RANGE INSTRUMENTATION PLANNING STUDY (U)

ABSTRACT

The emphasis in space technology over the past several years has shifted to very-long-range missiles, orbiting vehicles, and deep-space probes. Thus support from the test environment is now required on a truly global basis. For this reason, equipment compatibility and a means of integrating the operations of the existing ranges have become necessities.

TRW Space Technology Laboratories (formerly Space Technology Laboratories, Inc.) was awarded a contract by ESD to perform a study of the entire test environment problem for these classes of missions and tests. The primary objective was the definition of what the global test environment should be in the 1965 to 1970 period and the development of an implementation plan permitting the timely and efficient attainment of the recommended configuration.

Emphasis was placed on providing the capability to support the requirements imposed by the many programs involving missiles, large boosters, and spacecraft to be tested in the 1965 to 1970 period. Efficiency was emphasized because it was known that the costs associated with provision of a capability to support such a variety of missions would be very large under the best of circumstances.

STL's conclusion is that an integrated global test environment is not only feasible but highly desirable. The report presents specific recommendations for the choice of prime instrumentation in this integrated global test environment, and develops operational and management concepts appropriate to it. The report includes detailed recommendations, an implementation plan, and applied research and advanced development plans necessary or desirable to assure the timely implementation of the range and to provide a basis for a continuing upgrading of its capabilities.

Volume 1 consists of an overall introduction, a summary of the total report, and a presentation of the basic system concept.

Volume 2 contains a detailed description of the recommended instrumentation network and gives the implementation plan and cost estimates.

Volume 3 summarizes, as functions of time and location, the most stringent requirements imposed on the network; evaluates the network's capability of meeting the test requirements; and presents recommendations for applied research and advanced development programs required to implement the network or to advance the state of the art in pertinent instrumentation technology.

Volumes 4 through 8 contain supporting appendices for the findings, conclusions, and recommendations presented in Volumes 1 through 3.

C. V. HORRIGAN
Acting Director
Aerospace Instrumentation
Deputy for Engineering and Technology
Electronic Systems Division

CONTENTS

APPENDIX VIII. OPTICAL INSTRUMENTATION (Cont'd)

APPENDIX XII. TRACKING SYSTEMS ERROR ANALYSIS (Cont'd)

ILLUSTRATIONS

APPENDIX XIV. TECHNIQUES AND TRENDS IN AEROSPACE TELEMETRY (Cont'd)

APPENDIX XV: USE OF TELEMETRY FOR RANGE SAFETY

APPENDIX XVI. ONBOARD PREPROCESSING OF TELEMETRY DATA

VOLUME 1
SYSTEM CONCEPT

VOLUME 2
RECOMMENDED INSTRUMENTATION NETWORK

VOLUME 3
EVALUATION, REQUIREMENTS, AND TECHNOLOGY

1

3
UIREMENTS,
)LOGY

VOLUME 4
INSTRUMENTATION DATA REQUIREMENTS

VOLUME 5
TRACKING, TELEMETRY, AND COMMAND (TTC)

VOLUME 6
TTC AND LONG-HAL COMMUNICATIONS

2

VOLUME 6
TTC AND LONG-HAUL COMMUNICATIONS

VOLUME 7
DATA PROCESSING AND DISPLAY

VOLUME 8
MISCELLANEOUS CLASSIFIED APPENDICES

3

LIST OF ABBREVIATIONS

ac	alternating current
A/C	aircraft
ACIC	Aeronautical Chart and Information Center
AFC	automatic frequency control
AFCRL	Air Force Cambridge Research Laboratory
AFMTC	Air Force Missile Test Center
AFSC	Air Force Systems Command
AGC	automatic gain control
AICBM	anti-intercontinental ballistic missile
AIL	Airborne Instruments Laboratory
alt	altitude
AM	amplitude modulation
AMR	Atlantic Missile Range
AMS	Army Map Service
approx	approximately
ARDC	Air Research and Development Command
ARPA	Advanced Research Projects Agency
ARS	Air Rescue Service
BECO	booster engine cutoff
BO	burn out
BOA	broad ocean area
bpS	bits per sample
BTL	Bell Telephone Laboratories
BWO	backward wave oscillator
CCMTA	Cape Canaveral Missile Test Annex
cm	centimeter
COM	Chief Operations Manager
CONUS	Continental United States
cps	cycles per second
CRT	cathode-ray tube
CW	continuous wave
CY	calendar year
db	decibel
dbm	decibels referred to one milliwatt
dc	direct current

DCA	Defense Communications Agency
DCS	Defense Communications System
DE	Delco
deg	degree
deg/sec	degrees per second
DOD WGS	Department of Defense World Geodetic System
DSIF	Deep Space Instrumentation Facility
EAFB	Edwards Air Force Base
EBPA	electron beam parametric amplifier
EEG	electroencephalogram
EGO	Eccentric Geophysical Observatory
EKG	electrocardiogram
ESD	Electronic Systems Division
FDM	frequency division multiplex
FM	frequency modulation
FOT	frequency of optimum transmission
fps	feet per second
FSK	frequency-shift keyed
ft	foot
ft/sec	feet per second
g	gravity, acceleration due to
gc	gigacycles per second
GD/A	General Dynamics/Astronautics
GDOP	geometric dilution of precision
GE	General Electric
GERTS	General Electric Range Tracking System
GRCC	Global Range Control Center
HF	high frequency
hr	hour
HU	Hughes Products
ICGM	Intercontinental Global Missile
IF	intermediate frequency
IFCS	information flow control station
IGC	inertial guidance and control
IMCC	Integrated Mission Control Center
in.	inch

IR	infrared
IRBM	intermediate range ballistic missile
IRIG	inter-range instrumentation group
ISB HF	independent sideband high frequency
JPL	Jet Propulsion Laboratory
^{o}K	degrees Kelvin
kbits/sec	kilobits per second
kc	kilocycles per second
Kev	thousands of electron volts
km	kilometer
kw	kilowatt
LASV	Low-Altitude Supersonic Vehicle
LF	low frequency
LOS	line of sight
LRCC	local range control center
LUF	lowest usable frequency
m	meter
MATS	Military Air Transport Service
max.	maximum
mc	megacycles per second
MCC	mission control center
MEC	Microwave Electronics Corporation
MECO	main engine cutoff
megw	megawatt
Mev	millions of electron volts
MH	Minneapolis Honeywell
mi	miles
MILS	missile impact location system
Mil Spec	military specification
MIT	Massachusetts Institute of Technology
mm Hg	millimeters of mercury
MMRBM	mobile, medium-range, ballistic missile
mr	milliradian
msec	millisecond
MO	Motorola
MTBF	mean time between failures

MTS	members of the technical staff
MUF	maximum usable frequency
mw	milliwatt
NASA	National Aeronautics and Space Administration
nmi	nautical mile
NMFPA	U. S. Naval Missile Facility, Point Arguello
OAO	Orbiting Astronomical Observatory
OD	Operations Directive
OGO	Orbiting Geophysical Observatory
ORV	ocean range vessel
OSO	Orbiting Solar Observatory
PACM	pulse-amplitude code modulation
PAFB	Patrick Air Force Base
PAM	pulse-amplitude modulation
PCA	polar cap absorption
PCM	pulse-code modulation
PD	pulsed doppler
PDM	pulse duration modulation
PELT	precision early launch tracker
PH	Philco
PIRD	Program Instrumentation Requirements Document
PM	phase modulation
PMR	Pacific Missile Range
PN	pseudonoise
POGO	Polar Orbiting Geophysical Observatory
PPE	preliminary planning estimate
ppi	plan position indicator
ppm	parts per million
pps	pulses per second
PRF	pulse repetition frequency
PSK	pulse-shift keyed
R and D	Research and Development
RARR	range and range rate
RAY	Raytheon
RCA	Radio Corporation of America
ref	reference

RF	radio frequency
RIPS	Range Instrumentation Planning Study
RISE	Research in Supersonic Environment
rms	root mean square
rss	root sum square
RTG	radio-isotope thermoelectric generators
SCF	Satellite Control Facility
sec	second
SGLS	Space-Ground Link Subsystem
SLAM	Supersonic Low-Altitude Missile
smi	statute mile
S/N	signal-to-noise
SOFAR	Sound Firing and Ranging
SPO	Systems Project Office
Sps	samples per second
SRM	Systems Requirements Model
SSB	single sideband
SSD	Space Systems Division
SSN	sunspot number
STL	TRW Space Technology Laboratories
STV	special test vehicle
SWF	short-wave fadeout
SY	Sylvania
TASI	time assignment speech interpolation
TDM	time division multiplex
TI	Texas Instruments
TLM	telemetry
TR	Transitron
TTC	tracking, telemetry, and command
TTY	teletype
TV	television
TWT	traveling-wave tube
UFS	Unified Frequency System
UHF	ultra-high frequency
μrad/sec	microradians per second
USA WGS	United States Army World Geodetic Systems

USAF WGS	United States Air Force World Geodetic System
μsec	microsecond
VAFB	Vandenberg Air Force Base
VECO	vernier engine cutoff
VHF	very-high frequency
VLF	very-low frequency
w	watt
WE	Western Electric
wpm	words per minute
ws	watt-second
WSMR	White Sands Missile Range
Xpdr	transponder

Appendix VI. INTEGRATED TRACKING, TELEMETRY, AND COMMAND SYSTEMS

A. INTRODUCTION

An integrated tracking, telemetry, and command (TTC) system is one which performs the three primary spacecraft communications functions utilizing a single RF link in each direction between the vehicle and the ground station. Angle-tracking may be accomplished by any of the usual techniques. Range is extracted by impressing a suitable modulation on the uplink which, via the vehicle transponder, is repeated as a modulation on the downlink, and the two-way propagation delay is measured on the ground. Relatively coarse range-rate data may be obtained by differentiation of the range data, but precise range-rate measurement requires the use of doppler techniques, wherein the vehicle transponder retransmits a frequency that is coherently related to its received frequency. In some applications either the range or the range-rate measurement function is not used. In any case, both the uplink and downlink are used for the tracking function. Command data is transmitted by impressing a command modulation on the uplink RF carrier used for the tracking function, and telemetry data is handled in a similar fashion on the downlink.

B. SYSTEM CONSIDERATIONS

1. GENERAL

The use of an integrated TTC system has many advantages, especially those of minimizing equipment requirements in both the vehicle and the ground stations. However, no one system design can be optimum for all applications. For example, no one integrated system could simultaneously provide transmission of high quality TV from a spacecraft, megabit-per-second command rates from the ground, extremely precise tracking of boosters during thrust periods, tracking of passive vehicles, and tracking of a reentry vehicle through the ionization sheath. All of these functions place certain constraints on the system design which frequently are mutually incompatible. Some of the constraints of an integrated TTC system design which limit the universality of its application are discussed below.

2. TYPE OF CARRIER MODULATION

As far as the tracking function is concerned, either CW or pulsed techniques would be suitable. Telemetry and command information can be added to a CW tracking system by providing additional subcarriers, and to a pulsed system by multiple-pulse coding. As long as the required data rates are low relative to the PRF, addition of a command function to a pulsed radar presents no particular problem. A more serious limitation, however, exists with respect to telemetry, wherein expected data rates will in almost every case exceed the capability of a pulsed system. We therefore conclude that an integrated TTC system must utilize a CW carrier. This immediately makes the integrated system nonoptimum for skin-tracking of passive vehicles.

Because of its relative inefficiencies in detection, amplitude modulation is not attractive, and an integrated system will use either FM or PM. If the system is to measure doppler range rate, at least the ground receiver will utilize a phase-locked carrier tracking loop. Low-index phase modulation is then the preferred choice, since this form of modulation leaves a clean carrier which can be tracked for doppler extraction. If the range-rate measurement is not required, FM could be used, as is done in the SHF system for Dyna-Soar (Section C of this appendix). However, most integrated TTC system designs to date have included the doppler capability, and this capability is considered essential in any versatile general-purpose system. Biphase modulation, a specialized form of phase modulation which suppresses the carrier component, can be used when the data is a single digital bit stream, since a matched receiver can reconstruct the carrier component for doppler extraction. This is not attractive for the uplink, since the vehicle receiver required is rather complex. When several kinds of modulation are required on the downlink (digital or analog telemetry, voice, ranging information), one is forced into the use of subcarriers. The most versatile form of carrier modulation, which simultaneously permits extraction of doppler information and a variety of data channels, is ordinary low-index phase modulation.

There is a practical upper limit to the amount of data which can be modulated onto the tracking carrier. This limit is generally high enough to

be of only academic interest in the case of the command link, but it can be of concern to an extremely high data bandwidth telemetry system. When the data bandwidth is this large, the overriding concern in the design of the communication link is the recovery of this data with the least possible error rate, with the result that these considerations overshadow the tracking considerations. For example, under the above condition, it may well be more efficient to utilize wideband FM, with a frequency-following phase-locked receiver at the ground terminal.

If the telemetry data bandwidth is inordinately large relative to the tracking information bandwidth, some of the advantages of integrating the functions tend to disappear. The exact break-point can be the subject of a detailed tradeoff study, but it appears to be somewhere in the vicinity of several megacycles per second.

3. TYPE OF TRANSPONDER

The type of transponder must be matched to the form of carrier modulation chosen. When phase modulation is used, a phase-locked transponder, while not essential to a two-way doppler measurement system, is the obvious choice for an integrated TTC system. The phase-locked loop provides a carrier frequency for retransmission which is coherently offset from its received frequency. Doppler information is extracted on the ground by comparing the transmitted and received carrier frequencies, taking into account the coherent frequency offset effected by the transponder. The phase-locked transponder permits coherent detection of the command modulation, which for a given set of uplink parameters (transmitter power, antenna gains, receiver noise figure, etc.) maximizes the output signal-to-noise ratio and hence minimizes the probability of command bit error.

Telemetry and/or voice subcarriers can be combined and phase-modulated onto the downlink carrier. Ranging information from the uplink can be coherently detected and remodulated along with the data subcarriers. At the ground station, extraction of the data and ranging information is a straightforward matter.

4. MULTIPLE-STATION TRACKING

For telemetry and command functions, it is sufficient to establish two-way communications with the spacecraft from only one station at a time. Nothing (except perhaps some degree of reliability through redundancy) is gained by having stations at different locations simultaneously communicating with the vehicle. This is not always true, however, for the tracking function. In some situations it is desirable to have the capability of simultaneously measuring range and range rate to the vehicle from at least three widely separated geographic locations (i. e., trilateration). As described in the previous section, measurement of these parameters from one station presents no problem and, in fact, measurement of doppler from several stations simultaneously, using state-of-the-art atomically stabilized oscillators for frequency references, is entirely feasible. The most difficult problem is that of multiple-station ranging.

When the beacon consists of a single-channel, phase-locked transponder, rapidly time-sequenced interrogation (synchronized) is feasible under certain circumstances. An example of rapidly time-sequenced interrogation by properly synchronized ground stations may be found in the Secor system. In this system, the ground station transmission periods are synchronized so that no overlap will occur at the vehicle transponder, and up to four interrogating ground stations each sample the transponder at a rate of approximately 30 samples per second. This relatively high sampling rate implies the necessity for a broadband transponder to rapidly acquire the signal transmitted from each station, with the result that it is not feasible to take advantage of the narrow vehicle transponder bandwidths which are normally achievable with a phase-locked unit.

At the same time, in order to assure satisfactory performance of the ground receiving systems, it is necessary that these ground receivers by phase-locked receivers whose bandwidths are small relative to the sampling rates, so that the sampled nature of the input signal does not produce substantial performance degradation. In addition, there is a severe problem of stability of the phase-locked receiving system considered as a servomechanism. This is because, for stable operation, the uncompensated dynamic effects must give rise to sample-to-sample

carrier phase shifts substantially less than 90 degrees. For typical conditions, this requires at least acceleration compensation and may give rise to considerable difficulties with the phase errors introduced by jerk. This stability problem becomes progressively more difficult as the carrier frequency increases, inasmuch as the phase shifts scale directly with carrier frequency. The result is that the ground receiving system design becomes extremely difficult and complex if the receiving system is to be capable of operating with relatively extreme vehicle dynamics and with a carrier frequency in the microwave region. In particular, this is true for a system which operates in the 2-gc band, in which the stabilization of the ground receiving system appears prohibitively difficult. The desirability of using the 2-gc band will be discussed in Section D. 2 of this appendix.

In view of the situation here described, both for the beacon and for the ground receiving system, it must be concluded that an integrated CW TTC system with a single-channel transponder will not prove satisfactory for essentially simultaneous interrogation by a number of ground tracking stations. A partial solution to the limitation imposed by this would be to employ an interferometer configuration in the ground tracking stations. While somewhat higher accuracies might be achievable in this way than with a precision monopulse or conical scan tracker, the cost, complexity, and the siting and operational problems of such a system would be very large. An alternative solution would be to employ a multiple-channel, phase-locked transponder. However, this type of operation is almost tantamount to employing a number of distinct transponders equal to the number of ground stations which are to be able to interrogate the beacon simultaneously. In view of the normal limitations on space vehicle size, weight, and power, the use of multiple-channel phase-locked transponders does not appear to be a satisfactory general solution to the trilateration problem, although it might well be employed under special circumstances.

The one type of CW tracking system which does not fall within the range of the preceding discussion of simultaneous interrogation of a phase-locked transponder by a number of ground stations is the system typified by the Goddard range and range-rate system. In this system,

the basic transponder is essentially noncoherent, and doppler data are obtained by transmitting a suitable multiple of the transponder local oscillator frequency along with frequency-offset versions of the signals received on each of three receiving channels. By use of appropriate receiving and combining techniques in the ground receiving systems, the doppler data can be reconstituted from the received signal even though the transponder is not strictly coherent. The transponder employed for the Goddard range and range-rate system does employ a three-channel receiving system and a combiner through which the signals received from the three IF's are combined and modulated onto a single retransmitted carrier. This carrier is locally generated in the transponder from the same crystal oscillator which provides the receiver local oscillator signal after appropriate frequency multiplication. Although this type of system does indeed permit simultaneous trilateration, it is not attractive for use in an integrated TTC system. This is because the basic character of the system does not encourage recovery of a clean carrier onto which telemetry data are modulated on the downlink. While undoubtedly the system could be modified to provide some capability in this direction, its potentialities for use as an integrated TTC system are distinctly limited relative to the possibilities inherent in a system employing a phase-locked transponder. We must conclude that a system of the Goddard range and range-rate type should be regarded as a special-purpose CW tracking system with very limited possibilities for the transmission of additional data. For this reason, it is not considered to be a suitable system configuration for expansion into a general-purpose integrated TTC system.

C. THE DYNA-SOAR INTEGRATED TTC SYSTEM

The Dyna-Soar communications and tracking subsystem consists essentially of a C-band pulsed radar transponder, a two-way UHF system (used as a command or voice backup and as a recovery aid), and an integrated TTC system operating in the SHF band. This TTC system differs in many respects from other system designs. The SHF uplink carrier is modulated with commands, voice, and ranging information. The SHF downlink is modulated with telemetry data, voice, and ranging information. The ground antenna angle tracks on the SHF signal. All of these features are consistent with the usual objectives of an integrated system;

however, the tracking system does not measure range rate. Presumably, this is because the function was not specifically required by this particular mission. Consequently, the use of phase modulation and a phase-locked transponder are not required. The Dyna-Soar system uses FM in both directions, and the vehicle-transmitted carrier is not coherently related to its received carrier.

The parameters chosen for the ranging system are not very stringent, and again were apparently chosen to fit the particular mission requirements. The specified performance parameters are approximately:

Resolution	1500 ft
Accuracy	4500 ft
Maximum Unambiguous Range	500 mi

The angle-tracking portion of the system is designed for moderate precision (about 0.2 deg). For most space vehicle applications, these angle and range specifications would be inadequate. The choice of carrier frequency was dictated by the requirement to maintain communications during the critical reentry period when an ionized sheath is built up around the vehicle that would render communications impossible at lower frequencies. It is somewhat higher than would normally be chosen for a general purpose integrated TTC system.

In conclusion, the Dyna-Soar SHF integrated TTC system choices of carrier frequency, modulation method, transponder configuration, and tracking performance are not optimized for general purpose space vehicle applications, although they may well be for that particular mission or one with very similar characteristics.

D. A GENERAL-PURPOSE INTEGRATED TTC SYSTEM FOR SPACE VEHICLE APPLICATIONS

1. REQUIREMENTS

It has been shown in the previous sections that, while an integrated TTC system can provide distinct advantages in terms of hardware economies, it is not universal in its applications. Specifically, it should not be considered as the solution to the problems of skin-tracking, reentry tracking, ultra-high precision tracking of booster vehicles, trilateration ranging, and transmission of extremely high data bandwidths.

The integrated system designed for support of space vehicles under a wide variety of free-flight conditions should be capable of tracking in four coordinates (range, range rate, azimuth, and elevation). The ranging system should be of moderate precision (less than 100 ft) and should be unambiguous out to at least several thousand miles. Range rate and angular tracking accuracies should be consistent with performance achievable from coherent doppler techniques (a few tenths of a foot per second) and good quality antenna and servo design (about one milliradian). Concerning angular tracking accuracies, once the carrier frequency is chosen to be high enough to avoid significant ionospheric refraction errors and as long as the antenna diameter is large enough to make λ/D sufficiently small, the achievable performance is primarily dependent on the degree of sophistication built into the mechanical structure of the antenna and the servo, and is rather independent of the remainder of the RF system design. The bandwidth of the command data channel should be sufficient to accommodate the expected command bit rates, along with allowance for redundant coding for security purposes. The telemetry system should be capable of accommodating both analog and digital telemetry, and for manned missions provision should be included for two-way voice communications.

While the concept developed in this section is designed primarily for the free-flight regime, it should nevertheless prove applicable in most respects to other instances in which integrated TTC systems might be employed.

2. CHOICE OF FREQUENCY BAND

The system would operate in the 2-gc band, for a number of reasons. First, the carrier frequency is sufficiently high so that ionospheric errors (which are inversely proportional to the square of frequency) do not preclude the possibility of precision tracking for trajectory and orbit determination. Ionospheric errors are worst at low elevation angles, when the vehicle is within the ionosphere, and when the component of vehicle velocity transverse to the line of sight from the tracking station is large.

The parameters for a rather severe case considered in a recent National Academy of Sciences report (Reference 1) are:

Target altitude	160 nmi
Target range	660 nmi
Transverse velocity	10,000 ft/sec
Elevation angle	6 degrees

With these parameters, the uncorrected ionospheric errors for a 2,000-mc system and a normal ionosphere are as shown below:

Range bias	10 ft
Angle bias	8 μrad
Range-rate error	0.3 ft/sec*

These errors can be reduced considerably by using a Chapman model of the ionosphere to correct the ionospheric biases. (A "rule-of-thumb" estimate for the standard deviation of the corrected values is one-third of the correction made.) Thus, in particular, the one-sigma value of the range rate error after such correction would be about 0.1 ft/sec.

Galactic noise is very low in this band and low-noise parametric and maser amplifiers are feasible, so that the sensitivity of ground receiving systems may be made extremely high. Spacecraft transmitters of relatively high efficiency are currently available and state-of-the-art advances within the next few years will provide substantial increases in transmitter efficiency and power output. The availability of solid-state transmitters with adequate power outputs (several watts) in the 2-gc band (see Appendix XXI) is extremely important for transponder weight and reliability considerations.

In this portion of the spectrum, the wavelength is short enough to permit precision doppler tracking and to render feasible extremely precise angle tracking with antenna apertures of reasonable size. At the same time, the wavelength is sufficiently long so that the mechanical tolerances can be met for fabrication of suitable antennas with diameters

* An obvious numerical error in Reference 1 has been corrected to obtain the range rate error given.

as large as 250 feet. Adequate spectrum space is available to accommodate data links with multimegacycle bandwidths and to permit the simultaneous operation of a relatively large number of vehicles. It is feasible both to achieve substantial vehicle antenna gain with apertures of reasonable size or to design wide coverage vehicle antenna patterns if desired. Finally, at this wavelength and with ground apertures of the sizes required, beamwidths will be sufficiently wide so that acquisition and beam-steering will not pose insurmountable problems, and sufficiently narrow to render possible increased efficiency in spectrum utilization by taking advantage of the directivity to achieve vehicle discrimination and to employ time-sharing among several vehicles on the same frequency channel.

The wavelength at 2 gc is also short enough to permit construction of low sidelobe antennas, which is important for low noise receiving systems as well as reduction of mutual interference. This 2-gc band, which appears to be optimum for a wide variety of orbital and deep space missions, is not the optimum frequency band for precision guidance and tracking during the initial powered flight of a launch vehicle. On the contrary, because of the increased instantaneous accuracies which are required for this latter type of operation to compensate for the fact that the vehicle is accelerating and its motion is not essentially Keplerian, tracking systems operating in the C- or X-bands appear to be a superior choice. This circumstance illustrates that different types of operation will, in general, require the use of different frequency bands and different types of systems if optimum performance is to be obtained.

3. OVERALL SYSTEM CONFIGURATION

Because of the requirement for relatively wide-bandwidth telemetry, a pulsed system is considered unsuitable. The system configuration contemplated for a CW integrated TTC system for use in the 2-gc band on a variety of space missions includes a basic phase-locked transponder in the vehicle and a ground station consisting of a frequency synthesizer, a power amplifier transmitter, a low-noise receiving system, an antenna and servo, and doppler extraction equipment. The ground receiving

system would employ a CW monopulse technique for angle-tracking,* although conical scan could be used, and the station would be equipped with telemetry demodulation equipment, command generation equipment, and encoding and decoding equipment compatible with the spacecraft equipment described in the following paragraphs.

In the interest of flexibility and to accommodate the great number of commands which may be required, the basic command system would be digital. A simple tone command system might be employed as a backup, to provide a limited command capability in case of failure of the digital system. The primary telemetry system would be digital, again because of the flexibility and efficiency of digital data transmission techniques, while provision would be made for transmission of analog telemetry data (FM/FM and PAM/FM) where required. The term "telemetry" includes all data transmission from the spacecraft and does not refer exclusively to the transmission of spacecraft housekeeping information. The emphasis in both the command and telemetry systems would be upon flexibility to meet the requirements of a wide variety of missions. For this purpose, a modular or building block concept would be employed, so that the command and telemetry system required for a particular mission could be assembled quickly and efficiently from a number of standard modules. In general, the choice of modules would differ with the required bit rates, which might range from a hundred or so bits per second, or even less, to one megabit per second. Digital telemetry or commands would be encoded on the transmission from or to the space vehicle either by use of direct biphase modulation with residual carrier or by biphase or frequency modulation of a subcarrier. Analog data transmission from the spacecraft would be by frequency or phase modulation of a subcarrier and a similar technique would be employed for tone commands or voice transmission on the uplink. An

---

* Monopulse is particularly advantageous when tracking a tumbling vehicle, since the amplitude fluctuations caused by the tumbling motion can cause adverse effects on a conical scan system if they contain frequency components near the nutation frequency.

important consideration for some missions would be the security of the command link and the telemetry (data) link. Such security would be provided by suitable encryption and decryption units available in add-on modular form. The modular telemetry system would incorporate provision for various types of data storage and pretransmission data processing for redundancy reduction and efficient coding, as required.

The basic phase-locked transponder would be a very sensitive double-conversion unit, generically similar to those which have been employed in previous programs. The transponder design would be compatible with either a solid-state transmitter with an output from a fraction of a watt to a few watts or a relatively high-power transmitter employing a traveling wave tube or an amplitron. The choice of the particular transmitter configuration would be made on the basis of mission requirements, with particular reference to output power required, efficiency, and the reliability requirements of the mission; the solid-state transmitter, while somewhat less efficient than an amplitron transmitter, would be considerably more reliable. A final modular add-on capability would be a CW ranging unit (multitone or swept subcarrier) for use on those missions where precision range information was required.

In the preceding system design discussion, emphasis has been placed on achieving a system concept which permits the utmost in flexibility and versatility at minimum cost and in a fashion compatible with the basic components of the system. For this reason, the modular or building block approach is felt to be the only satisfactory design approach in that it permits the system to be tailored to the specific mission requirements without requiring extensive new design and development, while retaining full compatibility with the basic system components. In addition, the basic system may be developed and placed in operation in minimal time, and the additional building blocks and add-on modular features need be developed only as required. Reliability is not compromised for the sake of versatility since all functions which are not required for a specific mission are deleted, with the additional consequence that size, weight, and power requirements are minimized. Moreover, the modular building block concept permits extreme flexibility in the form factor of the assembled spacecraft communications (TTC) package, in order to fit within the confines of the space available for various missions.

Although digital techniques have been strongly emphasized, it has not been felt desirable to insist that all data transmission on the up and down links be required to be in a digital format since for special purposes there are distinct advantages to be obtained from retaining an analog format. These advantages include simplicity of the spacecraft equipment required for vibration and video data and voice transmission, and the relatively efficient performance which may be achieved by FM transmission of this information, particularly if large deviation FM is used and frequency-following demodulators are employed in the receiving system.

4. THE DATA SUBSYSTEM INTERFACES

Present practice with telemetry and command systems places the interface between range and range user at the transmitted RF link. Compatibility is achieved by specification of carrier frequencies and modulation forms. Tracking systems utilizing vehicle transponders generally have the complete transponder package defined under range cognizance, and the interface with the user is in the area of prime power, physical requirements, and antenna pattern design. Adoption of the concept of a general-purpose range-operated TTC system would mean that the data system interfaces would bear a closer resemblance to those presently encountered with tracking systems. That is, the bulk of the vehicle package would be defined under range cognizance.

The modular design of the telemetry system would place the hardware and subsystem interface between the range user and the range at the telemetry video inputs. The net limitations would not be much more severe on the range user than present IRIG telemetry standards, the main difference being that the range-specified transponder would eliminate the need for the user to develop telemetry modulators, transmitters, transmitter couplers and associated power supplies. The user would, however, be responsible for design, fabrication, and installation of the TTC transponder antenna system on his vehicle. Telemetry subsystem checkout and calibration should be little more complex than at present. Digital telemetry word and frame structures and rates should be determined by flight computer and experiment requirements.

For most applications of an integrated TTC system, it is unlikely that telemetry bit rates greater than 1 megabit/sec per RF link will be required for instrumentation. (Certain missions may require 10 or 20 megabits/sec for transmission of payload data.) Analog data encoding accuracies of greater than 8 bits will be required in the integrated systems based on realizable analog transducer accuracies and resolutions. The TTC telemetry subsystem capability should provide for a minimum of one PCM telemetry multiplex of up to 1 megabit/sec capacity, and one FM/FM multiplex of at least 100-kc baseband bandwidth. The output interface for the telemetry function would be the same as that of present day practice.

The command system interface would be similar to that of telemetry with the input being at the video input to the ground station command encoder, and the output being at the switch closure or gates in the spacecraft.

Minimum requirements for voice communications on manned missions will include one link up and one down, capable of simultaneous operation with any or all other TTC system functions. Voice link requirements are not very demanding on the TTC system in terms of information rates or accuracy (about 3-kc bandwidth). Both ground and vehicle TTC subsystems would provide for direct audio signal inputs and demodulated audio outputs. Use of the link for other compatible purposes, e.g., time-sharing it with facsimile, would be left to the discretion of the user.

REFERENCES

1. "Report of the Ad Hoc Panel on Electromagnetic Propagation," (Draft Copy), Advisory Committee to Air Force Systems Command, National Academy of Sciences, National Research Council, ACASC: 103, 1962, pp 91-92.

Appendix VII. GLOTRAC

A. INTRODUCTION

An important metric system, recently developed and now being readied for operational use, is the Glotrac system. The purpose of this appendix is to review briefly some of its historical background, to describe its present configuration, and to discuss possible methods for upgrading the capabilities of this system.

Approximately three years ago, requirements were placed on the National Ranges for a metric capability that could not be fulfilled with any existing system. Specifically, these requirements were for accurate metric instrumentation (particularly with respect to velocity) of booster burn periods in widely dispersed geographic areas, outside the coverage of the Mistram system then under development. This capability was required for low (approximately 100 miles) altitude events in three areas (500 to 1000 nmi downrange from Cape Canaveral, the Ascension Island area, and the Manus Island area in the Western Pacific), and high (approximately 20,000 nmi) altitude events in two areas (over the Equator at approximately 90 deg East and 105 deg West). The locations of these events were determined by the requirements of two possible trajectories for placing a satellite in a 24-hour synchronous equatorial orbit using a second stage booster capable of three burn periods.

It was in response to these requirements that the development of the Glotrac system was inititated in 1961. It was immediately apparent that a single station tracking radar could not be built to meet the very high accuracy requirements. The emplacement of interferometers at locations suitable for instrumentation of the required areas was also unattractive, because of the high cost of this type of system and because of the difficulty in obtaining suitable land masses for their deployment. Further, it could be forseen that future space missions would have similar requirements in other geographical areas, and it was therefore desirable to use a type of instrumentation which was inherently mobile and did not require the extensive site preparation of an interferometer.

The Glotrac system was configured about the basic concept of trilateration (or more generally multi-lateration), which had been under study prior to initiation of hardware development. This concept is ideally suited for instrumentation of burn periods at locations widely dispersed throughout the world, since it permits siting flexibility and requires nominal (i. e., msec) timing synchronization between stations.

B. THE PRESENT GLOTRAC SYSTEM

The Glotrac hardware, as originally developed, provides independent range rate measurements from each station for a velocity trilateration, but does not provide for simultaneous range measurements from all stations. Instead, it utilizes a variety of methods for position determination, and different methods can be used at each set of stations (or "segment," as they have come to be known). One method of determination is to simply use an independent pulsed radar (e. g. FPS-16 or TPQ-18) measuring range, azimuth, and elevation (RAE) from a site which need not necessarily be located with one of the rate measurement stations. The resultant position determination is less accurate than that of a range trilateration, and in fact the position determination accuracy is essentially that of the single station radar.* As can be seen by a review of the error propagation equations in Appendix XII, the reduced accuracy of position determination reflects in a degradation of velocity determination, since position errors couple into velocity errors in a significant way. A variation of this method which could be applied would be to make pulsed radar measurements from two of the stations, and to combine these radar data in a statistically redundant fashion. It is easy to visualize that this situation would provide better results. If this were carried one step further, one would have a complete three-station range and range rate solution. In any of these cases, however, observe that two vehicle transponders are required, since the range measurement is made by a pulsed radar technique, while the range rate is measured with a CW system.

---

* It should be mentioned that doppler data simultaneously taken from other stations can enhance the position determination accuracy, and in principle a six-station pure doppler configuration can determine vehicle position without any range or angle measurements.

Another means of measuring range with the Glotrac system is through the "ranging module," by means of which range is measured from a Glotrac master station utilizing a CW technique. In this configuration, the CW carrier used for measurement of two-way doppler is modulated with ranging sidetones which, after being transponded in the phase-locked doppler transponder and returned to the ground, are detected and processed to provide a range measurement from the master station. Since angles are not measured by the Glotrac CW equipment (in a precise sense), this information alone is insufficient for determination of vehicle position, and it must still be augmented by data from an RAE radar using a separate vehicle transponder, and preferably located at a site other than that used to measure CW range.

One obvious combination of hardware to achieve a complete three-station range and range rate solution is to install the CW ranging module at the Glotrac master station containing the transmitter used for multiple station doppler, and to install a C-band pulsed radar at those slave stations which are passive receiving sites for the CW portion of the system. Such a combination is indicated in the PMR Development Plan of January 1963, which lists the following:

- Buka - $\dot{R}$ transmitter, $\dot{R}$ receiver, CW ranging
- Los Negros and Ponape - MPS-25 and $\dot{R}$ receiver

When the vehicle is mutually visible to all three stations, a complete solution exists and the angular data obtained from the two radars are redundant, i.e. they make an insignificant contribution to the solution. When the vehicle is visible to either Los Negros or Ponape, but not mutually visible to all three, a radar solution (RAE) exists for position, but no solution exists for velocity except that obtained by numerical differentiation of the radar position data.

As can be seen from the preceding description, there is a wide variety of possible methods for determining vehicle position using the Glotrac system in conjunction with the C-band pulsed radars. Still another Glotrac configuration is that in which position and velocity are measured by interferometric techniques. The Glotrac system has been designed so that its transponder is compatible with the Azusa Mark II (modified) at Cape Canaveral, thus in the vicinity the Azusa ground station can be used.

There are also plans to install a rate-only interferometer configuration at Ascension Island, since suitable land masses are not available for a trilateration configuration and since the expected work load and political stability of the territory apparently justify the investment for an installation of this type. Position information from Ascension is obtained by a TPQ-18 pulsed radar.

The original decision to implement Glotrac so that it depended on the pulsed radars, with the attendent requirement for two vehicle transponders, was apparently heavily influenced by the short time remaining before the first scheduled launch of the program which was to have used this system, and possibly by funding limitations. Whatever the reasons, it was recognized from the beginning that this situation was not optimum for the long run. The Glotrac was therefore designed to provide a growth potential, in which the system could evolve into one in which both range and range rate measurements could be made from all stations (using CW techniques), and the dependence on the pulsed radars could be severed.

C. THE IMPROVED GLOTRAC SYSTEM

1. GENERAL

There are several methods by which range measurements can be made from each of the Glotrac stations. As described in Appendix VI, a phase-locked CW transponder is ideally suited for measuring range and range rate from a single station, in which the return signal is compared with the transmitted signal to achieve the desired measurements. If range and doppler data are to be simultaneously measured at the other stations, using the same transponded signal transmitted from the vehicle, the other station must have a time and frequency reference similar to that at the master station with which to compare the received signal.

Doppler data extraction requires only a suitable frequency reference, which is available in the form of atomically stabilized oscillators. If the carrier is generated at the transmitting site by such an oscillator, and the signal received at another site is compared with an independent oscillator whose frequence relative to the first is known with sufficient accuracy, usable doppler data can be extracted at the passive receiving site (or any number of such sites). The physical interpretation of doppler at the outlying site is not range rate from that site, but rather rate of change of

the range sum from the master station to the vehicle to the slave station. This is precisely the doppler implementation utilized in the existing Glotrac system design. State-of-the-art oscillators are available today whose accuracy and long-term stability are such that they contribute substantially less than 0.1 ft/sec error to the range-sum rate measurement.

By contrast, the measurement of range at the outlying stations in a manner analagous to that just described for a range rate measurement requires the slave station to have a time standard whose epoch is synchronized to that of the master station to about 10 nanoseconds for a 10-ft error in (one-way) range sum measurement. Techniques for achieving this accuracy over distances of hundreds of miles are not expected to be available in this decade. (A method for achieving this kind of time synchronization by means of a satellite is described in Appendix X.)

Several possible methods for achieving simultaneous range measurement (or the equivalent thereof) from multiple ground stations, based on utilizing the Glotrac CW techniques and hardware, have been under study for some time. At present there is no one implementation which can be labeled "The Improved Glotrac System." Three prominent possibilities will be described in the following paragraphs. An optimum choice of precisely which method should be used to implement the improvement phase depends on the particular mission requirements to which the improved system would be applied. The three principal implementations considered herein are:

- Multiple master stations, as planned for use at WSMR
- One master station and multiple slave stations, using multiple coherent transponder channels, as described in the document "Analysis of Azusa/Glotrac and Mistram Needs," PAWA Document MT 63-55922, dated 15 February 1963
- One master station and multiple slave stations, using one coherent transponder channel and one or more wideband transponder channels

Simplified block diagrams of these three implementations are given in Figures 1, 2, and 3, respectively. The first implementation is fairly well defined since plans are progressing to utilize this system for trajectory determination in the Guidance Evaluation Missile (GEM) program.

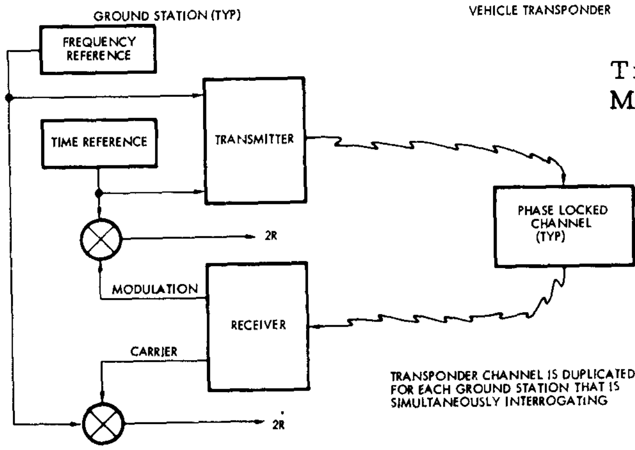

Figure 1.

Trilateration With Improved Glotrac - Multiple Master Stations

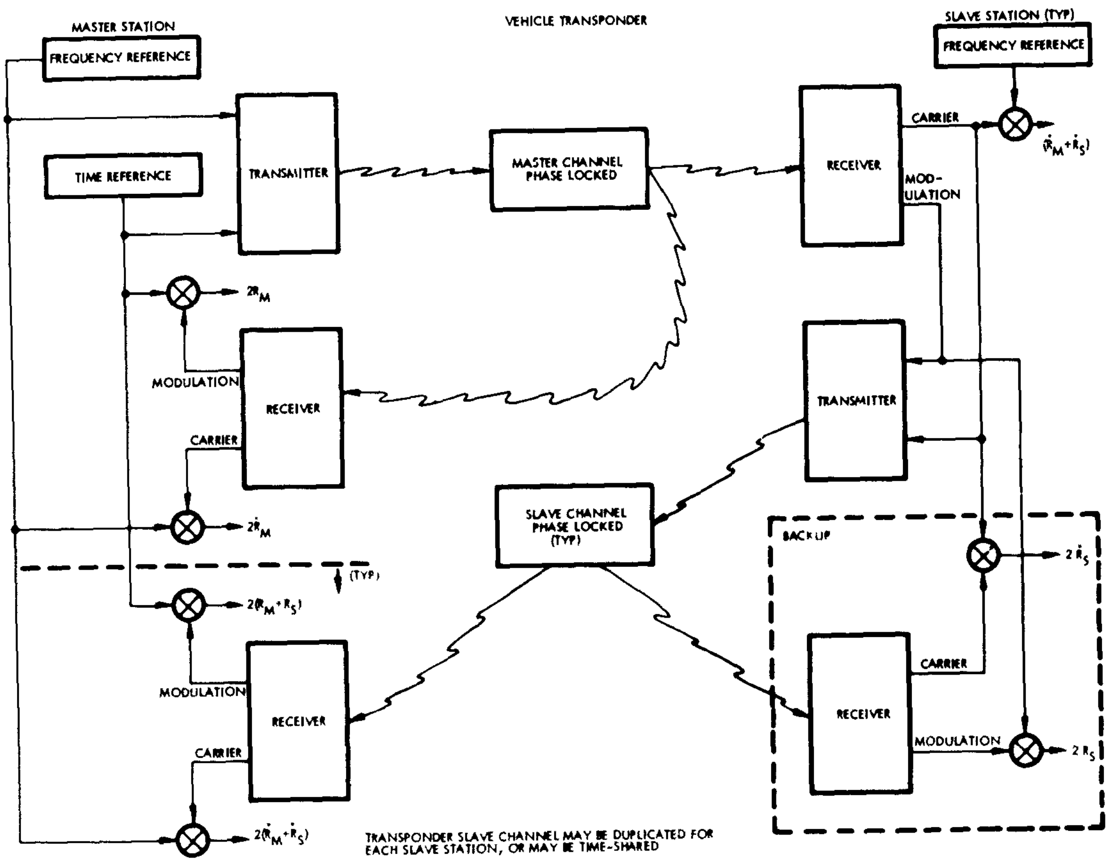

Figure 2. Trilateration With Improved Glotrac - Coherent Transponder Channels

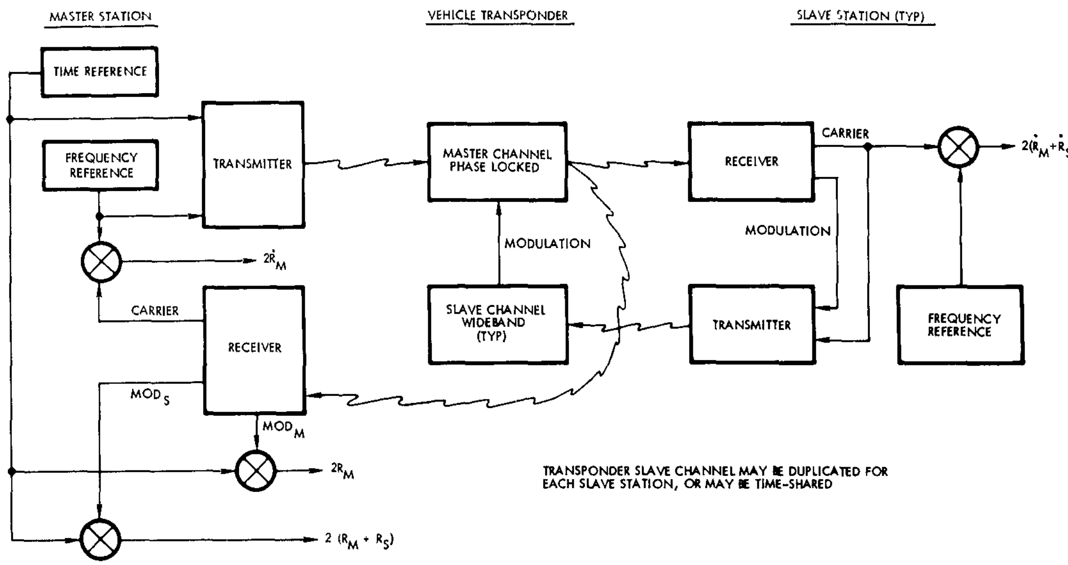

Figure 3. Trilateration With Improved Glotrac—Coherent and Wideband Transponder Channels

The other two implementations are more preliminary and hence leave several design decisions open to choice. They each contain several possible variants which will be briefly described, but these variants are considered to be minor details rather than fundamental in character.

2. MULTIPLE MASTER STATIONS

As seen in Figure 1 each ground station consists of the following elements: a transmitter, a receiver, a doppler extraction unit and a ranging module. The last two items have been simply designated by circles containing an "X." Each ground station is identical except for a frequency offset in the transmitter which is required to avoid mutual interference in the transponder. In this configuration the frequency reference need not be an atomically stabilized oscillator, but its use is being planned at WSMR because the Glotrac systems as presently implemented contained these oscillators. The transponder is seen to consist of multiple phase-locked loops, each essentially identical except for the frequency offset between channels. The weight, volume, and power

requirements of the vehicle transponder are essentially n times those of a single transponder, where n is the number of channels used. The use of a common mechanical structure and the integration of certain of the circuitry (e. g. the power supplies) will reduce these figures somewhat. The deployment plan at WSMR is for use of six ground stations and a 4-channel vehicle transponder. At each segment of the trajectory, the four stations having optimum geometry will be used in an active mode, while the other two will receive passively. The configuration choices, including the number of ground stations, the number of transponder channels, and the method of sharing the transponder channels, have been made to optimize the accuracy for GEM application.

A possible variation of the above has been considered at WSMR. This variation would utilize a single-channel vehicle transponder. Doppler measurement would be as presently implemented in the Glotrac system. Range measurements would be made by transmitting the ranging reference signals from the master station to each of the other ground stations. The accuracy requirements for synchronization of the stations in this application are identical to those required by the baseline synchronization links of an interferometer system. However, the implementation considered here would be to measure range sums at the slave stations rather than range differences as implemented in the Mistram system. This type of application is more feasible at WSMR where the stations are confined to a limited geographical area. However, this type of range loop measurement does not appear feasible for applications in which the baselines are several hundred miles long.

3. MASTER AND SLAVE STATIONS USING MULTIPLE COHERENT TRANSPONDER CHANNELS

A simplified block diagram of this implementation is shown in Figure 2. The slave station itself is a coherent transponder in which the signal transmitted to the vehicle is derived from the signal that has been transponded via the vehicle from the master station. A suitable frequency offset is provided so that the retransmitted signal will enter the slave channel of the transponder. The slave channel is like the master channel in that it is a phase-locked loop, and its output frequency is coherently

offset from its input. The output of the slave channel can be received at the master station, where it is compared with the original transmitted references to provide output data of range sum and range sum rate.

By duplicating the sections of Figure 2 marked "Typical" (slave station, transponder channel, and slave station receiver at master station), the master station can continuously derive range sum and range sum rate to each of two slave stations. An attractive feature of this configuration is that all of the data necessary to measure position and velocity is available at the master station; therefore only one high speed data handling and transmission system would be needed for real time data. In a fashion similar to that described in Section C. 2 of this Appendix, more than three stations could be used with a three-channel transponder by effecting a handover at the appropriate places in the trajectory. The slave station range sum and range-sum-rate data, in conjunction with the master station range and range-rate data, are then computer-processed to provide a three-station range and range-rate trilateration solution.

An alternative to this method is to use only one slave channel in the transponder and to time-share it rapidly between slave stations, under control of the master station. This mode of operation requires use of the command and timing feature (designed into the present Glotrac system) by means of which the master station, via its vehicle transponder channel, controls the sequencing operation at the slave stations. The slave station transmitters must be turned on and off at the sampling rate, which is undetermined at present but probably greater than once per sec. Each slave station may have the same nominal carrier center frequency, but differences in doppler shift from each slave station will cause the phase-locked loop in the transponder slave channel to unlock when the sequencing takes place. The slave station transponder must have a sufficiently wide loop bandwidth to permit rapid lock-on to the new signal within a small fraction of the sampling period. The same is true for the slave station receiver at the master ground station.

Range sum rate is extracted at each slave station on a continuous basis. In the data reduction process, the difference between slave station range sum rate and master station range rate can be integrated to interpolate the slave station range between the periods of active range measurement. By this means all of the necessary data is available on the ground to compute a three-station range and range-rate trilateration solution. The technique of synchronization of the stations via the transponder, for correlating the data-taking operations and time-tagging the data itself, should not be interpreted as synchronization of the sort which would permit the resultant system to be viewed as a wide baseline interferometer.

When the two-coherent-channel configuration with sequencing is compared to the three-coherent-channel configuration, it is seen that the former has the advantage of less transponder weight, volume and power, and the disadvantages of more complexity in the ground station (principally because of the sequencing process), increased computational requirements in the data processing, and increased requirements on the ground data transmission since all of the required data is not extracted directly at the master station. Figure 2 illustrates an optional method for extraction and recording of backup data at the slave station. If there is one transponder channel per active slave station, the atomic frequency reference and the extraction of range sum rate at the slave station is also a redundant backup. However, if the transponder slave channel is time-shared, the performance of these functions is essential to the solution.

Transponder weight, volume, and power requirements given in Section C. 2 of this appendix are applicable to this section as well, since each channel is a complete phase-locked loop using essentially identical circuitry. It is assumed that the transmitter power output of each transponder channel would remain the same as that of the present design and that the frequencies would be sufficiently separated to permit combining the two (or three) transmitter outputs with a low-loss multicoupler to feed a common antenna.

D. MASTER AND SLAVE STATIONS, USING WIDEBAND TRANSPONDER FOR SLAVE STATION RANGING

A simplified block diagram of this configuration is shown in Figure 3. By comparison with Figure 2 it is seen that the manner in which the transponder and the various ground stations are interrelated is similar, the principal difference being that the slave channel of the transponder is noncoherent. The result is that range sum rate cannot be extracted at the master station, but it is available at the slave station.

The transmitted carrier frequency at the slave station could be derived by coherently offsetting its received carrier as shown in Figure 3, or from an atomically stabilized oscillator. The prime advantage of this mechanization is that minimum hardware addition is required in the vehicle transponder. The local oscillator and input mixer can be common with the master channel. The second signal is amplified in an auxiliary IF strip whose center frequency is offset from that used within the phase-locked loop. The local oscillator tracks the signal from the master station, and the center frequency of the signal within the auxiliary IF strip is separated by the nominal offset introduced at the slave station plus the two-way doppler shift resulting from range rate to the slave station. Therefore, the IF bandwidths must be wide enough to accommodate this doppler shift, plus that bandwidth required to include the ranging sidebands on the signal itself. (If the slave station transmitter carrier were derived from an independent frequency reference, the bandwidth requirement would be about the same.) For a range rate to the slave station of plus or minus 20, 000 ft/sec, the IF bandwidth requirement is 400 kc for doppler effects plus 200 kc to accommodate the modulation sidebands. To maintain the signal-to-noise ratio above threshold in this IF strip requires sufficient signal strength to provide at least a 10 db S/N ratio in a 600-kc bandwidth. Comparing this with the coherent loop whose bandwidth is a small fraction of the above, and with a lower threshold requirement, it is seen that the noncoherent channel requires at least an order of magnitude more ground transmitter power than does the coherent channel in order to reach the threshold. Furthermore, since the noncoherent channel is open loop, it will not have the modulation phase stability of

the coherent loop, which utilizes modulation wipeoff, and it will therefore result in less accurate ranging.

Two principal means have been considered at AFMTC for retransmission of the output of this auxiliary channel. The first method is to demodulate the ranging tones by means of a discriminator and then to remodulate them on the transmitted carrier derived from the phase-locked loop. In order to distinguish these ranging tones from those in the master channel, the slave station ranging tones must be of different frequency. This could be accomplished by demodulation of the range tones at the slave station and coherently offsetting these tones before remodulation onto the slave station transmitted carrier. (The proposed technique appears to require considerable care in its implementation to avoid the introduction of phase ambiguities in the (coherent) frequency translation process.) A second method for handling the output of the transponder auxiliary channel would be to eliminate the tone demodulation and simply utilize the entire output of the IF strip as an additional modulation on the master channel carrier. This would appear as a subcarrier whose nominal frequency is at the center of the auxiliary IF strip, and the result would be a system which, as far as the slave stations are concerned, is essentially identical in configuration to the Goddard range and range rate system. With either method of retransmitting this slave channel information, the transmitter power must be shared between the two signals with a net reduction in power of approximately 3 db for each.

The foregoing discussion shows that the use of a noncoherent slave channel results in a considerable S/N degradation in both the down and the up links. For some applications at short ranges this degradation may be acceptable, but it is not considered optimum for general purpose system application. As in the case of the multiple coherent channels (Figure 2 in Section C.3 of this Appendix), two separate slave channels could be used with two slave stations to achieve a three-station range solution, or a single channel could be time-shared. Since the prime advantage to this is minimization of added hardware in the vehicle, the time-sharing scheme is almost certainly preferable. The present Glotrac type G transponder is constructed with some unused volume to permit system growth. It is estimated that this volume is sufficient to

accommodate the circuitry required to implement one noncoherent slave channel as described in this Section.

APPENDIX VIII. OPTICAL INSTRUMENTATION

This appendix presents (1) a review of current metric and other optical instrumentation, and (2) a discussion of future requirements and trends in optical instrumentation. No attempt has been made to detail specifications of all existing optical instrumentation since information as to accuracies and details of specific instruments is readily available in other publications. Requirements for future optical instrumentation and the advantages and disadvantages of metric optical instruments are discussed in full, and the future approach to metric optics that may combine electronic and optical measuring systems is presented.

A. CURRENT METRIC OPTICAL INSTRUMENTATION

1. INTRODUCTION

Metric optical instrumentation may be used to provide missile position, velocity, and acceleration data for all portions of the trajectory. A metric camera records space-coordinate, event-time information on a film or plate, which is subsequently used as a basis for measurement and calculation of missile position. The velocity and acceleration data provided are a byproduct of obtaining missile position at known-time intervals. The metric optical instrumentation system comprises the cameras which record the information, the film reading equipment, and the mathematical techniques which convert the photographic images into digital data. The basic techniques of reading and data reduction are common to all metric camera systems.

Three basic types of metric cameras are currently available: fixed cameras, cinetheodolites, and ballistic cameras. Fixed cameras and ballistic cameras remain fixed in space and angular position, and photograph the object as it moves through the field of view. The angular position of the film plane is established by reference points in the object field or by external graduated dials on the camera. Cinetheodolites remain in fixed-space position, but change angular position as the operator tracks the missile through its flight. The angular position of the cinetheodolite is measured internally and recorded on the film frame with the event.

These three types of cameras have been developed and employed to cover unique portions of the trajectory. Fixed cameras are used in the region liftoff through 5,000-ft-altitude range. The cinetheodolite provides metric data up to 100,000-ft altitude. The ballistic camera is used to cover all other portions of the missile trajectory, at ranges up to 1,000 miles from the camera site.

2. BALLISTIC CAMERAS

The ballistic camera system is the most accurate optical instrumentation available. It has three primary applications on the range

- Determination of missile trajectory position data
- Calibration of electronic guidance and tracking systems
- Geodetic surveying by photogrammetric techniques.

The principle which gives the ballistic camera its ultimate accuracy is the use of the star field as the calibration target. The ballistic camera is fixed in space and angular position, and obtains a record of the flight by photographing a light source on the missile as it passes through the field of view. Exposures of the star field on the same film plate serve to determine the angular orientation of the camera. The film plate consists of an optically flat glass plate coated with a photosensitive emulsion. The spatial position of the instrument is predetermined by survey, which may be photogrammetric, using the camera itself. Graduated dials on the horizontal and vertical axes are used to point the camera in the direction of planned missile flight.

In operation, a look angle is set, using the graduated dials, so that the vehicle will pass through the field of view. Shortly before the test, the shutter is opened for a short time to record a star position at that known time. The vehicle angles are then computed from the position of the missile on the plate.

Position is determined from the azimuth and elevation date from several cameras. Angle is determined by using the location of the camera, the orientation of the film plate, and the angle between the film plate and vehicle. The location of the camera is found by first-order survey; the orientation of the plate is obtained by comparing the positions of stars on

the plate with their known positions at that time, and the vehicle angles are then computed from the position of the missile on the plate.

a. Application

The principal use of the ballistic camera system is in the calibration of electronic guidance and tracking systems by determination of trajectory. These data are used to correct residual and bias errors in the electronic instruments. Simultaneous determinations of the flight path are made by the electronic equipment and by the ballistic camera photographing a light source that is on board the missile or aircraft. For missile application, the commonly used light sources are pyrotechnic flares or flashing strobe lights. Aircraft calibrations are generally made using strobe light sources carried aboard the aircraft. The requirements for an onboard light source have limited the employment of ballistic cameras to night flights carrying the required auxiliary light equipment.

The potential of the ballistic camera for range photography has been considerably broadened by the development of synchronized shutters which permit use of the rocket exhaust as the light source, and by filter and film combinations which permit its use in daylight. The star field may be recorded on the plate either the night before the launch or as soon as possible thereafter. Critical temperature control of the instrument during the intervals between exposures is a requirement to obtain accurate measurements with this technique. With this capability the ballistic camera may be employed during the launch phase to augment or replace other metric camera systems. Because of the wider field of view of the ballistic camera, it can provide data over a longer flight interval than the ribbon frame camera currently used for early launch coverage.

b. Ballistic Camera Operational Problems

In common with all photographic systems employed for range instruments, the ballistic camera system is weather sensitive. It is, in fact, more susceptible to weather than other metric optical instrumentation because it is generally used for trajectory measurements at long slant ranges. Ideally, for triangulation purposes, the cameras used to obtain data on a flight would be located 120 deg apart. In practice, however, missile ranges do not permit this ideal location and the cameras

are located at close to optimum sites along the proposed trajectory. The geographical separation of individual camera sites may be several hundred miles, so that each station may lose data because of local cloud cover. Little can be done for this problem except to provide redundant cameras and sites to minimize the possibility that local cloud cover will cause complete loss of data. Where ballistic camera data is a definite requirement, the problem can be handled only by launch scheduling (holding or postponing the launch until weather conditions are satisfactory at all camera sites).

The other principal operational problem of the ballistic camera, i. e. , the requirements for an auxiliary light source aboard the missile, was discussed in Section A. 2. a.

Aside from the payload penalty and flight system complexities introduced by onboard flares or strobe lights, there is the problem of telemetry RF interference. Flares have caused momentary transmission blackouts on detonation, and the high-voltage discharges of strobe lights have caused noise spikes on telemetry data channels. These effects cause loss of telemetry data at critical moments when it is most needed in order to correlate onboard events with external data.

The development of the synchronous shutter and flame-chopping technique may not completely solve the problem for all applications of the ballistic camera system since some rocket engines used on upper stages may have flames with insufficient luminous intensity to provide satisfactory images on the plate. The synchronous shutter will, however, permit the use of a continuous light source rather than the present individual flare or strobe light technique.

c. Ballistic Camera System Development

Since the first application of the ballistic camera for range instrumentation purposes, the ballistic camera system has undergone intensive development in the following major areas:

> Improvements have been made in the camera shutters to provide synchronous operation of the shutters on multiple camera installations. Further improvements have been made in the screen shutters used to block out portions of the field for daylight photography.

The focal length of the lenses used on ballistic cameras has been increased from 210 to 1000 mm. This is not simply a change in lens focal length, but represents several complete new ballistic camera instruments.

A number of improvements have been made in the film and filter combination employed in ballistic cameras to permit operation in restricted areas of the spectrum.

The mobility of the ballistic camera has been greatly improved by the development of system accessories, i. e., portable astrodomes, mounts, timing systems, etc. Although the development of the ballistic camera system has approached its practical limit, the following areas are being considered for future development.

1. Mobile Complete Systems

At present the mobility of the ballistic camera applies only to the photographic instrument itself. The plate must be returned to the laboratory for processing, reading and data reduction. This, of course, entails some delay in the delivery of data to the range user, especially when the plates are exposed at sites far from the mainland laboratories. The mobile complete system would provide processing and plate reading capability at the camera site. After processing and reading, the data points would be transmitted by radio or teletype to the laboratory for computation and data reduction.

2. Longer Focal Length Cameras

Studies have been made to consider extension of the focal length of ballistic cameras beyond 1,000 nmi. This increase in focal length means the development of a new ballistic camera. The extension of the camera focal length is accompanied by several new operational problems. For example, as the focal length is increased, the field of view decreases so that more cameras would be required to cover the same trajectory interval. Alternatively, a tracking mount can be considered for use with a long focal length ballistic camera; however, this introduces a new set of errors which could offset any advantage gained by the focal length increase.

3. CINETHEODOLITES

The cinetheodolite is the only tracking metric optical instrument. It is employed to provide position, velocity, and acceleration data from liftoff through the limits of its optical resolution, which for practical purposes is approximately 100,000-ft altitude. The cinetheodolite is composed of a camera mounted on a refined transit with provisions for recording the angular information (camera elevation and azimuth) on the film frame. Range time is also simultaneously recorded on the film.

The cinetheodolite commonly used throughout most ranges in the United States is the Askania, or one of a number of modifications of the Askania, made by various optical groups within the United States. A description of the Askania K^{th} 53 is given below:

> The Askania K^{th}53 cinetheodolite consists of a 35-mm camera (with double width frame) and two sighting telescopes. Two operators use handwheels to track the target, one in azimuth and the other in elevation. The film records target image, azimuth and elevation dial readings, time, and a sequential frame count.
>
> An optical train projects images of the azimuth and elevation dials, which give the direction of the optical axes upon the film. Electronic controls synchronize the strobe lamps which provide light for photographing the dial readings at each site. Range timing in binary code and a numerical frame count are also recorded on each frame.
>
> The camera is pulse-operated at rates of one, two, or five frames per second and has a film capacity of 110 ft using standard 35-mm film; the usable picture area is approximately 1.5 x 0.9 in. Each camera is equipped with lighted fiducial marks.
>
> From the position on the film of a point on the missile and the angle dial readings, the azimuth and elevation of the missile can be computed. Data recorded at the same time by two or more cinetheodolites are used to

find vehicle position. Pulses from central timing operate all of the cameras at the selected frame rate to ensure that all instruments record data at the same time.

The Askania $K^{th}53$ covers missile flight in the 0- to 100,000-ft range, providing backup coverage for the fixed camera system from 0 to 10,000 ft. It is a principal source of position data from 2,000- to 100,000-ft altitude, when photographic conditions permit.

One range (Eglin) has adopted the Contraves EOTS, a more recently developed instrument which has provision for electromechanically aided tracking and slaving, a feature which is not found in the manually operated Askania instrument.

a. Cinetheodolite Operational Problems

The cinetheodolite has been extensively developed since World War II, so that most of the technical problems have been solved. The principal operational problem of weather, as with all optical instrumentation, must be lived with.

b. Cinetheodolite Development

The development of the cinetheodolite beyond its current state of the art will probably be limited to increasing instrument mobility and flexibility. Some consideration has also been given to adding remote tracking capabilities so that the cinetheodolite can be employed within the extended danger zones which will be required for multimillion-pound thrust launch vehicles.

4. FIXED METRIC CAMERAS

The term, "fixed metric camera," is used to describe the ribbon frame camera that was first developed in 1942 by the California Institute of Technology. This camera is employed for the acquisition of space position, velocity, acceleration, and attitude data from liftoff to approximately 5,000-ft altitude.

The ribbon frame cameras use lenses up to 10 in. in focal length and take pictures with a frame size which is dependent on the frame rate selected. The missile is photographed on the long axis of a narrow film frame 5 in. long (hence, the name "ribbon frame"). The azimuth and elevation references for the ribbon frame camera are obtained in one of three ways:

- By target boards included within the field of view of the camera (shutter boards).
- By target boards which are offset from the field of view of the camera and which are photographed prior to making the film run; the camera is then aligned by means of calibrated azimuth dials.
- By use of the calibrated azimuth and elevation dials alone; however, the end accuracy is about one-half that of the target board method.

The standard fixed metric (ribbon frame) cameras are the CZR-1 and RC-5, which are functionally identical but have minor design differences. They provide azimuth and elevation angles for the first 5,000 ft of missile flight, from which position, velocity, and acceleration data may be derived. Roll and attitude data can also be obtained.

A large cylindrical, focal plane shutter drum encloses a continuous-motion film transport drum and a ribbon frame film. The shutter and film move at a constant rate; therefore, the number of frames per second depends upon shutter drum openings. The shutter drum has six slots spaced 60 deg apart. The slots may be closed off by shutter slides. One open slot will give 30 frames per second; two open slots opposite one another give 60 frames per second; three alternate open slots will give 90 frames per second; and all slots open will give 180 frames per second. Whenever the frame speed is changed, an aperture slide or framer must be inserted in the camera aperture to change the vertical dimension of the individual picture. The shutter drum is directly coupled to its synchronous motor, which operates at 1800 rpm.

A timing projector is located within the stationary cylinder of the film drum. This projector, which consists of a neon bulb and its wiring, is used to record a serial, elapsed-time code along the edge of the film. In this way, recorded data may be correlated to reference time.

A three-axis precision gimbal mount allows accurate leveling of the camera. Azimuth dials and target boards are used for prelaunch orientation. An electronic driver unit performs switching functions and supplies timing pulses in response to information from central timing.

5. BAKER-NUNN SATELLITE TRACKING CAMERA

a. Introduction

The Baker-Nunn camera is a tracking central projection instrument capable of detecting moving objects as faint as 15th magnitude with tracking accuracies of 2 arc-sec. The cameras, located throughout the world and tied into a central control site in Massachusetts, have achieved considerable success in the determination of artificial satellite orbits, unknown or dead satellite surveillance, and reduction of land mass global survey uncertainties; and they have contributed generally to a better understanding of the earth's atmosphere and shape, and to sun-earth relationships.

The USAF is using Baker-Nunn cameras for space surveillance, for which purposes a directional accuracy of 2 arc-sec is desirable. To attain the latter, considerable computational time is required since up to 60 star images must be used as references. A new star atlas is being compiled with star maps of the same scale as the camera photographs. It has been estimated that this new atlas will contain more than one million stars, as contrasted with the best existing star atlases containing about 30,000 stars each.

b. Discussion

The Baker-Nunn camera is related to the ballistic camera in the sense that they are both central projection instruments as contrasted with theodolites, the other main category of optical instruments. Central projection optical instrument operation is based on the principle that there exists a single fixed point (usually within a compound lens) such

that it, any given point of the object, and a corresponding point in the image are colinear. This is true only to the extent, however, that atmospheric anomalies and lens distortions can be minimized or accounted for in the data reduction process. Unlike ballistic cameras, Baker-Nunn cameras track the target in order to enhance sensitivity. They have achieved documented accuracies, in the field, of 2.8 arc-sec for 13th to 14th magnitude objects.

The Baker-Nunn camera optical system is a modified Schmidt type, with a 20-in. aperture and an f/1 focal ratio. It can only be operated at night to avoid damage to the aspherically-curved, Pyrex glass film back-up plate by solar radiation. The effective focal length is 500 mm. Photographs covering a field of view of 5 x 30 deg are taken on 55 mm film. Supporting data, including timing, are also recorded on each photograph, which measures about 12 x 2 in. Film transport is automatic, synchronized to a double shutter which serves the dual purpose of photographic shutter and image beam interrupter. Overall exposure times per frame can be selected at 0.2, 0.4, 0.8, 1.6, and 3.2 sec, plus one additional arbitrarily long interval. Kodak Royal X Recording Safety Film in 950-ft magazines is used. Resolving power of the camera is such as to produce minimum star image diameters of 20 μ on the film. The camera is suspended within a three-gimbal mount equipped with sidereal drive (angular velocity of 1 deg/4 min about the polar axis). Overall height of the Baker-Nunn camera is about 12 ft.

In operation, it is presumed that the satellite will be tracked so that the orbital path lies in the direction of the 30-deg frame axis. The considerable relative velocity of artificial satellites requires very precise time recording and photographic image coordinate determination, e.g., 1 msec and 0.0001 in. on the film would be required for 1 arc-sec determination.

The Smithsonian Baker-Nunn camera net includes:

Arequipa, Peru	Naimi Tal, India
Curacao, N. W. I.	San Fernando, Spain (northern tip)
Johannesburg, So. Africa	Shiray, Iran
Jupiter, Florida	Tokyo, Japan
Las Cruces, New Mexico	Villa Dolores, Argentina (northern sector)
Mauai, Hawaii	Woomera, Australia

c. Conclusions

Although Baker-Nunn cameras are limited, as are all other optical devices, by their inability to operate under all weather conditions, they have proved highly useful for satellite orbit determination and general surveillance on NASA and USAF programs. It is understood that, as of July 1963, Baker-Nunn cameras are the only cameras still capable of tracking the ANNA flashing light which is growing very faint.

For extremely precise satellite tracking and geodetic research, the Baker-Nunn camera net and each individual camera therein must be precisely calibrated. A beginning has been made with the Edwards AFB Baker-Nunn installation, but considerable work of this nature remains to be done.

Some experiments have indicated film-base instabilities resulting from the fact that at present the Baker-Nunn cameras employ film only 0.006 in. thick stretched over an aspherical backup plate under 14-lb tension. It has been suggested that this disadvantage can only be eliminated by redesign of the Baker-Nunn camera to use an absolutely flat film plane or, eventually, plane-glass photographic plates.

Continuation of the Baker-Nunn camera net and possibly its expansion are recommended to conduct research in the field of geodesy, geophysics, etc., and in tracking of dead satellites. The cooperative use of this network will be useful in the areas of geodetic and calibration satellites. However, no real advantage can be seen in transferring the existing management of the network from the Smithsonian Astrophysical Observatory to any other agency.

6. INFRARED (IR) TRACKERS AND SPECTROMETERS

a. Introduction

Infrared instrumentation coverage during launch and reentry operations will undoubtedly be of increasing interest in the 1965 to 1970 period. This coverage can be expected to include IR spectral intensity measurements, azimuth and elevation tracking data, and possibly image recording by IR radiation using video recording techniques. Combustion temperature and fuel-oxidizer ratio determinations can be made as a function of altitude from IR spectral data taken at launch. Reentry temperatures

c. Conclusions

Although Baker-Nunn cameras are limited, as are all other optical devices, by their inability to operate under all weather conditions, they have proved highly useful for satellite orbit determination and general surveillance on NASA and USAF programs. It is understood that, as of July 1963, Baker-Nunn cameras are the only cameras still capable of tracking the ANNA flashing light which is growing very faint.

For extremely precise satellite tracking and geodetic research, the Baker-Nunn camera net and each individual camera therein must be precisely calibrated. A beginning has been made with the Edwards AFB Baker-Nunn installation, but considerable work of this nature remains to be done.

Some experiments have indicated film-base instabilities resulting from the fact that at present the Baker-Nunn cameras employ film only 0.006 in. thick stretched over an aspherical backup plate under 14-lb tension. It has been suggested that this disadvantage can only be eliminated by redesign of the Baker-Nunn camera to use an absolutely flat film plane or, eventually, plane-glass photographic plates.

Continuation of the Baker-Nunn camera net and possibly its expansion are recommended to conduct research in the field of geodesy, geophysics, etc., and in tracking of dead satellites. The cooperative use of this network will be useful in the areas of geodetic and calibration satellites. However, no real advantage can be seen in transferring the existing management of the network from the Smithsonian Astrophysical Observatory to any other agency.

6. INFRARED (IR) TRACKERS AND SPECTROMETERS

a. Introduction

Infrared instrumentation coverage during launch and reentry operations will undoubtedly be of increasing interest in the 1965 to 1970 period. This coverage can be expected to include IR spectral intensity measurements, azimuth and elevation tracking data, and possiblv image recording by IR radiation using video recording techniques. Combustion temperature and fuel-oxidizer ratio determinations can be made as a function of altitude from IR spectral data taken at launch. Reentry temperatures

and data on reeentry vehicle ablative and heat-shield material performance can be obtained from IR spectral coverage at reentry. Launch and reentry IR spectrum "signatures" of as wide a variety of missions as possible are extremely important for the establishment of IR surveillance criteria to enable distinguishing enemy rocket launchings and vehicle reentries from similar but more benign phenomena.

Azimuth and elevation information can be obtained from IR trackers during launch and reentry to a considerable degree of accuracy if the trackers are land-based on precisely surveyed, stable, sites. Of course, tracking data can also be obtained from airborne or shipboard IR equipment as well, but it is subject to the same degradations as RF or visible optical tracking data obtained under the same circumstances. (See Appendixes XXXVI and XXXVIII for discussions on instrumented aircraft and ships, respectively.) It should also be mentioned that, although IR trackers have better haze-penetrating ability than visible light optical trackers, they are still by no means all-weather tracking systems, as are radar tracking systems operating from X-band down.

The following section contains a description of a current land-based IR measurement system as an example of the present state of the art in the field.

b. The AMR Land-Based IR Measurement System

AMR currently employs a tracking IR radiation measurement system at Patrick AFB to measure IR energy in the plume at launch, and another system located on Ascension Island to measure reentry IR phenomena.

The IR spectral measurement portions of the systems include a three-channel IR radiometer using a 12-in. f/3 Cassegrainian optical system, covering the following regions:

- 1.2 to 3.3 microns:
  Cooled lead sulfide detector
  Noise equivalent power density (NEPD), 2×10^{-14} watt/cm^2
  Six-decade logarithmic signal compression
  Signal bandwidths selectable at 0.2, 1.0, 5.0, and 20 cps.

- 1.2 to 7 microns:
  - Thermistor detector
  - NEPD sensitivity, 8.5×10^{-11} watt/cm^2
  - Four-decade logarithmic signal compression
  - Signal bandwidths selectable at 0.2, 1.0, 5.0, and 20 cps.
- 1.8 to 22 microns:
  - Thermistor detector
  - NEPD sensitivity, 8.5×10^{-11} watt/cm^2
  - Four-decade logarithmic signal compression
  - Signal bandwidths selectable at 0.2, 1.0, 5.0, and 20 cps.

Multielement IR scanners can be used to plot energy density variations in a rocket plume or reentry plasma as a function of position by scanning the field past a vertical detector array at the rate of 10/sec. Resolution runs as high as 0.1 mil in azimuth and elevation with a sensitivity of 10^{-12} watt/cm^2, or 1.0 mil in azimuth and elevation with a sensitivity of 10^{-13} watt/cm^2. The logarithmically compressed output covers five decades. Total field of view is 2.8 x 2.8 mils for the 0.1 mil system, and 28 x 28 mils for the 1.0 mil system.

The target acquisition portion of the IR tracker subsystem uses a modified Cassegrainian optical system with a left/right split field and an upper/lower dual-frequency light-chopping reticle to obtain target quadrant position data. For tracking, another modified Cassegrainian optical system is used, again with a left/right split field, each with its own PbS detector array; but with light-chopping reticles arranged so as to scan one across one-half field from left to right and the other from top to bottom. Separate azimuth and elevation output errors are obtained such that voltage amplitude is proportional to image displacement from the center of the field, and polarity is a function of direction from center. Characteristics are:

Tracking precision:	±0.05 mil
Tracking output:	voltage is a linear function of position error
Tracking field of view:	4 x 4 mil

Acquisition field of view: 4 x 4 deg
Sensitivity (NEPD): 10^{-13} watt/cm^2

In addition to the IR-measuring portions of the system just described, these instruments contain the following units:

Ultraviolet (UV) - Visible Photometer: S-1 and S-13 responses, covering the 0.24 to 1.0 μ region in six steps at a 2.4 sec scan rate, or capable of continuously monitoring any fixed portion of this region as determined by accessory filters; 5-decade logarithmically compressed output; field of view selectable at either 3 x 6, or 6 x 6 mils.

Boresight camera

Boresight TV

Magnetic tape recorder (records all tracking and spectrometer data outputs)

Azimuth and elevation encoders

Mk 51 telescope and mount (for manual track override of the IR tracker)

Nike-Ajax radar pedestal.

7. METRIC PHOTOGRAPHY DATA REDUCTION

The metric photographic instrument provides only an observation of the missile at a known time. This observation must then be translated into digital data and missile performance parameters. Triangulation, using two or more cameras and film measurements, is the key to obtaining reduced metric data from the film frame. This provides space position-time information and a series of individual measurements at known time intervals permits computation of velocity and acceleration. For daylight launches, missile attitude, e.g., pitch, yaw, and roll, can be measured and calculated when a suitable target pattern is provided on board the missile.

The mathematical technique employed is to determine the intersection of the rays from two or more cameras to the missile. A ray is considered to be the light beam extending from a point on the missile to a point on the film surface within the camera. Precise measurements of the X and Y coordinates of the image on the film determine the direction of the light ray. The mathematics are handled by electronic computers, and programs for reduction of data from as many as eight instruments have been developed.

The basic data, i. e., the X and Y film measurements which are fed to the computer, must be manually read, using precision comparators or theodolite film readers. In the case of ribbon frame camera or cinetheodolite data, trained film readers can read from 50 to 300 frames per hour. Ballistic camera plate reduction, because of the greater reading precision required, is somewhat slower.

This manual film reading process which is required before the computer can reduce the information into useful data is obviously one of the limiting factors in metric optical instrumentation. A number of improvements have been made in the film reading process in an effort to automate it, but complete automation with the film recording systems is impossible at present.

B. NEW METRIC OPTICAL INSTRUMENTATION DEVELOPMENTS

1. INTRODUCTION

Prior to further discussion of the future of metric optical instrumentation, the singular advantages which optical instrumentation has provided for range applications should be reviewed. These are:

- Metric optical instrumentation has provided accurate position and attitude information in the interval from liftoff to 5,000-ft altitude where electronic systems could not provide accurate information.
- The ballistic camera has provided trajectory information to an accuracy which permits the data to be used for the calibration of electronic tracking and guidance systems.

- The optical instrumentation system is completely external to the missile, requires no transponder or missileborne equipment, and can obtain data during malfunctions of the missile electrical system. The ballistic camera with its requirement for a missileborne flashing light is an exception to this statement, but with the flame-chopping capability it, too, becomes a completely external instrumentation system.
- A byproduct of photographic instrumentation is a time and space coordinated photographic record of the flight which may be used for engineering analysis of flight problems.

Some of the new developments in metric optical instrumentation which will be discussed subsequently do not have these singular advantages.

2. DISCUSSION

From the preceding, it is apparent that the existing metric optical instrumentation systems have reached or are fast approaching the limits of practical development; but the current status of the three metric optical instrumentation systems could be affected by the following considerations:

In the future, the fixed (ribbon frame) camera could be replaced in its entirety by the fixed ballistic camera where a photographic record is not required. The attitude data which was formerly taken from ribbon camera films could be obtained by tracking engineering sequential cameras, thereby making them metric cameras, as well, in this application. Use of the ballistic camera results in more accurate position data over a longer flight interval during the early launch phase.

The cinetheodolite appears to have been developed to a practical limit as noted before. Future developments will probably be limited to accessories to the instrument rather than to breakthroughs in camera design or lens

improvement. These accessories will provide greater flexibility and mobility for the cinetheodolite system but will not necessarily improve data gathering ability or data accuracy.

The ballistic camera has also been developed to a point where the prospects for further refinement are somewhat slight. The primary applications foreseen for ballistic cameras include precision geodetic work and calibration of electronic tracking systems. In the latter capacity, they may be employed in various ways, including uses with calibration missiles and satellites.

The future of optics as an instrumentation medium will probably be as a copartner with electronics and a new family of electro-optical instruments. These instruments can utilize the best features of electronic and optical systems to provide more accurate data more quickly than either electronic or optical systems can provide alone. Prominent among the electro-optical developments which have been proposed for improved instrumentation are:

Use of electronic image sensing and dissection devices to provide real time tracking outputs.

Use of video recording techniques to replace film as the recording medium to eliminate processing operations, i. e. , developing, fixing, etc.

Use of the laser as a short range radar for early launch coverage.

Use of infrared sensors and detectors for all-weather tracking.

Several of these are currently being employed for some applications in range instrumentation or are undergoing development. Their continued development is recommended in light of impact on the powered-flight phases of future ballistic missile and space programs.

3. SPECIFIC RECOMMENDATIONS

An approach to electro-optical instrumentation which appears to combine the advantages of both would be to substitute an electronic image-sensing device, such as a TV-camera-type pickup tube or solid-state photosensitive mosaic, for film, using an electronic image coordinate determining system for real-time extraction and readout of position and velocity information (and possibly attitude, at close range). Simultaneously, the information could be recorded or transmitted to remote locations in at least two formats. Coordinates could be handled as digital information and tape-recorded in the usual parallel binary format, or transmitted in real time via a PCM link. The composite picture might be recorded in the same manner, but more likely would be recorded in a format similar to that of present-day TV video recording. When combined with shaft position encoder outputs, video tape could record the image and pertinent timing, as well as azimuth and elevation information. However, the present state of the art in resolution of photo-electric sensing devices, and obtainable video recording bandwidth fall far short of that effectively realized in present-day photo-optical instruments, as will be illustrated in Section D.

The use of the laser as a direction-finding and ranging device is an attractive scientific problem which will be discussed in more detail in Section E. This optical radar would, however, be as susceptible to weather constraints as present-day incoherent optical instrumentation systems at the same ranges.

Infrared tracking devices have a definite use on the range where the advantages of IR seekers, detectors, and trackers can be utilized. Already in operation are a number of infrared tracking devices for acquisition and homing, IR spectral measurements, penetration aid measurements, and other specialized uses. The application of infrared techniques is recommended as a continuing range instrumentation development program for those applications where the photographic image by visible illumination is either not paramount or cannot be obtained.

C. CURRENT NONMETRIC (ENGINEERING SEQUENTIAL OR SURVEILLANCE) OPTICAL INSTRUMENTATION

1. INTRODUCTION

Nonmetric optics, more commonly referred to as engineering sequential or surveillance photography, comprises all of the photographic equipment employed in launch support to obtain event-time data. This distinguishes it from documentary photography which is not time correlated and from metric optics which provides event-time-position data.

There are four general applications of engineering surveillance photography in launch support operations.

- The study of individual events: Cameras are employed to record, usually in slow motion, the occurrence and duration of specific events occurring during the launch operation. The application is usually to a specific known or suspected problem area and the equipment is for the individual applications.
- Fixed surveillance: Cameras are employed to record all events taking place in the launch stand area for some time prior to ignition until after the launch vehicle leaves the camera's field of view or the film runs out, whichever occurs first.
- Short range or intermediate range tracking: Cameras on tracking mounts record the flight of the vehicle from liftoff or very shortly thereafter through the limits of optical and/or atmospheric image loss.
- Long-range tracking cameras: Tracking cameras slaved to other target acquisition means acquire the vehicle and record its flight from acquisition through the limits of optical and atmospheric image loss.

These are the current applications of engineering sequential photography, and it is reasonable to expect that they will continue unchanged

throughout the 1965 to 1970 period. While the applications for engineering sequential photography will remain constant, the requirements and operating problems encountered will undergo some changes during the 1965 to 1970 period.

Engineering sequential photography is one of the more reliable external data collection systems. Loss of data due to missile onboard system malfunctions is impossible, and loss of data due to camera malfunction or operator error is exceptional. Currently, the problems encountered with fixed cameras are predominately operational. These include:

- Loss of data due to film run-out. The fixed cameras employed around the launch stand are controlled remotely. The operation of these cameras is controlled by the master countdown and cameras are started at specific times in the count to record individual events. Particularly in the case of high-speed cameras, (e. g. , Fastax which has no stop and restart capability), operation continues until the film is exhausted. If a hold occurs in the countdown subsequent to camera startup or if the count is recycled for any reason after cameras have been started, no data can be obtained unless the cameras are reloaded. There are a great many applications of high-speed cameras in and around the missile to record events taking place in the last few minutes of the countdown, and during engine startup and missile liftoff. It is often physically impossible, due to the hazardous conditions around the launch stand, to permit camera reloading in the event of film run-out. Further, project officers have been extremely reluctant to call additional hold time for the purpose of camera reloading.

- Loss of data due to changes in exposure conditions. Again a problem which faces only fixed, nonattended cameras is the loss of data because the exposure conditions have changed radically between the time the cameras were set up and the time of operation.

With modern films, exposure changes of some magnitude can be tolerated without loss of significant data. Automatic electronic exposure control is becoming increasingly commonplace. However, countdowns which extend through daylight hours into night, or vice versa, still create exposure problems.

- Data quantity. A continuing problem with engineering surveillance photography is the processing and viewing of the mass of data obtained. Since many thousands of feet of film may be exposed on a typical launch, this processing and viewing requires a substantial investment in money and manpower.

2. RECORDING OPTICAL TRACKING INSTRUMENT (ROTI)

The ROTI is a tracking telescope which makes time-correlated photographs of objects in space at long ranges. The optical system is Newtonian, with large aperture and variable focal length. It has two tracking telescopes and two visual null devices for use by azimuth and elevation operators.

The telescope is supported by a modified Navy Mk 30, 5-in. gun mount driven by a hydraulic servo system for azimuth and elevation changes.

Controls are available for automatic focusing and exposure. Automatic focusing uses range data from the target acquisition bus. The exposure device compares the light entering the telescope with that from a standard light source and automatically adjusts the exposure time.

The 70-mm motion picture camera is adjustable for frame rate, shutter opening, and "off-on" operation. It uses either 400- or 1,000-ft capacity darkroom-loading, daylight-threading magazines. It is equipped with a variable shutter, timing lights, fiducial markers, film footage counter, and a film runout switch.

The ROTI is protected by a weather-proofed, air-conditioned astrodome. The astrodome is automatically positioned in azimuth by a drive assembly synchronized to the telescope rotation. A curved door slides overhead to expose the telescope.

Three tracking modes are provided: slaved to the target acquisition bus, slaved operation with operator override (servo error voltages are presented to the operator for correction), and operator tracking by joystick.

3. INTERCEPT GROUND OPTICAL RECORDER (IGOR)

The IGOR tracking telescope is used to photograph the flight of the missile as a function of time. As the camera records the images seen through the main objective telescope, timing marks are exposed along the edge of the film.

The objective telescope is an 18-in. Newtonian system with a fixed focal length of 90 in. Optical amplifiers give effective focal lengths of 180, 360, and 500 in. The system provides high resolution over a 2-1/4 x 2-1/4 focal plane. The telescope is mounted on a modified Navy Mk 27 5-in. gun mount. Either the 70-mm flight research camera or the 35-mm Mitchell camera may be used.

The IGOR is equipped with automatic focus and exposure controls and sighting telescopes. The three tracking modes provided are: slaved to the target acquisition bus, slaved operation with operator override (servo error voltages are presented to the operator for correction), and operator tracking by handwheel.

D. NEW NONMETRIC OPTICAL INSTRUMENTATION DEVELOPMENTS

To aid in the solution of the present operational problems and the anticipated future operational problems, studies are recommended on the following systems.

- Airborne optical tracking systems. This appears to be one approach to the problem of atmospheric limitations on nonmetrical coverage of events taking place at long distances from ground tracking sites, e.g., photography of vehicle reentry. Two difficult requirements here, however, would be the maintenance of accurate time correlation with ground tracking sites, and the continuous knowledge of accurate aircraft position. The first requirement might be met with an onboard atomic clock synchronized with base clocks before takeoff, and the second through

use of either an accurate onboard inertial or stellar-inertial navigation system or transmission to the aircraft of position as determined from ground-based electronic tracking systems, or a combination of both schemes. Alternatively, a TACAN-type navigation system could be used, as discussed in Appendix XXXVII.

- Electronic image recording. The use of magnetic tape recording and video camera techniques might solve a number of operational problems for engineering surveillance photography. For example, it is considered feasible to develope magnetic tape recording systems to replace the film in fixed cameras employed on and around the launch stand. These could be remotely erased and rewound in the event of premature startup. Another approach would be to substitute suitable TV cameras for the photographic cameras, transmitting the video by hardline or microwave links to central control for monitoring in real time and video recording. However, it should be emphasized that no systems of electronic image scanning and video recording have yet been devised that could provide image quality comparable to that of today's better engineering sequential cameras, e. g. , ROTI, IGOR, etc. See Table I for effective video upper cutoff frequencies of some of the popular engineering sequential cameras currently in use.

  Video recording systems, to date, have not been attainable with upper cutoff frequencies much above 14 mc for magnetic tape or 30 mc for thermoplastic tape (an order of magnitude, at least, below the effective upper cutoff frequency of the ROTI system). TV image scanning devices (photoelectric transducers), on the other hand, have been built with resolutions approaching those of 70-mm camera systems, e. g. , 2000 lines/frame. Scanning problems become serious, however, at reasonable frame rates with resolutions such as these, when a

Table I. Effective Video Upper Cutoff Frequencies of Typical Nonmetric Cameras (1) (3)

Format	Frame Rate (N) Frames/sec	No. Lines Per Frame (n)	Video Bandwidth (f_c) Mc
70 mm film (2-1/4 x 2-1/2 in.) ROTI or IGOR with 70 mm camera	60 (max)	4000	340
35 mm film, double frame 36.3 x 24.5 mm), Cinetheodolite K[th] 53	5 (max)	1715	7.68
35 mm film, single frame (22.0 x 16.0 mm), IGOR with 35 mm Mitchell	60 (max)	1120	36.8
16 mm film (10.26 x 7.49 mm)	24 (sound)	524	3.2[(2)]
16 mm film (10.26 x 7.49 mm) Fastax, etc.	2500	524	33.3
8 mm film (4.88 x 3.68 mm)	16	275	0.5675

Notes:

(1) Based on $f_c = (w/h)n^2N/2\sqrt{2}$ where W/h = aspect ratio (i.e., W = width, h = height); n = no. lines per frame = (lens/film resolution) x h; lens/film resolution = 70 lines/mm, assumed herein. See Morton and Zworykin, Television, John Wiley & Sons, New York, 1954.

(2) Bandwidth most closely equivalent to that of the present NTSC, 525 line, 30 fps TV standard.

(3) f_c's for the equivalent formats in color could range all the way from 3 x f_c (black and white) for a three-color equal bandwidth system to scarcely more than 1 x f_c (black and white) for a three-color, mixed-highs system with color subcarrier frequency interlacing.

high degree of sweep linearity is required with good reproducability and stability. High sensitivity is also a requirement.

Considerable effort is underway to produce a high-resolution, high-sensitivity solid-state photosensitive mosaic image-sensing device that would not require

scanning in the usual sense, but would produce a continuous matrix-type output as a function of elemental image brightness. Published estimates have placed achievement of useful devices such as these at 5 to 10 years in the future. The advantages of the solid-state image sensor include real-time data readout capability, reduction of information redundancy, and higher reliability.

- Remote control tracking equipment. To solve the problem of larger danger zones with larger thrust boosters, means must be provided for remotely operating the short and intermediate range cameras which are located within the danger zone. This can be accomplished by use of remotely controlled tracking mounts using TV sighting systems or master-slave controls. The current state of the art in TV and servomechanisms is believed to be adequate for most of these tasks.

E. LASERS IN RANGE INSTRUMENTATION

1. INTRODUCTION

The purpose of this section is to assess the possible utility of lasers as a part of the 1965 to 1970 global test range. This involves answers to questions such as:

To what areas of range instrumentation might lasers be applied?

What are the theoretical advantages of lasers versus other types of instrumentation?

What are the theoretical limitations of lasers versus other types of instrumentation?

What are the practical limitations of lasers with the present state of the art?

What are the prospects for overcoming the present limitations as a result of advances in the state of the laser art?

The laser is a device which ideally produces coherent light waves at a discrete frequency. All other light sources emit either broad continuous spectra or multiple-line spectra with broad lines having a band of frequencies rather than single frequencies.

Coherent light waves may be treated similarly to other coherent electromagnetic waves of lower frequency and, therefore, many techniques of electronic communications may be used. These include modulation, mixing or translation of frequency, frequency multiplication, demodulation, correlation, reflection, refraction, etc. However, the frequencies of light waves are of the order of 10^{14} to 10^{15} cps, some 10^4 to 10^5 times higher than present microwave frequencies. Optical techniques may be used for beam formation and transmission, but tolerances consistent with the wavelength must be met in order to benefit from the coherent property of the light.

2. RANGE INSTRUMENTATION APPLICATIONS

a. Tracking

Tracking is one broad area of range instrumentation to which lasers might be applied. All the functions performed by radar trackers and some performed only by optical instrumentation (e. g. , external attitude determination) are theoretically possible using coherent light waves instead of radio waves to illuminate the target. However, only range and angle measurement using high power pulses and low-power CW amplitude-modulating techniques are practical, at present. This is due to the fact that amplitude modulation is the simplest form of modulation to generate and detect. For example, Hughes Aircraft proposed and demonstrated feasibility of a range-only optical radar (Colidar Coherent Light Radar). It consists of the following elements:

Optical transmitter. (Laser operating in a pulsed reflector mode controlled by a Kerr cell.) Coherent light pulses have a peak power of 600 kw, pulse width of 0. 12 μsec, and rise time of 40 nsec. (Equivalent to transmitter and feed of pulsed radar)

Transmitting optics for spreading or concentrating the laser beam. (Equivalent to radar antenna)

Receiving optics for collecting returned light waves in a narrow frequency band centered at the laser output frequency. (Equivalent to receiving antenna and feed of radar)

Photomultiplier tube to convert the returned light pulses into an electrical signal. At present, the best available light detector appears to be the photomultiplier tube with S20 photo cathode. (Equivalent to antenna feed, preamp, and receiver, through video detector, of pulse radar)

Signal processing circuitry for extracting range, including a standard frequency generator, counter, PRF generator, counter and laser controls, and digital readout. (Equivalent and similar to range measurement circuitry of pulse radar)

Figure 1 shows operating range as a function of peak power, visibility, and beamwidth.

Angle tracking is readily obtained by any of the methods used in angle tracking radar, such as conical scan, nutation, or simultaneous lobing. The receiver must be capable of producing appropriate signals which measure the magnitude and direction of the deviation of the received target image from a reference position on the photo-sensitive surface. For example, the optical equivalent of a simultaneous lobing system would consist of dividing the field of view into four quadrants, each illuminating a separate photocathode. The four photocathode-output signals would be combined in difference circuits to produce the azimuth and elevation error signals. The four photocathode signals would be summed to produce the return pulse for the range system.

RCA is developing an optical tracking radar expected to be able to track the S-66 satellite scheduled for launch into a 600-nmi orbit during 1963 by NASA. According to RCA, the transmitter, using a crystal of neodymium-activated calcium tungstate, is expected to reach a peak power of 10 megw with a 1-μsec pulse length and a maximum pulse repetition frequency of 1000/sec. The

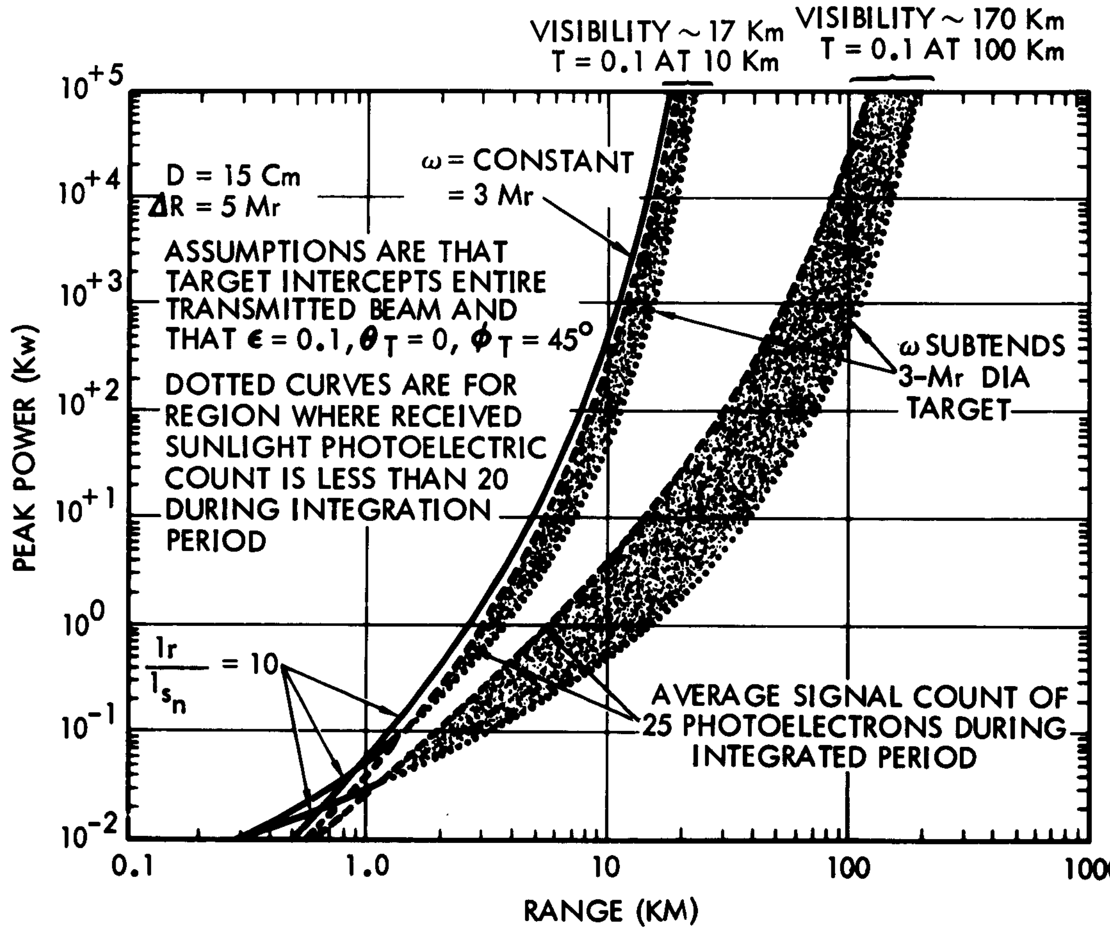

Figure 1. Required Power Versus Range For a Colidar Systems

transmitting optics will consist of a lens to focus the light into a beam expected to have a spread of about 0.5 mrad.

A separate receiving optical system with a 20-in. diameter aperture will be used. The S-66 satellite will be equipped with 35 in.^{2} of corner reflectors in order to return sufficient power for accurate tracking. Design objectives are range accuracy of 6 ft and angular accuracy of 0.02 mrad.

The Cloudcroft Satellite Surveillance System, under development jointly by Technical Research Group, Syosset, N. Y., and American Astrophysics, Monrovia, Calif., under USAF Aeronautical Systems Division contracts, is being designed to track targets as small as 10 ft^2 in area at ranges of up to 100 mi, with a beam dispersion of only 300 ft^2 at that distance. A 48-in. tracking telescope and a pair of 15-in. auxiliary visual acquisition telescopes will be mounted on a precision tracking mount.

Perkin Elmer has designed a precision laser tracking system for AMR intended for real-time readout of position accurate to 0.05 ft from 0 to 500 ft altitude, 0.2 ft from 500 to 5,000 ft, 2 ft from 5,000 to 50,000 ft; velocity accurate to 0.02 ft/sec from 0 to 500 ft, 0.2 ft/sec from 500 to 5,000 ft, 0.5 ft/sec from 5,000 to 50,000 ft; and acceleration accurate to 0.01 ft/sec^2 from 500 to 5,000 ft. The optical tracker uses a gas laser which produces a CW output at 6328 Å, with 100-mc amplitude modulation for ranging. The system configuration consists of multiple optical trackers distributed around the launch area, and a computing system to derive position, velocity, and acceleration using data from one or more of the optical trackers. The mount is designed for an accuracy of 2 arc-sec. The design is now being evaluated by the Air Force.

b. Communications

Communication is another broad area of range instrumentation to which lasers might be applied. As in the case of tracking, many companies are engaged in research in some aspect of laser communication techniques. Bell Telephone Laboratories are conducting performance studies on laser-generated light beams in underground pipes as the carrier for telephone communications. General Electric is reported to be

working on a closed-circuit light carrier TV system with a range of 10 miles. Light carrier systems have been proposed as the ground-to-satellite link for a communications satellite system. Douglas Aircraft has demonstrated that red light (6943 Å) from a ruby laser can penetrate reentry plasmas.

3. THEORETICAL ADVANTAGES OF LASERS FOR RANGE INSTRUMENTATION

The theoretical advantages of lasers for range instrumentation derive from the coherence of the light. Coherence makes it possible to obtain extremely high directivity with small optical elements. Since coherent light obeys the same laws as lower frequency electromagnetic waves, focusing is determined by the ratio of the wavelength to the diameter of the aperture, or

$$\theta \simeq \frac{\lambda}{D} \text{ rad}$$

where θ is the 6-db beamwidth, λ and D are in the same units. For visible light λ is 4×10^{-5} to 7×10^{-5} cm, so that the beamwidth is 40 to 70 μrad for a 1-cm aperture. High directivity also means high power gain in the beam:

$$\text{gain} \simeq 20\ A/\lambda^2$$

where A is the aperture area and λ is the wavelength. The theoretical power gain advantage of visible light versus present microwaves, for a given aperture area is greater than 80 db.

Signal-to-noise ratio also improves in optical transmission, for a given aperture size, since the received power increases with the square of the frequency, while the noise due to photon fluctuations increases directly with the carrier frequency; a S/N improvement of about 40 db for visible light versus present microwaves should be attainable.

Extremely wide information bandwidth is another theoretical advantage of coherent light. Even if only one percent of the carrier frequency of visible light is achieved as the modulation bandwidth, it represents a bandwidth of 4 to 7×10^6 mc/sec. This would make available an almost unlimited number of communications channels carried on a single beam.

The use of light waves is advantageous for tracking, when maximum accuracy is desired, because corrections for the index of refraction of the atmosphere can be made more exactly for the light waves than for microwaves, since the index of refraction is much smaller and is much less variable for light waves than for microwaves. This results from the fact that the index of refraction is only slightly dependent upon atmospheric water vapor for light waves, while it is strongly dependent upon water vapor for microwaves. Through the use of a subcarrier of microwave frequency, the same resolution is available without the additional tropospheric refraction error.

4. THEORETICAL DISADVANTAGES OF LASERS FOR RANGE INSTRUMENTATION

Although high directivity improves power gain and S/N ratio, the extremely narrow beam theoretically possible with coherent light requires a corresponding increase in the accuracy of pointing of the beam. The acquisition problem is even worse, since acquisition depends upon the cross-sectional area of the beam. The time required to cover a given area, by scanning the area at a given rate of scan, increases as the square of the frequency, some 10^8 times as long for visible light as for microwaves. It is obvious that acquisition aids are required, particularly if the transmitter and receiver are in relative motion. The acquisition aids might involve beam spreading, use of auxiliary microwave equipment, or passive IR or UV detectors to point the optical beam during acquisition.

In either case, acquisition becomes one limitation of the system, since the acquisition range threshold is determined either by the auxiliary microwave receiving equipment, or by the threshold of the optical system with the spread beam. Thus, if beam spread is used for acquisition, the acquisition range decreases inversely with the beam spreading factor, unless the transmitter power is increased to maintain the same power density in the spread beam, or the target dwell time is increased.

For reasonable acquisition time, the beam would require spreading from a few microradians to approximately 20 mrad, a factor of several thousand. The increase in power necessary to maintain the same range with the spread beam as with the narrow beam is of the order of several

million. Since it is unlikely that power output increases of that order of magnitude are possible, beam spreading will limit the maximum useful range.

Light transmission through the atmosphere suffers from attenuation due to absorption by gas molecules and scattering by dust particles and water droplets in fog, clouds and precipitation, although these effects can be minimized to a certain extent in the IR region.

5. PRACTICAL LIMITATIONS WITH PRESENT STATE OF THE ART

Atmospheric attenuation is a serious limitation on the use of lasers for range instrumentation if all weather capabilities are required. Even over relatively short distances, transmission could be blacked out by clouds so that range use for ground instrumentation would be possible only in clear weather.

Extraneous light causes another problem in optical transmission systems. Sunlight and ambient and back-scattered light cause external noise. Rejection of extraneous light is presently limited by the sharpest available optical band pass filters which have band widths of about 10^5 mc. The noise bandwidth is therefore four to six orders of magnitude larger than presently realizable information bandwidths, permitting significant amounts of noise to reach the detector even with extraneous wideband light brightness several orders of magnitude below laser brightness. In addition, internal noise is caused by dark current, and shot and flicker noise in the detector.

Present precision small-to-medium size antenna mounts have a pointing accuracy of about 0.05 mrad. In order to achieve or even approach the directivities and power gains theoretically possible, tolerances of the optical systems mounts and servos would have to be improved by about four orders of magnitude. This is certainly impractical at present, and pointing accuracy is now, and will remain for some time, a limitation on the narrowest light beam which may be used.

The efficiency of the overall conversion of energy in producing coherent light waves is another limitation in the use of lasers for spacecraft use. If modulation is involved, the power required for modulation must be included in the power input, further decreasing the efficiency.

Until recently, the efficiencies of lasers were so low (0.03 percent) that use in spacecraft would be impractical because of the large power sources required. Even with predicted improvements to about 5-percent efficiency, light-pumped lasers would still be impractical compared to present lower frequency equipment with efficiencies of about 50 percent. Development of electrically pumped lasers capable of efficiencies approaching 100 percent, during the last year, promises to overcome this limitation. Also under investigation are solar-pumped and radioisotope-pumped lasers. The latter schemes would be particularly advantageous for space work.

6. PROBLEMS OF PRESENT LASERS

The laser is essentially a fixed-frequency device whose frequency is determined by its energy levels. The emitted frequency is dependent upon doping, for ruby and other crystalline materials. Laser frequencies are affected by temperature. Ruby, for example, has a frequency temperature coefficient of about 0.001 percent/C^o.

Present lasers are only quasicoherent in their output. CW types, using a mixture of gases, such as helium and neon, have line widths reported from a fraction of a cps to several kc. However, they suffer badly from microphonics, producing frequency fluctuations of hundreds of kc when mechanically disturbed. Output powers are low, typically in the 1- to 50-mw range.

Crystal lasers, operated in the pulsed mode, achieve peak powers in the megawatt range, for fractional microsecond width pulses, but suffer badly from multimoding, with frequency differences as large as several hundred mc.

7. PROSPECTS FOR OVERCOMING PRESENT LIMITATIONS

The prospects for overcoming some of the limitations of present lasers are very good, since they are largely dependent upon materials and mechanical design.

During the last year, electrically pumped junction semiconductor materials have been discovered to lase, with energy conversion approaching 100 percent. Total power, however, is very low, in the microwatt

range. Further development of these lasers might make spacecraft use of lasers practical if suitable means can be devised to produce the required low temperatures ($4^{\circ}K$), or if lasers can be found that will operate at spacecraft ambient. With development of better lasers and modulation components, optical mixing may permit frequency translation to lower frequencies where electrical filtering may be used to improve the rejection of noise due to extraneous light if problems of doppler shifts can be solved. The limitations of acquisition and pointing accuracy might be overcome through development of electro-optical or combined electromechanical and electro-optical methods of beam steering capable of extremely rapid scanning and required accuracy.

Research is necessary to obtain more information about atmospheric attenuation. With present knowledge, it does not appear that the prospects are good for overcoming atmospheric attenuation, particularly through clouds.

8. CONCLUSIONS

With the present state of the art there are a few promising applications of lasers in range instrumentation for the 1965 to 1970 era. One of the most promising is early launch tracking. The limitations previously discussed do not apply under launch conditions. Test launches usually take place in clear weather, since visibility is required for photographic purposes. Over the short distances involved in early-launch tracking, the beam may be spread sufficiently so that the pointing and acquisition problem may be overcome.

With advances in the state of the art in lasers, particularly in efficiency, modulation-demodulation methods, and beam-pointing accuracy, continuous transmission of information through the reentry plasma may be possible, and satellite-to-satellite communication links may become feasible for data and information transmission, if multiple satellite systems become a part of the test environment. It is unlikely, however, that the latter will take place in time to be of service during the 1965 to 1970 era.

BIBLIOGRAPHY

A. J. Brandenberger, "The Use of Baker-Nunn Cameras for Tracking of Artifical Satellites," Photogrammetric Engineering, Vol 28, November 1962.

"Space Trajectories," Academic Press, 1960, p 271.

Appendix IX. INSTRUMENTATION FOR VEHICLE ATTITUDE MEASUREMENT

1. INTRODUCTION

The purpose of this appendix is to examine the instrumentation to be employed for vehicle attitude measurement during the 1965 to 1970 period. The basic question is the extent to which "exotic" attitude measuring instrumentation will be available for range use during this period. "Exotic" refers to systems and devices essentially distinct from the conventional noncoherent optical techniques currently employed. These conventional techniques make use of such instrumentation as theodolites and tracking telescopes to determine attitude from photographic records of the vehicle, together with records of the direction in which the tracking instruments were pointing at the time the photographs were made. The accuracies attainable with these conventional techniques are typically on the order of from one to a few degrees, which is sufficient for most current applications.

As with almost any other type of measurement, attitude measurement accuracies greater than those attained with current techniques would be desirable, though they are, for the most part, not mandatory. It is therefore appropriate to discuss briefly some of the means which might be employed for improved attitude measurement accuracies, and to evaluate the feasibility of employing these techniques during the 1965 to 1970 period.

2. BASIC RF ATTITUDE MEASUREMENT TECHNIQUES

It is clearly possible, in principle, to employ RF techniques for vehicle attitude determination. One method measures the normal to the wavefront arriving at the vehicle from a ground-based transmitter by means of monopulse or conical scan techniques, and also measures the polarization of the received signal. These data are then relayed to the ground via telemetry. A second RF technique employs an interferometer-type antenna array on the vehicle and suitable data processing equipment to determine the direction of arrival of a signal from a ground transmitting station relative to the vehicle frame of reference. Here, as previously, the resultant data is telemetered to the ground.* In either case, it is

* See Paragraph 3. below for a description of a preferred variant of this technique, in which the direction of transmission is reversed.

assumed that the vehicle is tracked by external instrumentation, so that the direction of the ray arriving at the vehicle from the ground station associated with the attitude determining system is known in the external coordinate system relative to which the vehicle attitude is to be determined.

Consider now the number of independent parameters which must be measured to determine the vehicle attitude relative to an external frame of reference. These parameters are pitch, yaw, and roll (or an alternative set of equivalent parameters). The first system described, which employs a monopulse or conical scan tracker and a radio polarimeter, measures a set of three independent angular-attitude parameters. This fact can be seen immediately by realizing that the establishment of the direction of the normal to the incident wavefront determines two angular parameters related to the vehicle attitude, while measurement of the polarization of the incident wave provides the third angular-attitude parameter. Here, of course, use must be made of the knowledge of the normal to the incident wavefront and the direction of the polarization vector within the wavefront in the external coordinate system. As indicated previously, this information is obtained from the external tracking data.

The situation is somewhat more complex as regards attitude determination from the measurements made by the vehicle-borne interferometer, which measures only the direction of the normal to the incident wavefront relative to the vehicle coordinate system. That is, only two independent angular parameters are measured. To obtain an additional independent angular parameter related to the vehicle attitude, it is necessary to employ a second ground transmitting station as part of the attitude measuring system. If the same vehicle-borne interferometer array is employed to determine the direction of the normal to this second incident wavefront relative to the vehicle frame of reference, two additional angular measurements related to the vehicle attitude are obtained, of which only one can be independent of the two angular measurements made on the signal received from the first ground station. In this case, the vehicle attitude is overdetermined by the addition of the second ground station. This fact causes no difficulty inasmuch as the data reduction process either can make use of a least-squares method to solve for the

best estimate of vehicle attitude employing all four angular measurements, or can ignore one of the measurements.* In general, preference would be given to the least-squares data reduction method because of the increased accuracy attainable with this method of data reduction.

The use of the same interferometer array on the vehicle for the simultaneous reception of signals from two ground transmitting stations requires that some means be employed to distinguish the signal received from one station from that received from another. The simplest method of distinguishing these signals would be to transmit on somewhat different frequencies and to separate these frequencies in the receiving system prior to data processing. Any method of effecting the separation of the signals received from the two ground stations implies a requirement for a dual-channel receiving system and duplication of the data extraction circuitry.

Although the techniques described above have been confined either to interferometric configurations or to configurations which measure the normal to the wavefront and the polarization of the received wave, the basic principles involved are somewhat more general and could be employed, for example, with a system which made use of modulation techniques instead. The interferometer system should be expected to yield considerably better attitude accuracies than the radio polarimeter system because of the difficulty of making an accurate polarization measurement with a radio polarimeter, and because of the accuracy deterioration caused by ionospheric effects. While ionospheric refraction will cause some error in the interferometer system, this error will usually be negligible at any reasonable carrier frequency; whereas, in the case of the radio polarimeter, the error caused by Faraday rotation of the polarization vector will be so large as to very seriously degrade the system accuracy unless the carrier frequency is well up in the microwave region. When due account is taken of these factors, it appears that the preferred RF technique would be the interferometric technique.

* It would be simpler not to make the redundant interferometer measurement, since it is necessary only to measure the angle of the normal to the incident wavefront relative to the baseline established by one pair of the three or more antenna elements which constitute the interferometer array.

3. A PREFERRED VARIANT OF THE RF ATTITUDE MEASUREMENT SYSTEM

The preceding discussion has assumed that the direction of transmission for the RF attitude measurement system is from ground to vehicle and that the resultant data, in either digital or analog form, are telemetered to the ground after extraction in the vehicle. While this technique is quite feasible, there are certain disadvantages associated with the necessity for performing the data extraction in the vehicle. In discussing these disadvantages, only the interferometric technique will be considered. To avoid the necessity for providing multiple receiving and data processing channels in the vehicle, it is only necessary to reverse the direction of transmission by transmitting from vehicle to ground through the individual elements of the vehicle-borne interferometer array, and by receiving and processing the data at the ground stations associated with the attitude measuring system. With this mode of operation, it is necessary to mark the signals transmitted from the individual vehicle antennas with some type of modulation so that the ground receiving stations can determine from which antenna of the vehicle interferometer array each signal was received. As a practical matter, this separation would normally be performed by transmitting at slightly different frequencies from each of the elements of the vehicle-borne interferometer array, and also by transmitting a reference signal which defined the frequencies and phases of the offset frequencies.* The vehicle implementation would make use of a number of phase-locked loops, which would permit the generation of distinct frequencies whose offsets from the nominal carrier frequency would be carefully controlled in frequency and phase.

While the reverse configuration described above has the disadvantage that it requires the transmission of separate signals from each of the elements of the vehicle interferometer array and, thus, necessitates both the synthesis of these signals and the use of a separate vehicle transmitter for each element of the vehicle interferometer array, the fact that the

* The frequency offset described is indeed a form of modulation scheme. In fact, it can be characterized as single sideband suppressed carrier modulation.

complete receiving, timing, and data extraction system can be confined to ground installations outweighs these disadvantages. Since the received interferometer phase data are carried on the beat frequencies between the signals received from different elements of the vehicle antenna array, together with the received reference frequency, the receiving system can be very tightly narrowbanded at its output. Accordingly, the vehicle transmitter powers can be quite small. For these reasons, it is probable that the interferometer configuration which employs vehicle-to-ground transmission would be preferred over the interferometer configuration described in Paragraph 2. above. An additional advantage of this reverse configuration is that it permits the use of an arbitrary number of ground receiving and data extraction stations, with the result that no handover problem exists as the vehicle moves downrange along its trajectory.

Even with the reverse configuration, which appears to offer some simplification in the vehicle equipment, it must be conceded that a fair amount of additional vehicle equipment is required for RF attitude measurement. This factor alone might prove decisive in the question of the use of this type of attitude determination system for a number of applications. However, the problems discussed below will prove much more decisive.

4. VEHICLE ANTENNA PROBLEMS AND THEIR IMPLICATIONS

While the preceding discussion has shown the feasibility of employing RF techniques for vehicle attitude determination, it has ignored one very significant factor, namely, the vehicle antenna problems implied by both of the RF techniques described. In either case, there is a very serious problem in the placement of suitable vehicle antennas. This problem is most apparent in a consideration of the fact that most vehicle attitude measurements by means of external instrumentation are required during powered flight. The requisite antenna structures cannot be mounted on the aft end of the vehicle (the obvious location) because of the placement of the rocket motors and the flame problems associated therewith. Accordingly, the antennas must be placed on other portions of the vehicle, virtually eliminating the possibility of employing anything except the simplest antennas.

These antenna problems would seem to rule out the possibility of employing a monopulse or conical scan receiving antenna mounted on the side of the vehicle because of the severe problems encountered with aerodynamic loading and heating during the vehicle's passage through the lower atmosphere. This antenna configuration was rejected in Paragraph 2 above because of the severe accuracy limitations of the system employing a radio polarimeter. Moreover, even if both of these criticisms are ignored, the mechanical problems associated with mounting a gimbaled dish on the side of a missile or booster vehicle, except possibly for certain very special applications, are prohibitive.

The arguments cited above appear to leave the interferometer configuration, which permits the use of extremely simple antennas, as the only remaining possibility for vehicle attitude measurement by RF techniques. Even here, however, suitable antenna placement poses major problems. It is, indeed, possible to employ flush-mounted slot antennas. On the other hand, it is extremely difficult, if not impossible, to place these antennas on the vehicle in such a fashion that a suitable line of sight will be available to all antennas simultaneously, without blocking by the vehicle itself and without the introduction of severe multipath problems caused by reflections from the vehicle. Any significant multipath would render the data obtained with this vehicle configuration completely invalid.

This brief examination indicates that the prospects of installing suitable vehicle antennas are not encouraging. Accordingly, the conclusion of this examination of RF attitude measuring techniques is that while such techniques are feasible in principle, they will not constitute a practical solution to the attitude measurement problem except possibly in very special cases (which do not include ballistic missiles or boosters for space vehicles). On the other hand, the techniques might prove useful in the case of satellite vehicles, in which considerably more latitude might exist concerning placement of the antennas, inasmuch as such vehicles are not so constrained by aerodynamic loading and thermal problems and would not introduce the additional problems of mounting the antenna structure in the presence of the rocket motors and the associated flame and flame attenuation.

Since there may well exist cases in which the RF attitude measuring techniques might prove practical and valuable, even though these cases are probably limited to satellite vehicles, it appears reasonable to plan for continued research on these techniques and their applications. At the same time, in planning a global test environment, heavy dependence should not be placed on the availability of such devices, nor should they be scheduled for implementation at any specific time. The research program should commence as a study program to determine the applicability of these techniques to various types of vehicles and missions. If the results of this study program are encouraging, a research program should be instituted to construct a system suitable for further evaluation. Only after adequate experimental confirmation has been obtained should plans be made for development of a system for range operations.

5. "EXOTIC" OPTICAL TECHNIQUES FOR ATTITUDE MEASUREMENT

When the entire antenna structure is sufficiently small that it can be suitably emplaced on the vehicle (preferably at a single location), the preceding arguments concerning the impracticability of installing suitable vehicle antennas are not valid. In the consideration of optical techniques, the situation described here applies. An optical system which determines the direction of arrival of an incident beam and its polarization should prove eminently practicable for attitude measurement, and the recent advent of coherent optical techniques appears to render this approach to the problem even more feasible. Alternatively, the advent of coherent optical techniques should also render feasible the use of the interferometric method for vehicle attitude determination. In either case, transmission would be from ground to vehicle. If the interferometric method were employed, it could be used for phase comparisons either directly on the optical carrier, or on a very high frequency microwave modulation imposed on the carrier. Although, even in the interferometric case, it presently appears preferable to transmit from ground to air, the system employing the reverse direction of transmission should be explored in greater detail in the future.

Despite the possibility of achieving extremely high attitude measurement accuracies by coherent optical techniques, they are subject to some very severe limitations, relative to RF techniques, in any

tracking application. One of the most serious of these limitations is the lack of an all-weather capability. This fact alone implies that the improved optical techniques described will not constitute a panacea to the vehicle attitude determination problem. In addition, as with optical tracking techniques generally, there exists a problem of achieving sufficient receiving cross section without requiring a beamwidth so narrow as to pose difficult or impossible acquisition and tracking problems. Then, too, there is the usual problem of achieving optical transmitter powers comparable to those which are readily achieved at radio frequencies. This is a particularly difficult problem if a coherent CW optical signal is required. Finally, the problem of assuring that the optical windows on the vehicle will not be distorted or obscured is significant in a number of applications, including ballistic missiles and launch vehicles. For example, coating could certainly be expected to occur with a silo-launched missile, such as Minuteman.

It can be concluded that work on optical techniques, particularly coherent optical techniques, for vehicle attitude determination should be continued, but that the basic limitations of optical techniques for tracking will continue to prove decisive for many applications. Nevertheless, R and D programs for the study of optical attitude measurement systems should be instituted and plans should be made for the development and incorporation of such systems when their operational capability is confirmed. Since these coherent optical attitude measurement systems will constitute an upgrading of the current optical attitude measurement capabilities, and will not solve the fundamental problems associated with the use of optical techniques in tracking applications, the situation will not be catastrophic in case these systems should not become available in reliable operational form. Therefore, although it seems feasible to tentatively plan for their incorporation, it will also be desirable to maintain the present optical attitude measuring capability by means of theodolites, tracking telescopes, and similar conventional techniques.

Mention should be made of the possibility of measuring vehicle attitude by the use of star trackers. This technique is certainly feasible, but has a number of the problems described earlier for optical techniques in general. In addition, it requires relatively sophisticated equipment on

board the vehicle. In general, for use during the launch phase, it is considerably less attractive than the "exotic" attitude measuring techniques.

6. INERTIAL TECHNIQUES FOR ATTITUDE MEASUREMENTS

In view of the foregoing discussion, it does not appear that any of the "exotic" attitude measurement techniques described will permit a significant increase of our attitude measuring capabilities, at least for general range use. While some of these techniques may prove very useful in special cases and for special vehicles, they will, in general, not prove applicable to the problem of vehicle attitude determination for the work-horse vehicles (ballistic missiles and space vehicle boosters). The only technique which appears to show any promise for improved attitude measurement for these applications is that of attitude measurement by inertial means. When an inertial guidance system is included as a part of the vehicle, the attitude data available from this system can be telemetered. In those cases in which a suitable inertial guidance system is not available, or in backup attitude measurements, an auxiliary inertial system could be employed. This system would be very crude compared to a precision inertial guidance system. But even a relatively crude inertial platform should provide data far in excess of foreseeable requirements for vehicle attitude measurement. It should also be observed that the inertial attitude measuring system has an outstanding advantage, relative to the optical systems, in that it has an all-weather capability. While the addition of such a platform to a vehicle would constitute an additional item of expense and would add a certain amount of size and weight, these factors might be made quite small by employing a system developed specifically for attitude measurement. That is, the system should be designed only to the required tolerances, rather than to the specifications typical for an inertial guidance system. An inertial system developed solely for attitude measurement need not have a specification for very low drift over long time periods; since once injection into orbit (either a parking orbit or a final orbit) has been achieved, the task of attitude determination may be taken over by star and horizon sensors.

A study should be made to determine the availability of systems suitable for the use here proposed. In the eventuality that such systems are not available with reasonable size, weight, and power requirements, and at reasonable costs, a design study should be carried out to determine funding and lead-time requirements to develop such a system. Institution of a development program should await a clearly defined user requirement.

Appendix X. TIME SYNCHRONIZATION BETWEEN WIDELY SEPARATED POINTS

1. INTRODUCTION

Markowitz has pointed out that there are two basic aspects of time-keeping: determination of epoch and determination of the unit or interval (Reference 1). Whereas epoch specifies when an event occurred, the time unit is concerned with time interval and is independent of when the time interval occurs.

Three basic types of epoch time are published by the United States Naval Observatory. These times are based upon:

- The rotation of the earth about its axis
- The revolution of the moon around the earth
- The natural resonance phenomenon of the atoms in cesium gas.

The Naval Observatory communicates seven kinds of time to the various users. There are three kinds of universal time (UT0, UT1, and UT2), two kinds of sidereal time (true sidereal and mean sidereal), ephemeris time, and atomic (A1) time. Universal time is based upon the rotation of the earth and is closely related to mean solar time. UT0 is uncorrected universal time; UT1 is universal time corrected for observed polar motion; and UT2 is universal time corrected for polar motion and for extrapolated seasonal variation in speed of rotation of the earth. Sidereal time is also derived from the earth's rotation, but is based upon the earth's rotation with respect to the vernal equinox. Ephemeris time is based upon the moon's revolution about the earth. Atomic time is derived from the atomic resonance phenomenon.

The systems described in this appendix will generally be based upon UT2 time, since this will convenience the largest number of users. For range use only, any time base would suffice.

In a global test environment and in most other timing applications, the problem of interest is to set and maintain all clocks in the system in agreement with one another to a certain desired precision. The more precise the agreement must be between clocks in the system, the more

difficult the problem; and inasmuch as some of the clocks must be in widely separated locations to be useful in a global test environment, the problem is compounded.

Morgan has proposed the following three methods as solutions to the problem of time synchronization of widely separated clocks (Reference 2):

- Transportation of a master clock to each location where synchronization is desired
- Two-way transmission of radio signals between a master clock and the slave clock or clocks
- One-way transmission of radio signals from a master clock to the slave clock or clocks.

Method 1 would require almost continuous scheduled flying of the standard to service all the sites. Synchronization more than once a day would probably not be feasible, and a special trip with the standard would be necessary in case of a failure which interrupted a local clock. In general, it does not seem practical to synchronize many clocks to fractional millisecond accuracy. All the systems described in this appendix basically involve one-way transmission of radio signals from a master clock to a local clock or clocks (Method 3), although (as described later for the satellite system) Method 2 may be useful in a special application, such as removal of transit time. This study concerns itself with three probable systems, using Methods 2 or 3, for attaining time synchronization over a major part of the free world in the 1965 to 1970 period. These are current systems (primarily VLF radio), current and proposed LORAN-C chains for timing use, and a possible satellite system.*

2. SYSTEMS FOR GLOBAL TIME SYNCHRONIZATION

a. Current Systems

At the present time, HF radio, WWV (Beltsville, Maryland, 2.5, 5, 10, 15, 20, 25 mc) and WWVH (Maui, Hawaii, 5, 10, 15 mc) and VLF radio NBA (Summit, Canal Zone, 18 kc) and GBR (Rugby, England, 16 kc) are available for time synchronization use on a semiglobal basis.

* The discussion of advantages and disadvantages of both the VLF and LORAN-C systems was taken primarily from the IRIG study (Reference 3).

WWVL (Fort Collins, Colorado, 20 kc) is expected to be operational in the early part of 1963. For fractional millisecond synchronization on a global basis, VLF appears feasible.* The stability of VLF propagation, compared to HF propagation, and the need for long-range coverage for time synchronization use indicates that a VLF system is preferable to HF radio (HF timing accuracies are, at best, ±1 msec). Therefore, only VLF systems will be considered here.

1. VLF CW Systems

When a VLF CW signal is received at a point on the earth some distance from an earth-based transmitter, the signal consists of a contribution due to the groundwave and contributions due to the various skywave modes. In such a CW system, the range is extremely limited (only a few hundred miles) where the ratio of groundwave to skywave is large enough to attain accuracies approaching those inherent in a pulse system.

2. VLF Pulse Systems

In a pulse system, however, it is possible to resolve the various transmission modes and measure their phase separately. Figure 1 depicts ground wave resolution. Since variation in propagation time for the groundwave mode is considerably less than for skywave modes (random ionospheric variations have very little effect on the propagation time of the groundwave mode), it is desirable to select the groundwave portion of the signal as the reference for either frequency or time.

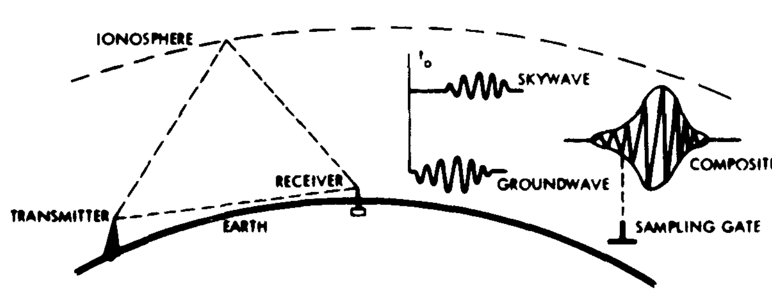

Figure 1. Groundwave Resolution

* For limited geographical areas, direct cable is also used. Timing synchronization along AMR is maintained to ±50 μsec at those sites connected to the submarine cable.

(a) Use as Time or Frequency Synchronization. The VLF system for time or frequency synchronization (NBA, GBR, WWVL) employs a relatively slow-rising pulse (when not being used for communications) every second on the second. The transmitted pulse is approximately 0.3 sec in duration and has a rise time of approximately 15 msec. Once each 15 min, a station programmer inserts the station call letters in international Morse code. The 29th, 56th, 57th, 58th, and 59th second pulses of each minute are omitted. During the last 5 min of each hour, the second pulses from 51 to 55 are omitted to identify the minute. The basic principle is that it is possible to estimate the time required for VLF pulse bursts to propagate over the surface of the earth to an accuracy of from 5 to 10 μsec. Once the local clock is set to agree with the master standard, the local timing oscillator can be slaved (phase-lock loop) to the VLF timing signals from a master station, thus providing continuous synchronization.

(b) Accuracy. In the VLF band, antenna-bandwidth limitations and antenna-detuning problems limit the shape and rise time of the transmitted pulse and, hence, the system accuracy. The slow rise time of the transmitted pulse makes determination of the pulse beginning difficult. This is the major limitation on the accuracy of the system. Currently, real-time system accuracy from 500 μsec to 1 msec is realizable; it is not anticipated that the probable eventual accuracy will be much better than ±50 μsec (Reference 3). Obviously, periods of sunrise and sunset effects (periods of extreme phase instability) should be excluded. The sunrise and sunset periods of instability are approximately half an hour for each ionospheric reflection point involved.

(c) Advantages. The advantages of the VLF pulse system are as follows:

- Essentially world-wide timing coverage can be provided by existing transmitter over at least part of each day.
- Relatively inexpensive equipment is required at each receiving station ($2500 to $4500 per timing receiver).
- Synchronizing signals occur at 1-pps rate during

periods when communications are not being handled.

- The duty cycle of the transmitted pulse (30 percent) simplifies the task of phase measurements.

- Good and predictable phase stability exists in spite of skywave contamination effects.

- Phase-locking of slave to master provides continuous time synchronization.

(d) Disadvantages. The disadvantages of the VLF pulse system are as follows:

- Slow rise time of transmitted pulse (approximately 15 msec)makes determination of pulse beginning difficult (probably in range 100 to 500 μsec).

- Due to slow pulse rise times, all usable portions of the transmitted pulse suffer from skywave contamination.

- At present, NBA transmissions are interrupted to handle communications (interruptions are infrequent; NBA is part of a Navy emergency communications net).

b. Current and Proposed LORAN-C Chains

LORAN-C is a pulse navigation system which uses a carrier frequency of 100 kc. A LORAN-C chain consists of a master station and two or more slave stations. For navigation purposes, synchronized pulse transmissions from a master-slave pair of stations generate hyperbolic lines of position which are loci of points of constant time difference. Transmissions from two pairs of stations (generally the master station is common to each pair) generate a set of hyperbolic grids. Receivers measure time difference of arrival of the pulses from each pair and obtain a fix on these grids. This navigation system utilizes techniques for selecting a given cycle and a point on that cycle; thus, this navigation system satisfies the requirements for a precision time synchronization system. At the present time, five localized LORAN-C chains are in operation: East Coast, North Atlantic, Mediterranean, Aleutians, and Hawaii.

Each station of the current LORAN-C chain transmits a group of eight pulses (the master station has a ninth pulse for identification) with

a uniform spacing between pulses of 1 msec. Each pulse has a rise time of approximately 70 μsec and a duration of approximately 160 μsec. These pulse groups time-share the group repetition interval, and the spacings between pulse groups are known constants for any particular chain. (See Figure 2.)

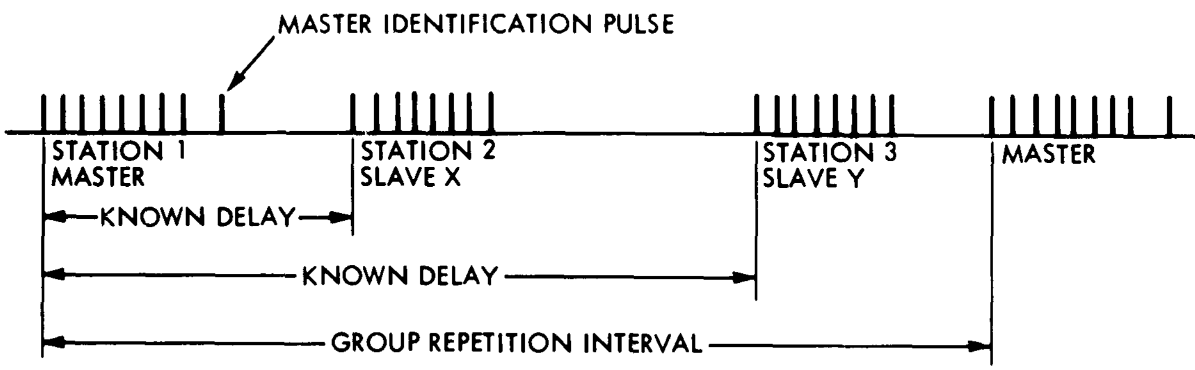

Figure 2. LORAN-C Time-Sharing of Group Repetition Intervals

For example, the East Coast chain has a group repetition rate of 20 pps and, hence, a group repetition interval of 50 msec. When LORAN-C is used as a time synchronization system, a signal from only one station is sufficient, since the time relationship of pulse groups within a group repetition interval is known.

For timing purposes, it is essential that the location of the receiver be known, since the transmission time between the transmitter and the receiver must be determined independently. Propagation delay calculation (and therefore timing accuracy) is directly dependent upon relative position accuracy. If the relative position accuracy is within 1000 ft, then the best attainable timing accuracy is approximately 1 μsec; 10,000 ft, 10 μsec; etc. It has been shown (References 4, 5, 6) that groundwave propagation times can be calculated to an accuracy between 0.1 and 1.0 μsec, and it has been estimated that skywave propagation times can be calculated to an accuracy better than 10 μsec. The inaccuracy in the computation of transmission times is the major error in the system and is due primarily to uncertainties in the conductivity and dielectric constant of the earth and the refractive index of the medium. Synchronization via groundwave LORAN-C reception is obviously preferable and groundwave coverage from any particular station is possible within a radius of some 1500 mi over land and 2000 mi over sea water.

There is little doubt, however, that LORAN-C clocks may be synchronized with skywaves (References 4, 5) to within 10 μsec.

A slaved LORAN-C clock has been developed by NBS (References 5, 6, 7) and consists of four major functional components: a timing receiver, local oscillator, clock divider, and readout register and display. The receiver uses sampling techniques to separate the first signal (groundwave if within groundwave coverage) from subsequent skywave signals. Synchronous detection techniques discriminate against nonsynchronous noise, and frequency and phase of the local oscillator are phase-locked to that of the transmitter oscillator. Thus, an inexpensive local oscillator may be used since it is continuously (from a sampled data point of view) synchronized with the transmitter oscillator and the slaved clock is constrained to run at a rate controlled by the LORAN-C master transmitter. The clock divider consists of 15 trochoidal beam-switching tubes acting as decimal counters. The first tube operates at 1 mc, the second at 100 kc, and so on, to the 15th, which operates once every several hundred days. Carry outputs trigger bistable multivibrators which drive the following beam-switching tube. An additional input to the bistable multivibrator provides the capability of adding counts to each decade as an aid in setting the clock. The seconds and minutes counters automatically reset to zero on their 60th count. The hours counters are arranged to reset to zero on their 24th count. Upon command, the readout system will display visually the time from 1 μsec to 1000 days. To resolve ambiguity on initially setting the clock, a seconds pulse from WWV (or equivalent source) is used as a read command to set the clock within 10 msec. Then a pulse derived from the LORAN-C receiver is used to set the clock to within 1 μsec (groundwave). (See Figure 3.)

1. Proposed LORAN-C Timing System

Interchain timing synchronization (monitored by the United States Frequency Standard (USFS) at Boulder, Colorado, for instance) would provide timing coverage for most of the world using both groundwave and skywave signals. It has been proposed (Reference 3) that establishment of a LORAN-C station between Boulder, Colorado and the East Coast and another station in the Southwestern United States would provide groundwave coverage for the entire continental United States. Similar techniques could be used to synchronize the remaining LORAN-C chains.

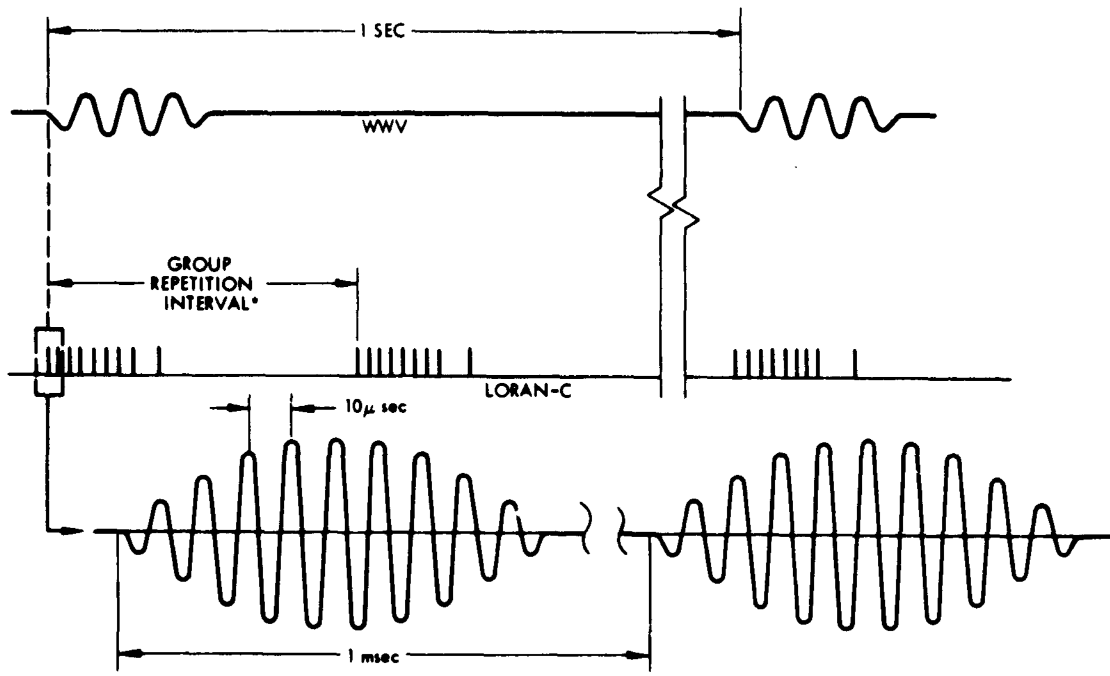

Figure 3. Synchronization of LORAN-C with WWV Time Signal

(a) Advantages. The advantages of the LORAN-C timing system are as follows:

- Fast pulse rise time (approximately 70 μsec) allows the signal to be detected before skywave contamination occurs for groundwave coverage to about 2000 mi.
- Sophisticated techniques, plus fast-pulse rise time, enable determination of a known point of the pulse to within 0. 1 μsec using existing techniques.
- For groundwave coverage, extremely good phase stability (less than 0. 1 μsec for pure groundwave condition) is possible.
- Essentially worldwide timing coverage could be integrated to provide worldwide navigation coverage from the same uninterrupted transmissions (accuracies: groundwave 1 μsec, skywave 10 μsec).

- After initial "set," local timing oscillator can be slaved (phase-locking) to the master oscillator to provide continuous time synchronization.

(b) Disadvantages. The disadvantages of the LORAN-C timing system are as follows:

- Groundwave coverage limited to approximately 2000 mi over the sea and 1500 mi over land.
- Complex signal codings due to a large variety of repetition rates result in costly timing receivers. (IRIG estimates $30,000 each without quantity requirement.)
- Limited groundwave coverage necessitates a large number of transmitter chains to make full use of the LORAN-C 1-μsec synchronization capabilities. (IRIG estimates approximately $500,000, plus building facilities per transmitting station.)
- Nonintegral repetition rates (e.g., 10.01001 . . . pps) cause unduly complicated operational problems to maintain time synchronization.

c. Possible Satellite Systems

It is certainly possible that, in the foreseeable future, systems requiring time synchronization to a precision at least two orders of magnitude greater than ±1 μsec will evolve. Examples of such possible systems are given in the following section.

1. Satellites with Active Relays

It is the purpose of this section to discuss a possible satellite system which it appears could maintain timing synchronization to an accuracy from 1 to 10 nsec. It is not intended that the system described should be construed to be optimum in any sense, but certain features do possess definite advantages over possible alternatives.

(a) Stability. It is important to realize that for this contemplated satellite system, continuous synchronization will not be possible. Therefore, it is imperative that a high-precision frequency

standard (probably an atomic oscillator) be employed at each ground station which requires 10 nsec accuracy.

Current research and development work is oriented toward developing atomic oscillators with a long-term stability of 1 part in 10^{14} per day. It is anticipated that in the 1965 to 1970 period, atomic oscillators with a long-term stability (averaged over a day) of 1 part in 10^{13} and a short-term stability on the order of 1 part in 10^{12} will be available. Several factors contribute to the accumulative timing error between two clocks, each controlled by an atomic oscillator of nominally identical frequency:

More-or-less constant frequency offset. Once this has been determined experimentally, an appropriate correction may be made since this would represent a linear drift with time (this would probably have to be checked periodically).

Short-term stability. It has been shown theoretically (Reference 8) that short-term, random, frequency deviations lead to a probable accumulative phase error increasing with time, even though the average frequency error over a long time approaches zero. This probable accumulative phase error increases proportional to the square root of the number of successive half-cycles of free-running operation. (This would constitute an estimate of a time-varying standard deviation of a probabilistic error distribution due to short-term, random frequency deviations.)

Long-term stability. For estimation of time errors, this is usually treated as a probable average drift rate per day.

It is not well understood at this time how to combine these effects for a precise estimate of time errors between calibrations. Further detailed study (partly experimental) is required. Typically, in the literature, a rough estimate is made using the long-term stability as

the basis for a calculation of an average drift rate per day. A more conservative approach (to determine gross feasibility) would be to use the short-term stability as the basis for calculating a probabilistic expected error rate. For a short-term stability of 1 part in 10^{12}, a probable linear error rate of approximately 90 nsec per day would be a conservative estimate. Calibration some 10 times a day would maintain time synchronization with the master clock within a probable ±10 nsec, on the average.

(b) Orbits. Selection of useful orbits and satellite placement within these orbits is complicated by the very large number of possible alternatives. A particularly attractive choice, for several reasons apparent from the discussion to follow, would be a number of satellites in synchronous (24-hour) equatorial orbits. Three such satellites, equally spaced, would provide line-of-sight coverage to a substantial portion of the world.

If the function of the satellite is to relay a radio timing signal from a master clock to a local clock, it is obvious that the transit time involved is many orders of magnitude greater than the desired timing tolerances. Measurement of the round-trip transit time, by means of a transmission from Station 1 to the satellite, to Station 2, back to the satellite, and back to Station 1, would provide a means for removing this transit time. In the case of the 24-hour equatorial satellite, this transit time is constant and the transmitted time would be advanced (at the master station) by exactly one-half of the round-trip transit time. Since the above argument invokes reciprocity, a few comments may be in order concerning nonreciprocal propagation effects in the contemplated frequency range. Two such effects briefly considered were nonstationary medium and Faraday rotation. A very rough calculation (1-gc CW signal) indicated that one could expect a phase uncertainty due to nonstationary medium on the order of a few electrical degrees which would be negligibly small. For CW signals at a frequency of 1 gc or greater, phase shift due to Faraday rotation is estimated to be less than an electrical degree. Design of the satellite transponder to achieve a delay stability of a few nanoseconds at most would be necessary. Note also the assumption that the slave transmitter and receiver pairs are matched to the master transmitter and receiver pair.

For a satellite in anything except a "stationary" orbit, it would be necessary in the transit time correction to account for changes in propagation path lengths, which occur during the correction process. For example, an uncertainty in path length of 10 ft would introduce a timing uncertainty of 10 nsec. Unfortunately, the relatively large range rates (with respect to the earth) of low- and medium-altitude satellites introduce an uncertainty in excess of 10 ft and thus do not appear practical for a 10-nsec system.

As the orbital altitude decreases, the line-of-sight coverage to the surface of the earth also decreases; a low-orbit or medium-orbit system would require placement of a larger number of satellites than are required for the synchronous (24-hour) system to achieve equivalent coverage.

The discussion to this point has emphasized satellites in equatorial 24-hour orbits. It is well known that, unless launched from a point on the equator, it would be more difficult (and would require larger boosters) to attain an equatorial 24-hour orbit than to attain an inclined 24-hour orbit (such as the 30-degree inclination for Syncom). The relatively low range-rates of such an inclined 24-hour orbit permit corrections for propagation path length changes (in the transit time removal described for the equatorial case) to an accuracy better than 10 nsec and, with such corrections, a system of satellites in 24-hour orbits inclined with respect to the equator would be feasible for global time synchronization to the desired accuracy.

As mentioned previously, to synchronize the system clocks to the desired accuracy, it would be necessary to calibrate each clock in the system (with respect to the master standard) several times a day. It is clearly an advantage to have a relay satellite in "view" every instant of the day (as would be the case for the synchronous satellite), since use of the satellite transponder would undoubtedly be time-shared with numerous ground stations. The time-sharing considerations would be considerably more stringent if time synchronization were a secondary function of the transponder aboard a communications satellite.

(c) Timing Coding. If the timing information were transmitted in the form of pulse bursts, the most severe limitation on the system accuracy would be the rise time and shape of the pulse envelope. To achieve pulse rise times sufficiently fast to assure that pulse beginning could be resolved to a few nanoseconds would require tremendous bandwidth and does not appear economically attractive.

A more attractive alternative is the transmission of timing signals in the form of a sequence of sinusoidal subcarriers. The ground station would produce a reference carrier plus sideband pairs obtained by phase modulation of the carrier frequency with several harmonically related sidetones. Both the carrier frequency and the subcarriers would be synthesized from the master frequency standard. Ambiguity-resolution possibly could be achieved by appropriate amplitude modulation of one of the subcarriers. Several advantages of this form of implementation are:

- The removal of transit time could be implemented very simply by phase shifters prior to transmission of the timing signals.
- Precision phase measurements to obtain desired timing accuracy can be made using a phase comparison technique.
- Small information bandwidth required.
- Stabilization of the time delays in the transmitting and receiving equipment to a few nanoseconds at most may be achieved by careful implementation of modulation feedback techniques such as have been employed successfully in certain precision CW tracking and guidance systems.

(d) Satellite Stabilization and Antenna Requirements. The system could be reasonably implemented using spin-stabilization of the satellite with the spin axis of the synchronous satellite aligned normal to the orbit plane in order to satisfy the satellite stabilization and antenna requirements. A linearly polarized dipole antenna, with the antenna pattern axis aligned with the spin axis, would provide effective coverage

that is relatively phase insensitive to the direction of the incoming signal. Phase uncertainty introduced by the satellite spin at 1 gc is anticipated to be on the order of 30 electrical degrees, at worst, which would cause a timing error much less than 1 nsec.

(e) Multipurpose Satellite System. The great expense in implementing a satellite system such as just described is probably not economically justified if the sole purpose of the system were to achieve the time synchronization function.

Incorporation of the time synchronization system as a secondary function on a synchronous communication satellite system (such as Syncom) seems an attractive solution. This could be accomplished either by including a separate transponder for time synchronization or by time-sharing the communication transponder. However, it should be noted that time-sharing the communication transponder would impose requirements on the transponder for timing use considerably more stringent than would have to be satisfied for communication only.

(f) Advantages. The advantages of the active ring satellite system are as follows:

- Potential time synchronization accuracy is at least two orders of magnitude better than any other system contemplated.
- Incorporation of time synchronization system as a secondary function of communication satellite system is possible.

(g) Disadvantages. The disadvantages of the active relay satellite system are as follows:

- Very large development and implementation expenses are involved, particularly if timing is the sole function obtained.
- A satellite failure would eliminate synchronization with the master standard over a large area for days, and possibly for weeks.

- Extensive problems would exist in the development of hardware to achieve system stabilities of a few nanoseconds.

2. Alternative Systems

At this time, an active relay satellite shows the most promise for a satellite system used as part of a precision time synchronization system. However, two alternative approaches are proposed, listing some of their major disadvantages, compared to the use of satellites as active relays.

(a) Satellites as Passive Relays. The disadvantages of this system are as follows:

- Imperfections in satellite (reflector) symmetry could cause multipath effects of sufficient magnitude to make desired accuracies unattainable.
- A passive satellite of practical size would require extremely powerful transmitters.
- The possibility of obtaining precision timing in conjunction with a relatively wideband communication satellite system is impractical for reasonable transmitter powers.

(b) Atomic Clocks in Satellites Transmitting Time Signals. The disadvantages of this system are as follows:

- It would still be desirable to synchronize satellite clocks with a master standard on the earth.
- Carrying an atomic clock, frequency synthesizer, timing receivers, timing transmitter, and so on, in the satellite would necessitate a satellite of considerable volume and large payload.

3. SYSTEM APPLICATIONS OF SATELLITE TIMING SYSTEMS

Since the preceding discussion has indicated the possibility of achieving worldwide time synchronization to an accuracy far exceeding

presently established requirements, it is appropriate to discuss the potential applications of this capability to problems of general interest.*

a. Tracking

A 1- to 10-nsec time synchronization capability opens up the possibility of designing a very long baseline (hundreds of miles) interferometer. The time synchronization system would serve the function of baseline synchronization, and a 10-nsec timing uncertainty would represent a 10-ft error in range sum (or range difference) measurement. With a baseline of 1700 nmi, this represents a worst-case angular error of 1 μrad. With sufficient care, range rate could be measured to 0.1 fps, resulting in an angular rate measurement of 0.01 μrad/sec. These measurements would be made using a CW signal, suitably modulated with ranging information, transmitted from a single station. The vehicle would utilize a single-channel, phase-locked transponder, and the remaining stations would operate in a passive reception mode only. Performance of the type indicated here represents a significant improvement over present-day interferometers without the problems of baseline synchronization by ground links.

b. Communication

1. Secure Communications Systems

Typically, these systems function by modulating the intelligence onto a very broadband carrier for transmission and by demodulating this carrier by means of a correlation process with a similar broadband reference carrier in the receiver. The receiver-reference waveform must be a locally generated model of the transmitted carrier which is properly phased with respect to this carrier as received. The output bandwidth of the correlator is made equal to the bandwidth of the intelligence transmitted. The broadband carrier modulation is essentially random (pseudorandom) in character, which means that, although it is basically causal, its structure is so complex that it is supposedly unknown to any hostile agency which might be interested in jamming the communications link.

* Not all of these applications are of major interest for range purposes.

Even if the receiver-reference frequency is identical to that of the received carrier, phase control is essential since the correlation time of a broadband signal is approximately equal to the reciprocal of its RF bandwidth occupancy. Accordingly, when RF bandwidths of many megacycles are employed, with correlation times of fractions of a microsecond, very accurate synchronization between the received carrier modulation and the locally generated reference modulation is required for successful signal demodulation.

<u>2.</u> <u>Nonsecure Digital Communications</u>

It is well known that a matched filter for a received binary digital waveform is an integrate-and-dump detector, i.e., one which integrates the received signal (at video) for the duration of one bit, makes a binary 0-1 decision, restores the output of the integrator to the null level, and repeats the process on the next bit. In order to successfully perform this operation, fairly accurate bit sync knowledge is required, usually about 1/10th of the bit length. A 10-nsec timing error would then permit "optimum" detection of a 10-megabit/sec signal. If the timing function were accomplished via a communication satellite, it would serve a very important role in the communication function itself.

<u>c.</u> <u>Aircraft Navigation</u>

An accurate time standard carried in an aircraft would permit implementation of a one-way TACAN navigation system, in which range and angle to the TACAN site would be passively measured in the aircraft. Position information could be derived to a few tens of feet. The advantages of this type of navigation are:

- The aircraft would not have to carry a transmitter.
- There would be no possibility of saturating the TACAN station, as is the case with the present two-way interrogating system.

It should be noted that, for an application of this type, the aircraft clock would be synchronized before take-off from the airport, and the standard would be maintained by an atomically stabilized oscillator acting as a flywheel.

d. Geodesy

An improved tracking system of the sort described in Paragraph 3.a. above, operating with satellites whose orbits are known to a high degree of precision, would permit improved accuracy in the knowledge of the tracking station's location.

4. CONCLUSIONS

Possible time synchronization over most of the world through 1965 to 1970 is summarized as follows:

System	Current	Possible 1-3 Years	Possible 1965-70
VLF	±500 μsec	±100 μsec	± 50 μsec
LORAN-C	-	± 1 μsec	±0.5 μsec
Synchronous Satellite System	-	-	±1 to 10 nsec

For applications requiring time synchronization to no better than ±500 μsec, VLF radio is already operational. Multichannel receiving equipment is relatively inexpensive and operation is quite reliable.

The majority of timing requirements in the immediate future requires time synchronization to no better than ±1 μsec. LORAN-C groundwave has a proven capability of achieving this accuracy. Existing chains should be synchronized to a common master standard and additional stations built to provide coverage for most of the world.

For very high precision timing synchronization requirements (1 to 10 nsec), a synchronous satellite system serving as active relays for microwave CW timing signals (probably with a carrier frequency of 1 to 10 gc) appears feasible. From an economic point of view, it appears desirable to incorporate this precision timing function within a synchronous communication satellite system.

REFERENCES

1. W. Markowitz, "Time Measurement Techniques in the Microsecond Region," The Engineer's Digest, No. 135, July-August 1962, pp 9-18.

2. A. H. Morgan, "Precise Time Synchronization of Widely Separated Clocks," NBS Technical Note No. 22, July 1959.

3. "Preliminary Plan for Global Timing Synchronization," prepared by Tele-Communications Working Group of the Inter-Range Instrumentation Group, IRIG Document No. 106-62, August 1962.

4. R. H. Doherty, G. Hefley, and R. F. Linfield, "Timing Potentials of LORAN-C," IRE Proceedings, Vol 49, No. 11, November 1961.

5. R. H. Doherty, T. L. Davis, and E. L. Berger, "LORAN-C Timing Tests," NBS Report 6754, 14 March 1961.

6. H. Lidkea, et al, "LORAN-C Timing Receiver Specifications," NBS Report 7240, 29 March 1962.

7. T. L. Davis and R. H. Doherty, "Widely Separated Clocks with Microsecond Synchronization and Independent Distribution Systems," IRE Wescon Convention Record, 1960.

8. W. A. Edson, "Noise in Oscillators," IRE Proceedings, Vol 48, No. 8, August 1960.

Appendix XI. GEOPHYSICAL CONSIDERATIONS IN METRIC INSTRUMENTATION

1. INTRODUCTION

For the purpose of range instrumentation planning, it is of interest to consider the effects of uncertainties in those geophysical properties which affect the trajectories of missiles and space vehicles being tracked by the test ranges, viz., gravitational potential and atmospheric density (drag fluctuations). These uncertainties must be taken into account in precise orbit prediction (e.g., for a satellite to calibrate a range instrumentation system, such as Mistram) and in certain test operations, such as the Guidance Evaluation Missile (GEM), where complete trajectory is interpolated from measurements taken at the end points by using free-fall calculations. It is the purpose of this appendix to briefly assess the uncertainties in computed trajectories arising from imperfect knowledge of the geophysical properties mentioned here.

The status of today's geophysical knowledge is sufficient to preclude any problems in current weapons system applications (impact prediction) (Reference 1). Thus, this appendix will consider geophysical uncertainties in orbit prediction. To permit analytic treatment, the discussion will be restricted to circular orbits. Specifically, uncertainties one revolution after epoch will be considered. It is assumed that the orbital parameters are perfectly known at epoch so that only the geophysical uncertainties will propagate. In real life, of course, the orbital parameters would be determined by observations and, hence, the observational uncertainties would contribute to the total uncertainty.

2. GRAVITATIONAL POTENTIAL

The earth's gravitational potential external to the earth may be represented by a series of spherical harmonics (Ref 2).

$$U = \frac{GM}{r}\left(1 - \sum_{n=2}^{\infty} J_n^{(0)} \left[\frac{R}{r}\right]^n P_n^{(0)} (\cos\theta)\right)$$

$$+ \sum_{n=2}^{\infty} \sum_{m=1}^{n} J_n^{(m)} \left[\frac{R}{r}\right]^n P_n^{(m)} (\cos\theta) \cos m\left[\lambda - \lambda_n^{(m)}\right] \quad (1)$$

where

G = universal gravitational constant

M = earth's mass

R = mean equatorial radius of the earth

r = geocentric distance

θ = polar angle

λ = east longitude

$P_n^{(m)}$ = Legendre polynomials or order n

$\left.\begin{matrix}\cos(\theta) \\ J_n^{(m)}\end{matrix}\right\}$ = associated constant empirical Legendre coefficients.

$$P_n^{(0)} = P_n\text{; Legendre zonal harmonic}$$

$$P_n^{(m)},\ n \neq m\text{; Legendre tesseral harmonic}$$

$$P_n^{(m)},\ n = m\text{; Legendre sectorial harmonic.}$$

The terms involving $\cos m\left[\lambda - \lambda_n^{(m)}\right]$ take into account the variations of U with longitude.

The series representation in equation (1) must be truncated to be useful; a good approximation is obtained by using

$$U = \frac{GM}{r}\left(1 - \sum_{n=2}^{7} J_n^{(0)} \left[\frac{R}{r}\right]^n P_n^{(0)} (\cos\theta)\right.$$

$$\left. + \sum_{n=2}^{4} \sum_{m=1}^{n} J_n^{(m)} \left[\frac{R}{r}\right]^n P_n^{(m)} (\cos\theta) \cos m\left[\lambda - \lambda_n^{(m)}\right]\right) \quad (2)$$

where $J_2^{(1)} = 0$.

The second order zonal term in the series, $J_2\left[\frac{R}{r}\right]^2 P_2 (\cos\theta)$, essentially represents the oblateness of the geoid and is by far the largest perturbing term. This term causes large precessional motions in the orbit, both a rotation of the orbital plane (nodal* regression, e.g., the angle ϕ_r in Figure 1 exemplifies nodal regression after one revolution) and a rotation of the line of apsides.** These are secular (increasing with time) perturbations, to which all the higher-order even zonal harmonics contribute (although to much lesser extent than does the second harmonic). In addition, the second harmonic term causes a nonsecular periodic perturbation in geocentric distance, which will be discussed subsequently; the second harmonic contributions to uncertainties along the orbit and orthogonal to the orbit plane will also be discussed subsequently.

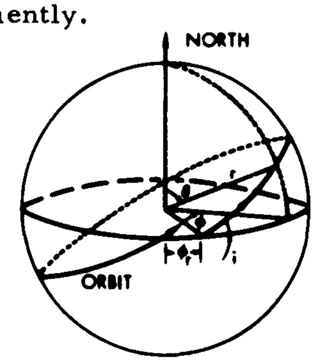

Figure 1. Orbit Showing Nodal Regression

* Those points on the celestial sphere where the satellite crosses the equator are called the nodes.

** The major axis of an orbit, extended indefinitely, is called the line of apsides. Since, by definition, a circular orbit does not have a unique major axis, no unique line of apsides exists.

The third-order zonal term in Equation (2) causes a slow change in the orbital elements, primarily in the eccentricity, with a period equal to that of the rotation of the line of apsides. All the higher-order odd zonal harmonics contribute, to a much lesser extent, to this periodic perturbation. As a first approximation, it is of interest to examine the uncertainties in a circular orbit due to uncertainties in J_2 (second-order zonal coefficient), neglecting higher order terms. Uncertainties will exist in geocentric distance (radial perturbation), position along the orbital path, and position orthogonal to the orbit plane.

The best values quoted in the literature for the zonal coefficients are probably those of Kozai (Reference 4) Thus

$$J_2 = (1082.48 \pm 0.06) \times 10^{-6}$$

where 0.06×10^{-6} is the rms scatter in his determination of J_2 and will be referred to subsequently as σ_J.

The radial error may be estimated by

$$\sigma_r = \frac{\sigma_J \quad R}{1 + \frac{h}{R}} \qquad (3)$$

where R is the mean equatorial radius of the earth and h is the height of the circular orbit.

The uncertainty in position along the orbit (one revolution from epoch) is directly related to uncertainty in period. The period, taking into account the oblateness of the earth, is given by

$$T = T_o \left\{ 1 - J_2 \left(\frac{1}{1 + \frac{h}{r}} \right)^2 \left[\cos^2 i + \cos i \sin^2 i - \frac{1}{2} \sin^2 \right] \right\} \qquad (4)$$

where i is the inclination angle of the orbit and T_o is the period for a spherical earth (Reference 4). The uncertainty in the period may be estimated by

$$\sigma_T = \sigma_J \left(\frac{1}{1 + \frac{h}{R}} \right)^2 \left[\cos^2 i + \cos i \sin^2 i - \frac{1}{2} \sin^2 i \right] T_o \qquad (5)$$

At some intermediate orbit inclination, the period of the satellite will be independent of the oblateness term J_2. This occurs when the trigonometric term in Equations (4) and (5) vanishes. This is the case when the orbit plane is inclined at approximately 69 deg to the equator (i = 69 deg). Arbitrarily taking the inclination angle to equal 45 deg

$$\frac{\sigma_T}{T} \text{ (i = 45 deg)} = \frac{\sigma_J \left(\frac{1}{1 + \frac{h}{R}} \right)^2 (0.604)}{\left\{ 1 - J_2 \left(\frac{1}{1 + \frac{h}{R}} \right)^2 (0.604) \right\}} \qquad (6)$$

The uncertainty in position along the orbit (one revolution from epoch), with i = 45 deg, is given by

$$\sigma_p = 2\pi \; (R + h) \; \frac{\sigma_T}{T} \quad \text{(i = 45 deg)} \qquad (7)$$

The uncertainty in position orthogonal to the orbit plane at time t is related to the uncertainty in nodal regression. Nodal regression (ϕ_r in Figure 1) has been shown in References 5 to equal

$$\phi_r = 2\pi J_2 \left(\frac{R}{R + h} \right)^2 \cos i = \frac{2\pi J_2 \cos i}{\left(1 + \frac{h}{R} \right)^2} \text{ rad} \qquad (8)$$

Thus, the uncertainty in nodal regression may be expressed

$$\sigma_{\phi_r} = \frac{2\pi\sigma_J \cos i}{\left[1 + \frac{h}{R} \right]^2} \text{ rad} \qquad (9)$$

Then the uncertainty in position arc orthogonal to the orbit plane (one revolution from epoch) may be expressed

$$\sigma_{\perp} = \frac{2\pi\sigma_J \cos i \sin i}{\left(1 + \frac{h}{R}\right)^2} \left[R + h\right] \tag{10}$$

and for i = 45 deg

$$\sigma_{\perp} = \frac{\pi\sigma_J (R + h)}{\left(1 + \frac{h}{R}\right)^2} \tag{11}$$

From Equations (3), (6), (7), and (11), Table I was constructed for the various uncertainties at several orbital altitudes. It should be noted that the values in this table represent approximate standard deviations and the actual error will, of course, be larger part of the time.

Table 1. Estimate of Uncertainties in Orbit Prediction Due to Uncertainty in the Coefficient of the Second Zonal Harmonic in the Earth's Gravitational Potential Expansion (One Revolution from Epoch)

Orbital Altitude h (nmi)	Uncertainty in Geocentric Distance r σ_r (ft)	Uncertainty in Position Arc Along the Orbit σ_P (ft)		Uncertainty in Position Arc Orthogonal to the Orbit Plane $\sigma_{\perp}$ (ft)	
100	1.17	4.6	(0.00021)*	3.8	(0.00018)*
200	1.13	4.5	(0.00020)*	3.7	(0.00017)*
300	1.10	4.4	(0.00019)*	3.6	(0.00016)*
500	1.05	4.2	(0.00017)*	3.4	(0.00014)*
1000	0.93	3.7	(0.00014)*	3.1	(0.00011)*

* The numbers in parentheses refer to the geocentric angle (in mr) subtended by the uncertainty in position arc.

It was shown in the previous section (Table I) that, although the second order zonal term is by far the largest perturbing term in the earth's potential, the coefficient J_2 is known to sufficient precision that errors in orbit prediction due to uncertainty in J_2 are quite small.

It is of interest to consider uncertainties in orbit prediction due to uncertainties in the coefficients of the tesseral harmonics. Kozia (Reference 6), inhis analysis of the effects of tesseral harmonics on the orbits of close earth satellites, concludesthat there are no secular perturbations of the first order in any orbital elements and that the amplitudes of the long-periodic (integral fractions of a day) terms are greater by an order of magnitude than the short-periodic terms. These results have been used to calculate the approximate long-periodic perturbations in position coordinates (resulting from neglect of tesseral harmonic terms through the fourth order) for a near-circular, near-polar satellite orbit. Combining these results with the uncertainties in the coefficients of the tesseral harmonics as derived by Kozai (Reference 6) yields Table II, which represents an estimate of uncertainties in position coordinates of such a satellite even if tesseral harmonic terms through the fourth order are included in the expression for the potential of the earth as in equation (2). Note that because the tesseral coefficients are known to such poor precision the position uncertainties in Table II are very much greater than the position uncertainties in Table I. The total uncertainty in each position coordinate would be on the order of hundreds of feet.

3. ATMOSPHERIC DENSITY

Since the earth's atmosphere is not symmetric,drag fluctuations such as fluctuations in atmospheric density (diurnal bulge), perturbations due to solar activity and magnetic storms, and other effects must be taken into account in precise orbit prediction.

It is not possible to predict the atmospheric parameters perfectly and, hence, drag fluctuations lead to pronounced orbital uncertainties below 200 nmi. Probably the 1962 Paetzold model (Reference 7) represents the state of the art. It appears that the atmospheric parameters are predictable on the basis of this model to within 10 percent.

Table II Estimate of Uncertainties in Orbit Prediction Due to Uncertainties in the Coefficients of Tesseral Harmonics in the Earth's Gravitational Potential Expansion

Coefficient	Period (Hrs)	Uncertainty in Geocentric Distance σ_r (ft)	Uncertainty in Position Arc Along the Orbit σ_p (ft)	Uncertainty in Position Arc Orthogonal to the Orbit Plane $\sigma_\perp$ (ft)
$J_2^{(2)}$	12	0	433	94
$J_3^{(1)}$	24	44	0	0
$J_3^{(2)}$	12	124	0	0
$J_3^{(3)}$	8	342	0	0
$J_4^{(1)}$	24	0	193	243
$J_4^{(2)}$	12	0	258	21
$J_4^{(3)}$	8	0	92	92
$J_4^{(4)}$	6	0	880	228

It is not the purpose of this appendix to discuss atmospheric models or problems in detail. The reader is referred to References 7 and 8 for a good discussion. Rather, it is of interest to consider the errors in orbital predictions due to drag fluctuations as analyzed by Moe (References 9, 10, 11).

Figure 2 presents the uncertainty in position arc along the orbit path due to uncertainties in the atmospheric model for a 100 nmi circular orbit. It is important to note that these curves refer to a particular representative satellite $\frac{W}{C_D A} = 100\ \mathrm{lb}/\mathrm{ft}^2$. For any particular vehicle with a particular $\frac{W}{C_D A}$ ratio, the ordinates of the curves in Figure 2 are inversely proportional to the $\frac{W}{C_D A}$ ratio.

Figure 3 provides a curve yielding coefficients to apply to the curves in Figure 2 to obtain errors for orbital altitudes above 100 nmi.

Table III presents the errors in position arc for various orbital altitudes obtained from Figures 2 and 3. In addition, an estimate of uncertainties in geocentric distance due to atmospheric density uncertainties is presented using as a rule-of-thumb (derived from empirical experience) that the uncertainties in geocentric distance are approximately 0. 1 times the magnitude of the corresponding uncertainty in position arc. It is important to note that the values in Table 2 represent one standard deviation.

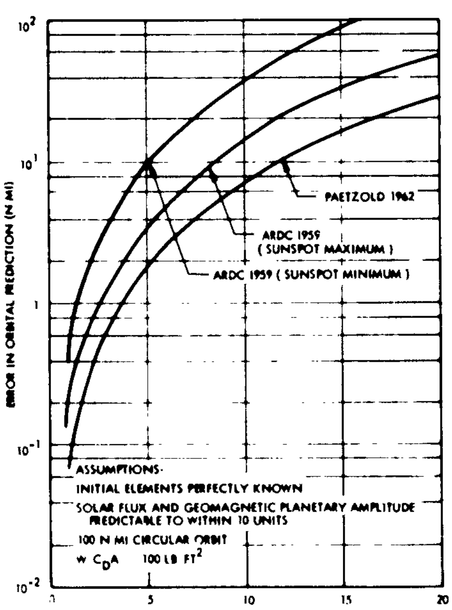

Figure 2. Errors in Orbital Predictions Using Paetzold's and the ARDC Atmosphere

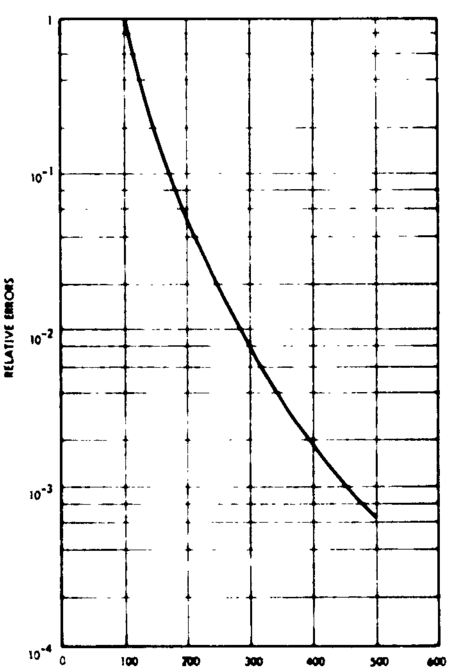

Figure 3. Relative Error Caused by Drag Fluctuations in Predictions for Circular Orbit

Table III. Estimate of Uncertainties in Orbital Prediction Due to Uncertainties in the Atmospheric Model (One Revolution from Epoch)

Orbital Altitude (nmi)	Uncertainty in Geocentric Distance σ_r (ft)	Uncertainty in Position Arc Along the Orbit σ_p (ft)	
100	50	500	(0.0023)*
200	4.0	40	(0.00018)*
300	0.5	5	(0.000022)*
500	0.04	0.4	(0.0000015)*
1000	negligible	negligible	

* The numbers in parentheses refer to the geocentric angle (in mr) subtended by the uncertainty in position angle.

4. CONCLUSIONS

Consideration of Table III indicates that, for orbits above 300 nmi errors due to drag fluctuations should present no problems. Considerable work is being done on the derivation of atmospheric parameters from observational data. However, no startling breakthrough is anticipated in the 1965-70 period as far as improvements on a "prediction" model of atmospheric density. Below 200 nmi, errors due to imperfect knowledge of atmospheric density variation can interfere significantly with precise orbit prediction.

From Table II, it is apparent that errors in orbit prediction due to uncertainties in the tesseral harmonic coefficients are likely to be greater than 100 ft in each position coordinate. Thus, the uncertainties are sufficiently large to pose a serious problem at this time in connection with the metric instrumentation problem. However, it is felt that reduction of satellite data (particularly ANNA and TRANSIT) over the next few years should reduce the uncertainties in the tesseral harmonic

coefficients by perhaps an order of magnitude and reduce the corresponding position uncertainties by a like amount. It appears that work toward improvements in the values for the tesseral harmonic coefficients is vital for such range projects as a calibration satellite.

Calibration and/or geodetic satellites will probably impose the most stringent requirements on orbit prediction during the 1965-70 period. It is likely that the major source of error will be the uncertainty in the orbital parameters as determined by observations. For the calibration satellite, it is quite likely that the range system under test will be the source of the observational data used to determine the initial orbital parameters - a "bootstrap" technique. Errors due to the uncertainties in the determination of the orbital parameters will likely be comparable to or outweigh errors due to geophysical uncertainties.

It is of interest to consider a specific test operation (of importance in weapon system evaluation) in light of the previous discussion on precise orbit prediction. Often it is desirable to determine a missile's position and velocity vector at the point of injection into free flight using metric data taken at a later time (reentry, for example) and "extrapolating back" to the injection point via free flight computations. If this free flight portion of the trajectory is approximated by a segment of a circular 100 nmi orbit, the previous results can be used to estimate geophysical uncertainties in missile position at injection. For example, consider the segment to be 1/5 of a 100 nmi circular orbit, using Table II and Figure 2, yields (in the notation of Tables II and III).

Uncertainties in the Tesseral Harmonic Coefficients (Gravitational Potential)			Uncertainties in the Atmospheric Density Model	
σ_r (ft)	σ_p (ft)	$\sigma_\perp$ (ft)	σ_r (ft)	σ_p (ft)
$>$ 100	$>$100	$>$ 100	10	100

The geophysical uncertainties will very likely be comparable to the errors due to uncertainties in the metric data taken at reentry. This points out again the need for more precise values for the empirical tesseral coefficients in the gravitational potential expression.

REFERENCES

1. A. D. Wheelon, "Free Flight of a Ballistic Missile," ARS Journal December 1959.

2. W. M. Kaula, "A Review of Geodetic Parameters," for presentation to International Astronomical Union Symposium No. 21, "The System of Astronomical Constants," Paris, 27-31 May 1963.

3. L. Blitzer, "Effect of Earth's Oblateness on the Period of a Satellite," Jet P ropulsion Laboratory, April 1957.

4. Y. Kozai, "Numerical Results from Orbits," Smithsonian Institute Astrophysical Observatory Special Report 101, 1962.

5. L. Blitzer and M. Weisfeld and A. D. Wheelon, "Perturbations of a Satellite Orbit Due to the Earth's Oblateness," Journal of Applied Physics, Vol 27, No. 10, pp 1141-1149, October 1956.

6. Y. Kozai, "Tesseral Harmonics of the Potential of the Earth as Derived from Satellite Motions," Smithsonian Institute Astrophysical Observatory Special Report 72, 9 August 1961.

7. H. K. Paetzold, "Model for the Variability of the Terrestrial Atmosphere Above 150 km after Satellite Acceleration," to appear in Space Research III, North Holland Publishing Co. , Amsterdam.

8. L. G. Jacchia, "Variations in the Earth's Upper Atmosphere as Revealed by Satellite Drag," Smithsonian Institute Astrophysical Observatory, 31 December 1962.

9. K. Moe, "Errors in Orbital Predictions for Artificial Satellites of Earth," Nature, Vol 192, No. 4798, 14 October 1961.

10. K. Moe, "Errors in Orbital Predictions for Meteorological and Geodetic Satellites," presented at the American Geophysical Union meeting in Washington, D. C. , 25-28 April 1962.

11. K. Moe, "Stochastic Models of the Errors in Orbital Predictions for Artificial Earth Satellites," ARS Journal, November 1962.

APPENDIX XII. TRACKING SYSTEMS ERROR ANALYSIS

A. INTRODUCTION

1. PURPOSE

Although the instrument measurement and survey errors of the various tracking systems may be known, it is still necessary to propagate these errors into the resultant errors in determination of the missile or spacecraft position and velocity. Only in this way can the tracking potential of each system be evaluated for various missions. The purpose of this appendix is to show the method by which error propagation equations were derived, and to list these equations along with applicable assumptions and limitations.

2. TRACKING SYSTEMS STUDIED

In the present study, formulas were generated for the propagation of the instrument and survey error of four different radio tracking systems into errors in determination errors of vehicle position and velocity. These four systems are representative of those now being used or planned for use in the near future which appear to offer the best potential for meeting future mission requirements. The systems for which the formulas have been developed are:

- Radar: measuring range (R), azimuth (A), and elevation (E)
- Interferometer: measuring range, range rate, direction cosines, and direction cosine rates
- General Electric Range Tracking System (GERTS): a combination of radar position measurement and interferometer velocity measurement
- Trilateration: measuring range and range rate from three stations

The Mistram system can be treated as an interferometer by dividing errors in range difference measurements by the baseline length to derive an equivalent error in direction cosine, and by treating the time derivatives of these measurements in the same fashion. Another network which

is a modification of the complete trilateration network is one in which vehicle position is determined from one or two radars measuring range, azimuth, and elevation, and vehicle velocity is determined by a three-station range-rate trilateration. In this case, the position error would result from the appropriate propagation of the radar RAE measurements, and would be worse than that obtained from a range trilateration. In addition, the velocity error is somewhat worse than that obtained with the range and range-rate trilateration network because of the manner in which position errors propagate into velocity errors.

3. APPROACH

Although the equations for the radar and interferometer were derived successfully by matrix methods, analysis of the trilateration network by the same method proved impractical. Instead, a vectorial approach was chosen for the derivation which, in turn, provided a geometric interpretation of the problem. A graphical method was developed to assist in evaluating the error coefficients. One of the primary reasons for the detailed study of the trilateration case was that the trilateration approach appears to be the only feasible method for satisfying mission requirements far down range of the launch area where the interferometer trackers (Mistram, Azusa) are no longer capable of accurate tracking. These stations are located in widely dispersed areas throughout the world.

The sources of error were divided into two categories: those originating as errors in the measurement; and those originating in location of the measurement system. For obvious reasons, it was desirable that the metric error due to those effects be kept separate.

Rather than dividing the vehicle metric error components due to these error sources into errors in a specific coordinate system such as (σ_x, σ_y, σ_z), the errors are derived in terms of a total mean-square position, σ_P^2, or velocity, σ_V^2, error. This is in conformity with the mission requirements which are also given in this manner.

B. SURVEY ERRORS

1. GENERAL

Survey errors are of two general types: internal and external. Internal survey errors for a gimbaled tracking antenna consist of errors in the determination of the direction of the azimuth reference (usually true North), and in the direction of the elevation reference, (usually the direction connecting the origin of the local coordinate system and the earth's center of mass). Internal survey errors for an interferometer system consist of errors in measurement of baseline lengths and baseline orientations with respect to true North and true local vertical. These types of survey errors are considered to be contributors to the total measurement error of the instrument itself, and their effects are lumped under "instrumental" error sources. That is, if all such internal errors are taken into account in quoting the accuracies of the direction cosines and their time derivatives in the case of the interferometers, and in quoting the azimuth and elevation accuracies in the case of the tracking radars, only the station location errors need be attributed to survey errors. External survey errors are defined as the errors in the location of the origin of the local tracker coordinate system, with respect to a reference coordinate system, usually geocentric.

Station location errors contribute to total mean-square error in determination of vehicle position and velocity in the reference coordinate system. An interferometer is considered a "single point tracker" in the context of external survey errors, since the baseline measurements are made with respect to a single,local coordinate system. The same holds true for the GERTS system, which is a hybrid combination of a gimbaled range, azimuth, and elevation (RAE) radar and a rate interferometer.

The station location error problem is treated somewhat differently in the case of the trilateration network, since the stations are generally separated by hundreds of miles. The data used for analysis of the network performance are the range and range-rate errors of the individual radars, whose location errors with respect to some reference coordinate system are assumed to be uncorrelated. Methods of treating these uncorrelated station location errors are developed in Section F of this appendix. If the station locations are determined with respect to the prime coordinate system to which vehicle position and velocity are eventually referenced,

these methods alone will suffice. If the station locations are determined with respect to some common intermediate datum, then the methods of Section F are used to determine vehicle position and velocity errors with respect to this intermediate datum, and the location errors of this datum with respect to the prime coordinate system are treated in the same fashion as those of a "single point tracker" in the following discussion.

2. POSITION ERRORS

Consider a tracking system located at (x_o, y_o, z_o) which is believed to be located at (0, 0, 0) in the reference Cartesian coordinate system and let the position of the vehicle being tracked be (x, y, z) in this reference system. We suppose that the directions of the reference coordinate axes are known at the tracking station, so that the only survey error is an error in knowledge of the station position. In this case, the station will make position measurements which, when transformed into the reference coordinate system, may be expressed in terms of the coordinates x', y', z'. These measurements are related to the true vehicle position by

$$\begin{aligned} x' &= x - x_o \\ y' &= y - y_o \\ z' &= z - z_o \end{aligned} \tag{1}$$

From Equation (1), it is apparent that the errors in determination of the vehicle coordinates in the reference coordinate system are given by

$$\begin{aligned} x' - x &= - x_o \\ y' - y &= - y_o \\ z' - z &= - z_o \end{aligned} \tag{2}$$

and that the square of the resulting position error $\delta\bar{R}$ is

$$(\delta\bar{R})^2 = x_o^2 + y_o^2 + z_o^2 = (\delta\bar{S})^2 \tag{3}$$

where $\delta\bar{S}$ is the survey position error. If we let σ_S^2 be the mean-square value of the location error, it follows immediately that the mean-square error in vehicle position determination due to external survey error is

$$\sigma_{PS}^2 = \sigma_S^2 \tag{4}$$

and this result holds true for all systems whose measurements are made with respect to a single reference point. The derivation of Equation (4) has not taken into account rotation of the local coordinate system due to latitude and longitude errors in the station location, since Equation (1) assumed that the directions of the reference axes are known. Suppose that the true directions of North, East, and vertical are accurately determined and there is no error in station altitude. A station-location error of L will result in a vehicle position error of $L\frac{R_o + h}{R_o}$, where R_o is the earth radius and h is the vehicle altitude. This degree of sophistication in the present analysis is unnecessary for two reasons:

- There is considerable uncertainty in assigning accurate values to the station location errors
- At extremely high altitudes, when the factor $\frac{R_o + h}{R_o}$ differs significantly from unity, trilateration networks are employed whose station-location errors are separately analyzed.

3. VELOCITY ERRORS

Differentiation of Equation (1) yields

$$\begin{aligned} \dot{x}' &= \dot{x} \\ \dot{y}' &= \dot{y} \\ \dot{z}' &= \dot{z} \end{aligned} \tag{5}$$

which shows that the tracking station determines the velocity components in the local coordinate system correctly. The important point here is simply that the velocity vector is the time rate of change of a position vector without regard to the choice of the origin for the position vector.

From Equation (5) it follows that the mean-square velocity error due to station-location error is

$$\sigma_{VS}^2 = 0 \tag{6}$$

Equation (6) does not mean that station-location errors are of no concern to the determination of vector components of vehicle velocity, since the rotation of the local coordinate system will introduce a corresponding angular rotation error of the measured velocity. The effect of these errors, however, will usually be much smaller than the instrumental errors. For example, if $|\overline{V}|$ = 30,000 ft/sec and $|\delta\overline{S}|$ = 210 feet, the resultant error is 0.3 ft/sec in a direction normal to $\overline{V}$.

C. RAE RADAR

1. VARIATIONAL EQUATIONS

Consider an RAE radar located at the origin of a Cartesian coordinate system in which the z axis lies in the direction of the local vertical. Let the Cartesian coordinates of the vehicle being tracked by the radar be x, y, z. The Cartesian coordinates are given in terms of the radar coordinates by

$$\begin{aligned} x &= R \cos E \cos A \\ y &= R \cos E \sin A \\ z &= R \sin E \end{aligned} \tag{7}$$

While the natural coordinate system for the radar is the spherical polar coordinate system, the fact that the directions of the unit vectors in this natural coordinate system are functions of the vehicle position complicates a direct analysis of the manner in which errors propagate into position and velocity errors. For this reason, it seems preferable to refer the errors to a fixed Cartesian coordinate system from the outset and to make use of matrix methods for the analysis.

We first derive the variational equations that show the manner in which variations in R, A, E are related to variations in x, y, z. We shall make use of the fact that if $\eta_1, \eta_2, \ldots, \eta_m$ are functions of $\xi_1, \xi_2, \ldots, \xi_n$, the variations in the η_k's are expressible in terms of the variations in the ξ_k's by means of the matrix formula

$$\begin{bmatrix} \delta\eta_1 \\ \delta\eta_2 \\ \vdots \\ \delta\eta_m \end{bmatrix} = \begin{bmatrix} \frac{\partial\eta_1}{\partial\xi_1} & \frac{\partial\eta_1}{\partial\xi_2} & \cdots & \frac{\partial\eta_1}{\partial\xi_n} \\ \frac{\partial\eta_2}{\partial\xi_1} & \frac{\partial\eta_2}{\partial\xi_2} & \cdots & \frac{\partial\eta_2}{\partial\xi_n} \\ \vdots & \vdots & & \vdots \\ \frac{\partial\eta_m}{\partial\xi_1} & \frac{\partial\eta_m}{\partial\xi_2} & \cdots & \frac{\partial\eta_m}{\partial\xi_n} \end{bmatrix} \begin{bmatrix} \delta\xi_1 \\ \delta\xi_2 \\ \vdots \\ \delta\xi_n \end{bmatrix} \tag{8}$$

From Equations (7) and (8), we have

$$\begin{bmatrix} \delta x \\ \delta y \\ \delta z \end{bmatrix} = M_1 \begin{bmatrix} \delta R \\ \delta E \\ \delta A \end{bmatrix} \tag{9}$$

where

$$M_1 = \begin{bmatrix} \cos E \cos A & -R \sin E \cos A & -R \cos E \sin A \\ \cos E \sin A & -R \sin E \sin A & R \cos E \cos A \\ \sin E & R \cos E & 0 \end{bmatrix} \tag{10}$$

From Equation (9) we have

$$(\delta x)^2 + (\delta y)^2 + (\delta z)^2 = \begin{bmatrix} \delta x \\ \delta y \\ \delta z \end{bmatrix}^T \begin{bmatrix} \delta x \\ \delta y \\ \delta z \end{bmatrix} = \begin{bmatrix} \delta R \\ \delta E \\ \delta A \end{bmatrix}^T M_1^T M_1 \begin{bmatrix} \delta R \\ \delta E \\ \delta A \end{bmatrix} \tag{11}$$

where the superscript T indicates the transpose of the matrix. From Equation (10) we find that

$$M_1^T M_1 = \begin{bmatrix} 1 & 0 & 0 \\ 0 & R^2 & 0 \\ 0 & 0 & R^2 \cos^2 E \end{bmatrix} \tag{12}$$

which illustrates the orthogonal character of the R, A, E coordinate system. From Equations (11) and (12), we now have

$$(\delta \bar{R})^2 = (\delta x)^2 + (\delta y)^2 + (\delta z)^2 = (\delta R)^2 + (R \delta E)^2 + (R \cos E \, \delta A)^2 \tag{13}$$

While the result expressed by Equation (13) is well known, the derivation given serves to introduce the methodology employed in the remainder of this analysis.

The corresponding variational equations for $\delta\dot{x}$, $\delta\dot{y}$, $\delta\dot{z}$ are derived as follows. From Equation (7) we find, by differentiation with respect to time, that

$$\begin{aligned}
\dot{x} &= \dot{R}\cos E\cos A - \dot{E}R\sin E\cos A - \dot{A}R\cos E\sin A \\
\dot{y} &= \dot{R}\cos E\sin A - \dot{E}R\sin E\sin A + \dot{A}R\cos E\cos A \\
\dot{z} &= \dot{R}\sin E + \dot{E}R\cos E
\end{aligned} \tag{14}$$

Next we write

$$\begin{bmatrix} \delta\dot{x} \\ \delta\dot{y} \\ \delta\dot{z} \end{bmatrix} = \begin{bmatrix} M_2 & M_3 \end{bmatrix} \begin{bmatrix} \delta\dot{R} \\ \delta\dot{E} \\ \delta\dot{A} \\ \delta R \\ \delta E \\ \delta A \end{bmatrix} = M_2 \begin{bmatrix} \delta\dot{R} \\ \delta\dot{E} \\ \delta\dot{A} \end{bmatrix} + M_3 \begin{bmatrix} \delta R \\ \delta E \\ \delta A \end{bmatrix} \tag{15}$$

where

$$M_2 = \begin{bmatrix} \frac{\partial\dot{x}}{\partial\dot{R}} & \frac{\partial\dot{x}}{\partial\dot{E}} & \frac{\partial\dot{x}}{\partial\dot{A}} \\ \frac{\partial\dot{y}}{\partial\dot{R}} & \frac{\partial\dot{y}}{\partial\dot{E}} & \frac{\partial\dot{y}}{\partial\dot{A}} \\ \frac{\partial\dot{z}}{\partial\dot{R}} & \frac{\partial\dot{z}}{\partial\dot{E}} & \frac{\partial\dot{z}}{\partial\dot{A}} \end{bmatrix} \tag{16}$$

and

$$M_3 = \begin{bmatrix} \frac{\partial\dot{x}}{\partial R} & \frac{\partial\dot{x}}{\partial E} & \frac{\partial\dot{x}}{\partial A} \\ \frac{\partial\dot{y}}{\partial R} & \frac{\partial\dot{y}}{\partial E} & \frac{\partial\dot{y}}{\partial A} \\ \frac{\partial\dot{z}}{\partial R} & \frac{\partial\dot{z}}{\partial E} & \frac{\partial\dot{z}}{\partial A} \end{bmatrix} \tag{17}$$

From Equation 14, for the elements of M_2 we have

$$
\left.
\begin{aligned}
\frac{\partial \dot{x}}{\partial \dot{R}} &= \cos E \cos A \\
\frac{\partial \dot{x}}{\partial \dot{E}} &= -R \sin E \cos A \\
\frac{\partial \dot{x}}{\partial \dot{A}} &= -R \cos E \sin A \\
\\
\frac{\partial \dot{y}}{\partial \dot{R}} &= \cos E \sin A \\
\frac{\partial \dot{y}}{\partial \dot{E}} &= -R \sin E \sin A \\
\frac{\partial \dot{y}}{\partial \dot{A}} &= R \cos E \cos A \\
\\
\frac{\partial \dot{z}}{\partial \dot{R}} &= \sin E \\
\frac{\partial \dot{z}}{\partial \dot{E}} &= R \cos E \\
\frac{\partial \dot{z}}{\partial \dot{A}} &= 0
\end{aligned}
\right\} \qquad (18)
$$

From Equations (18), (16), and (10) we see that*

$$M_2 = M_1 \qquad (19)$$

* That the relationship expressed by Equation (19) is valid is not a peculiarity of the spherical polar coordinate system but holds in the general case. To establish this result, we have only to observe that from the usual formula for partial differentiation

$$\dot{\eta}_k = \sum_{j=1}^{n} \frac{\partial \eta_k}{\partial \xi_j} \dot{\xi}_j$$

from which it follows that

$$\frac{\partial \dot{\eta}_k}{\partial \dot{\xi}_j} = \frac{\partial \eta_k}{\partial \xi_j}$$

Also, from Equation (14) for the elements of M_3, we have

$$\left.\begin{aligned}
\frac{\partial \dot{x}}{\partial R} &= -\dot{E} \sin E \cos A - \dot{A} \cos E \sin A \\
\frac{\partial \dot{x}}{\partial E} &= -\dot{R} \sin E \cos A - \dot{E}R \cos E \cos A + \dot{A}R \sin E \sin A \\
\frac{\partial \dot{x}}{\partial A} &= -\dot{R} \cos E \sin A + \dot{E}R \sin E \sin A - \dot{A}R \cos E \cos A \\
\\
\frac{\partial \dot{y}}{\partial R} &= -\dot{E} \sin E \sin A + \dot{A} \cos E \cos A \\
\frac{\partial \dot{y}}{\partial E} &= -\dot{R} \sin E \sin A - \dot{E}R \cos E \sin A - \dot{A}R \sin E \cos A \\
\frac{\partial \dot{y}}{\partial A} &= \dot{R} \cos E \cos A - \dot{E}R \sin E \cos A - \dot{A}R \cos E \sin A \\
\\
\frac{\partial \dot{z}}{\partial R} &= \dot{E} \cos E \\
\frac{\partial \dot{z}}{\partial E} &= \dot{R} \cos E - \dot{E}R \sin E \\
\frac{\partial \dot{z}}{\partial A} &= 0
\end{aligned}\right\} \qquad (20)$$

Equation (15) may now be written

$$\begin{bmatrix} \delta\dot{x} \\ \delta\dot{y} \\ \delta\dot{z} \end{bmatrix} - M_1 \begin{bmatrix} \delta\dot{R} \\ \delta\dot{E} \\ \delta\dot{A} \end{bmatrix} + M_3 \begin{bmatrix} \delta R \\ \delta E \\ \delta A \end{bmatrix} \qquad (21)$$

whose transpose is

$$\begin{bmatrix} \delta\dot{x} \\ \delta\dot{y} \\ \delta\dot{z} \end{bmatrix}^T = \begin{bmatrix} \delta\dot{R} \\ \delta\dot{E} \\ \delta\dot{A} \end{bmatrix}^T M_1^T + \begin{bmatrix} \delta R \\ \delta E \\ \delta A \end{bmatrix}^T M_3^T \qquad (22)$$

If we let

$$(\delta\overline{V})^2 = (\delta\dot{x})^2 + (\delta\dot{y})^2 + (\delta\dot{z})^2 = \begin{bmatrix}\delta\dot{x}\\ \delta\dot{y}\\ \delta\dot{z}\end{bmatrix}^T \begin{bmatrix}\delta\dot{x}\\ \delta\dot{y}\\ \delta\dot{z}\end{bmatrix} \tag{23}$$

then, from Equations (21) and (22), we have

$$(\delta\overline{V})^2 = \begin{bmatrix}\delta\dot{R}\\ \delta\dot{E}\\ \delta\dot{A}\end{bmatrix}^T M_1^T M_1 \begin{bmatrix}\delta\dot{R}\\ \delta\dot{E}\\ \delta\dot{A}\end{bmatrix} + \begin{bmatrix}\delta\dot{R}\\ \delta\dot{E}\\ \delta\dot{A}\end{bmatrix}^T M_1^T M_3 \begin{bmatrix}\delta R\\ \delta E\\ \delta A\end{bmatrix} + \begin{bmatrix}\delta R\\ \delta E\\ \delta A\end{bmatrix}^T M_3^T M_1 \begin{bmatrix}\delta\dot{R}\\ \delta\dot{E}\\ \delta\dot{A}\end{bmatrix}$$

$$+ \begin{bmatrix}\delta R\\ \delta E\\ \delta A\end{bmatrix}^T M_3^T M_3 \begin{bmatrix}\delta R\\ \delta E\\ \delta A\end{bmatrix} \tag{24}$$

Since the transpose of a scalar is once again a scalar, we have

$$\begin{bmatrix}\delta\dot{R}\\ \delta\dot{E}\\ \delta\dot{A}\end{bmatrix}^T M_1^T M_3 \begin{bmatrix}\delta R\\ \delta E\\ \delta A\end{bmatrix} = \begin{bmatrix}\delta R\\ \delta E\\ \delta A\end{bmatrix}^T M_3^T M_1 \begin{bmatrix}\delta\dot{R}\\ \delta\dot{E}\\ \delta\dot{A}\end{bmatrix} \tag{25}$$

which permits Equation (24) to be simplified to the form

$$(\delta\overline{V})^2 = \begin{bmatrix}\delta\dot{R}\\ \delta\dot{E}\\ \delta\dot{A}\end{bmatrix}^T M_1^T M_1 \begin{bmatrix}\delta\dot{R}\\ \delta\dot{E}\\ \delta\dot{A}\end{bmatrix} + \begin{bmatrix}\delta R\\ \delta E\\ \delta A\end{bmatrix}^T M_3^T M_3 \begin{bmatrix}\delta R\\ \delta E\\ \delta A\end{bmatrix} + 2 \begin{bmatrix}\delta\dot{R}\\ \delta\dot{E}\\ \delta\dot{A}\end{bmatrix}^T M_1^T M_3 \begin{bmatrix}\delta R\\ \delta E\\ \delta A\end{bmatrix} \tag{26}$$

Before evaluating the matrices in Equation (26), it will be convenient to introduce the statistical considerations.

2. STATISTICAL CONSIDERATIONS

If the errors δR, δE, and δA are uncorrelated and have zero-mean values (on an a priori basis), it follows from Equation (13) that the instrumental mean-square position error is given by

$$\sigma_{PI}^2 = \sigma_R^2 + R^2 \sigma_E^2 + R^2 \cos^2 E \, \sigma_A^2 \tag{27}$$

which, under the conditions

$$\sigma_E^2 = \sigma_A^2 \tag{28}$$

can be written

$$\sigma_{PI}^2 = \sigma_R^2 + \sigma_{A,E}^2 R^2 (1 + \cos^2 E) \tag{29}$$

where σ_R, σ_E, and σ_A are the equivalent rms errors in R, E, A after such smoothing as may be performed in data reduction.

The above point pertaining to data smoothing is sufficiently important to warrant additional discussion. In general, radar data are filtered digitally in the course of reduction of the raw output data. A transformation to a reference Cartesian coordinate system is usually made prior to the final smoothing. The radar outputs, of course, are already smoothed by the action of the range- and angle-tracking servos, and some additional smoothing may, on occasion, be performed on R, E, A prior to the transformation to the reference coordinate system. The nonlinearity of the coordinate transformation implies a considerable complication in assessing the effects of smoothing after the coordinate transformation when the nominal values of R, E, A cannot legitimately be considered to be constant over the smoothing interval, although it gives rise to no particular problems in smoothing the data. The alternative is to smooth the R, E, A data directly and then effect the transformation to the reference coordinate system. If the smoothing is properly done in both cases, the results should be comparable. Since the error analysis is so much more tractable when the numerical smoothing, differentiation, etc., are performed on the measured parameters R, E, A, such smoothing will be assumed for the remainder of this analysis of the R, E, A radar performance.

When numerical (digital) filtering or differentiation is performed, the efficiency of the smoothing operation, relative to the raw data, is strongly dependent on the spectral characteristics of the raw data. Obviously, the sampling rate must be sufficiently high relative to the spectrum of the data to avoid aliasing. The output R, E, A data will, of course, have low-pass spectra, and the spectral widths will be determined by the bandwidths of the range, azimuth, and elevation servo systems. If the output of a data channel is sampled with a sampling frequency equal to twice the spectral width of the data (that is, at a sampling rate equal to twice the noise bandwidth of the servo system), the resulting data samples will contain all the information obtainable from the data source and, in fact, will permit reconstruction of the original output data. This result from interpolation theory is the well-known sampling theorem.

The statistical version of the sampling theorem states, in addition, that if the output noise (which is presumed to be stationary over the period of interest) is gaussian, then samples taken at a sampling frequency equal to twice the noise bandwidth are statistically independent. Since the servo bandwidths are narrow relative to the noise bandwidth at the servo input, the gaussian assumption should be valid for the fluctuating portion of the radar output. This assumption does not, of course, take into account the causal cyclic errors in the equipment (which should be small in a well-designed radar).

On the basis of the preceding discussion, it is clear that in an analysis of the effects of numerical filtering operations, there is no essential loss of generality in the assumption that the data samples are taken at a sampling rate equal to twice the bandwidth of the appropriate servo system, that the fluctuating parts of these samples are statistically independent, and that the digital filtering process is designed to optimize the resulting radar data (position and velocity data). These remarks are applicable to the interpretation of Equation (27), but are especially critical for the analysis of the mean-square velocity error. For this reason, the following discussion is concentrated on the velocity error.

A reasonable numerical differentiation formula for obtaining $\dot{R}, \dot{E}, \dot{A}$ from R, E, A is one based on optimizing the differentiation operator in a minimum mean-square error sense on the assumption that the data can

be adequately represented by a quadratic polynomial over the smoothing interval, subject to the constraint that the operator should yield the correct value of the function being smoothed when the input data are error-free. The operator is taken to be linear and the result of the smoothing (and differentiation) operation is to be applicable at the midpoint of the interval over which the samples are given. If samples $\eta_{-n}, \dots \eta_{-1}, \eta_o, \eta_1, \dots, \eta_n$ are given, the estimator for $\dot{\eta}_o$ is of the form

$$\hat{\dot{\eta}}_o = \sum_{k=-n}^{n} w_k \eta_k \tag{30}$$

where the carat over $\dot{\eta}_o$ indicates that the right-hand side is an estimate for $\dot{\eta}_o$ rather than $\dot{\eta}_o$ itself. When $\eta(t)$ can be fitted by a quadratic polynomial over the smoothing interval and when the samples are error-free, the value of the sum on the right is indeed $\dot{\eta}_o = \dot{\eta}(0)$; this is guaranteed by the constraint mentioned above. Specifically, the constraint requires that

$$\sum_{k=-n}^{n} w_k = 0, \qquad \Delta \sum_{k=-n}^{n} k w_k = 1, \qquad \sum_{k=-n}^{n} k^2 w_k = 0 \tag{31}$$

where Δ is the sampling period. The fact that these constraints are necessary if Equation (30) is to fit a quadratic function without error is easily verified. If the weights w_k are now determined, subject to Equation (31) to provide minimum mean-square error when the errors in the samples η_k are uncorrelated with equal variances and zero means, it is easily found that w_k is given by

$$w_k = \frac{3k}{n(2n+1)(n+1)\Delta} \qquad (-n \le k \le n) \tag{32}$$

and that the mean-square value of the estimate $\hat{\dot{\eta}}_o$ is given by

$$\sigma^2(\hat{\dot{\eta}}_o) = \frac{3\sigma^2(\eta)}{n(2n+1)(n+1)\Delta^2} \tag{33}$$

Here $\sigma^2(\eta)$ is the common variance of the η_k's. The results expressed by Equations (32) and (33) are well known, but a few points concerning these equations should be noted. First, the fact that $w_{-k} = -w_k$ shows that any constant bias in the samples η_k will have no effect on the digital filtering. This fact also follows from the first constraint in Equation (31) and is to be expected since the derivative of a constant is zero. When the errors are not only uncorrelated with identical means but also have a joint gaussian distribution, a linear operator is optimum for estimating $\dot{\eta}_o$ (and η_o, etc.) in the mean-square sense. This well-known result implies that for the case of interest, the estimator, Equation (30), with the w_k given by Equation (32) is absolutely optimum in a mean-square sense, subject to the constraints noted previously. In other words, in the radar case, we shall be doing as well as is possible with the available data.

Similar remarks are applicable to any smoothing operation performed on the sequence η_k to estimate η_o. In this case, the smoothing operator will be symmetric ($w_{-k} = w_k$) about the midpoint of the data interval rather than antisymmetric ($w_{-k} = -w_k$) as is the case in estimating $\dot{\eta}_o$. It is also worth observing that the total data interval (span of (2n+ 1) data points) over which smoothing is performed may well differ for estimating $\dot{\eta}_o$ and η_o.

It would be desirable to place the expression for $\sigma^2(\hat{\dot{\eta}}_o)$ in a form that shows the dependence on the smoothing time and the noise bandwidth (servo bandwidth) more explicitly. For this purpose, we write

$$m = 2n + 1 \tag{34}$$

so that m is the total number of data samples used in the smoothing process. For the right-hand side of Equation (33) we have

$$\sigma^2(\hat{\dot{\eta}}_o) = \frac{12\sigma^2(\eta)}{(2n)(2n+1)(2n+2)\Delta^2} = \frac{12\,\sigma^2(\eta)}{(m-1)(m)(m+1)\Delta^2}$$

which may be written as

$$\sigma^2(\hat{\dot{\eta}}_o) = \frac{12\sigma^2(\eta)}{m(m^2-1)\Delta^2} \tag{35}$$

Henceforth, we may omit the subscript zero as the result applies at any time, and we shall suppose that $\dot{\eta}$ is calculated from the estimate $\hat{\dot{\eta}}$, permitting us to drop the carat also for notational convenience.

Now, observe that

$$\Delta = \frac{1}{2B} \tag{36}$$

where B is the servo noise bandwidth and that

$$m\Delta = T, \qquad m = \frac{T}{\Delta} = 2BT \tag{37}$$

where T is the interval over which the smoothing (numerical differentiation) is performed. In general, we will have $m >> 1$, since otherwise no appreciable filtering is performed in the data reduction process. We may therefore write

$$\sigma^2(\dot{\eta}) \approx \frac{12\sigma^2(\eta)}{(m\Delta)^2 m} \tag{38}$$

which, on using Equation (37), may be rewritten as

$$\sigma^2(\dot{\eta}) = \frac{12\sigma^2(\eta)}{T^2(2BT)} \tag{39}$$

where we have replaced $\approx$ by $=$ for convenience in writing. Equation (39) is notable in that it no longer depends explicitly on the number of samples. The quantity 2BT is of some interest, however, as it is precisely the number of independent samples of a signal of bandwidth B in time T. The final form in which we shall use Equation (39) is

$$\sigma^2(\dot{\eta}) = \frac{6}{BT^3}\,\sigma^2(\eta) \tag{40}$$

Next we turn to a study of the correlation properties of optimum position and rate estimates. To make matters definite, we consider the range and range-rate errors, when range rate is obtained by numerical differentiation of range data. Thus we consider the estimate $\hat{R}$ obtained by filtering on $2m+1$ samples and the estimate $\hat{\dot{R}}$ which is obtained by filtering on $2n+1$ samples. These estimates are to apply at a common time. Let the original data be R_k, with errors

$$\delta R_k = X_k + Y \tag{41}$$

Here Y is a bias common to the measurements R_k, while the X_k's are the fluctuating part of the error. The samples are taken at a rate equal to twice the bandwidth of the range servo, so that the X_k's are uncorrelated (they may actually be taken to be independent) with zero means. Although Y is a bias, it may be taken a priori to be a random variable with zero mean. It is clear that both the resulting range error after smoothing, δR, and the resulting range-rate error after smoothing have zero means. We wish to show that they are also uncorrelated. For this purpose, we write the weights used in estimating R as u_k and the weights used in differentiating R as v_k. We recall that $u_{-k} = u_k$ and $v_{-k} = -v_k$. Hence for the resulting errors δR and $\delta \dot{R}$ we have from Equation (41)

$$\begin{aligned}\delta R &= u_o \delta R_o + \sum_{k=1}^{m} u_k \left(\delta R_k + \delta R_{-k}\right) \\ &= \left(\sum_{k=-m}^{m} u_k\right) Y + u_o X_o + \sum_{k=1}^{m} u_k \left(X_k + X_{-k}\right)\end{aligned} \tag{42}$$

$$\begin{aligned}\delta \dot{R} &= \sum_{j=1}^{n} v_j \left(\delta R_j - \delta R_{-j}\right) \\ &= \sum_{j=1}^{n} v_j \left(X_j - X_{-j}\right)\end{aligned} \tag{43}$$

On observing that the requirement that the estimator for R should be unbiased implies

$$\sum_{k=-m}^{m} u_k = 1 \tag{44}$$

We may rewrite Equations (42) and (43) as

$$\delta R = Y + u_o X_o + \sum_{k=1}^{m} u_k \left(X_k + X_{-k} \right) \tag{45}$$

$$\delta \dot{R} = \sum_{j=1}^{n} v_j \left(X_j X_{-j} \right) \tag{46}$$

Clearly, Y does not correlate with any terms on the right in Equation (46). Also, none of the terms involving the X's on the right of Equation (45) will correlate with any of the terms on the right in Equation (46) for $j \neq k$. If $j = k$, the product of the term on the right in Equation (45) with the corresponding term on the right in Equation (46) will be

$$u_k v_k \left(X_k + X_{-k} \right)\left(X_k - X_{-k} \right) = u_k v_k \left(X_k^2 - X_{-k}^2 \right) \tag{47}$$

which clearly has a zero mean since $\sigma^2(X_k) = \sigma^2(X_{-k})$. Using the notation $\langle X \rangle$ for the mathematical expectation of the random variable X, it follows that

$$\langle \delta R \delta \dot{R} \rangle = 0 \tag{48}$$

as was asserted.

The same argument shows that

$$\langle \delta E \delta \dot{E} \rangle = 0 \quad , \quad \langle \delta A \delta \dot{A} \rangle = 0 \tag{49}$$

Moreover, it is certainly reasonable to assume that the errors in R, E, A are mutually uncorrelated. It now follows from this reasonable hypothesis, and from Equations (48) and (49) that δR, δE, δA, $\delta \dot{R}$, $\delta \dot{E}$, $\delta \dot{A}$ are all uncorrelated. Since, in addition, they all have zero means, we see that the term involving $M_1^T M_3$ in Equation (26), when averaged, contributes nothing to the mean-square velocity error. Accordingly, the computation of the matrix $M_1^T M_3$ is unnecessary.

Consider now the contributions of the first and second terms on the right in Equation (26) to the mean-square velocity error. Since $\delta\dot{R}$, $\delta\dot{E}$, $\delta\dot{A}$ are uncorrelated, only the diagonal terms in $M_1^T M_1$ contribute to the mean-square velocity error. In similar fashion, since δR, δE, δA are uncorrelated, only the diagonal terms in the matrix $M_3^T M_3$ contribute to the mean-square velocity error.

Denoting the diagonal elements of the matrix $M_3^T M_3$ by a_{11}, a_{22}, a_{33}, we have, from Equation (17)

$$
\begin{aligned}
a_{11} &= \left(\frac{\partial \dot{x}}{\partial R}\right)^2 + \left(\frac{\partial \dot{y}}{\partial R}\right)^2 + \left(\frac{\partial \dot{z}}{\partial R}\right)^2 \\
a_{22} &= \left(\frac{\partial \dot{x}}{\partial E}\right)^2 + \left(\frac{\partial \dot{y}}{\partial E}\right)^2 + \left(\frac{\partial \dot{z}}{\partial E}\right)^2 \\
a_{33} &= \left(\frac{\partial \dot{x}}{\partial A}\right)^2 + \left(\frac{\partial \dot{y}}{\partial A}\right)^2 + \left(\frac{\partial \dot{z}}{\partial A}\right)^2
\end{aligned} \tag{50}
$$

which, from Equation (20) becomes (after some reduction)

$$
\begin{aligned}
a_{11} &= \dot{E}^2 + \dot{A}^2 \cos^2 E \\
a_{22} &= \dot{R}^2 + \dot{E}^2 R^2 + \dot{A}^2 R^2 \sin^2 E \\
a_{33} &= (\dot{R} \cos E - \dot{E} R \sin E)^2 + \dot{A}^2 R^2 \cos^2 E
\end{aligned} \tag{51}
$$

From Equations (12), (26), and (51), we then have for the total instrumental mean-square velocity error

$$
\begin{aligned}
\sigma_{VI}^2 = {} & \sigma_{\dot{R}}^2 + R^2 \sigma_{\dot{E}}^2 + (R \cos E)^2 \sigma_{\dot{A}}^2 + (\dot{E}^2 + \dot{A}^2 \cos^2 E)\, \sigma_R^2 \\
& + (\dot{R}^2 + \dot{E}^2 R^2 + \dot{A}^2 R^2 \sin^2 E)\, \sigma_E^2 \\
& + \left[(\dot{R} \cos E - \dot{E} R \sin E)^2 + \dot{A}^2 R^2 \cos^2 E\right] \sigma_A^2
\end{aligned} \tag{52}
$$

Note that

$$
V^2 = \dot{R}^2 + (R\dot{E})^2 + (R\dot{A} \cos E)^2 \qquad (53
$$

from which
$$\frac{V^2 - \dot{R}^2}{R^2} = \dot{E}^2 + \dot{A}^2 \cos^2 E \tag{54}$$

which could be substituted into Equation (52), if convenient. If the fluctuating components of the error on the azimuth and elevation measurements have the same statistical properties and if these measurements are digitally smoothed and differentiated with the same operator, it follows that

$$\sigma^2_{\dot{E}} = \sigma^2_{\dot{A}} \tag{55}$$

Using Equations (28), (54), and (55), we can write Equation (52) in the form

$$\sigma^2_{VI} = \sigma^2_{\dot{R}} + \sigma^2_{\dot{A},\dot{E}} R^2 (1 + \cos^2 E) + \sigma^2_R \left(\frac{V^2 - \dot{R}^2}{R^2}\right) + \sigma^2_{A,E}\left[(R\dot{E})^2(1 + \sin^2 E) + \dot{R}^2(1 + \cos^2 E) + (R\dot{A})^2 - R\dot{E}\dot{R} \sin 2E\right] \tag{56}$$

It is still required to determine precisely what values of $\sigma^2(R)$, $\sigma^2(E)$, and $\sigma^2(A)$ should be used in calculating $\sigma^2(\dot{R})$, $\sigma^2(\dot{E})$, and $\sigma^2(\dot{A})$ by means of Equation (40). Since $\sigma^2(\eta)$ in Equation (40) is the variance of that portion of η which fluctuates from sample to sample, it does not include the contribution of the random bias. With the notation of Equation (41), we find that the variance which should be used in calculating $\sigma^2(\dot{R})$ from Equation (40) is $\sigma^2(X) = \sigma^2(X_k)$. To clearly identify the variances, we shall write the variance of the bias portion of a measurement error as $\sigma^2_b(\;\;)$, and the variance of the fluctuating or noiselike portion as $\sigma^2_n(\;\;)$. For example, we have

$$\sigma^2\left(R_k\right) = \sigma^2_b\left(R_k\right) + \sigma^2_n\left(R_k\right) \tag{57}$$

Then $\sigma^2(\dot{R})$, $\sigma^2(\dot{E})$, and $\sigma^2(\dot{A})$ in Equation (52) are to be calculated from the formulas

$$\sigma^2(\dot{R}) = \frac{6}{B_R T_R^3} \sigma^2_n(R) \tag{58}$$

$$\sigma^2(\dot{E}) = \frac{6}{B_E T_E^3} \sigma_n^2(E) \tag{59}$$

$$\sigma^2(\dot{A}) = \frac{6}{B_A T_A^3} \sigma_n^2(A) \tag{60}$$

The quantities $\sigma^2(R)$, $\sigma^2(E)$, $\sigma^2(A)$ which appear in Equation (52) are the mean-square values of the smoothed R, E, A measurements. Their precise values cannot be expressed in terms of the corresponding quantities $\sigma_b^2(\ )$ and $\sigma_n^2(\ )$ until the smoothing time T and the servo bandwidths are specified. However, in practice $\sigma^2(R)$, $\sigma^2(E)$, $\sigma^2(A)$ will generally be estimated from specified performance data without recourse to the details of the smoothing procedure. In any case, we see from Equation (45) that we shall always have

$$\sigma(R) \geq \sigma_b(R), \quad \sigma(E) \geq \sigma_b(E), \quad \sigma(A) \geq \sigma_b(A) \tag{61}$$

where equality holds when and only when the fluctuating components are absent.

To summarize, the mean-square instrumental error for position is given by Equation (27), where the values of σ_R^2, σ_A^2, and σ_E^2 to be used are the sums of the contributions from bias errors and fluctuation errors, after such smoothing as may be applied. The mean-square instrumental error for velocity is given by Equation (52), where the values for σ_R^2, σ_A^2, and σ_E^2 are the same as used in Equation (27) and the values of $\sigma_{\dot{R}}^2$, $\sigma_{\dot{A}}^2$, $\sigma_{\dot{E}}^2$ to be used are given by Equations (58), (59), and (60).

D. AZUSA AND MISTRAM INTERFEROMETERS

1. GENERAL

For this analysis, it is assumed that the interferometer legs are orthogonal and lie in a horizontal plane, and that the origin of coordinates is taken to lie at the phase center of the antenna employed for range and range-rate measurement. While these assumptions are not strictly valid, for Mistram in particular, they preserve the essential features of both the Mistram and Azusa tracking systems to a degree sufficient for an error analysis in which the effects of internal errors are included in the error estimates for the basic parameters measured by these systems. Finally, when the range to the vehicle is large relative to the interferometer baseline, we may view the interferometer portion of the system as measuring the cosines of the angle of arrival of the incident wave with respect to the directions of the baselines, together with their time derivatives. The geometry is illustrated in Figure 1 below, in which the range to the vehicle is assumed to be sufficiently great so that the parallel-ray geometry constitutes an adequate approximation. This is the case of primary interest for the applications of both the Mistram and Azusa tracking systems.

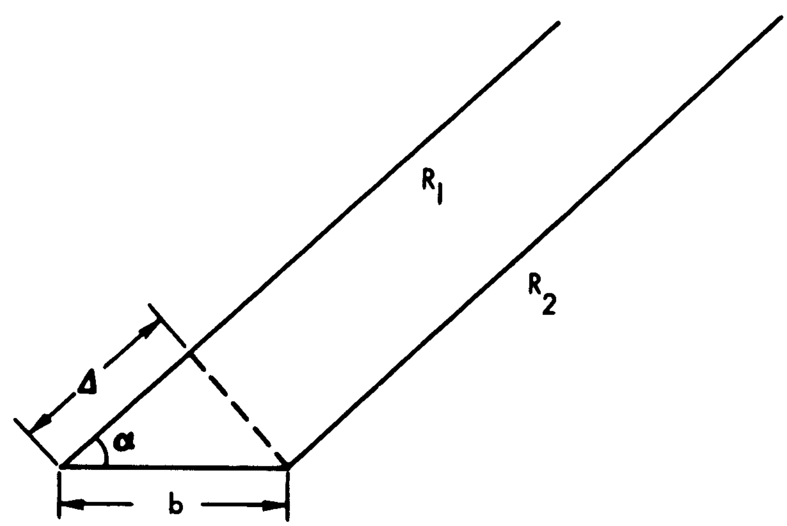

Figure 1. Parallel-Ray Geometry

From the figure it is clear that what the system actually measures by phase-comparison techniques is the range difference $\Delta = R_1 - R_2$, but that

$$\cos \alpha = \frac{\Delta}{b} = \frac{R_1 - R_2}{b} \tag{62}$$

so that the interpretation in terms of direction cosines is completely equivalent to the interpretation in terms of range differences. In the Azusa case, the cosine interpretation is most common, and accuracies are quoted in terms of errors in the direction cosines and the direction cosine rates, whereas in the Mistram case, accuracies are generally quoted in terms of the errors in the range differences, P and Q, and their time derivatives.

For the purpose of this analysis, it will prove notationally more convenient to employ the interpretation in terms of the cosines of the angles of arrival of the incident wave with respect to the directions of the system baselines. Since the baselines are taken to be orthogonal, we may suppose the baselines to lie in the X-Y plane and to be centered at the origin of the reference Cartesian coordinate system in which the positive direction of the Z axis lies upward along the local vertical. Moreover, we may take the interferometer legs to lie along the X and Y axes, respectively. With these assumptions and the additional convention that the angle of arrival of the incident ray is measured with respect to the positive direction of the appropriate X or Y coordinate axis, it follows that the cosines measured by the interferometer are precisely the direction cosines of the line of sight to the vehicle with respect to the Cartesian coordinate axes. If we write the direction cosines of this line of sight with respect to the X, Y, and Z axes as ℓ, m, n respectively, the three basic position parameters measured by the tracking system are R, ℓ, m. (Here R is range to the vehicle.) The remaining direction cosine is determined from the condition

$$\ell^2 + m^2 + n^2 = 1 \tag{63}$$

where it is understood that $n \geq 0$ since the vehicle must be above the horizon. The corresponding rate parameters are $\dot{R}$, $\dot{\ell}$, $\dot{m}$ (and the derived quantity $\dot{n}$, when convenient). The details of the manner in which the position and rate parameters are measured differ somewhat between Azusa and Mistram, but these differences are not germane to the present analysis.

2. VARIATIONAL EQUATIONS

The Cartesian coordinates of the vehicle are given by

$$\begin{aligned} x &= R\ell \\ y &= Rm \\ z &= Rn \end{aligned} \tag{64}$$

We will employ the matrix technique in a manner entirely analogous to its use in Section C of this appendix (the RAE radar). In this way, we obtain at once the expressions

$$\begin{bmatrix} \delta x \\ \delta y \\ \delta z \end{bmatrix} = M_1 \begin{bmatrix} \delta R \\ \delta \ell \\ \delta m \end{bmatrix} \tag{65}$$

and

$$\begin{bmatrix} \delta \dot{x} \\ \delta \dot{y} \\ \delta \dot{z} \end{bmatrix} = \begin{bmatrix} M_1 M_3 \end{bmatrix} \begin{bmatrix} \delta \dot{R} \\ \delta \dot{\ell} \\ \delta \dot{m} \\ \delta R \\ \delta \ell \\ \delta m \end{bmatrix} = M_1 \begin{bmatrix} \delta \dot{R} \\ \delta \dot{\ell} \\ \delta \dot{m} \end{bmatrix} + M_3 \begin{bmatrix} \delta R \\ \delta \ell \\ \delta m \end{bmatrix} \tag{66}$$

where the matrices M_1 and M_3 are given by

$$M_1 = \begin{bmatrix} \frac{\partial x}{\partial R} & \frac{\partial x}{\partial \ell} & \frac{\partial x}{\partial m} \\ \frac{\partial y}{\partial R} & \frac{\partial y}{\partial \ell} & \frac{\partial y}{\partial m} \\ \frac{\partial z}{\partial R} & \frac{\partial z}{\partial \ell} & \frac{\partial z}{\partial m} \end{bmatrix} \tag{67}$$

and

$$M_3 = \begin{bmatrix} \frac{\partial \dot{x}}{\partial \dot{R}} & \frac{\partial \dot{x}}{\partial \dot{\ell}} & \frac{\partial \dot{x}}{\partial \dot{m}} \\ \frac{\partial \dot{y}}{\partial \dot{R}} & \frac{\partial \dot{y}}{\partial \dot{\ell}} & \frac{\partial \dot{y}}{\partial \dot{m}} \\ \frac{\partial \dot{z}}{\partial \dot{R}} & \frac{\partial \dot{z}}{\partial \dot{\ell}} & \frac{\partial \dot{z}}{\partial \dot{m}} \end{bmatrix} \tag{68}$$

The fact that the matrix coefficient of the vector $(\delta\dot{R}, \delta\dot{\ell}, \delta\dot{m})$ in Equation (66) is the same as the coefficient of the vector $(\delta R, \delta\ell, \delta m)$ in Equation (65) is a consequence of the fact that

$$\frac{\partial \dot{x}}{\partial \dot{R}} = \frac{\partial x}{\partial R}, \qquad \frac{\partial \dot{x}}{\partial \dot{\ell}} = \frac{\partial x}{\partial \ell} \qquad \frac{\partial \dot{x}}{\partial \dot{m}} = \frac{\partial x}{\partial m}$$

with similar results for the other two Cartesian coordinates. The notation employed for the matrices is the same as that used in Section C of this appendix to emphasize the identity of the underlying methodology.

In evaluating the elements of M_1 and M_3, it will prove convenient to employ Equation (63) to obtain formulas for $\frac{\partial n}{\partial \ell}, \frac{\partial n}{\partial m}, \frac{\partial \dot{n}}{\partial \dot{\ell}}$, and $\frac{\partial \dot{n}}{\partial \dot{m}}$. Differentiation of Equation (63) with respect to ℓ yields

$$\ell + n\frac{\partial n}{\partial \ell} = 0$$

whence

$$\frac{\partial n}{\partial \ell} = -\frac{\ell}{n} \tag{69}$$

In the same fashion we find that

$$\frac{\partial n}{\partial m} = -\frac{m}{n} \tag{70}$$

To obtain expressions for the partial derivatives of $\dot{n}$ with respect to ℓ and m, we first differentiate Equation (63) with respect to time to obtain

$$\ell\dot{\ell} + m\dot{m} + n\dot{n} = 0 \tag{71}$$

On differentiating Equation (71) with respect to ℓ, we get

$$\dot{\ell} + \dot{n}\frac{\partial n}{\partial \ell} + n\frac{\partial \dot{n}}{\partial \ell} = 0$$

which may be solved for $\frac{\partial \dot{n}}{\partial \ell}$ in the form

$$\frac{\partial \dot{n}}{\partial \ell} = -\frac{1}{n}\left(\dot{\ell} + \dot{n}\frac{\partial n}{\partial \ell}\right) \tag{72}$$

Substitution of Equation (69) on the right side of Equation (72) finally yields

$$\frac{\partial \dot{n}}{\partial \ell} = \frac{\dot{n}\ell - n\dot{\ell}}{n^2} \tag{73}$$

In a similar fashion we have

$$\frac{\partial \dot{n}}{\partial m} = \frac{\dot{n}m - n\dot{m}}{n^2} \tag{74}$$

As a final preliminary, we differentiate Equation (64) with respect to time to obtain

$$\begin{aligned} \dot{x} &= \dot{R}\ell + R\dot{\ell} \\ \dot{y} &= \dot{R}m + R\dot{m} \\ \dot{z} &= \dot{R}n + R\dot{n} \end{aligned} \tag{75}$$

By use of Equations (64), (69), (70), (73), (74), and (75), we may immediately write the following explicit expressions for the matrices M_1 and M_3 defined by Equations (67) and (68)

$$M_1 = \begin{bmatrix} \ell & R & 0 \\ m & 0 & R \\ n & -R\frac{\ell}{n} & -R\frac{m}{n} \end{bmatrix} \tag{76}$$

$$M_3 = \begin{bmatrix} \dot{\ell} & \dot{R} & 0 \\ \dot{m} & 0 & \dot{R} \\ \dot{n} & -\dot{R}\frac{\ell}{n} + R\left(\frac{\dot{n}\ell - n\dot{\ell}}{n^2}\right) & -\dot{R}\frac{m}{n} + R\left(\frac{\dot{n}m - n\dot{m}}{n^2}\right) \end{bmatrix} \tag{77}$$

Precisely as in the previous analysis of the R, A, E radar, we obtain from Equations (65) and (66) the quadratic forms

$$(\delta\overline{R})^2 = (\delta x)^2 + (\delta y)^2 + (\delta z)^2 = \begin{bmatrix} \delta R \\ \delta \ell \\ \delta m \end{bmatrix}^T M_1^T \ M_1 \begin{bmatrix} \delta R \\ \delta \ell \\ \delta m \end{bmatrix} \tag{78}$$

and

$$(\delta\overline{V})^2 = (\delta\dot{x})^2 + (\delta\dot{y})^2 + (\delta\dot{z})^2 = \begin{bmatrix} \delta\dot{R} \\ \delta\dot{\ell} \\ \delta\dot{m} \end{bmatrix}^T M_1^T \ M_1 \begin{bmatrix} \delta\dot{R} \\ \delta\dot{\ell} \\ \delta\dot{m} \end{bmatrix}$$

$$+ \begin{bmatrix} \delta R \\ \delta \ell \\ \delta m \end{bmatrix}^T M_3^T \ M_3 \begin{bmatrix} \delta R \\ \delta \ell \\ \delta m \end{bmatrix} + 2 \begin{bmatrix} \delta\dot{R} \\ \delta\dot{\ell} \\ \delta\dot{m} \end{bmatrix}^T M_1^T \ M_3 \begin{bmatrix} \delta R \\ \delta \ell \\ \delta m \end{bmatrix} \tag{79}$$

3. STATISTICAL CONSIDERATIONS

To obtain the mean-square values of $(\delta\overline{R})^2$ and $(\delta\overline{V})^2$ we have now only to take the expectations on the right and sides of Equations (78) and (79). For this purpose it is essential to have some information concerning the statistical properties of the errors δR, $\delta \ell$, δm, $\delta\dot{R}$, $\delta\dot{\ell}$, $\delta\dot{m}$. These properties are the subject of the following discussion.

In general, it is to be expected that the errors $\delta \ell$, δm will be correlated because a portion of these errors is caused by propagation phenomena common to both legs of the interferometer. For the Mistram case, the fact that a common receiving system is employed at one end of the ℓ and m legs of the interferometer also implies that instrumental errors in this receiving system will be common to both the ℓ and m measurements. Similar comments are applicable to correlation among the errors $\delta\dot{\ell}$ and $\delta\dot{m}$. The correlation between a direction cosine error, $\delta \ell$, and the cosine rate error, $\delta\dot{\ell}$, may also be expected to depend, at least partially, on the details of the system implementation. The same holds almost without exception, for the various possible pairs of errors.

The net result of this state of affairs is to introduce a degree of complexity which renders a precise evaluation of the mean-square position and velocity errors impractical without a very detailed consideration of the system implementation and of the propagation phenomena which play such an important role in determining the performance of a precision tracking system.

Moreover, to evaluate the performance of the tracking system in question, we propose to be as realistic as possible by employing experimental data concerning the rms values of the errors $\delta\dot{R}$, $\delta\dot{\ell}$, $\delta\dot{m}$, δR, $\delta\ell$, δm. Unfortunately, while the rms values of these quantities have been measured, inferred, or estimated from experimental data, no significant information is available concerning the correlations between them. For the same reason, no reliable information is available concerning permanent biases in the measured parameters. As a consequence, the only reasonable statistical hypothesis permitting use of available data is that the errors in the measured parameters have zero means and are uncorrelated. While this hypothesis is certainly not strictly valid, it is felt to constitute the best single hypothesis permitting effective use to be made of available data. In any event, the resulting accuracy estimates (while not exact) should be adequate for planning purposes.

Subject to the hypothesis (introduced above) that the errors in the measured parameters have zero means and are uncorrelated (on an *a priori* basis), it follows that $\delta\overline{R}$ and $\delta\overline{V}$ also have zero means, so that we may use their variances for their mean-square values. If we now take the expectations in Equations (78) and (79), it follows from the foregoing statistical hypotheses that the mean-square values of $\delta\overline{R}$ and $\delta\overline{V}$ are given by

$$\sigma_I^{\,2}(\delta\overline{R}) = b_{11}\,\sigma^2(R) + b_{22}\,\sigma^2(\ell) + b_{33}\,\sigma^2(m) \tag{80}$$

and

$$\sigma_I^{\,2}(\delta\overline{V}) = b_{11}\,\sigma^2(\dot{R}) + b_{22}\,\sigma^2(\dot{\ell}) + b_{33}\,\sigma^2(\dot{m}) + c_{11}\,\sigma^2(R) + c_{22}\,\sigma^2(\ell) + c_{33}\,\sigma^2(m) \tag{81}$$

where we have employed b_{jk} for the elements of the matrix $M_1{}^T M_1$ and c_{jk} for the elements of the matrix $M_3{}^T M_3$. The subscript I indicates that the errors given by Equations (80) and (81) are the so-called "instrumental" errors, referred to previously.

By straightforward matrix multiplication and use of Equation (63) we find at once from Equation (76) that

$$\begin{aligned} b_{11} &= 1 \\ b_{22} &= R^2\left(1+\left(\frac{\ell}{n}\right)^2\right) \\ b_{33} &= R^2\left(1+\left(\frac{m}{n}\right)^2\right) \end{aligned} \tag{82}$$

and from Equation (77)

$$\begin{aligned} c_{11} &= \dot{\ell}^2 + \dot{m}^2 + \dot{n}^2 \\ c_{22} &= \dot{R}^2 + \left[\dot{R}\,\frac{\ell}{n} + R\left(\frac{n\dot{\ell} - \dot{n}\ell}{n^2}\right)\right]^2 \\ c_{33} &= \dot{R}^2 + \left[\dot{R}\,\frac{m}{n} + R\left(\frac{n\dot{m} - \dot{n}m}{n^2}\right)\right]^2 \end{aligned} \tag{83}$$

In principle, Equations (80), (81), (82), and (83) complete the error analysis. However, it will be worthwhile to pursue the implications of these equations somewhat further to exhibit their geometrical significance and to obtain formulas more convenient for numerical computation. For this purpose, it is reasonable to make the additional assumption that

$$\begin{aligned} \sigma(\ell) &= \sigma(m) \\ \sigma(\dot{\ell}) &= (\dot{m}) \end{aligned} \tag{84}$$

Under the conditions of Equation (84), Equations (80) and (81) become, respectively,

$$\sigma_I{}^2\,(\delta\bar{R}) = \sigma^2\,(R) + (b_{22} + b_{33})\,\sigma^2\,(\ell) \tag{85}$$

and

$$\sigma_I^2(\delta\overline{V}) = \sigma^2(\dot{R}) + \left(b_{22} + b_{33}\right)\sigma^2(\dot{\ell})$$
$$+ c_{11}\,\sigma^2(R) + \left(c_{22} + c_{33}\right)\sigma^2(\ell) \tag{86}$$

We now have

$$b_{22} + b_{33} = R^2\left\{2 + \left(\frac{\ell}{n}\right)^2 + \left(\frac{m}{n}\right)^2\right\}$$
$$= R^2\left\{1 + \frac{\ell^2 + m^2 + n^2}{n^2}\right\}$$
$$= R^2\left(1 + \frac{1}{n^2}\right) \tag{87}$$

On recalling that n = sin E, where E is the elevation angle, we see that

$$b_{22} + b_{33} = R^2\,(1 + \csc^2 E) \tag{88}$$

A straightforward calculation using the equivalent spherical polar coordinate expressions for ℓ, m, and n yields, after some simplifications,

$$c_{11} = \dot{E}^2 + \dot{A}^2\cos^2 E$$

$$c_{22} + c_{33} = 2\dot{R}^2 + \left(R\dot{E}\csc^2 E - \dot{R}\cot E\right)^2 + R^2\dot{A}^2\cot^2 E \tag{89}$$

The expression for c_{11} may be given an alternative interpretation by observing that

$$\dot{E}^2 + \dot{A}^2\cos^2 E = \frac{(R\dot{E})^2 + (R\dot{A}\cos E)^2}{R^2} = \frac{V^2 - \dot{R}^2}{R^2} \tag{90}$$

since $(R\dot{E})^2 + (R\dot{A}\cos E)^2$ is the square of the component of the vehicle velocity normal to the line of sight. By means of Equation (90), we have

$$c_{11} = \frac{V^2 - \dot{R}^2}{R^2} \tag{91}$$

The basic equations for determination of the instrumental position and velocity errors are then

$$\sigma_{PI}^2 = \sigma_R^2 + R^2 (1 + \csc^2 E) \sigma_{\ell, m}^2 \tag{92}$$

$$\sigma_{VI}^2 = \sigma_{\dot{R}}^2 + R^2 \left(1 + \csc^2 E\right) \sigma_{\dot{\ell}, \dot{m}}^2 + \frac{V^2 - \dot{R}^2}{R^2} \sigma_R^2$$

$$+ \left[2\dot{R}^2 + \left(R\dot{E} \csc^2 E - \dot{R} \cot E\right)^2 + R^2 \dot{A}^2 \cot^2 E\right] \sigma_{\ell, m}^2 \tag{93}$$

E. GERTS

1. GENERAL

The GERTS tracking system is a combination of a CW interferometer system which measures range rate, $\dot{R}$, and direction cosine rates (or, equivalently, range-rate differences), $\dot{\ell}$ and $\dot{m}$, with a pulse radar which measures range, R, azimuth, A, and elevation, E. The procedure to be followed for the analysis will be similar to that employed for the R, A, E radar and for the Asuza and Mistram tracking systems. Some care is required to account properly for the fact that basically different coordinate systems (measured parameter sets) are employed for position and rate measurement. The notation and conventions used in these analyses will be employed without additional explanation. It is understood that the position-measuring radar is located at the origin of the reference Cartesian coordinate system.

The Cartesian coordinates are given in terms of the measured parameters by

$$\begin{aligned} x &= R \cos E \cos A \\ y &= R \cos E \sin A \\ z &= R \sin E \end{aligned} \tag{94}$$

while rates are given by Equation (75), derived in the interferometer analysis analysis and repeated below for reference.

$$\begin{aligned} \dot{x} &= \dot{R}\ell + R\dot{\ell} \\ \dot{y} &= \dot{R}m + R\dot{m} \\ \dot{z} &= \dot{R}n + R\dot{n} \end{aligned} \tag{75}$$

In Equation (75), the range, R, and the direction cosines, ℓ and m, are now determined by means of the R, A, E measurements of the tracking radar. The direction cosines are given explicitly in terms of the measured angles by

$$\begin{aligned} \ell &= \cos E \cos A \\ m &= \cos E \sin A \\ n &= \sin E \end{aligned} \tag{95}$$

E. GERTS

1. GENERAL

The GERTS tracking system is a combination of a CW interferometer system which measures range rate, $\dot{R}$, and direction cosine rates (or, equivalently, range-rate differences), $\dot{\ell}$ and $\dot{m}$, with a pulse radar which measures range, R, azimuth, A, and elevation, E. The procedure to be followed for the analysis will be similar to that employed for the R, A, E radar and for the Asuza and Mistram tracking systems. Some care is required to account properly for the fact that basically different coordinate systems (measured parameter sets) are employed for position and rate measurement. The notation and conventions used in these analyses will be employed without additional explanation. It is understood that the position-measuring radar is located at the origin of the reference Cartesian coordinate system.

The Cartesian coordinates are given in terms of the measured parameters by

$$\begin{aligned} x &= R \cos E \cos A \\ y &= R \cos E \sin A \\ z &= R \sin E \end{aligned} \qquad (94)$$

while rates are given by Equation (75), derived in the interferometer analysis analysis and repeated below for reference.

$$\begin{aligned} \dot{x} &= \dot{R}\ell + R\dot{\ell} \\ \dot{y} &= \dot{R}m + R\dot{m} \\ \dot{z} &= \dot{R}n + R\dot{n} \end{aligned} \qquad (75)$$

In Equation (75), the range, R, and the direction cosines, ℓ and m, are now determined by means of the R, A, E measurements of the tracking radar. The direction cosines are given explicitly in terms of the measured angles by

$$\begin{aligned} \ell &= \cos E \cos A \\ m &= \cos E \sin A \\ n &= \sin E \end{aligned} \qquad (95)$$

Also, the quantity $\dot{n}$ is a derived rather than measured quantity. By use of Equation (71), $\dot{n}$ may be expressed as

$$\dot{n} = -\frac{\ell\dot{\ell} + m\dot{m}}{n}$$

from which we obtain by substitution, using Equation (95)

$$\dot{n} = -\dot{\ell}\cot E \cos A - \dot{m} \cot E \sin A. \tag{96}$$

Substitution of the result expressed by Equation (96) into Equation (75) and use of Equation (95) yields the rate equations

$$\begin{aligned} \dot{x} &= \dot{R} \cos E \cos A + R\dot{\ell} \\ \dot{y} &= \dot{R} \cos E \sin A + R\dot{m} \\ \dot{z} &= \dot{R} \sin E - R \cot E \quad (\dot{\ell} \cos A + \dot{m} \sin A) \end{aligned} \tag{97}$$

which express $\dot{x}$, $\dot{y}$, $\dot{z}$ directly in terms of the measured parameters.

In the following analysis, only the instrumental velocity error will be derived, based on Equation (97). Since the position determination of the GERTS is precisely that of an RAE radar, the mean-square position error is given by Equation (27).

2. VARIATIONAL EQUATION

The variational equation has the form

$$\begin{bmatrix} \delta\dot{x} \\ \delta\dot{y} \\ \delta\dot{z} \end{bmatrix} = N_1 \begin{bmatrix} \delta\dot{R} \\ \delta\dot{\ell} \\ \delta\dot{m} \end{bmatrix} + N_2 \begin{bmatrix} \delta R \\ \delta E \\ \delta A \end{bmatrix} \tag{98}$$

where

$$N_1 = \begin{bmatrix} \frac{\partial \dot{x}}{\partial \dot{R}} & \frac{\partial \dot{x}}{\partial \dot{\ell}} & \frac{\partial \dot{x}}{\partial \dot{m}} \\ \frac{\partial \dot{y}}{\partial \dot{R}} & \frac{\partial \dot{y}}{\partial \dot{\ell}} & \frac{\partial \dot{y}}{\partial \dot{m}} \\ \frac{\partial \dot{z}}{\partial \dot{R}} & \frac{\partial \dot{z}}{\partial \dot{\ell}} & \frac{\partial \dot{z}}{\partial \dot{m}} \end{bmatrix} \tag{99}$$

and

$$N_2 = \begin{bmatrix} \frac{\partial \dot{x}}{\partial R} & \frac{\partial \dot{x}}{\partial E} & \frac{\partial \dot{x}}{\partial A} \\ \frac{\partial \dot{y}}{\partial R} & \frac{\partial \dot{y}}{\partial E} & \frac{\partial \dot{y}}{\partial A} \\ \frac{\partial \dot{z}}{\partial R} & \frac{\partial \dot{z}}{\partial E} & \frac{\partial \dot{z}}{\partial A} \end{bmatrix} \tag{100}$$

From Equation (98) the square of the velocity error $\delta\overline{V}$ is

$$(\delta\overline{V})^2 = (\delta\dot{x})^2 + (\delta\dot{y})^2 + (\delta\dot{z})^2 = \begin{bmatrix}\delta\dot{R}\\ \delta\dot{\ell}\\ \delta\dot{m}\end{bmatrix}^T N_1^T N_1 \begin{bmatrix}\delta\dot{R}\\ \delta\dot{\ell}\\ \delta\dot{m}\end{bmatrix}$$

$$+ \begin{bmatrix}\delta R\\ \delta E\\ \delta A\end{bmatrix}^T N_2^T N_2 \begin{bmatrix}\delta R\\ \delta E\\ \delta A\end{bmatrix} + 2 \begin{bmatrix}\delta\dot{R}\\ \delta\dot{\ell}\\ \delta\dot{m}\end{bmatrix}^T N_1^T N_2 \begin{bmatrix}\delta R\\ \delta E\\ \delta A\end{bmatrix} \qquad (101)$$

Next we differentiate Equation (97) to obtain explicit expressions for the matrices N_1 and N_2. In this way, we obtain

$$N_1 = \begin{bmatrix} \cos E \cos A & R & 0 \\ \cos E \sin A & 0 & R \\ \sin E & -R \cot E \cos A & -R \cot E \sin A \end{bmatrix} \qquad (102)$$

and

$$N_2 = \begin{bmatrix} \dot{\ell} & -\dot{R} \sin E \cos A & -\dot{R} \cos E \sin A \\ \dot{m} & -\dot{R} \sin E \sin A & \dot{R} \cos E \cos A \\ \cot E \cdot(\dot{\ell} \cos A + \dot{m} \sin A) & \dot{R} \cos E + R \csc^2 E \cdot(\dot{\ell} \cos A + \dot{m} \sin A) & -R \cot E \cdot(-\dot{\ell} \sin A + \dot{m} \cos A) \end{bmatrix} \qquad (103)$$

Henceforth, we shall write for the elements of the matrices in Equation (101),

$$N_1^T N_1 = \left[\alpha_{jk}\right], \qquad N_2^T N_2 = \left[\beta_{jk}\right] \qquad (104)$$

3. STATISTICAL CONSIDERATIONS

We turn now to the essential statistical considerations. As for the position- and rate-tracking interferometer analyzed previously, we make the assumption that the various instrumental errors in the measured position and rate parameters are uncorrelated and have zero means. Actually, one would expect some correlation between $\delta\dot{\ell}$ and $\delta\dot{m}$, for the

reasons explained in the earlier analysis. However, for present purposes, the statistical hypotheses considered seem most appropriate on the same basis as in the interferometer error analysis.

Under the statistical hypotheses indicated above, we may take the expectation on both sides of Equation (101) to obtain

$$\sigma_{VI}^2 = \alpha_{11}\sigma_{\dot{R}}^2 + \alpha_{22}\sigma_{\dot{\ell}}^2 + \alpha_{33}\sigma_{\dot{m}}^2 + \beta_{11}\sigma_R^2 + \beta_{22}\sigma_E^2 + \beta_{33}\sigma_A^2 \tag{105}$$

The assumption that $\delta\dot{R}$, $\delta\dot{\ell}$, $\delta\dot{m}$, δR, δE, and δA are all uncorrelated and have zero means makes it unnecessary to calculate any elements of the matrix $N_1^T N_2$.

From Equation (102) we have

$$\begin{aligned} \alpha_{11} &= 1 \\ \alpha_{22} &= R^2(1 + \cot^2 E\cos^2 A) \\ \alpha_{33} &= R^2(1 + \cot^2 E\sin^2 A) \end{aligned} \tag{106}$$

From Equation (103), after simplification, we have

$$\begin{aligned} \beta_{11} &= \dot{E}^2 + \dot{A}^2\cos^2 E = \frac{V^2 - \dot{R}^2}{R^2} \\ \beta_{22} &= \dot{R}^2 + (\dot{R}\dot{E}\csc E)^2 - 2R\dot{R}\dot{E}\cot E = (\dot{R} - R\dot{E}\cot E)^2 + (R\dot{E})^2 \\ \beta_{33} &= \cos^2 E(\dot{R}^2 + R^2\dot{A}^2\cot^2 E) \end{aligned} \tag{107}$$

We can make the additional hypothesis that

$$\sigma_{\dot{\ell}} = \sigma_{\dot{m}} \tag{108}$$

which is eminently reasonable on physical grounds. From Equation (106) we have

$$\alpha_{22} + \alpha_{33} = R^2(1 + \cot^2 E) = R^2\csc^2 E \tag{109}$$

From Equations (106), (108), and (109), we can write Equation (105) in the form

$$\sigma_{VI}^2 = \sigma_{\dot{R}}^2 + (R \csc E)^2 \sigma_{\dot{\ell}, \dot{m}}^2 + \beta_{11} \sigma_R^2 + \beta_{22} \sigma_E^2 + \beta_{33} \sigma_A^2 \qquad (110)$$

Equations (110) and (107) now provide the expressions for mean-square instrumental velocity error of the GERTS.

F. TRILATERATION NETWORKS

1. INTRODUCTION

The method of analysis used for the radar and interferometer proved impractical for the trilateration network. This resulted, principally, because there is no one natural Cartesian coordinate system for the problem; and the expressions resulting from the squaring of partial derivatives became too unwieldy. Instead, a vectorial approach was used permitting derivation of expressions for σ_P^2 and σ_V^2 without introducing a coordinate system. However, to utilize these expressions for calculation of numerical results, a Cartesian coordinate system must be introduced.

The development proceeds in the following manner:

- Step 1. Variational equations are derived for the vector position error, $\delta\overline{R}$, and velocity error, $\delta\overline{V}$, in terms of variations in range and range rate from each of three stations, without regard to the sources of these variations.
- Step 2. Vector expressions are developed for the equivalent variations at each station $\left(\delta\overline{R}_k, \delta\dot{\overline{R}}_k, k = 1, 2, 3\right)$ caused by both instrument and station location errors. These expressions are then substituted into the results of Step 1 to derive expressions for $\delta\overline{R}$ and $\delta\overline{V}$ in terms of the instrument and survey errors.
- Step 3. Utilizing the results of Step 2, expressions are derived for the mean-square position and velocity errors in terms of the statistical properties of the basic error sources.

2. VARIATIONAL EQUATIONS

a. General

During the analysis, it will be necessary to make use of the following result which is stated as a lemma:

Let $\overline{a}_k$ (k = 1, 2, 3) and $\overline{x}$ be vectors in three-dimensional space and let b_k (k = 1, 2, 3) be scalars. The necessary and sufficient condition that the set of equations

$$\overline{a}_k \cdot \overline{x} = b_k \qquad (k = 1, 2, 3) \tag{111}$$

should have a unique solution is that

$$(\bar{a}_1 \, \bar{a}_2 \, \bar{a}_3) \neq 0, \tag{112}$$

where $(\bar{a}_1 \bar{a}_2 \bar{a}_3)$ is the triple scalar product, which is given by $\bar{a}_1 \cdot \bar{a}_2 x \bar{a}_3$ or any cyclic variation thereof. When the condition of Equation (112) is satisfied, the unique solution of Equation (111) is given by

$$\bar{x} = \frac{b_1\left(\bar{a}_2 \times \bar{a}_3\right) + b_2\left(\bar{a}_3 \times \bar{a}_1\right) + b_3\left(\bar{a}_1 \times \bar{a}_2\right)}{(\bar{a}_1 \, \bar{a}_2 \, \bar{a}_3)} \tag{113}$$

b. <u>Position Error</u>

Consider first the manner in which variations δR_1, δR_2, δR_3 in the measured ranges R_1, R_2, R_3 cause a vector variation $\delta \bar{R}$ in the vehicle position defined by the trilateration network. The vectors from the three tracking stations will be written as $\bar{R}_1$, $\bar{R}_2$, $\bar{R}_3$ or in general $\bar{R}_k$ from the kth tracking station. The unit vectors in these directions will be designated as $\bar{u}_1$, $\bar{u}_2$, $\bar{u}_3$ or, in general, $\bar{u}_k$.

Now

$$\bar{R}_k \cdot \bar{R}_k = R_k^2 \tag{114}$$

from which

$$\bar{R}_k \cdot \delta \bar{R}_k = R_k \, \delta R_k \tag{115}$$

Noting that $\delta \bar{R}_k = \delta \bar{R}$, Equation (115) thus becomes

$$\bar{R}_k \cdot \delta \bar{R} = R_k \, \delta R_k \tag{116}$$

and after division by R_k

$$\bar{u}_k \cdot \delta \bar{R} = \delta R_k \quad (k = 1, 2, 3) \tag{117}$$

Use of the lemma, Equation (113), therefore gives

$$\delta \bar{R} = \frac{\left(\bar{u}_2 \times \bar{u}_3\right) \delta R_1 + \left(\bar{u}_3 \times \bar{u}_1\right) \delta R_2 + \left(\bar{u}_1 \times \bar{u}_2\right) \delta R_3}{(\bar{u}_1 \, \bar{u}_2 \, \bar{u}_3)} \tag{118}$$

Equation (118) may be put in a form better suited to geometrical interpretation. Let us determine the geometrical interpretation for the coefficients of δR_1, δR_2, δR_3. First define a unit vector $\bar{u}_{23}$ by the equation

$$\bar{u}_{23} = \frac{\bar{u}_2 \times \bar{u}_3}{\left| \bar{u}_2 \times \bar{u}_3 \right| \operatorname{sgn}\left(\bar{u}_1 \, \bar{u}_2 \, \bar{u}_3\right)} \tag{119}$$

where $\left|\bar{x}\right|$ is the length of a vector $\bar{x}$ and sgn x is $+1$ if $x > 0$, and -1 if $x < 0$.

The coefficient of δR_1 in Equation (118) may now be written in the form

$$\frac{\left(\bar{u}_2 \times \bar{u}_3\right)}{\left(\bar{u}_1 \, \bar{u}_2 \, \bar{u}_3\right)} = \frac{\bar{u}_{23}}{\bar{u}_1 \cdot \bar{u}_{23}} \tag{120}$$

It is apparent that $\bar{u}_{23}$ is a unit vector normal to the plane defined by the second and third tracking stations and the vehicle. It is also obvious that although reversal of the order of multiplication of $\bar{u}_2$ and $\bar{u}_3$ causes the sign of the numerator in Equation (120) to reverse, the sign of the denominator also is reversed and, therefore, the unit normal vector $\bar{u}_{23}$ is invariant in direction with regard to the order of multiplication.

The physical interpretation of this fact is that the direction of $\bar{u}_{23}$ does not depend on the direction in which the stations are numbered (i.e., clockwise or counterclockwise) when looking down at the earth from the vehicle. It can be shown that the direction of $\bar{u}_{23}$ is always upwards and away from station 1, as illustrated in Figure 2. (The observer is looking along the edge of the plane formed by the intersection of $\bar{R}_2$ and $\bar{R}_3$ at the vehicle.)

A physical interpretation of the direction of $\bar{u}_{23}$ can be gained by considering a positive displacement in the length of $\bar{R}_1$, while the lengths of $\bar{R}_2$ and $\bar{R}_3$ are held constant. This displacement would cause the plane $\bar{R}_2$, $\bar{R}_3$ to rotate about the line joining stations 2 and 3, and the apparent position of the vehicle would be displaced in the direction $\bar{u}_{23}$, normal to this plane.

The scalar product $\bar{u}_1 \cdot \bar{u}_{23}$ is given by

$$\bar{u}_1 \cdot \bar{u}_{23} = \cos \phi_1' \tag{121}$$

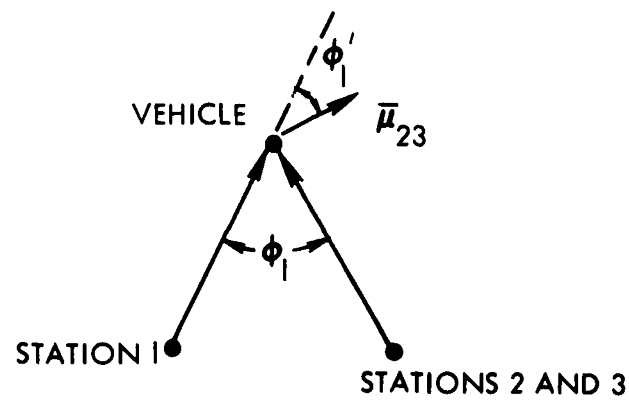

Figure 2. Direction of $\bar{u}_{23}$

where ϕ_1' is the angle between the directions of $\bar{u}_1$ and $\bar{u}_{23}$. Since, from Equation (119), $\bar{u}_1 \cdot \bar{u}_{23} > 0$, the angle ϕ_1 is acute and the result may be placed in an alternative form where

$$\phi_1 = 90^0 - \phi_1' \tag{122}$$

As thus defined, ϕ_1 is the acute angle between $\bar{R}_1$ and the plane defined by $\bar{R}_2$ and $\bar{R}_3$. In terms of ϕ_1, Equation (121) becomes

$$\bar{u}_1 \cdot \bar{u}_{23} = \sin \phi_1 \tag{123}$$

The same result holds for the other two terms on the right of Equation (118). Therefore, Equation (118) may be put in the following form to facilitate geometrical interpretation:

$$\delta\bar{R} = \bar{u}_{23} \csc \phi_1 \delta R_1 + \bar{u}_{31} \csc \phi_2 \delta R_2 + \bar{u}_{12} \csc \phi_3 \delta R_3 \tag{124}$$

c. Velocity Error

Differentiation of Equation (114) with respect to time and use of the fact that $\dot{\bar{R}}_k = \bar{V}$ yields

$$\bar{R}_k \cdot \bar{V} \quad R_k \dot{R}_k \tag{125}$$

from which

$$\bar{R}_k \cdot \delta\bar{V} + \bar{V} \cdot \delta\bar{R}_k = R_k \delta\dot{R}_k + \dot{R}_k \delta R_k \tag{126}$$

On recalling that $\delta\bar{R}_k = \delta\bar{R}$, Equation (126) can be expressed as

$$\bar{u}_k \cdot \delta\bar{V} = \delta\dot{R}_k + \frac{\dot{R}_k \delta R_k - \bar{V} \cdot \delta\bar{R}}{R_k} \tag{127}$$

Use of the lemma, Equation (113), gives as a solution of Equation (127)

$$\begin{aligned} \left(\bar{u}_1 \bar{u}_2 \bar{u}_3\right) \delta\bar{V} = {} & \left(\bar{u}_2 \times \bar{u}_3\right) \left\{\delta\dot{R}_1 + \frac{\dot{R}_1 \delta R_1 - \bar{V} \cdot \delta\bar{R}}{R_1}\right\} \\ & + \left(\bar{u}_3 \times \bar{u}_1\right) \left\{\delta\dot{R}_2 + \frac{\dot{R}_2 \delta R_2 - \bar{V} \cdot \delta\bar{R}}{R_2}\right\} \\ & + \left(\bar{u}_1 \times \bar{u}_2\right) \left\{\delta\dot{R}_3 + \frac{\dot{R}_3 \delta R_3 - \bar{V} \cdot \delta\bar{R}}{R_3}\right\} \end{aligned} \tag{128}$$

Making use of Equations (120) and (123), Equation (128) can be written

$$\begin{aligned} \delta\bar{V} = {} & \bar{u}_{23} \csc\phi_1 \left\{\delta\dot{R}_1 + \frac{\dot{R}_1 \delta R_1 - \bar{V} \cdot \delta\bar{R}}{R_1}\right\} \\ & + \bar{u}_{31} \csc\phi_2 \left\{\delta\dot{R}_2 + \frac{\dot{R}_2 \delta R_2 - \bar{V} \cdot \delta\bar{R}}{R_2}\right\} \\ & + \bar{u}_{12} \csc\phi_3 \left\{\delta\dot{R}_3 + \frac{\dot{R}_3 \delta R_3 - \bar{V} \cdot \delta\bar{R}}{R_3}\right\} \end{aligned} \tag{129}$$

Inserting the explicit expression for $\delta\bar{R}$, given by Equation (124), into Equation (129) and collecting terms yield

$$\begin{aligned} \delta\bar{V} = {} & \bar{u}_{23} \csc\phi_1 \delta\dot{R}_1 + \bar{u}_{31} \csc\phi_2 \delta\dot{R}_2 + \bar{u}_{12} \csc\phi_3 \delta\dot{R}_3 \\ & - \bar{B}_1 \delta R_1 - \bar{B}_2 \delta R_2 - \bar{B}_3 \delta R_3 \end{aligned} \tag{130}$$

where

$$\begin{aligned}\bar{B}_1 = {} & \bar{u}_{23} \csc \phi_1 \left[\bar{V} \cdot \bar{u}_{23} \csc \phi_1 - \dot{R}_1\right] / R_1 \\ & + \bar{u}_{31} \csc \phi_2 \left[\bar{V} \cdot \bar{u}_{23} \csc \phi_1\right] / R_2 \\ & + \bar{u}_{12} \csc \phi_3 \left[\bar{V} \cdot \bar{u}_{23} \csc \phi_1\right] / R_3\end{aligned} \tag{131}$$

$$\begin{aligned}\bar{B}_2 = {} & \bar{u}_{23} \csc \phi_1 \left[\bar{V} \cdot \bar{u}_{31} \csc \phi_2\right] / R_1 \\ & + \bar{u}_{31} \csc \phi_2 \left[\bar{V} \cdot \bar{u}_{31} \csc \phi_2 - \dot{R}_2\right] / R_2 \\ & + \bar{u}_{12} \csc \phi_3 \left[\bar{V} \cdot \bar{u}_{31} \csc \phi_2\right] / R_3\end{aligned} \tag{132}$$

$$\begin{aligned}\bar{B}_3 = {} & \bar{u}_{23} \csc \phi_1 \left[\bar{V} \cdot \bar{u}_{12} \csc \phi_3\right] / R_1 \\ & + \bar{u}_{31} \csc \phi_2 \left[\bar{V} \cdot \bar{u}_{12} \csc \phi_3\right] / R_2 \\ & + \bar{u}_{12} \csc \phi_3 \left[\bar{V} \cdot \bar{u}_{12} \csc \phi_3 - \dot{R}_3\right] / R_3\end{aligned} \tag{133}$$

Equations (124) and (130) are then the desired basic variational equations, giving position and velocity variations as a function of the individual scalar variations δR_1, δR_2, δR_3, $\delta \dot{R}_1$, $\delta \dot{R}_2$, $\delta \dot{R}_3$, without regard to the source of these variations.

3. INSTRUMENTAL ERRORS

a. General

Let the instrumental errors in range and range rate be represented by

$$\delta R_{Ik} = W_k + X \tag{134}$$

$$\delta \dot{R}_{Ik} = Y_k + Z \tag{135}$$

where W_k and Y_k represent errors uncorrelated between stations, and X and Z represent completely correlated (i.e., bias) errors, common to all three stations. The random variables W_k, X, Y_k, and Z may reasonably be taken to have zero mean values.

b. Position Error

For position error due to uncorrelated range error, substitution of Equation (134) into Equation (124) yields

$$\delta\bar{R}_W = \bar{u}_{23} \csc \phi_1 W_1 + \bar{u}_{31} \csc \phi_2 W_2 + \bar{u}_{12} \csc \phi_3 W_3 \tag{136}$$

and due to a common correlated range error

$$\delta\bar{R}_X = \left(\bar{u}_{23} \csc \phi_1 + \bar{u}_{31} \csc \phi_2 + \bar{u}_{12} \csc \phi_3\right) X \tag{137}$$

The coefficient of X in Equation (137) has a geometric interpretation more easily derived if the coefficient is expressed in the form resulting from substitution of Equation (134) into Equation (118), yielding

$$\delta\bar{R}_X = \frac{\left(\bar{u}_2 \times \bar{u}_3\right) + \left(\bar{u}_3 \times \bar{u}_1\right) + \left(\bar{u}_1 \times \bar{u}_2\right)}{\left(\bar{u}_1\ \bar{u}_2\ \bar{u}_3\right)} X \tag{138}$$

Define a unit vector $\bar{n}$ by the equation

$$\bar{n} = \frac{\left(\bar{u}_2 \times \bar{u}_3\right) + \left(\bar{u}_3 \times \bar{u}_1\right) + \left(\bar{u}_1 \times \bar{u}_2\right)}{\left| \left(\bar{u}_2 \times \bar{u}_3\right) + \left(\bar{u}_3 \times \bar{u}_1\right) + \left(\bar{u}_1 \times \bar{u}_2\right) \right| \operatorname{sgn}\left(\bar{u}_1\ \bar{u}_2\ \bar{u}_3\right)} \tag{139}$$

Consider the tetrahedron formed by the unit vectors $\bar{u}_1$, $\bar{u}_2$, and $\bar{u}_3$ emanating from the vehicle. The base of the tetrahedron is the plane containing the tips of these vectors, and the altitude, h, is measured from this base to the vehicle. Observe that $(\bar{u}_1 - \bar{u}_2)$ and $(\bar{u}_1 - \bar{u}_3)$ lie in the plane of the base of the tetrahedron and that the vector product $(\bar{u}_1 - \bar{u}_2) \times (\bar{u}_1 - \bar{u}_3)$, therefore, is normal to the plane of this base.

Now let a vector $\bar{m}$ be defined by the vector product

$$\begin{aligned} \bar{m} &= \left(\bar{u}_1 - \bar{u}_2\right) \times \left(\bar{u}_1 - \bar{u}_3\right) \\ &= \left(\bar{u}_1 \times \bar{u}_1\right) - \left(\bar{u}_1 \times \bar{u}_3\right) - \left(\bar{u}_2 \times \bar{u}_1\right) + \left(\bar{u}_2 \times \bar{u}_3\right) \\ &= \left(\bar{u}_2 \times \bar{u}_3\right) + \left(\bar{u}_3 \times \bar{u}_1\right) + \left(\bar{u}_1 \times \bar{u}_2\right) \qquad (140) \\ &= \text{numerator of } \bar{n} \end{aligned}$$

Note that $\bar{u}_1 \cdot \bar{m} = \left(\bar{u}_1\ \bar{u}_2\ \bar{u}_3\right)$ because vectors $\left(\bar{u}_3 \times \bar{u}_1\right)$ and $\left(\bar{u}_1 \times \bar{u}_2\right)$ are orthogonal to $\bar{u}_1$.

Designating the denominator of $\bar{n}$ in Equation (139) as d, and noting that $\bar{n} = \bar{m}/d$, Equation (138) may be written as

$$\delta \bar{R}_X = \frac{\bar{m}}{\bar{u}_1 \cdot \bar{m}} X = \frac{\bar{n}}{\bar{u}_1 \cdot \bar{n}} X \tag{141}$$

Note from Equation (139) that the sign of $\bar{n}$, and hence its direction, does not depend on whether the stations are numbered in a clockwise or counterclockwise direction. A reversal of the sense of station numbering will reverse not only the sign of each term in the numerator but also the sign of the triple scalar product in the denominator. It can be seen that $\bar{n}$ is directed from the vertex to the base of the tetrahedron. The altitude, h, of the tetrahedron is given by the projection of a side, i.e., $\bar{u}_1$ on a unit normal to the base of the tetrahedron, where this normal points from the vertex to the base.

Therefore,

$$h = \bar{u}_1 \cdot \bar{n} \tag{142}$$

and Equation (141) may be written as

$$\delta \bar{R}_X = \frac{\bar{n}}{h} X \tag{143}$$

c. Velocity error

Substitution of Equations (134) and (135) into Equation (130) yields the following expressions for velocity error due to the instrumental errors noted:

1. Due to uncorrelated range-rate error

$$\delta \bar{V}_Y = \bar{u}_{23}, \csc \phi_1 Y_1 + \bar{u}_{31} \csc \phi_2 Y_2 + \bar{u}_{12} \csc \phi_3 Y_3 \tag{144}$$

2. Due to correlated range-rate error

$$\delta \bar{V}_Z = \frac{\bar{n}}{h} Z \tag{145}$$

3. Due to uncorrelated range error

$$\delta \bar{V}_W = -\left(\bar{B}_1 W_1 + W_2 + \bar{B}_3 W_3\right) \tag{146}$$

4. Due to correlated range error

$$\delta \overline{V}_X = - \left(\overline{B}_1 + \overline{B}_2 + \overline{B}_3 \right) X \tag{147}$$

where the $\overline{B}_k$'s are given by Equations (131), (132), and (133).

Equation (145) may be derived by noting that the term Z enters into Equation (130) in exactly the same fashion that X enters into Equation (124), so that the derivation of Equation (143) is analogous.

4. SURVEY ERRORS

a. General

Let P_o be a fixed and known point on the earth's surface, let P_k be the assumed location of the kth tracking station, and let P be the vehicle position as shown in Figure 3.

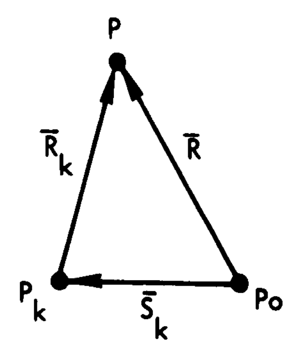

Figure 3. Survey Point Locations

From Figure 3, the following equation results.

$$\overline{R}_k = \overline{R} - \overline{S}_k \tag{148}$$

A variation in the station location results in a variation in $\overline{R}_k$ given by

$$\delta \overline{R}_{kS} = -\delta \overline{S}_k \tag{149}$$

Substitution of this result into Equation ((115) and division of both sides by R_k yield

$$\delta R_{kS} = - \overline{u}_k \cdot \delta \overline{S}_k \tag{150}$$

To derive the analogous expression for range rate, we make use of Equation (126) and note that, for a fixed trajectory, $\overline{V}$ will not vary with variations in the station locations. Substituting Equations (149) and (150) into Equation (126), and letting $\delta\overline{V} = 0$, yields

$$\delta\dot{R}_{kS} = \frac{1}{R_k}\left[\dot{R}_k\left(\overline{u}_k \cdot \delta\overline{S}_k\right) - \overline{V} \cdot \delta\overline{S}_k\right] \tag{151}$$

which may also be written as

$$\delta\dot{R}_{kS} = \frac{-1}{R_k}\left(\overline{V} - \overline{u}_k\dot{R}_k\right) \cdot \delta\overline{S}_k \tag{152}$$

Note that the term $\left(\overline{V} - \overline{u}_k\dot{R}_k\right)$ is the component of vehicle velocity normal to the line of sight from the kth station, and division by R_k gives the angular velocity of the line of sight.

Denoting this normal component of velocity as $V_{\perp k}$, Equation (152) can be written

$$\delta\dot{R}_{ks} = \frac{-1}{R_k}\,\overline{V}_{\perp k} \cdot \delta\overline{S}_k \tag{153}$$

b. Position Error

Substitution of Equation (150) into Equation (124) yields, for position error due to survey error

$$\begin{aligned}\delta\overline{R}_S = -\Big\{&\overline{u}_{23}\csc\phi_1\left(\overline{u}_1 \cdot \delta\overline{S}_1\right) + \overline{u}_{31}\csc\phi_2\left(\overline{u}_2 \cdot \delta\overline{S}_2\right)\\ &+ \overline{u}_{12}\csc\phi_3\left(\overline{u}_3 \cdot \delta\overline{S}_3\right)\Big\}\end{aligned} \tag{154}$$

c. Velocity Error

Substitution of Equations (150) and (153) into Equation (130) yields for velocity error due to survey error

$$
\begin{aligned}
\delta\bar{V}_S = {} & \bar{B}_1\left(\bar{u}_1 \cdot \delta\bar{S}_1\right) + \bar{B}_2\left(\bar{u}_2 \cdot \delta\bar{S}_2\right) + \bar{B}_3\left(\bar{u}_3 \cdot \delta\bar{S}_3\right) \\
& -\bar{u}_{23} \csc\phi_1 \left(\bar{V}_{\perp 1} \cdot \delta\bar{S}_1\right) / R_1 \\
& -\bar{u}_{31} \csc\phi_2 \left(\bar{V}_{\perp 2} \cdot \delta\bar{S}_2\right) / R_2 \\
& -\bar{u}_{12} \csc\phi_3 \left(\bar{V}_{\perp 3} \cdot \delta\bar{S}_3\right) / R_3
\end{aligned}
\tag{155}
$$

where the $\bar{B}_k$'s are given by Equations (131), (132), and (133).

5. STATISTICAL CONSIDERATIONS

a. General

The mean-square error in position and velocity is found by summing the mean-square errors resulting from each of the five error sources considered, since the random variables are uncorrelated and have zero means. The variational equations developed for position and velocity errors are summarized in Table I.

Table I. Variational Equations — Position and Velocity Errors

		Equation Number	
Error Source	Subscript	Position	Velocity
Instrumental			
Range - uncorrelated between stations	W	(136)	(146)
Range - correlated between stations	X	(143)	(147)
Range rate - uncorrelated between stations	Y		(144)
Range rate - correlated between stations	Z		(145)
Survey	S	(154)	(155)

To find the appropriate contributions to total mean-square position and velocity errors, each of the equations in the table must be squared and the mathematical expectation taken for each term.

Before performing the squaring and averaging operations, it will be convenient to discuss the statistical assumptions concerning the error sources and to derive some fundamental relations to be used subsequently.

b. Instrumental Errors

The range error is given by

$$\delta R_{Ik} = W_k + X \tag{134}$$

W_k and X are both random variables. W_k represents errors peculiar to each station, caused by such factors as receiver noise, equipment phase shifts, etc. It is assumed that the W_k's have zero means and are uncorrelated between stations. It is further assumed that

$$\sigma^2\left(W_1\right) = \sigma^2\left(W_2\right) = \sigma^2\left(W_3\right) = \sigma_R^2 \tag{156}$$

X represents a bias common to the range measurements taken from all three stations, resulting from such factors as a time delay in a beacon shared by all three stations and by the uncertainty in the velocity of propagation. Although X may appear essentially constant throughout a given flight phase, it must still be considered random on an <u>a priori</u> basis; and it is reasonable to assume that it has a zero mean. We take its mean-square value as

$$\sigma^2\,(X) = \sigma_{Rb}^2 \tag{157}$$

The range-rate error is given by

$$\delta \dot{R}_{Ik} = Y_k + Z \tag{135}$$

The interpretations are analogous to those of the range error; i.e., both are random variables with zero mean, the Y_k's are uncorrelated between stations, and

$$\sigma^2\left(Y_1\right) = \sigma^2\left(Y_2\right) = \sigma^2\left(Y_3\right) = \sigma_{\dot{R}}^2 \tag{158}$$

$$\sigma^2\,(Z) = \sigma_{\dot{R}b}^2 \tag{159}$$

The physical interpretation of a range-rate bias error, Z, is not so obvious as that of a common range bias. Certain propagation effects can cause this type of error, although their functional form will be more complex than that given by Equation (135). On physical grounds, it is reasonable for most applications to set Z equal to zero.

c. Survey Error

We shall assume the station location errors $\delta\overline{S}_k$ to be mutually uncorrelated with zero means, and

$$\sigma^2\left(\delta\overline{S}_1\right) = \sigma^2\left(\delta\overline{S}_2\right) = \sigma^2\left(\delta\overline{S}_3\right) = \sigma_S^2 \tag{160}$$

Equation (160) may not hold true if, for example, one or two of the stations are on ships while the others are on land. However, for planning purposes, such an assumption is justified on the grounds of simplification.

Let the survey error at any station be represented by

$$\delta\overline{S} = \overline{i}\delta x + \overline{j}\delta y + \overline{k}\delta z \tag{161}$$

in a local Cartesian coordinate system. When $\overline{k}$ is the direction of the local vertical, it is entirely reasonable to set

$$\sigma(\delta x) = \sigma(\delta y) \tag{162}$$

while we expect to have

$$\sigma(\delta z) < \sigma(\delta x) \tag{163}$$

considerable simplification results in the equations if we make the slightly pessimistic assumption that

$$\sigma(\delta x) = \sigma(\delta y) = \sigma(\delta z) \tag{164}$$

Even in this case, $\sigma^2(\delta x) + \sigma^2(\delta y)$ will contribute two-thirds of the mean-square displacement error, σ_S^2; thus from this point on, Equation (164) will be used.

In evaluating mean-square position and velocity errors resulting from survey errors, we will have occasion to take expected values of terms of the form $E\left\{\left(\overline{C}\cdot\delta\overline{S}_j\right)\left(\overline{D}\cdot\delta\overline{S}_k\right)\right\}$, where $\overline{C}$ and $\overline{D}$ are arbitrary vectors. Since the errors are uncorrelated between stations, we have

$$E\left\{\left(\overline{C}\cdot\delta\overline{S}_j\right)\left(\overline{D}\cdot\delta\overline{S}_k\right)\right\} = 0 \quad \text{for } j \neq k \tag{165}$$

For the case when $j = k$, it is convenient to introduce a local Cartesian coordinate system, in terms of which

$$\begin{aligned} \delta\bar{S} &= \bar{i}\delta x + \bar{j}\delta y + \bar{k}\delta z \\ \bar{C} &= \bar{i}c_1 + \bar{j}c_2 + \bar{k}c_3 \\ \bar{D} &= \bar{i}d_1 + \bar{j}d_2 + \bar{k}d_3 \end{aligned} \tag{166}$$

where the subscript k's have been omitted in the expression for $\delta\bar{S}$ as a matter of convenience . From Equation (166) we have

$$E\left\{\left(\bar{C}\cdot\delta\bar{S}\right)\left(\bar{D}\cdot\delta\bar{S}\right)\right\} = E\left\{\left(c_1\delta x + c_2\delta y + c_3\delta_3\right) \cdot \left(d_1\delta x + d_2\delta y + d_3\delta z\right)\right\} \tag{167}$$

Under the reasonable assumption that δx, δy, and δz are uncorrelated, Equation (167) can be written

$$E\left\{\left(\bar{C}\cdot\delta\bar{S}\right)\left(\bar{D}\cdot\delta\bar{S}\right)\right\} = c_1 d_1\sigma_x^2 + c_2 d_2\sigma_y^2 + c_3 d_3\sigma_z^2 \tag{168}$$

and making use of Equation (164), this reduces to

$$E\left\{\left(\bar{C}\cdot\delta\bar{S}\right)\left(\bar{D}\cdot\delta\bar{S}\right)\right\} = \left(c_1 d_1 + c_2 d_2 + c_3 d_3\right)\sigma_x^2 \tag{169}$$

which can be recognized as

$$E\left\{\left(\bar{C}\cdot\delta\bar{S}\right)\left(\bar{D}\cdot\delta\bar{S}\right)\right\} = \left(\bar{C}\cdot\bar{D}\right)\sigma_x^2 \tag{170}$$

From Equations (161) and (164), and the above assumption, we have

$$\sigma_S^2 = \sigma_x^2 + \sigma_y^2 + \sigma_z^2 = 3\sigma_x^2 \tag{171}$$

Substituting Equation (171) into Equation (170), we have

$$E\left\{\left(\bar{C}\cdot\delta\bar{S}\right)\left(\bar{D}\cdot\delta\bar{S}\right)\right\} = \frac{1}{3}\left(\bar{C}\cdot\bar{D}\right)\sigma_S^2 \tag{172}$$

6. DERIVATION OF MEAN-SQUARE ERRORS

a. Position Error

The contribution due to a range error, uncorrelated between stations, is obtained by squaring Equation (136) and taking the expectations of the terms.

Let

$$E\left\{\left(\delta R_W\right)^2\right\} = \sigma_{PW}^2 \tag{173}$$

Since the W_k's are uncorrelated, the expected values of all cross-product terms are zero, and making use of Equation (156) we have

$$\sigma_{PW}^2 = \left(\csc^2 \phi_1 + \csc^2 \phi_2 + \csc^2 \phi_3\right) \sigma_R^2 \tag{174}$$

Performing the same operations on Equation (143) and making use of Equation (157), we have (for a common range error)

$$\sigma_{PX}^2 = h^{-2} \sigma_{Rb}^2 \tag{175}$$

To find the effect of survey errors, the expectation of the quantity $\delta\bar{R}_S \cdot \delta\bar{R}_S$ is found by making use of Equation (154). Note that, from Equation (172)

$$E\left\{\left(\bar{u}_k \cdot \delta\bar{S}_k\right)^2\right\} = \frac{1}{3}\sigma_S^2 \tag{176}$$

Performing the indicated operation, we have

$$\sigma_{PS}^2 = \frac{1}{3}\left(\csc^2 \phi_1 + \csc^2 \phi_2 + \csc^2 \phi_3\right) \sigma_S^2 \tag{177}$$

Finally, the total mean-square position error is given by

$$\sigma_P^2 = \sigma_{PW}^2 + \sigma_{PX}^2 + \sigma_{PS}^2 \tag{178}$$

where the terms are given by Equations (174), (175), and (177).

b. Velocity Error

From Equations (146) and (156), we obtain

$$\sigma_{VW}^2 = \left(B_1^2 + B_2^2 + B_3^2\right) \sigma_R^2 \tag{179}$$

From Equations (147) and (157), we find that

$$\sigma_{VX}^2 = B^2 \sigma_{Rb}^2 \tag{180}$$

where we have defined a new vector, $\bar{B}$, by the equation

$$\bar{B} = \bar{B}_1 + \bar{B}_2 + \bar{B}_3 \tag{181}$$

and it has been convenient to write

$$\bar{B}_k \cdot \bar{B}_k = B_k^2 \qquad \bar{B} \cdot \bar{B} = B^2 \tag{182}$$

From Equations (144) and (158), we have

$$\sigma_{VY}^2 = \left(\csc^2 \phi_1 + \csc^2 \phi_2 + \csc^2 \phi_3\right) \sigma_{\dot{R}}^2 \tag{183}$$

From Equations (145) and (159), we obtain

$$\sigma_{VZ}^2 = h^{-2} \sigma_{\dot{R}b}^2 \tag{184}$$

To obtain the survey contribution, Equation (155) must be squared and expectations taken of terms of the form $E\left\{\left(\bar{u}_k \cdot \delta\bar{S}_k\right)\left(\bar{V}_{\perp k} \cdot \delta\bar{S}_k\right)\right\}$. From Equation (172), it is seen that this results in terms of the form $(\bar{u}_k \cdot \bar{V}_{\perp k})$. However, we have seen that these vectors are orthogonal; thus their dot product is zero. This means that although two terms contribute to velocity error from a survey error at each of these stations, these two contributions are uncorrelated in spite of the fact that they arise from the same error.

We also make use of the fact that from Equation (172)

$$E\left\{\left(\bar{V}_{\perp k} \cdot \delta\bar{S}_k\right)^2\right\} = \frac{1}{3} V_{\perp k}^2 \sigma_S^2 \tag{185}$$

But since

$$V^2 = V_{\perp k}^2 + \dot{R}_k^2 \tag{186}$$

we can write Equation (185) in the form

$$E\left\{\left(\bar{V}_{\perp k} \cdot \delta\bar{S}_k\right)^2\right\} = \frac{1}{3}\left(V^2 - \dot{R}_k^2\right)\sigma_S^2 \tag{187}$$

Performing the squaring operation and taking the expectations in Equation (155), and making use of Equations (176) and (187), yield

$$\sigma_{VS}^2 = \frac{1}{3}\left\{B_1^2 + B_2^2 + B_3^2 + \frac{V^2 - \dot{R}_1^2}{R_1^2}\csc^2\phi_1 + \frac{V^2 - \dot{R}_2^2}{R_2^2}\csc^2\phi_2 + \frac{V^2 - \dot{R}_3^2}{R_3^2}\csc^2\phi_3\right\}\sigma_S^2 \qquad (188)$$

Finally, the total mean-square velocity error is given by

$$\sigma_V^2 = \sigma_{VW}^2 + \sigma_{VX}^2 + \sigma_{VY}^2 + \sigma_{VZ}^2 + \sigma_{VS}^2 \qquad (189)$$

where the terms are given by Equations (179), (180), (183), (184), and (188).

7. NOTES ON THE GEOMETRICAL CONFIGURATION

Equations (174), (177), and (183) contain error coefficients of the form $\left(\csc^2\phi_1 + \csc^2\phi_2 + \csc^2\phi_3\right)$. This term reaches a minimum value of 3 when

$$\phi_1 = \phi_2 = \phi_3 = 90^\circ \qquad (190)$$

that is, when the three range vectors are orthogonal.

Equations (175) and (184) contain error coefficients of the form h^{-2}. Recalling that h is the height of the tetrahedron formed by the three unit vectors $\bar{u}_1$, $\bar{u}_2$, and $\bar{u}_3$, it is seen that this error coefficient is minimized when the three range vectors tend toward parallelism. This requirement is incompatible with that of minimizing $\csc\phi_k$ above.

To gain some insight into the effect of geometry, consider a network of ground stations laid out on an equilateral triangle with sides of length D, and the vehicle equidistant from each station at an altitude H above the plane formed by the three stations. In this case we can write

$$\sigma_{PW} = g_1\ \sigma_R \qquad (191)$$

$$\sigma_{PS} = g_1\ \sigma_S / \sqrt{3} \qquad (192)$$

$$\sigma_{PX} = g_2\ \sigma_{Rb} \qquad (193)$$

$$\sigma_{VY} = g_1 \ \sigma_{\dot{R}} \tag{194}$$

$$\sigma_{VZ} = g_2 \ \sigma_{\dot{R}_b} \tag{195}$$

where

$$g_1 = \sqrt{3} \csc \phi \tag{196}$$

and

$$g_2 = h^{-1} \tag{197}$$

The factors g_1 and g_2 are plotted in Figure 4 for the range of values

$$0.1 \leq H/D \leq 10 \tag{198}$$

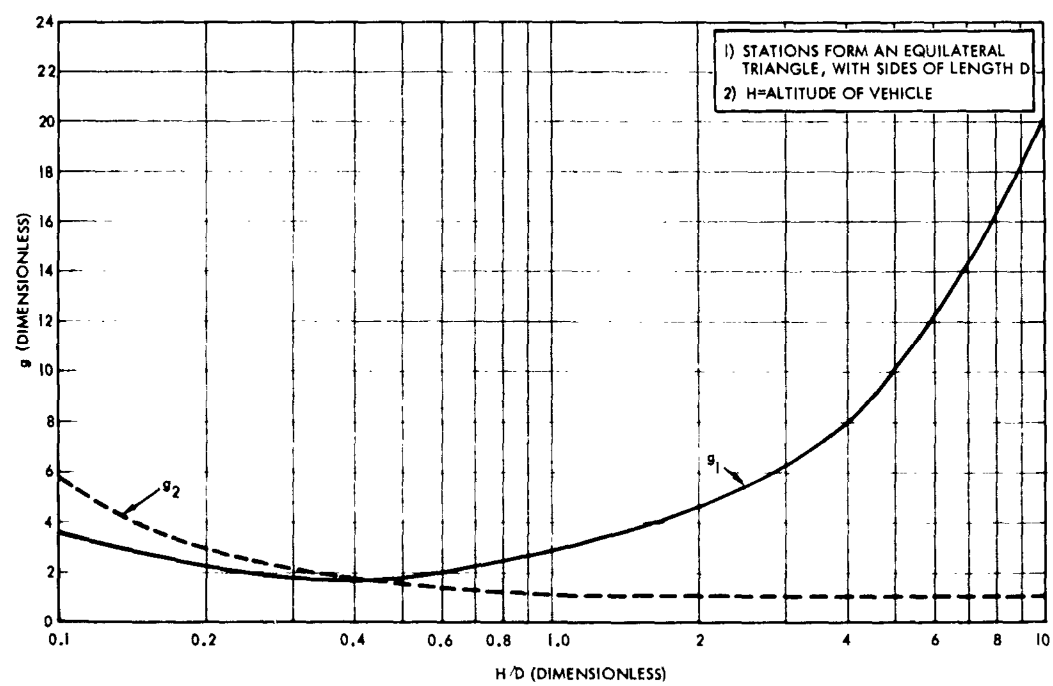

Figure 4. Coefficients of g, and g2 Versus H/D for a Vehicle Equidistant From Three Tracking Stations

The remaining error coefficients (by means of which range errors and survey errors contribute to a velocity error) do not lend themselves to any simple geometrical interpretation.

8. NOTES ON COMPUTATIONAL PROCEDURES

a. Graphical Solutions

For certain applications, when a range bias error can be neglected, the position error can be written from Equations (174), (177), and (178) as

$$\sigma_P^2 = \left(\csc^2\phi_1 + \csc^2\phi_2 + \csc^2\phi_3\right)\left(\sigma_R^2 + \sigma_S^2/3\right) \tag{199}$$

The terms $\csc\phi_k$ may be evaluated by graphical means, as follows. Consider a three-station configuration as shown in Figures 5a and 5b with the vehicle in the position shown. Figure 5a is a view looking down on the network configuration while Figure 5b is a view from the side with

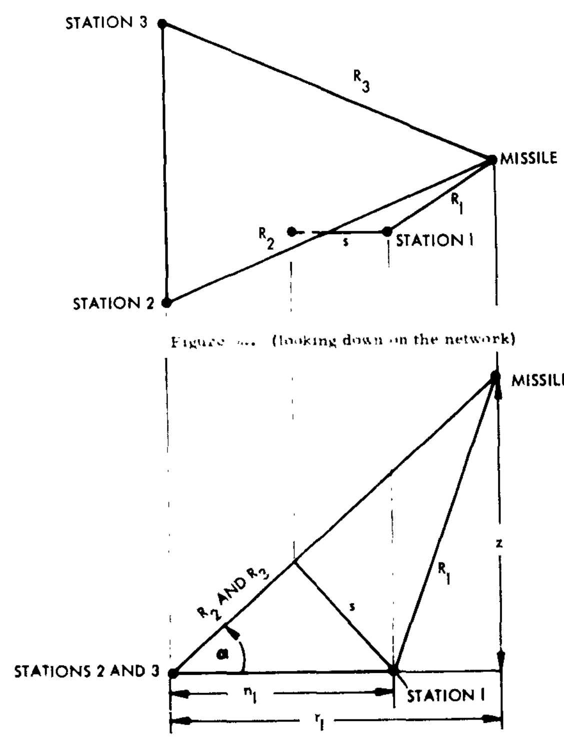

Figure 5a. (looking down on the network)

Figure 5b. (view from the side)

Figure 5. Three Station Configuration (R_1, R_2, R_3)

the plane formed by line-of-sight ranges R_2 and R_3 forming an angle with range R_1. This is not the angle ϕ_1 because the view is not from a direction where the true length of R_1 is shown. However, s, the perpendicular distance between station 1 and the plane formed by R_2 and R_3, is shown with its true length in Figure 5b, in which case, if this can be determined graphically, $\csc\phi_1 = \dfrac{R_1}{s}$.

Let

n_1 = perpendicular distance between the baseline of stations 2 and 3 and station 1

r_1 = perpendicular distance between the baseline of stations 2 and 3 and the projection of the missile on the plane formed by the three stations

z = height of the missile above the plane formed by stations 1, 2, and 3

α = angle between the plane formed by ranges R_2 and R_3 and the plane formed by stations 1, 2, and 3.

then

$$s = n_1 \sin \alpha \tag{200}$$

and

$$\sin \alpha = \frac{z}{\left(z^2 + r_1^2\right)^{1/2}} \tag{201}$$

Therefore,

$$s = \frac{n_1 z}{\left(z^2 + r_1^2\right)^{1/2}} \tag{202}$$

and

$$\csc \phi_1 = \frac{R_1 \left(z^2 + r_1^2\right)^{1/2}}{n_1 z} \tag{203}$$

The same procedure is used in solving for $\csc \phi_2$ and $\csc \phi_3$. The geometric coefficient in Equation (199) can consequently be represented by

$$(\csc^2 \phi_1 + \csc^2 \phi_2 + \csc^2 \phi_3)$$

$$= \left[\frac{R_1^2\left(1 + \frac{r_1^2}{z^2}\right)}{n_1^2} + \frac{R_2^2\left(1 + \frac{r_2^2}{z^2}\right)}{n_2^2} + \frac{R_3^2\left(1 + \frac{r_3^2}{z^2}\right)}{n_3^2}\right] \tag{204}$$

Therefore, the method for using the graphical procedure is to lay out the network on graph paper and measure n_1, n_2, and n_3. Given a missile trajectory, with respect to the network, the R's, r's, and z's can be obtained for various points of the trajectory and substituted into Equations (204) and (199) for use in the solution of the metric errors. Note also that Equation (204) can be used to evaluate Equation (183), which gives the vehicle velocity error resulting from an instrumental range-rate error.

b. Numerical Solutions

For cases when the graphical solutions are not sufficient, a fixed, right-handed Cartesian coordinate system must be introduced in which all vectors can be expressed as linear combinations of the unit vectors $\bar{i}$, $\bar{j}$, $\bar{k}$ defined by this system. The previously obtained formulas provide the framework of an orderly procedure for performing the specified vector operations in a step-by-step manner, or for programming a computer. When the vectors are expressed in terms of their $\bar{i}$, $\bar{j}$, $\bar{k}$ components, for example

$$\begin{aligned} \bar{A} &= \bar{i}a_1 + \bar{j}a_2 + \bar{k}a_3 \\ \bar{B} &= \bar{i}b_1 + \bar{j}b_2 + \bar{k}b_3 \\ \bar{C} &= \bar{i}c_1 + \bar{j}c_2 + \bar{k}c_3 \end{aligned} \tag{205}$$

we have

$$\bar{A} + \bar{B} = \bar{i}\left(a_1 + b_1\right) + \bar{j}\left(a_2 + b_2\right) + \bar{k}\left(a_3 + b_3\right) \tag{206}$$

$$A^2 = a_1^2 + a_2^2 + a_3^2 \tag{207}$$

$$\bar{A} \cdot \bar{B} = a_1 b_1 + a_2 b_2 + a_3 b_3 \tag{208}$$

$$\bar{A} \times \bar{B} = \begin{bmatrix} \bar{i} & \bar{j} & \bar{k} \\ a_1 & a_2 & a_3 \\ b_1 & b_2 & b_3 \end{bmatrix} \tag{209}$$

$$\bar{A} \cdot \bar{B} \times \bar{C} = (\bar{A}\ \bar{B}\ \bar{C}) = \begin{bmatrix} a_1 & a_2 & a_3 \\ b_1 & b_2 & b_3 \\ c_1 & c_2 & c_3 \end{bmatrix} \tag{210}$$

c. Pertinent Equations for Reference

- Position Error

$$\sigma_P^2 = \sigma_{PW}^2 + \sigma_{PX}^2 + \sigma_{PS}^2 \tag{178}$$

$$\sigma_{PW}^2 = \left(\csc^2\phi_1 + \csc^2\phi_2 + \csc^2\phi_3\right)\sigma_R^2 \tag{174}$$

$$\sigma_{PX}^2 = \frac{\sigma_{Rb}^2}{h^2} \tag{175}$$

$$\sigma_{PS}^2 = \left(\csc^2\phi_1 + \csc^2\phi_2 + \csc^2\phi_3\right)\frac{\sigma_S^2}{3} \tag{177}$$

- Velocity Error

Neglecting a correlated bias in the instrumental range-rate error

$$\sigma_V^2 = \sigma_{VW}^2 + \sigma_{VX}^2 + \sigma_{VY}^2 + \sigma_{VS}^2 \tag{189}$$

$$\sigma_{VW}^2 = \left(B_1^2 + B_2^2 + B_3^2\right)\sigma_R^2 \tag{179}$$

$$\sigma_{VX}^2 = B^2\sigma_{Rb}^2 \tag{180}$$

$$\sigma_{VY}^2 = \left(\csc^2\phi_1 + \csc^2\phi_2 + \csc^2\phi_3\right)\sigma_{\dot{R}}^2 \tag{183}$$

$$\sigma_{VS}^2 = \left\{B_1^2 + B_2^2 + B_3^2 + \frac{V^2 - \dot{R}_1^2}{R_1^2}\csc^2\phi_1 + \frac{V^2 - \dot{R}_2^2}{R_2^2}\csc^2\phi_2 + \frac{V^2 - \dot{R}_3^2}{R_3^2}\csc^2\phi_3\right\}\frac{\sigma_S^2}{3} \tag{188}$$

where the mean-square values of the error sources are:

σ_R^2, from an uncorrelated range measurement error

σ_{Rb}^2, from a range measurement error common to all stations

σ_S^2, from a survey error in the station location

$\sigma_{\dot{R}}^2$, from an uncorrelated range-rate measurement error;

and the terms in the error coefficients are:

R_1, R_2, R_3, ranges from stations 1, 2, 3 to the vehicle

$\dot{R}_1, \dot{R}_2, \dot{R}_3$, range rates at stations 1, 2, 3

V, absolute value of the vehicle's velocity

and the B vectors are as defined below:

$$\bar{B}_1 = \bar{u}_{23} \csc \phi_1 \frac{\bar{V} \cdot \bar{u}_{23} \csc \phi_1 - \dot{R}_1}{R_1} + \bar{u}_{31} \csc \phi_2 \frac{\bar{V} \cdot \bar{u}_{23} \csc \phi_1}{R_2} + \bar{u}_{12} \csc \phi_3 \frac{\bar{V} \cdot \bar{u}_{23} \csc \phi_1}{R_3} \tag{131}$$

$$\bar{B}_2 = \bar{u}_{23} \csc \phi_1 \frac{\bar{V} \cdot \bar{u}_{31} \csc \phi_2}{R_1} + \bar{u}_{31} \csc \phi_2 \frac{\bar{V} \cdot \bar{u}_{31} \csc \phi_2 - \dot{R}_2}{R_2} + \bar{u}_{12} \csc \phi_3 \frac{\bar{V} \cdot \bar{u}_{31} \csc \phi_2}{R_3} \tag{132}$$

$$\bar{B}_3 = \bar{u}_{23} \csc \phi_1 \frac{\bar{V} \cdot \bar{u}_{12} \csc \phi_3}{R_1} + \bar{u}_{31} \csc \phi_2 \frac{\bar{V} \cdot \bar{u}_{12} \csc \phi_3}{R_2} + \bar{u}_{12} \csc \phi_3 \frac{\bar{V} \cdot \bar{u}_{12} \csc \phi_3 - \dot{R}_3}{R_3} \tag{133}$$

$$\bar{B} = \bar{B}_1 + \bar{B}_2 + \bar{B}_3 \tag{181}$$

where

$\bar{u}_{12}$ is a unit vector normal to the plane formed by R_1 and R_2

$\bar{u}_{23}$ is a unit vector normal to the plane formed by R_2 and R_3

$\bar{u}_{31}$ is a unit vector normal to the plane formed by R_3 and R_1

and the sense is positive upwards and away from the opposite station.

In terms of the unit vectors $\bar{u}_1$, $\bar{u}_2$, and $\bar{u}_3$ lying along the corresponding range vectors and directed from the stations to the vehicle

$$\left.\begin{aligned} \bar{u}_{23} \csc \phi_1 &= \frac{\bar{u}_2 \times \bar{u}_3}{(\bar{u}_1\ \bar{u}_2\ \bar{u}_3)} \\ \bar{u}_{31} \csc \phi_2 &= \frac{\bar{u}_3 \times \bar{u}_1}{(\bar{u}_1\ \bar{u}_2\ \bar{u}_3)} \\ \bar{u}_{12} \csc \phi_3 &= \frac{\bar{u}_1 \times \bar{u}_2}{(\bar{u}_1\ \bar{u}_2\ \bar{u}_3)} \end{aligned}\right\} \tag{211}$$

which may be used to evaluate the B vectors.

We also have, in the same terms

$$\left.\begin{aligned} \csc^2 \phi_1 &= \left[\frac{\bar{u}_2 \times \bar{u}_3}{(\bar{u}_1\ \bar{u}_2\ \bar{u}_3)}\right]^2 \\ \csc^2 \phi_2 &= \left[\frac{\bar{u}_2 \times \bar{u}_3}{(\bar{u}_1\ \bar{u}_2\ \bar{u}_3)}\right]^2 \\ \csc^2 \phi_3 &= \left[\frac{\bar{u}_1 \times \bar{u}_2}{(\bar{u}_1\ \bar{u}_2\ \bar{u}_3)}\right]^2 \end{aligned}\right\} \tag{212}$$

$$\frac{1}{h^2} = \left[\frac{(\bar{u}_2 \times \bar{u}_3) + (\bar{u}_3 \times \bar{u}_1) + (\bar{u}_1 \times \bar{u}_2)}{(\bar{u}_1\ \bar{u}_2\ \bar{u}_3)}\right]^2 \tag{213}$$

which may be used to evaluate the remaining terms in the error coefficients.

Appendix XIII. THE SHIFT OF TELEMETRY FROM VHF TO UHF

1. INTRODUCTION

The allocation of the frequency band from 216 to 260 mc for telemetry purposes will expire on 1 January 1970 as stated by a joint DOD/IRAC directive. At that time, two new frequency bands are to be used for telemetry:

- 1435 to 1535 mc (1435 to 1485 inclusive is reserved for tests on manned aircraft)
- 2200 to 2300 mc.

The transition will be effected by 1970. The Department of Defense and the Inter-Range Instrumentation Group (IRIG) have assigned the responsibility for new and revised telemetry standards to the Telemetry Working Group (TWG). This appendix will discuss the advantages and disadvantages of the telemetry frequency change and its effect on future range instrumentation planning.

2. CONSIDERATION OF SYSTEMS COMPONENTS

a. Modulation Standards

The IRIG Document No. 106-60, Parts 2 through 5 (Reference 1) lists the modulation standards for telemetry systems as follows:

Part 2. FM/FM or FM/PM standard, including subcarrier frequencies, deviation ratios, frequency response, correction for zero drift and sensitivity, commutation rates, and calibration requirements.

Part 3. PDM/FM or PDM/PM or PDM/FM/FM standard, including frame rate and number of samples per frame with tolerances, subcarrier channels and pulse shape tolerances.

Part 4. PAM/FM or PAM/PM standard, to be added later.

Part 5. PCM standards, including bit rate versus receiver IF bandwidth, bit rate stability, word and frame structure, synchronization, commutation, premodulation filtering, and RF carrier modulation.

The telemetry radio frequency shift will not directly affect the choice of the modulation technique, as long as the required carrier-to-thermal noise ratio is provided by the radio system. The selection of a type of modulation is rather dictated by the amount of information per unit bandwidth to be transmitted during a particular mission, by the accuracy requirement of the data, and by the allowable system complexity. Reference 2 gives a theoretical efficiency comparison of several communication systems based on a figure of merit defined as the ratio of energy required per bit transmitted to a given noise spectral density. Orthogonal systems have been theoretically shown to consistently require less power to transmit at a given information rate than other systems, and closely approach Shannon's theoretical limit. The fact that orthogonal systems are basically of digital form may be a limiting factor in space application due to increased equipment complexity. FM systems with a phase-lock loop are next in efficiency, followed by FM systems with pulse counting discriminators and conventional FM. The efficiency difference between these latter systems increases rapidly with increasing information rates.

b. Satellite Transmitter

The development of CW transmitters* for the new telemetry bands should not present unsolvable difficulties. Today, experimental units are available delivering approximately 2 to 2.5 watts minimum. The following table compares four important parameters for space applications for TWT and solid-state transmitters:

*There is also an 80 to 100 watt, 2.2-gc amplifier being developed with expected efficiency of 23 percent; however, it will weigh about 15 pounds including power supply.

	TWT	Solid-State
CW output power	2 to 10 watts	2 to 2.5 watts
Efficiency	20 percent	10 percent
Weight, including driver and power converter for TWT	48 ounces	32 ounces
Predicted life	20,000 hours	undetermined, but high

The TWT transmitter is presently capable of delivering more power with better efficiency, but at the expense of some extra weight. For special applications, such as transmission with brief and frequent duty cycles, the solid-state transmitter is preferable.

With regard to system design, the frequency shift to 2 gc is advantageous, since the minimum CW breakdown electrical field (being approximately proportional to frequency) is almost 10 times higher. This eliminates the requirement of running the transmitter temporarily at reduced power, especially during launch, and helps to solve the problem of flame attenuation. (See Section 3. b.)

c. Antennas

1. Ground

The antenna problem must be considered in connection with the free-space propagation characteristics. The gain of a parabolic antenna is

$$G(\text{db}) = -52.6 + 20 \log \text{frequency (mc)} + 20 \log \text{diameter (ft)}$$

and the free-space loss is

$$L_{fs} = 37 + 20 \log \text{frequency (mc)} + 20 \log \text{distance (mi)}$$

The combined characteristic of antenna and free space is then

$$G - L_{fs} = -89 + 20 \log \text{diameter (ft} - 20 \log \text{distance) (mi)}$$

and is independent of frequency. According to Reference 3, most missile sites are already equipped with UHF antennas, while the satellite UHF antenna, either omnidirectional or high gain, will require some development time.

Of some significance is the fact that the Fresnel zone clearance for the ground antenna is less for UHF than for VHF, which results in lower towers. This can be important if the ground antenna is removed from the launch site to overcome the flame attenuation problem.

2. Airborne

A primary requirement of a missile or space vehicle telemetry system is to communicate comprehensive information concerning vehicle and on-board systems performance to the ground range stations. It is vitally important that this information be communicated when a malfunction occurs, to permit appropriate evaluation and the necessary corrective action. Since many malfunctions result in marked departure of the vehicle from nominal trajectories and, in the case of boost vehicles, require command destruct action, it is highly desirable that the on-board telemetry antenna system provide spherical coverage.

Attitude-independent telemetry links have been approached in the lower bands where the vehicle is incorporated in the antenna system design to provide nearly isotropic radiation coverage.

A close approximation to uniform 4-π steradian coverage is sometimes feasible if vehicle dimensions are small in comparison to the wavelength of the telemetry transmitter frequency, e. g., under one wavelength. This is especially true if no particular requirement is placed on spacecraft antenna polarization, i. e., if polarization may vary with pattern angle.

However, if the spacecraft is large, e. g., a few wavelengths or greater, then isotropic coverage presents a very difficult design problem.

Several approaches have been sought to obtain spherical coverage arrays in the UHF bands, and the results indicate rather complex

configurations. One type that most closely approaches spherical coverage and has received much attention is the circular array which makes up a band around the vehicle (Figure 1). The elements of the array can be horns, cavity-backed slots, or dipoles. In any case, a single transmitter feeds all elements simultaneously. The elements can be fed in two different ways.

First, all the elements can be fed in-phase. In this case, the radiation pattern is doughnut-shaped with nulls along the axes. The in-phase signals are obtained by power dividers. The power dividers are difficult to implement, however, since a large number of antenna elements are required to keep the ripple in the pattern to allowable values. The number of elements required, is, of course, dependent on vehicle size. For very large vehicles such as the Saturn C-5, 200 to 300 elements would be required.

Second, the elements can be fed in-phase rotation so as to obtain a total phase shift around the array of 2-π radians. This produces a bidirectional, fan-shaped beam which rotates around the array at the frequency of the RF energy. Spherical coverage is thus obtained. Again, it is difficult to implement the power divider and phase-shift structure necessary to obtain the desired signals for driving the individual elements.

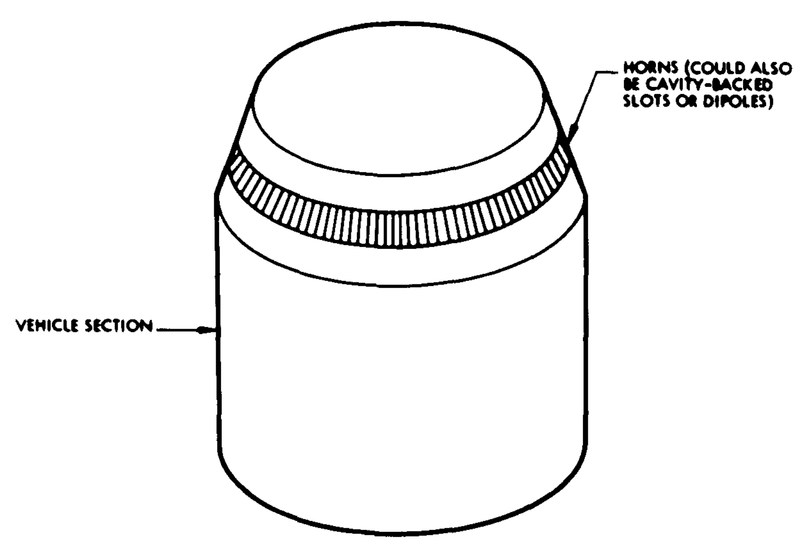

Figure 1. Spherical Coverage Antenna Array

Other approaches to obtaining spherical coverage have been made; however, most exhibit undesirable polarization, phase, and amplitude characteristics.

It may be concluded that the shift from the present VHF band to UHF (S-band) introduces significant antenna problems in the vehicle and the applications and requirements for each vehicle and mission must be studied to determine the tradeoffs that can be made. To obtain nearly spherical coverage on a large vehicle at S-band may require a prohibitively complex array. (The circular array would be categorized as impractical for a large vehicle.)

d. Summary

Table I compares basic system parameters of the present and future system standards. Except for better stability and different bandwidth assignments, the standards are equal. Therefore, no difficulties are expected.

In regard to component development, the satellite antenna and transmitter will require most of the efforts. While the antenna configuration must be matched to the space vehicle and must simultaneously meet the required system characteristics, the transmitter design must be carried from the experimental model to the final hardware which will meet systems and environmental specifications.

Looking at the systems performance, the new telemetry systems should and will be able to perform better. Besides slightly improved propagation characteristics and lower receiver noise temperature, a significant gain increase in the system is to be expected from the ground antenna. While the maximum gain of contemporary 260-mc antennas is 35 db, 60-db gain is practical at 2 gc. This is still 7 db more gain than required to compensate the increased path loss of 18 db. The more precise antenna steering performance should be obtainable with today's techniques. The new frequency bands will allow more IF bandwidth, which will be important for low orbit missions, while for deep-space probes, available weight-limited equipment does not allow the utilization of the wider bandwidth.

Table I. Comparison of Basic System Parameters of Present and Future Telemetry System Standards. (Reference 4)

Parameter	Present Frequency Band	Future Frequency Band
Transmitter frequency tolerance	0.01 percent	0.005 percent
Transmitter power	Less than 100 watts	Dictated by intended use
Spurious and harmonic emission	db below the carrier = 55 + 10 $\log_{10} P_t$ P_t = measured power output in watts	
Spurious, harmonics and fundamental signals radiated from equipment, cables and power leads	Per MIL-I-26600	
Receiver stability	0.005 percent	0.001 percent
Spurious response	More than 60 db below fundamental frequency	
Spurious emission	Per MIL-I-26600	
Bandwidth	Optimized for maximum information transfer per given bandwidth	
Bandwidth guideline		
For ±125 kc deviation, BW (60 db)	600 kc	1 mc
For ±1.4 mc deviation, BW (60 db)		10 mc
For PCM, BW (3 db)		1.5 times bit rate
BW (60 db)		3.6 times bit rate

3. GENERAL SYSTEMS ASPECTS

a. Propagation

Both the new and present telemetry RF frequencies are located close to the geometric mean of the so-called space frequency window, which reaches from 10 mc to about 10 gc. Therefore, the propagation characteristics will not vary appreciably between 260 mc and 2. 2 gc; if so, a very slight improvement at 1. 5 and 2. 2 gc will result. In addition, as described in detail in Reference 5, propagation losses at 1. 5 or 2. 2 gc are not noticeably increased by either uncondensed water vapor, molecular oxygen, ionospheric absorption, precipitation or auroral absorption.

Angle errors due to refraction can be 2 mrad for low elevation angles of approximately 5 deg.

Faraday rotation, if linear polarization is used, can cause 20-db attenuation between 1. 6 and 3. 1 gc. This difficulty can be avoided by circular polarization at the expense of 3-db loss, or by polarization diversity reception.

b. Launch Problems

During the powered flight of the missile, three phenomena affect the reception of telemetry signals:

Flame attenuation

Pressure shock wave during staging

Antenna ionization.

Signal attenuation of as much as 20 db has been observed when the RF signal passes through the rocket exhaust. The signal fades gradually over several seconds while the noise increases. The effect is most pronounced at receiving stations near the launch site, but also depends on the location of the satellite antenna. Consequently, there are two remedies for this problem:

The satellite antenna should be located as far away as possible from the exhaust.

For ground reception, a medium-gain antenna may be used near the launch site and a high-gain antenna downrange to insure a clear propagation path undisturbed by the rocket exhaust.

During the separation of the first and second stage, a shock wave that reflects RF waves is created around the missile. This results in varying signal attenuation, depending on signal strength and phase of the direct and reflected wave. The effect is equivalent to amplitude modulation (100 percent) which can confuse the automatic tracking equipment. Unfortunately, the effect is nonfrequency sensitive and has been observed with optical equipment as well. Therefore, the RF frequency shift will have no bearing on this case.

A gas subjected to RF electric fields will break down more easily with decreasing pressure. At a critical altitude, an antenna glow discharge can occur resulting in excessive RF power dissipation, high VSWR, and change in antenna impedance and antenna radiation pattern. Reference 6 shows that the minimum CW breakdown electrical field is approximately proportional to frequency. Therefore, the new RF telemetry frequencies will allow more RF power before breakdown. However, the antenna dimension may be smaller, so that the power advantage can be reduced again. The problem is not too critical and can be remedied by diversity reception, since the fading at different stations has been observed to be noncoherent.

c. Reentry Problem

The problem of reliable telemetry and communication during the reentry phase of a space flight has not been solved satisfactorily. The plasma sheath which forms around the space vehicle during reentry possesses a refraction index which depends on frequency. The resulting attenuation and phase-shift characteristics as functions of frequency are shown in Figures 3 and 4 of Reference 7. Other than use of super high frequencies (SHF), the solutions to the reentry attenuation problem which have been proposed involve either:

The suppression of the plasma sheath by recombination methods or cooling.

The use of the sheath to enhance propagation by electric and magnetic interaction.

No practical results are available at present.

Summarizing, the shift of the telemetry frequency to 2.2 gc will not assist in solving the reentry problem.

Reference 8 describes a 9-gc telemetry experimental system. Reference 9 reports the performance of a 5,000-mc telemetry system on a Polaris missile. For its particular shape and reentry characteristics, a signal fadeout of 8 to 12 db is reported for a duration of 4 sec, while VHF telemetry was lost for about 15 sec.

REFERENCES

1. "Telemetry Standards," Document 106-60 IRIG, Astia No. AD 253-641, reissued April 1961.

2. R. W. Sanders, "Communication Efficiency Comparison of Several Communication Systems," Proc. IRE, April 1960, pp. 575-588.

3. G. F. Bigelow, et al, "Microwave Telemetry at U. S. Missile Ranges," IRE Transaction on Military Electronics, Volume MIL-5, No. 4, October 1961, pp 266-272.

4. "Telemetry Frequency Utilization Parameters and Criteria," IRIG Recommendation No. 101-59, revised July 1960.

5. "Notes on Factors Affecting Communications Between Satellites and Earth Stations," Interim Engineering Report No. 154-R-8, ASTIA AD 202-388, Haller, Raymond and Brown, Inc., State College Pennsylvania, 10 January 1959.

6. A. D. MacDonald, "High Frequency Breakdown in Air at High Altitudes," Proc. IRE, Volume 47, March 1959, pp 436-441.

7. E. F. Dirsa, "The Telemetry and Communication Problem of Reentrant Space Vehicles," Proc. IRE, April 1960, pp 703-713

8. E. A. Brummer and R. F. Harrington, "A Unique Approach to an X-band Telemetry Receiving System," Proc. of the National Telemetry Conference, Volume I, Section 4-2, May 1962.

9. D. L. Anderson, et al, "A 5000-mc Telemetry Transmitting and Receiving System," Proc. of the National Telemetry Conference Volume I, Section 4-3, May 1962.

BIBLIOGRAPHY

W. H. Drake and F. S. Howell, "Radio Frequency Propagation to and from ICBM's and IRBM's," STL (inc).

W. F. Link and C. D. Eatough, "Experimental Optimization and Evaluation of Telemetry Systems," IRE Transaction, Set 8, September 1962.

"PCM Telemetry System — A Report Bibliography," (report abstracts concerning telemetry systems from 1957 to July 1962), ASTIA Document ARB-10899, STL No. 62-4547.

Reference Data for Radio Engineers, 4th Edition, IT and T Corporation, 1956.

Appendix XIV. TECHNIQUES AND TRENDS IN AEROSPACE TELEMETRY

A. INTRODUCTION

When studying the trends in contemporary telemetry systems and speculating about developments that may be expected, it is clear that certain requirements will continue to be of primary importance.

- Very large capacities for data transmission
- Great spectral efficiency, to minimize interference between simultaneous operations on limited bandwidths
- Efficient management and utilization of large facilities that already exist or are being built
- Greater consideration of the requirements for acquisition and processing systems when defining the parameters of vehicle telemetry (This includes consideration of ground extraction and distribution, time correlation, real-time requirements, and joint telemetry-tracking-command requirements.)
- Discriminating between the requirements of the "work horse" facilities which provide most of the general range support, and the specialized facilities which provide service to particular programs or special program phases (For example, telemetry for deep-space vehicles, operational satellite programs, or tactical weapons systems requires a considerable degree of freedom from range telemetry standards because these missions require that the telemetry be optimized with regard to specialized parameters.)

B. SOME TELEMETRY SYSTEMS FOR LARGE VEHICLES

Because of their historical development and standardization, their general adequacy for many requirements, and the evolutionary constraints that demanded their compatibility with existing ground stations, FM/FM, PCM/FM, PAM/FM, and PDM/FM are the "bread-and-butter" telemetry systems of today. An extensive evaluation of these systems and their probable adequacy for the post-1960 period was begun in 1957 by Aeronutronic Division of Ford Motor Company for the United States Army. This comprehensive study (Reference 1) lasted for several years. It included both experimental and analytical evaluations. Missile program requirements were of primary significance, and consideration was given (1) to the use of both the existing VHF and the new UHF spectrums, (2) to minimizing interference, (3) to the role of standardized and unified ground stations, and (4) to the configuration which might characterize a desirable new standard system.

Reports from the first phase of that study included the results of a "user requirements" survey. Some germane findings included:

- The indicated capacity required for an average missile telemetry system was 75 kbits/sec. A capacity of 200 kbits/sec was indicated as necessary to handle 75 percent of contemporary missile test programs.
- Rates of the order of 1000 kbits/sec and approximately 400 data channels were required by test programs of some large missiles.
- The combination of needing many channels per test, and needing wide ranges in requisite channel bandwidth and accuracy showed the need for flexibility in telemetry configurations.

Since that study, developments have been in the directions the report predicted. Two activities of interest are the incorporation of special multiplexers to handle abundant wideband vibration data for larger stages, and the demands of some programs for a large number of RF links to provide the required number of channels.

Centaur vehicle telemetry used two PAM/FM/FM systems (500 kc and 100 kc) plus incidental PCM telemetry integrated with tracking augmentation requirements (Reference 2). Additional telemetry was used for the Atlas booster and payload stages.

On early Saturn vehicles, as many as 1100 measurements were required for SA-5, including as many as 125 vibration channels, and data from a number of digital sources (Reference 3). The system devised for some of these vehicles combines PCM/FM (for high-accuracy data, data originating digitally, and data used in prelaunch monitoring and checkout), PAM/FM/FM (for functions requiring less than 1000 cps in bandwidth and poorer than 1 percent accuracy), and SS/FM (for vibration data).

The S-1 stage telemetry (for SA-5) has 4 PAM/FM/FM links (with IRIG FM/FM on some carriers, plus commutation and subcommutation which includes a nonstandard 70-kc ±30 percent subcarrier). Two SS/FM systems each provide a capability equivalent to 15 channels from 30 to 3000 cps.

The Douglas S-IV stage adds three PDM/FM/FM systems, each of which provides two commutated subcarriers, plus fifteen continuous subcarriers.

An instrumentation unit (above the S-IV stage) adds 4 more systems: 2 systems each contain 15 continuous subcarriers and 2 subcarriers submultiplexed with FM/FM (channels 2 and 6 on top of channels 14 and 17); one SS/FM system provides 10 vibration channels; one PCM/FM system provides variable word length (5 to 11 bits/word) and variable bit rate (N x 3.6 kbits/sec, up to 180 kbits/sec).

These brief examples illustrate several points:

- Systems of very large capacity are in use today.

- The common modulation and multiplexing techniques evaluated by Aeronutronic are seeing heavy current use, and some operations involve many simultaneous VHF carriers.
- Spectrum and data-handling loads are being further burdened by the incorporation of nonstandard techniques to meet special requirements.
- Some programs are beginning to employ other factors which enter into systems requirements consideration, such as adaptive system parameters (variable word length, variable rate, different power levels), and integration of flight telemetry with other activities or systems (static and dynamic testing, monitor-checkout-flight test, tracking augmentation, range safety and other real-time users).

Several conclusions were drawn from the Aeronutronic study with reference to optimizing employment of the enumerated standard systems (References 1, 4). Noteworthy items include:

- System bandwidth equal to the bit rate (plus some margin for system drifts and mistunings) was recommended for NRZ PCM/FM and it was pointed out that additional bandwidth is not advantageous and requires greater power to maintain threshold performance against random noise.
- PCM/FM systems should employ premodulation filtering (video bandwidth equal to one-half the bit-rate) to provide spectrum conservation.

- It was recommended that FM/FM employ an RMS carrier deviation of 40 to 60 kc and a receiver bandwidth of 300 kc (for IRIG subcarriers through 70 kc).
- For PAM/FM systems providing 1 to 3 percent accuracy, an optimum receiver bandwidth was determined to be five times the sample rate, and premodulation filtering with bandwidth equal to one-half the receiver bandwidth was recommended.

Comparative evaluations among the systems emphasized requisite receiver signal/noise ratios, receiver bandwidth/bit rate ratios, and resulting error rates. It was concluded that PCM generally had an inherent requirement for greater bandwidth than PAM, but that PCM/FM offered the best performance, in terms of both spectrum occupancy and power consumption, when accuracies exceeding 1 percent were required. PAM/FM was adjudged the better choice if lesser accuracies were acceptable. While these observations offer guides to more efficient application of the basic systems, previous observations point out the need for more sophisticated approaches to satisfying total needs for large multistage vehicles.

The Aeronutronic survey of user requirements for missile telemetry indicated a general mix of high-frequency/low-accuracy channels and low-frequency/high-accuracy channels; so, considering the aforementioned system characteristics, the study recommended a hybrid telemetry system (PACM/FM) combining PAM and PCM as a desirable new standard system. Evaluation of PACM/FM system hardware is in process, and the results should provide a good guide to the degree of application which the system warrants. However, the attractiveness of the philosophy makes it a strong enough contender to warrant further description.

PACM/FM, as proposed by Aeronutronic, (References 1, 4, 5) permits the intermixing of analog data samples (PAM) and digital data samples synchronously in a single, serial data stream. The basic concept involves

a highly modularized construction that allows a particular configuration to be assembled with parameters optimized to particular needs. Yet, the all-time-multiplexed nature of the system and certain design constraints should make possible ground stations which are sufficiently versatile to accommodate the various airborne permutations. In an extreme case, the system could be all PAM or all PCM, with airborne complexity comparable to existing systems of those types. In the full hybrid mode, this complexity has been compared to that of multiple-accuracy PCM. Advantages of this approach to handling the missile instrumentation requirement are given in Reference 5. They include:

- The use of PAM for low- and moderate-accuracy data, and of PCM for high-precision or naturally-digital data permits a reduction in requisite transmitter power (as compared to meeting both data requirements with a single modulation).
- Placing the mixed data load on a single carrier permits considerably better spectral utilization than does the number of independent carriers required to satisfy very high capacity missions with nonhybrid techniques.

Some basic constraints used in a preliminary design (Reference 4) include:

- Receiver bandwidth and transmitter power remain fixed during PAM and PCM portions.
- If some basic bit period τ_c is defined, then PCM word length = N τ_c (N = number of bits per word, and includes one parity bit in outlined system); M τ_c = PAM sample duration; and $N/_M = k$, where N, M, and k are integers. If required, the PCM word length is expanded

above basic system requirements to provide these integer relationships, which are made to simplify logic and circuit design. (Table I summarizes the relations among some parameters.)

- The basic sampling rate (frame rate) is selected to satisfy midrange requirements, and extremes are accommodated by subcommutation and supercommutation.
- The frame length is an integer multiple of both PAM samples and PCM words.
- Full-scale PAM amplitude is equal to maximum PCM bit amplitude.
- NRZ PCM and 100-percent duty cycle PAM are used.

Some values presented (Reference 4) for "typical" PACM vehicleborne data converters are shown in Table I.

Figure 1 shows the S/N ratio required for various data accuracies (RMS error) as a function of normalized bandwidth (receiver bandwidth B/sample rate f_s). PCM/FM values depict the effects of various receiver bandwidth/bit-rate ratios (τ_c = 1/B, 2/B, 3/B is equivalent to B = f_B, 2 f_B, 3 f_B) and of various word lengths (all include one parity bit).

Figure 2 is a simpler plot which assumes τ_c = 1/B (i.e., B = f_B), and illustrates the effects of incorporating a parity bit in the PCM words.

SS/FM has been mentioned (in References 3, 6, and 7) as one alternative to PAM/FM or FM/FM for handling abundant vibration data (or other requirements for many wideband channels). This single-sideband frequency modulation (SS/FM) technique translates many baseband slots up into nearly contiguous slots by SSB techniques and then frequency-modulates the carrier with that composite. In a particular system, 15 3-kc channels (actually 50 to 3000 cps) are translated into successive

Table 1. Some PACM Parameters

Bit Rate	8 to 800 kbits/sec
PAM Sample Duration	2, 3, or 4 bits
PCM Word Length	6, 9, or 12 bits
Number of PAM Prime Channels	126: (3 x PCM prime channels)
Number of PCM Prime Channels	Up to 21 (including frame sync)
Frame Length	Equivalent to 126 PAM samples
Power Consumption (excluding power supplies)	At 400 or 800 kbits/sec - 45 w At 250 kbits/sec, or less - 30 w
Weight	15.1 lb
Volume	0.18 cu ft

τ_c = Basic bit period

f_B = Bit rate = $\frac{1}{\tau_c}$ bit/sec

M = Number of bit intervals per PAM sample

τ_a = PAM sample duration and

= $M\tau_c$ (M = integer)

N = Number bits per PCM word (including parity)

$N\tau_c$ = PCM word or sample duration

f_s = Sample rate,

= $\frac{1}{N\tau_c}$ for PCM samples, and

$\frac{1}{M\tau_c} = \frac{1}{\tau_A}$ for PAM samples

B = Receiver bandwidth

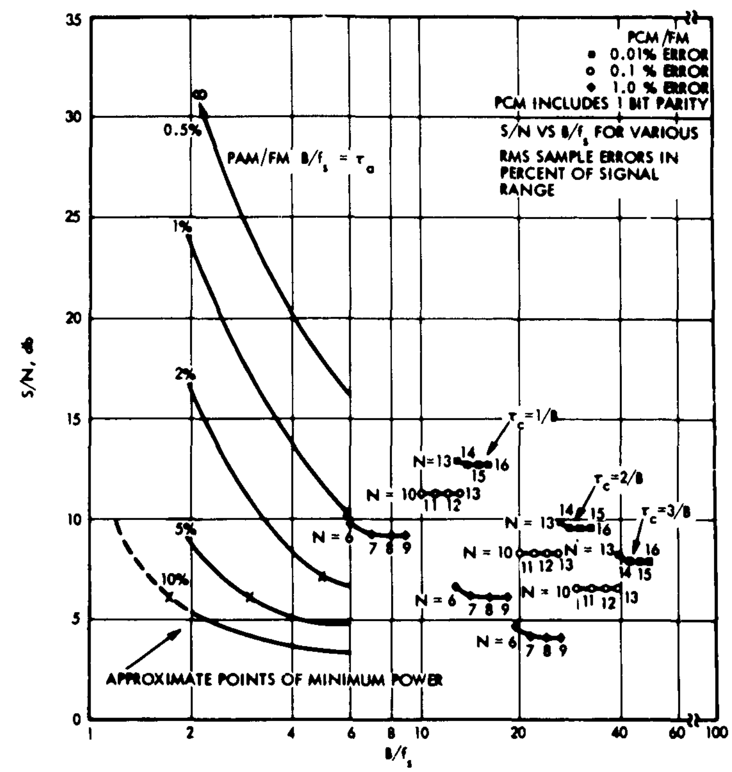

Figure 1. PACM Design Chart Adapted from G. J. Pastor, Reference 4

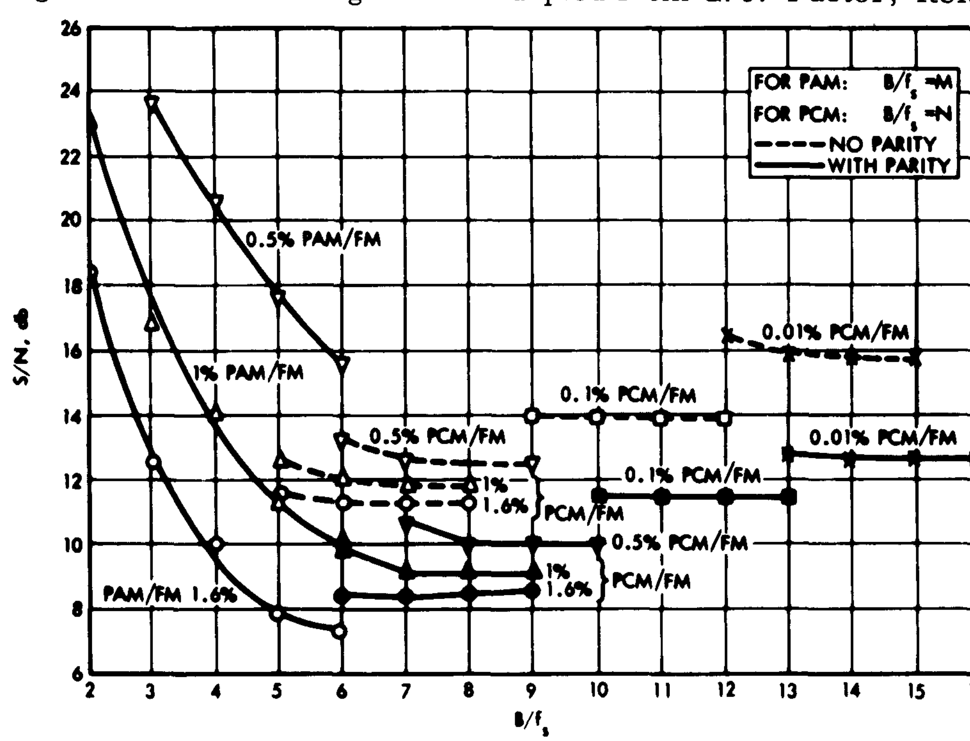

Figure 2. PCM/FM–PAM/FM Error Comp. from Reference 1 Aeronutronic Division, FMC

4.74 kc-wide channels, and a pilot tone is added at 75.83 kc for AGC and frequency reference (Reference 3). This provides a data bandwidth of (15) (2950) = 44.25 kc in about the same spectrum that would be required to provide a 4.53 kc data bandwidth (D. R. =5) or 22.67 kc (D. R. =1) with the standard IRIG FM/FM system. Also, the SS-FM channels constitute channels of identical bandwidth, while the IRIG channels provide radically different bandwidths (but permit uniform signal-noise ratios). This SSB multiplex is equivalent to the method commonly employed to stack 3 kc voice channels for telephone systems; however, voice traffic is not sensitive to phase and amplitude distortion. Reference 3 cites the highly efficient bandwidth utilization and poor phase response and amplitude accuracy of SSB multiplex as compared to other systems. While the basic RF transmission is IRIG-compatible, the ground data separation obviously requires specialized equipment. Thus, SS-FM offers an adequate means of handling difficult data now. However, alternative means, such as PAM/FM, PACM/FM, or an extension of contemporary FM/FM, might represent considerably better solutions for widespread, standardized use at general-purpose ranges.

Rorex and Frost (Reference 7) have described a hybrid system which accommodates wideband analog data and low-frequency high-accuracy digital data by frequency-division multiplexing. PCM data at a moderate bit rate (20 to 40 kbits/sec) receives premodulation filtering and occupies the lower portion of the baseband, and the SS subcarriers are translated to the upper portion. The composite signal for a particular PCM-SS/FM configuration being considered comprises 25.2 kbit/sec PCM and 10 single-sideband channels of 3-kc data bandwidth each. This composite baseband is 75 kc wide and uses an IRIG FM/FM RF spectrum. Reference 7 notes that such a hybrid is easily separated at the ground station, and that the two ground stations can be identical to those used for the same signals on separate carriers. Further, no synchronization between the two systems (PCM and SS) is necessary.

This system merits comparison with PACM/FM if a new standard system is to be derived. While current tests of PACM prototypes and of actual SS/FM systems will help to evaluate those modulation techniques,

preference for a particular hybrid as a standard system will be strongly dependent upon the anticipated mission requirements. The utility of SS/᷀M for vibration data acquisition will give impetus to its general use for booster stages and larger missiles, and the adaptability of time-multiplexed systems will make PACM attractive for complex missions involving considerable, multistage instrumentation of diverse bandwidth and accuracy requirements.

C. DEEP-SPACE TELEMETRY

Emphasis to this point has been on systems for handling the suborbital (and some earth-orbital) missions which represent the bulk of the loading on the general test facilities. These missions are characterized by requirements for (1) considerable capacity, and the possible requirement for many RF links, (2) generally adequate S/N ratios for effective use of FM carrier modulation, (3) necessity for wideband analog data of low or moderate accuracy, (4) various needs for integrating telemetry with other mission activities, and (5) a strong motivation for being compatible with some existing data acquisition and processing facilities.

Telemetric systems involving planetary and extra-orbital ranges present some considerably different considerations. Limitations imposed by power availability, transmission attenuations, antenna characteristics, noise levels, flight durations, and the data requirements of these missions all combine to emphasize the efficiency with which the communication system enables information transfer. Also these considerations deemphasize, to some degree, interprogram compatibility, total spectrum utilization, and the means for handling some input types (such as vibration data).

Some of the relationships among pertinent parameters are illustrated in Figures 3, 4, and 5. Figure 3 (from Reference 8) illustrates the degradation in S/N ratio which results from increased free-space propagation loss with vast ranges. The particular values depicted show that, even with very large antenna systems, severe restrictions on attainable bandwidth and S/N ratio preclude useful information rates at these ranges

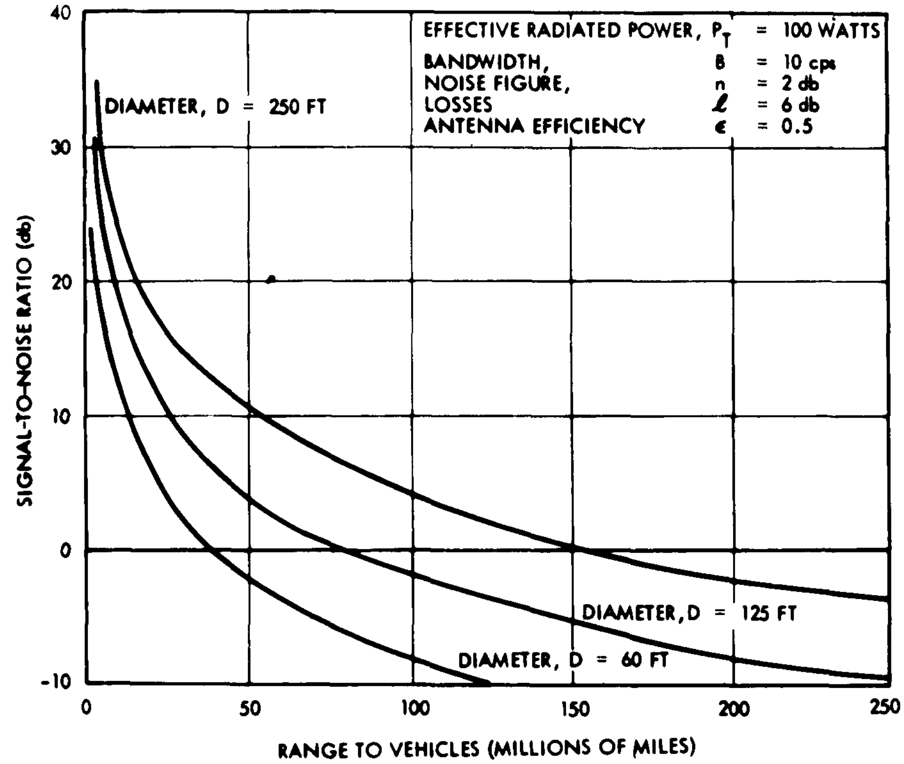

Figure 3. S/N Versus Range for Three Ground Antenna Sizes From Mueller, Reference 8

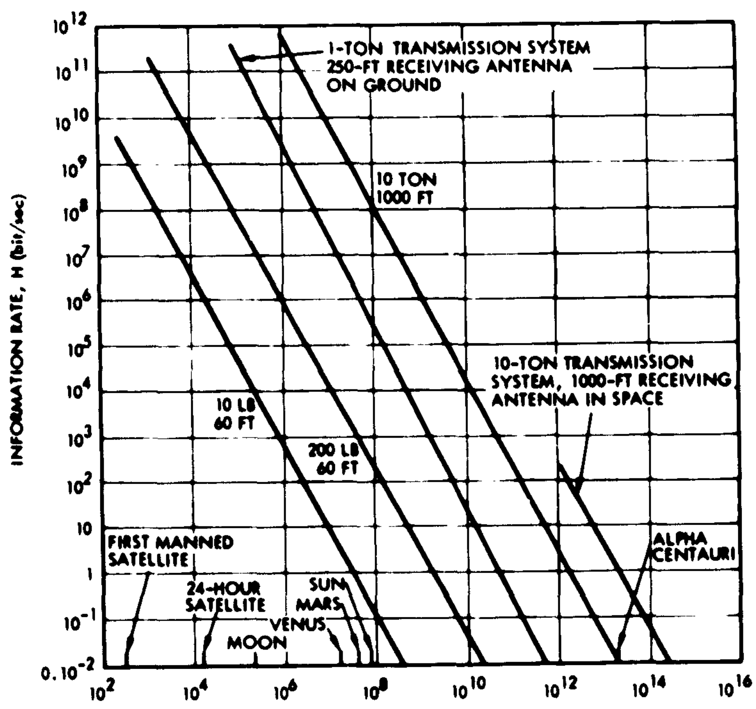

Figure 4. Information Rate Versus Range for Various Transmitter Weights and Antenna Systems

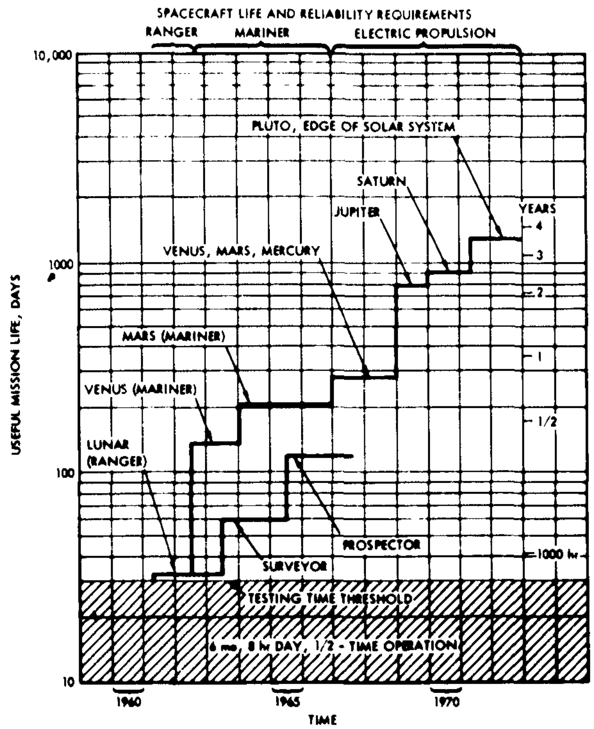

Figure 5. Required Life Versus Mission (From Riddle, Reference 9)

with high-threshold modulation-detection systems. Figure 4 (Reference 8) indicates information rates associated with some conceivable payload and antenna configurations, and also notes the ranges associated with some particular deep-space missions. Some of these missions reappear in Figure 5 (Reference 9), and the required mission lifetimes presented there suggest the importance of power consumption and mean-times-to-failure considerations for such hardware as telemetry components associated with these vehicles.

Many comparative evaluations have been made of modulation and demodulation techniques. Analytical studies of techniques for VHF and UHF transmission over interplanetary ranges have indicated the attractiveness of coherent PCM techniques because of existing conditions on requisite bandwidth, available power, hardware limitations, and transmission and environmental noise conditions. A simple comparison of several digital modulation techniques is presented in Figure 6 (Reference 10).

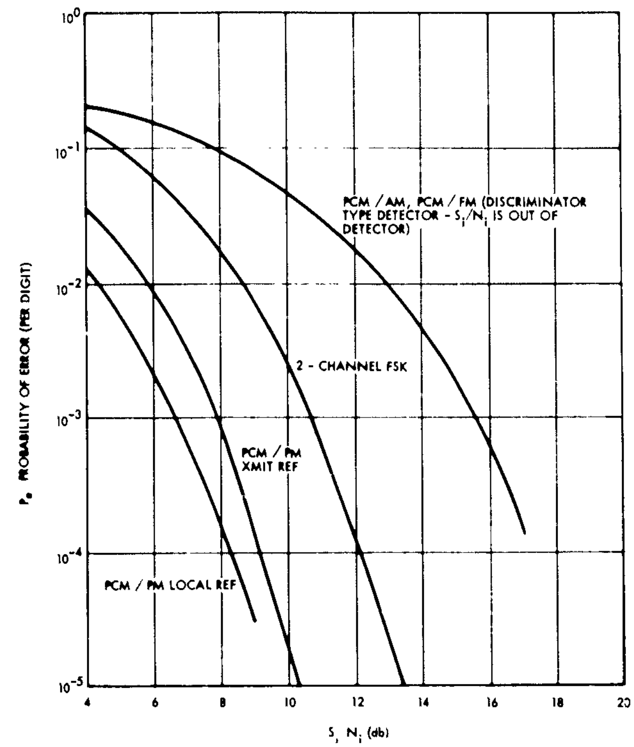

Figure 6. P_c Versus S_i/N_i for Various PCM Modulations, (From C. S. Weaver, Reference 10)

It may be observed that considerable improvement in error rate (for a particular S/N ratio) is obtainable if digital phase modulation and various coherent detectors are employed. Various PCM/PM telemetry systems, such as the "Telebit" system (Reference 8), have found favor for applications requiring the highly efficient communication necessitated by deep-space ranges. Sanders has presented the capabilities of various systems in terms of necessary received energy per transferred information bit to permit some specified probability of bit error, given some average power limitation and white Gaussian noise of some power density (Reference 11). His presentation indicates the theoretical advantage enjoyed by orthogonally coded, phase-coherent operation when it is desired to minimize that energy/bit requirement. Sanders (Figure 7) shows the lower limit for this energy/bit (β) measure which is provided by the

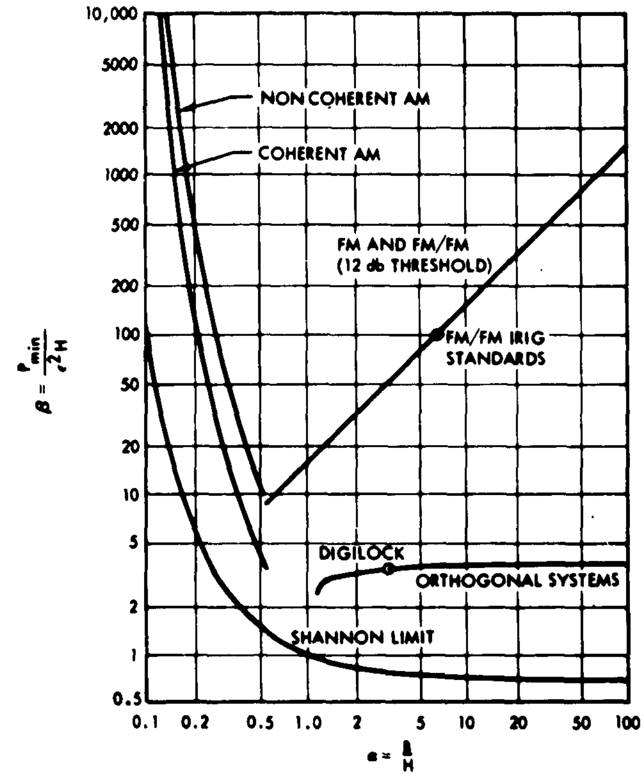

Figure 7. β vs B/H for Various Systems (rms Quantizing Noise = rms Error Due to Error Rate)

Shannon description of such channels, and indicates that redundantly-coded systems such as Digilock (Reference 11) (employing Reed-Muller coding) permit nearer theoretical approaches to this limit. Figure 8 presents Sanders' calculations of the β required to permit a probability of error less than 10^{-6} with various transmission techniques for various input signal resolution.

Viterbi (Reference 12) and others have also examined redundant coding techniques for telemetric applications, and have pointed out some advantages of orthogonal and biorthogonal code sets for use in reducing error probability at the expense of increased bandwidth. Viterbi shows that in the limit, as the number of bits per code word and the bandwidth approach infinity, the error probability approaches zero, provided that the ratio of received signal energy per bit to noise power per unit bandwidth exceeds ln 2 .

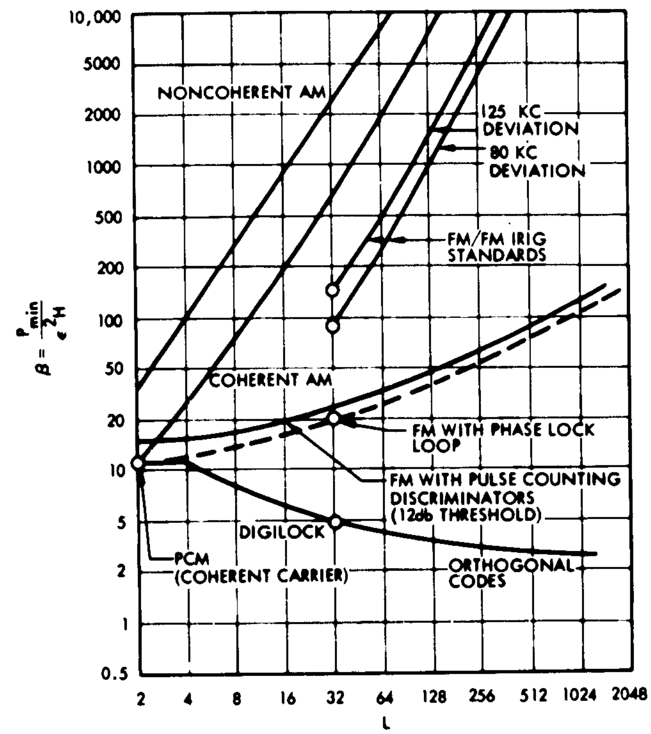

Figure 8. β_{os} Quantization Levels, L ($P_e = 10^{-6}$)

These more sophisticated techniques are of particular interest in missions (and mission phases) where transmission range requirements, power limitations, antennas, and receiving systems combine to require maximum transmission and detection efficiency. Systems of this sort will find continuing use for deep-space missions. Greater tolerance to transmission inefficiency, the hardware complexity of some sophisticated systems, the spectral occupancy required for large-capacity, high-rate systems, and the lack of compatibility with existing facilities at major ranges make these techniques inappropriate for suborbital and most earth-orbital missions.

REFERENCES

1. "Telemetry System Study," Final Report (3 Volumes), Aeronutronic Publication No. U-743, Aeronutronic Division of Ford Motor Co., December 1959.

2. C. R. Cearly, "Design of the Telemetry System of the Centaur Space Vehicle," Proceedings of the National Telemetry Conference, 1960, pp. 121-129.

3. R. F. Eichelberger, "The Saturn Telemetry System," Proceedings of the 1962 National Telemetry Conference, (Volume 2), pp. 13-1. 1 to 13-1. 12.

4. G. J. Pastor, "Practical Design of PACM Telemetry Equipment," Proceedings of the 1962 National Telemetering Conference (Volume 1), pp. 13-4. 1 to 13-4. 13.

5. D. E. Gilcrest, R. P. Kolb and D. E. Fineran, "PACM-FM Telemetry Evaluation," National Aerospace Electronics, 1962 National Conference Proceedings, pp. 103-111.

6. W. O. Frost, "SS/FM: A Telemetry Technique for Wideband Data," IRE Trans. on Space Electronics and Telemetry; December 1962, pp. 283-289.

7. J. E. Rorex and W. O. Frost, "Telemetry Considerations for Large Space Vehicles," IRE Trans. on S. E. T., June 1962, pp. 135-138.

8. G. E. Mueller, "A Pragmatic Approach to Space Communications," Proc. of the IRE, April 1960, pp. 557-566.

9. F. M. Riddle, "Communication With Deep-Space Vehicles," Proceedings of the 1962 National Telemetering Conference, (Volume 1), pp. 8-1. 1 to 8-1. 11.

10. C. S. Weaver, "A Comparison of Several Types of Modulation," IRE Trans. on Communication Systems, March 1962, pp. 96-101.

11. R. W. Sanders, "Communication Efficiency Comparison of Several Communication Systems," Proc. of the IRE, April 1960, pp. 575-588.

12. A. J. Viterbi, "On Coded Phase-Coherent Communications," IRE Trans. on S. E. T., March 1961, pp. 3-14.

Appendix XV. USE OF TELEMETRY FOR RANGE SAFETY

In Section III, in which the range safety system is outlined, it is specified that more use should be made of data telemetered from the vehicle under test in reaching the range safety decisions. In this appendix, an example of this concept is examined in detail.

The range safety purposes for which telemetry data can be utilized to advantage include:

- Anticipation of impending failures
- Confirmation of proper or erratic behavior
- Comparisons of confidence in various range safety inputs
- Combination of telemetry and tracking data to arrive at a best estimate of instantaneous impact point (IIP)
- Bridging tracking data dropouts with telemetry data
- Primary source of range safety information.

Arguments against the exhaustive use of telemetry data for range safety include:

- High system complexity and cost
- Possibility of incorrect evaluation of data by relatively inexperienced range personnel
- Coordination problems in providing range with telemetry calibrations, formats, and missile subsystem flight tolerance limits
- Complex equipment setup required for each flight
- Flight system simulation programs might be needed by the range.

Telemetry data can provide input to the range safety calculations in any one or a combination of the following modes:

- Coarse azimuth and elevation information from telemetry tracking antennas
- Continuous azimuth and elevation from CW tracking systems (COTAR)
- Flight component performance and status information
- Flight subsystem performance and status information
- Flight computer position and velocity outputs
- Position and velocity information computed by a simulated flight computer, using telemetry inputs.

Figure 1 illustrates a range safety system which could make maximum use of the above-mentioned information in addition to the usual external data, and in which the final safe/unsafe decision is still the range safety officer's decision. The inputs to the displays are:

Impact prediction plots based on:

- External data
- Internal data derived from (1) Flight computer position and velocity outputs, (2) Simulated flight computer position and velocity outputs, and (3) Telemetry carrier azimuth and elevation data

Present position plots based on same as above

Computed mission safe/unsafe indication

Flight system safe/unsafe indication based on telemetry data decisions

Flight subsystem safe/unsafe indications based on telemetry data decisions

Flight component safe/unsafe indications based on telemetry data decisions

Flight subsystem performance data

Flight computer output data

Simulated flight system performance based on telemetry input.

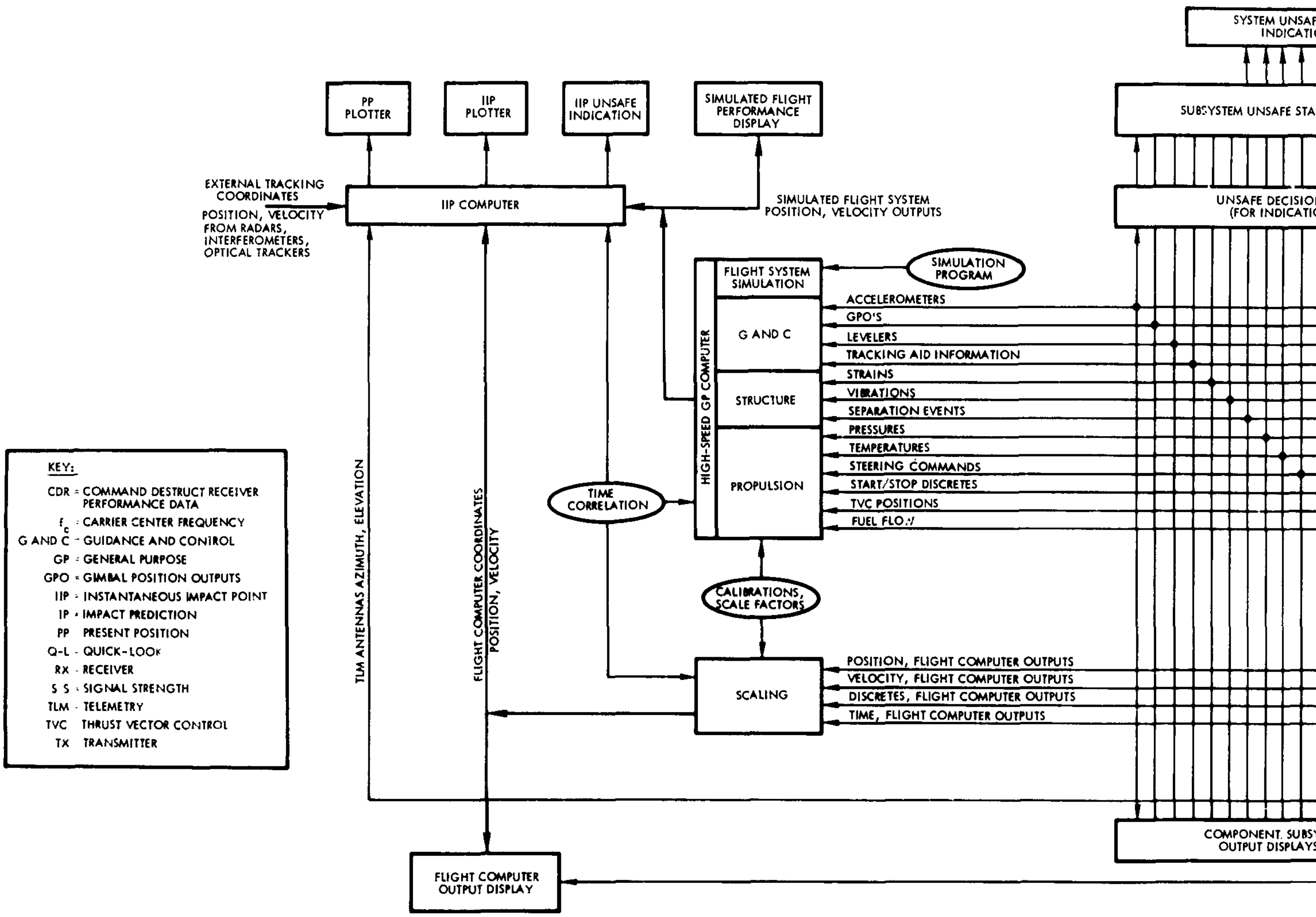
SYSTEM UNSAFE INDICATION
PP PLOTTER
IIP PLOTTER
IIP UNSAFE INDICATION
SIMULATED FLIGHT PERFORMANCE DISPLAY
SUBSYSTEM UNSAFE STATU
EXTERNAL TRACKING COORDINATES
POSITION, VELOCITY FROM RADARS, INTERFEROMETERS, OPTICAL TRACKERS
IIP COMPUTER
SIMULATED FLIGHT SYSTEM POSITION, VELOCITY OUTPUTS
UNSAFE DECISION (FOR INDICATION
FLIGHT SYSTEM SIMULATION
SIMULATION PROGRAM
HIGH-SPEED GP COMPUTER
G AND C
STRUCTURE
PROPULSION
ACCELEROMETERS
GPO'S
LEVELERS
TRACKING AID INFORMATION
STRAINS
VIBRATIONS
SEPARATION EVENTS
PRESSURES
TEMPERATURES
STEERING COMMANDS
START/STOP DISCRETES
TVC POSITIONS
FUEL FLOW
KEY:
CDR = COMMAND DESTRUCT RECEIVER PERFORMANCE DATA
f_c = CARRIER CENTER FREQUENCY
G AND C = GUIDANCE AND CONTROL
GP = GENERAL PURPOSE
GPO = GIMBAL POSITION OUTPUTS
IIP = INSTANTANEOUS IMPACT POINT
IP = IMPACT PREDICTION
PP PRESENT POSITION
Q-L - QUICK-LOOK
RX - RECEIVER
S S - SIGNAL STRENGTH
TLM - TELEMETRY
TVC THRUST VECTOR CONTROL
TX TRANSMITTER
TLM ANTENNAS AZIMUTH, ELEVATION
FLIGHT COMPUTER COORDINATES POSITION, VELOCITY
TIME CORRELATION
CALIBRATIONS, SCALE FACTORS
SCALING
POSITION, FLIGHT COMPUTER OUTPUTS
VELOCITY, FLIGHT COMPUTER OUTPUTS
DISCRETES, FLIGHT COMPUTER OUTPUTS
TIME, FLIGHT COMPUTER OUTPUTS
COMPONENT, SUBSYST OUTPUT DISPLAYS
FLIGHT COMPUTER OUTPUT DISPLAY

1

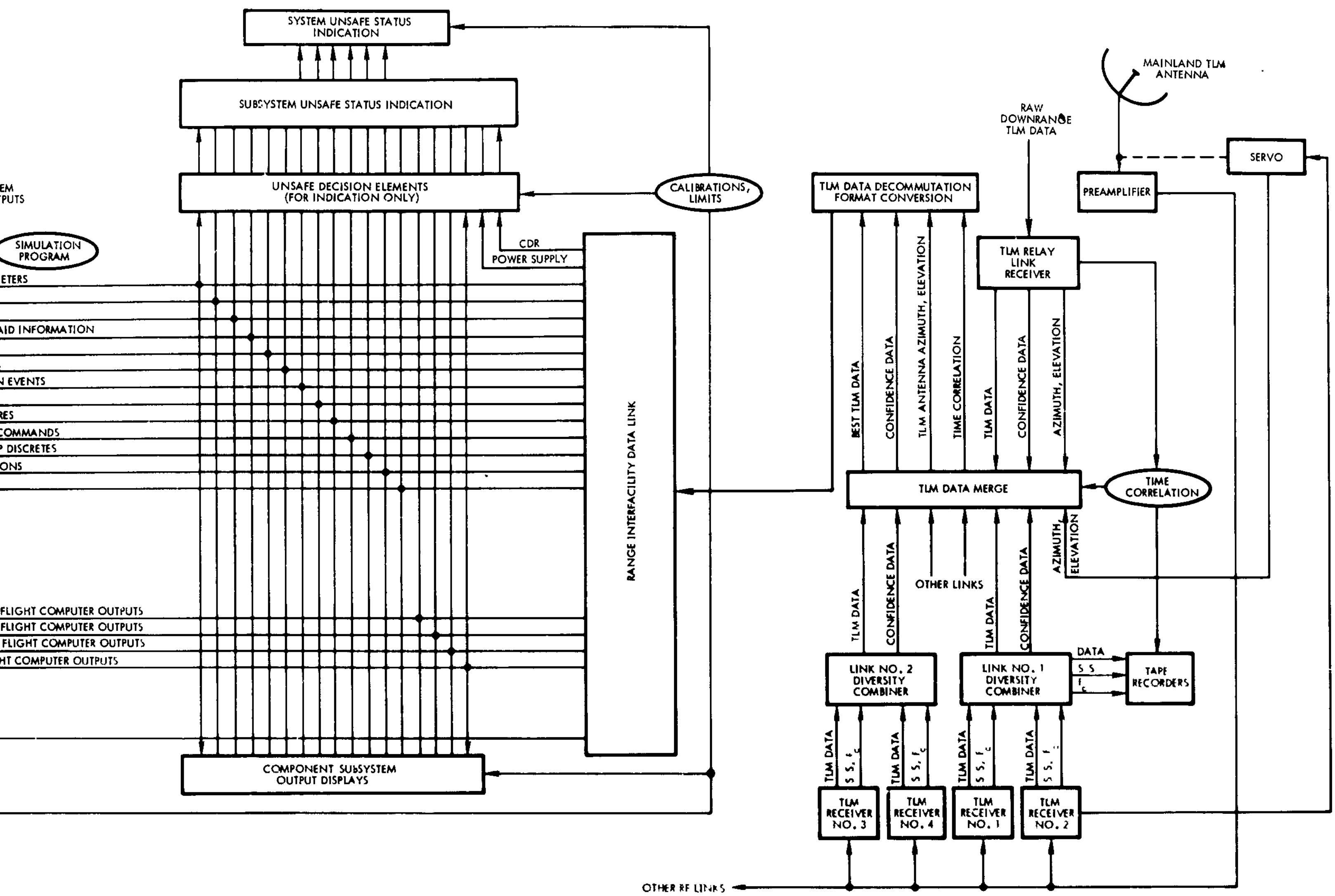

Figure 1. Comprehensive Use of Telemetry as an Adjunct to Range Safety

Information in categories 7 through 9 would, in all probability, not be very desirable if a man were in the link because he would have to act on the basis of his knowledge and memory of flight system nominal performance criteria. More desirable inputs to him would be flight system, subsystem and component safe/unsafe status indications (in that order), with decisions made by machine logic, using preprogrammed limits and calibrations. These indications would enable anticipation of onboard troubles. Perhaps the most valuable supplementary telemetry inputs for IIP computer would be scaled, time-correlated, flight computer position and velocity outputs. These can be utilized in the generation of a separate plot or combined with external data to obtain a best estimate of trajectory plot.

The impact prediction data most difficult to obtain will be position and velocity data from a simulated flight system operating in real time from telemetered inputs, including acceleration, platform position, guidance commands, etc. Not only will complete calibration and scale factor information be required, but a flight system simulation program capable of operation in real time will be needed.

If the telemetry receiving and processing station is not physically located very close to the range safety facility, a data link will be required between the two. Because of the accuracy, resolution, and data rates involved, a digital link is indicated. The telemetry data must be decommutated and converted to a suitable format for transmission and decision. Calibrations, scale factors, safe limits, and time correlations must be applied, either at the telemetry data processing station or at the range safety facility; and since a high launch rate can be expected, the hardware must be readily programmable. The supporting data will be furnished to the range by the contractors as magnetic tapes with last-minute revisions made by punched tape or cards. The telemetry decommutation problem could be expected to extend from reclocking and format conversion of digital telemetry data (such as that originating from the digital flight computer) to frequency discrimination, spectral analysis, and subsequent digitization before transmission to the range safety area.

Input to the decommutation facility will be raw, real-time telemetry data from one or more mainland receiving stations and raw or preprocessed data from downrange stations. The latter is extremely important if propagation interruptions and disturbances are to be minimized. Flame

attenuation and refraction effects become especially troublesome with tailon look angles, which are inevitable when tracking a missile from the launch site. The only means of filling in telemetry dropouts has been to merge mainland data with downrange data. If this is to be conducted in real time during a flight, downrange telemetry data must be relayed, with minimum delay, to the central mainland data processing facility. This will be feasible at the AMR when the Tel 4 (on Merritt Island), Vero Beach, and Grand Bahama Island complex of telemetry receivers and data communications links is installed. Alternatives would be to decommutate telemetry signals downrange and either make safe/unsafe subsystem decisions locally, or to reformat a minimum of decommutated data at reduced sampling rates and bandwidths for transmission to the central mainland data processing facility (Figure 2). The first alternative would necessitate calibration, TLM format, and performance tolerance information at each station. A third alternative (illustrated in Figure 1) is based on use of a high-capacity transmission link between downrange and mainland stations, possibly a satellite communications system. Selection of the telemetry data source or sources for merging would necessitate transmission of supporting data such as receiver signal strength, signal center frequency, etc., along with the telemetry data.

A formidable time correlation problem would develop when merging data from many sources and locations in real time. This might be resolved by careful and frequent calibration of transmission link and equipment delays with due allowance for continuously varying vehicle range. Possibly an easier method would be to transmit all telemetry data as a function of known onboard time, e.g., as a function of the flight computer clock. The only disadvantage of this method would be the use of a small portion of the total telemetry link information capacity and some additional onboard logic.

In Table I, Group 1 inputs from guidance can, by themselves, provide an additional trajectory input to the range safety IIP computer, and also an indication of impending disaster by differencing with external tracking data. The remaining groups of data can be used to anticipate failures or out-of-tolerance conditions in a particular flight subsystem, possibly

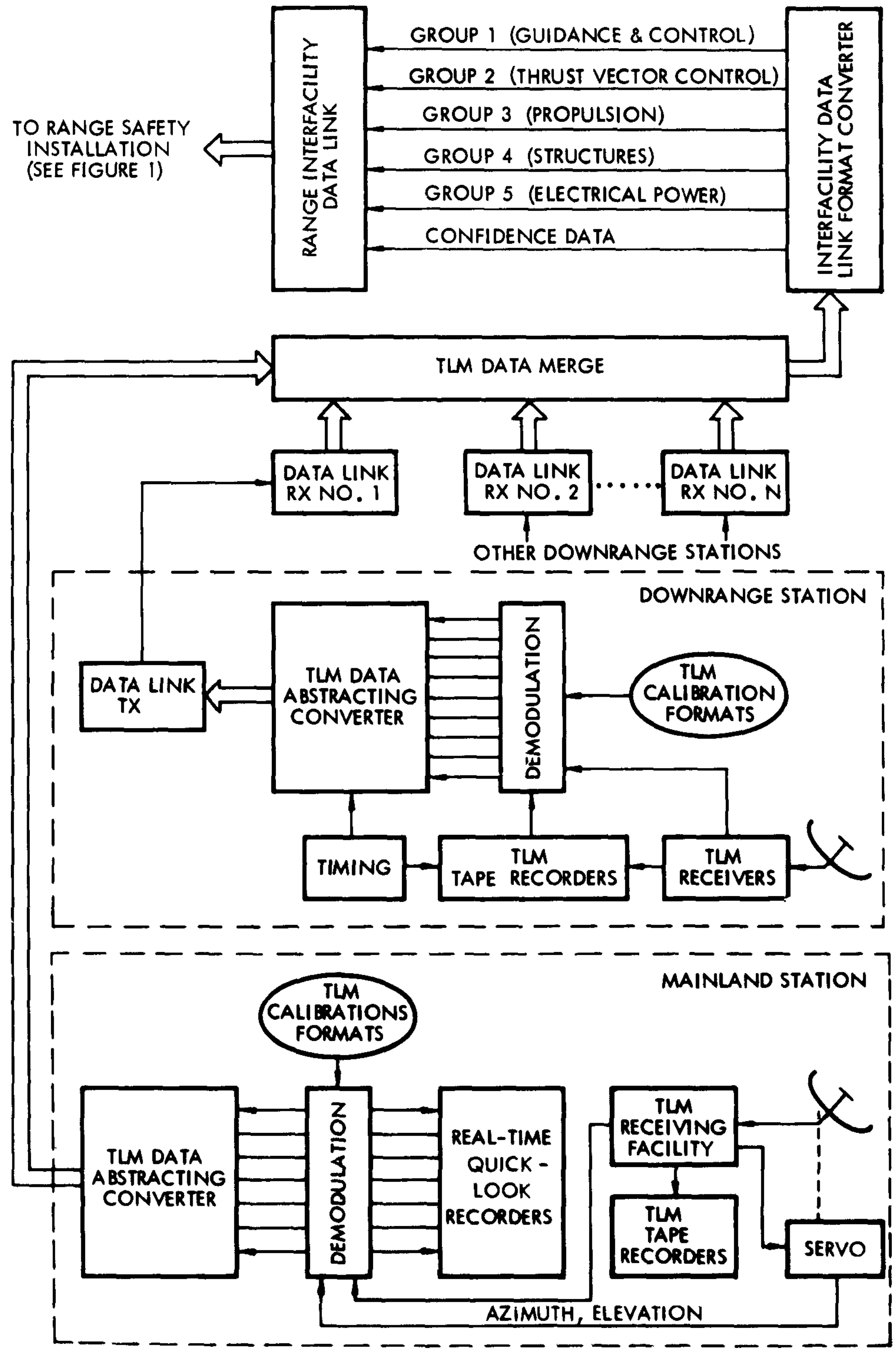

Figure 2. Telemetry Data Abstract as an Adjunct to Range Safety

Table I. Quantitative Description of Telemetered Data

Parameter	Sampling Rate (sps)	Bits Per Sample	Bits Per Second Subtotal
Guidance and Control (Group 1)			
Flight Computer Velocities			
$\dot{X}$	10	24	240
$\dot{Y}$	10	24	240
$\dot{Z}$	10	24	240
Flight Computer Positions			
X	10	24	240
Y	10	24	240
Z	10	24	240
Onboard Time			
t	10	17	170
Event Occurrences			
12	10	1	12
Total Bits Per Second, Group 1			1622
Thrust Vector Control (Group 2)			
Steering Commands			
Pitch	10	8	80
Yaw	10	8	80
Roll	10	8	80
Steering Errors			
Pitch	10	8	80
Yaw	10	8	80
Roll	10	8	80
Total Bits Per Second, Group 2			480
Propulsion (Group 3)			
Chamber Pressure (Solid Engines)	10	8	80
Fuel Flow (Liquid Engines)	10	8	80
Total Bits Per Second, Group 3			160
Structures (Group 4)			
Temperatures (10, Minimum)	1	8	80
Strain/ Breakwires (4, Minimum)	10	1 to 8	40 to 320
Triaxial Power Spectral Density	10	8	80
Total Bits Per Second, Group 4			200 to 480
Electrical Power (Group 5)			
Voltages (6, Minimum)	10	8	480
Total Bits Per Second, Group 5			480
TOTAL INFORMATION BITS PER SECOND, ALL GROUPS			2942 to 3222

before any significant trajectory deviation from the norm would be sensed from external data alone. In the case of missions like 3.1, 3.2, 3.3, and 3.5, these data are extremely useful.

The information in Table I, reduced to binary digital format, requires a total of only about 3000 bits/sec, which is low enough to be transmitted over voice-range RF or hardline communication links even after taking into account sync, parity, and timing requirements. This makes real-time inflight use of downrange telemetry data practical in the near future. However, a minimum amount of calibration and scale factor data, telemetry formats, and safe/unsafe tolerance limits still will be furnished to the range in advance of flights. Also, it should be noted that each contractor would be called upon to implement two distinct types of telemetry measurement philosophies on every flight, namely the usual comprehensive measurement technique to obtain most detailed information on the greatest number of parameters practical for fine-grained flight analysis; and also an abstractive measurement technique to reduce the most vital information to the smallest bandwidth possible for supplementing range safety.

Abstracting can be done either when programming the airborne telemetry subsystem or at the ground data processing stations, but it is the contractor's responsibility to provide information to the range for conducting the task.

Appendix XVI. ONBOARD PREPROCESSING OF TELEMETRY DATA

Preprocessing is the changing of raw, real-time data into some modified form before transmission from the experiment vehicle. The bandwidth requirements of a given mission can be reduced if preprocessing is possible. The following material was collected during a study of the feasibility of preprocessing data from an aerospace vehicle such as a satellite.

1. EFFECT OF RELIABILITY ON INFORMATION RATE

The reliability problem caused by the addition of components for preprocessing is generally treated separately from the theory associated with preprocessing of the data. However, in order to compare the capabilities of several telemetry systems, we must consider their average data handling capabilities over a long period of time (interval of the mission) rather than the idealized peak data capability of the system. In practice, a given system may perform at maximum capability for only a short time after calibration until a component degrades enough to change the information handling capability of the system.

It is not within the scope of this report to give rigorous mathematical support to the concept of the data handling capability of a system. However, we do want to relate the concept of a system's reliability with its information handling capabilities, since most reports consider information rate and system reliability as separate entities.

The information capacity of one channel is

$$C_{ch} = B_{ch} \log_2 \left[\frac{\text{Total discrete signal levels}}{\text{Uncertain discrete signal levels}} \right] \text{ bits/sec}$$

where B_{ch} is the number of bits transmitted per second for a given channel. For example, if $B_{ch} = 7$ bits/sec, and there are 128 total discrete signal levels with only one uncertain discrete level, the information capacity is

$$C_{ch} = 7 \times \log_2 \left[\frac{128}{1} \right] = 49 \text{ bits/sec}$$

Now consider a condition where a component changes enough to cause an uncertainty in the signal of eight discrete signal levels. In this case, the channel information capacity is

$$C_{ch} = 7 \times \log_2 \left[\frac{128}{8}\right] = 28 \text{ bits/sec}$$

In general, because of component degradation, the information rate of a channel is a function of time. The average information rate associated with a given channel over the entire mission is denoted as $\overline{C}_{ch}$.

$$\overline{C}_{ch} = \frac{1}{T}\int_{o}^{T=\text{duration of mission}} B \log_2 \left[\frac{\text{Total number of discrete levels}}{\text{Number of uncertain discrete levels}}\right] dt \quad (1)$$

Let DL_n represent the number of discrete signal levels in the nth channel. DL is usually a fixed value for each channel and is not dependent upon time. Let $U_n(t)$ represent the number of uncertain discrete levels. Because of component degradation, U is a function of time. For a calibrated digital system, DL is equal to the total number of quantization levels. U is the quantization uncertainty which always includes a range from minus one-half bit to plus one-half bit around the quantized signal. Thus U is taken as one bit in a digital system. In an analog system, the ratio $\frac{DL}{U}$ may be considered the dynamic range of the channel and is determined by the maximum input signal and the errors in channel signal response.

The instantaneous information capacity of the entire system is equal to the sum of the instantaneous information capacities of each channel.

$$C_{system}(t) = B_1 \log_2 \left[\frac{DL_1}{U_1(t)}\right] + B_2 \log_2 \left[\frac{DL_2}{U_2(t)}\right] \cdot B_n \log_2 \left[\frac{DL_n}{U_n(t)}\right]$$

The average information capacity of the system over the mission is:

$$\overline{C}_{system} = \frac{1}{T}\int_{o}^{T=\text{duration of mission}} C(t)\, dt = \int_{o}^{T} \left\{B_1 \log_2 \left[\frac{DL_1}{U_1(t)}\right] \cdot B_n \log_2 \left[\frac{DL_n}{U_n(t)}\right]\right\} dt \quad (2)$$

We now have an expression for the average information rate per system which takes into account the degradation of the channel accuracy due to changes in component values. The accuracy of the above expression may be open to question; however, the purpose of the above work is not so much to derive a usable expression as it is to stress the importance of component reliability in evaluating the relative merits of various telemetering systems.

2. TYPES OF INFORMATION IN A SIGNAL

Transmitted data that represents events or states which could be predicted is referred to as inactive data in this appendix. Signals which are so random in nature that it is not practical to attempt to obtain cause-and-effect relations about the phenomena which they represent are called disordered data. For this type of signal we are usually interested in a gross effect, such as the average values and dispersion of the signals over a particular time interval. The main interest during a specified time interval is in the amplitude of the quantity being measured and not in the order in which the various measurements were taken. Most vibration data would be considered as disordered data.

A common attribute of inactive data and disordered data is that considerable savings in transmitter power or bandwidth, or both, may be obtained by preprocessing the data before transmission.

3. PREPROCESSING OF INACTIVE DATA

During the past 6 months, the various aspects of this phase of the problem have been studied under the names of Adaptive Telemetry Study, Data Redundancy Reduction, and Format Control (changing the sampling rates of the various channels). Some of the study results can be seen in References 1 and 2. Reference 1 is a quick-look study of the problem and is valuable because it briefly discusses the advantages and disadvantages of the various techniques that could be used for preprocessing inactive data. Reference 2 covers at some length basic considerations governing the prediction of data.

Preprocessing of certain data can substantially reduce the data transmitted from the spacecraft during parts of the flight. In Reference 3, data taken from Explorer VI indicated that if the only data transmitted

were that which changed from the immediate past value, only 20 percent of the data taken would have had to be transmitted. For Pioneer V, the redundancy was even larger and only about 5 percent of the data taken could be considered nonredundant. It appears that a separate program is required for each mission to determine if the objectives of the flight can best be served by eliminating the transmission of inactive data.

4. PREPROCESSING OF DISORDERED DATA

By definition, the information contained in disordered data is found in the amplitude of the measurement and not in the order of occurrence of the measurements. The transmission of a quantity's frequency spectrum or its statistical characteristics is the most common means for representing data in cases where the order in which the data was procured is not important. An illustration of this approach is the data acquisition system used in the Goddard experiment:

> The Goddard experiment is designed to measure the ultraviolet radiation from stars over a range of spectral wavelengths. Six parallel data channels accumulate pulses that represent the intensity of radiation at six different incremental portions of the ultraviolet spectrum. Data accumulated at each position is stored in spacecraft memory. Compression techniques are employed to reduce the number of bits which must be stored. (Reference 4)

The general problems encountered in the measurement of the signal's spectral density are discussed at length in References 5 through 11. A fundamental difficulty arises in obtaining spectral data when the conditions of the flight are changing rapidly. As the frequency band for a measurement is made narrower, the transient response of the associated filter network becomes increasingly larger. For a specified accuracy of spectral density data, a compromise is required between the spectral bandwidths of various frequency bands and the time during which the statistics of the signal remain constant. Because of this requirement, it is necessary that the data be obtained in a form suitable to its eventual use. For example, measurements of a vibration spectrum in an operating missile may be used to determine the structural design of a future missile.

The designer may require information about a relatively narrow spectrum, with a corresponding increase in the time required per measurement. Here, it would be important that the bandwidth associated with the spectral density measurements be appropriate to the ultimate use of the data. The "uncertainty principle" associated with measurements on atomic particles also applies to measurement of the spectral density. The time required for any measurement is inversely proportional to the bandwidth and directly related to the accuracy desired.

The statistics of a signal may be obtained from raw data and transmitted in place of the data itself. Reference 11 considers this problem and points out the conditions where a savings in transmitted data is realized. Over a small interval of the flight in which the data statistics do not change and the order of the measurements has no significance, data compression can be obtained by sending a signal's statistical parameters, such as its amplitude-probability density or significant moments of the amplitude-probability density function. The price paid for this type of data compression is considerably increased hardware complexity.

5. TELEMETRY BIT RATE REQUIREMENTS

The maximum bit rate required to sample a single channel is primarily determined by the frequency spectrum of the signal, and the desired accuracy of the sample. In theory, it is possible to sample at slightly greater than twice the highest frequency present in the data spectrum; however, in order to recover all of the information contained in the highest frequency of the signal, an "ideal" but physically nonrealizable filter is required in the demodulation process. In practice, the accuracy of the recovery of sampled data is dependent on the nonideal characteristics of the demodulator filter and sampled data rate. The data reconstruction errors caused by poor demodulator filter characteristics may be compensated to any desired degree by increasing the sampling rate. Before any calculations can be made on the required bit rate (and, therefore, the system bandwidth) for a specified accuracy of data reproduction, we would have to know something about the manner in which the transmitted sample data is to be reconstructed. In the following calculations of required telemetry bit rate, the assumption is made that the data are to be sampled at three times the highest frequency present in the signal and that the demodulation filter will reconstruct the

sampled data to the required accuracy. With this assumption, B_r^{CH}, the bit rate required for a single channel of data which is converted to a binary digital code for transmission is

$$B_r^{CH} \geq 3\, f_{max}\, N_B$$

where f_{max} is the maximum frequency present in the data and N_B is the number of bits required to transmit the data with the specified accuracy.

Where there are many channels in which the data is converted to a binary code before transmission, the overall system bit rate required is equal to the sum of the bit rates associated with each channel. For an m-channel system:

$$B_r^{system} = \sum_{i=1}^{m} B_{r_i}^{channel} = 3 \sum_{i=1}^{m} f_{max_i}\, N_{B_i}$$

The total bandwidth required is approximately equal to the system bit rate. Bandwidth (cps) = B_r^{system} (bits/sec).

In systems where the amplitude is not converted to a binary form before transmission, for example, PAM, the required bit rate per channel is again determined by the required accuracy. Roughly speaking, for a few percent error, the bandwidth required per analog channel will be equal to the sample rate. The precise error in the sampling process is a function of the entire telemetry system's frequency response. It is felt that in a PAM system the assumption that the required bandwidth is equal to the reciprocal of the bit rate will be sufficiently accurate for the purpose intended; however, further study on this problem is recommended. The overall system bandwidth is the sum of the bandwidths required by each digital channel and analog channel.

$$\text{System Bandwidth} = 3\left[\underbrace{\sum_{i=1}^{m} f_{max_i}\, N_{B_i}}_{\text{PCM}} + \underbrace{\sum_{i=1}^{n} f_{max_i}}_{\text{PAM}}\right]$$

6. BANDWIDTH REQUIRED BY TIME-OF-EVENT MEASUREMENTS

It appears that the time of occurrence of an event with respect to a reference event can best be determined by counting the pulses which occur in a high-frequency pulse train during the interval separating the two events. Then the number of pulses stored in a counter is a measure of the time duration between events. The clock frequency chosen must be high enough so that an error of one count will not cause a count error in excess of the required measurement accuracy. If the measurement must be transmitted with minimum delay after the event, a means must be found for inserting the word representing the measurement into the telemetry format as soon as possible. The initial reference time marker could be defined by the occurrence of a synchronizing bit and transmitted every frame. The number of bits which would have to be transmitted for a given measurement accuracy is:

$$N_B^T = \log_2 \frac{\text{time duration of 1 frame (sec)}}{\text{allowable error of measurement (sec)}}$$

As an example, if it were required to measure the occurrence of an event with respect to the synchronization signal to ±100-μsec accuracy, a 10-kc clock source is required. If a new frame occurs at 3-sec intervals, the number of bits required for transmission is:

$$N_B^T = \log_2 \frac{3 \text{ sec}}{10^{-4} \text{ sec}} \approx 15 \text{ bits}$$

For an amplitude-modulated transmission, the data bandwidth must be multiplied by a factor of two; for single-sideband transmission, the transmission bandwidth is equal to the data bandwidth.

In the calculation of the bandwidths required to transmit a given information rate, it is commonly assumed that a bandwidth of $1/\tau$ is required to transmit a pulse of width τ. The following graph shows that the optimum signal-to-noise ratio occurs when f_c, the system bandwidth, is less than $1/\tau$. For a system transmission characterized by a gaussian response (several RC low-pass filters having the same cutoof frequency), the ideal bandwidth system is $f_c \approx 0.3/\tau$. For a double-sideband system,

the total data bandwidth would be $2 \times 0.3/\tau$. Thus calculated, the data bandwidths are larger than the bandwidths required for a maximum S/N ratio. The optimum transmission bandwidth required is determined by the type of modulation employed and the overall data frequency response of the transmission system and data reconstruction network. (See Figure 1. Also see Reference 12.)

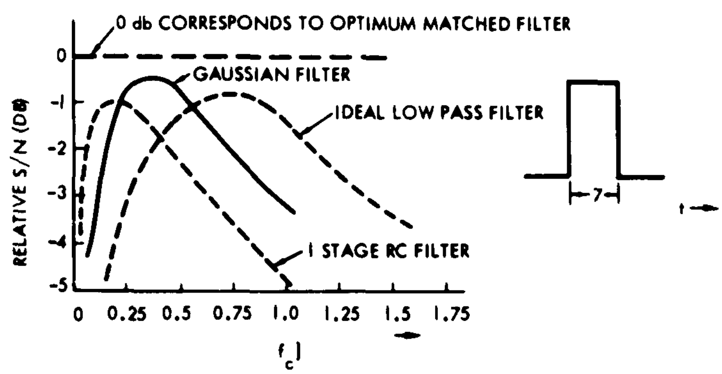

Figure 1. Peak S/N Ratio for Various Filters

7. SUMMARY

A good example of preprocessing data from a space vehicle can be seen in the Goddard experiment. It is discussed in Reference 4.

It appears that all the types of data on the mission will be suitable for preprocessing because maximum data activity will occur during a small portion of the mission, leaving much of the mission time unused for telemetry purposes. The longer a mission, the more valuable will preprocessing be. On short missions, especially if the data changes continuously, preprocessing is of little or no value.

The effect that preprocessing has on reliability is a most important consideration in deciding upon the feasibility of preprocessing for a given case. An approach to this problem is to determine the change in information rate that can be realized through preprocessing. Information rate must, in this case, be taken as a function of accuracy, component degradation, and component failure.

It appears that one of the major tasks in the design of systems for telemetering data from space will be to determine a tradeoff between the degradation of data accuracy caused by preprocessing of data and the potential increased transmission and reception accuracy provided when preprocessing of data allows smaller data bandwidths to be utilized. It is believed that component reliability and system transmission characteristics should be included in the expression for the system information rate and that this expression may be used as a basis for determining the type of telemetry system to be used for a specific mission.

Clearly, preprocessing of data, if reliable components are used, will increase the system information capabilities in the initial phases of the mission. The use of data preprocessing will reduce the required bit rate with a consequent reduction in transmitted power for a given signal-to-noise ratio. It is entirely possible, because of the lower power requirements, that an improved data transmission reliability over the entire mission can be obtained by using data preprocessing techniques.

Although preprocessing has a significant effect on the airborne system development, the effect on ground station capability is largely one of data interpretation and analysis. In a sense, it can be considered to have no effect on the space-to-ground link because it provides improved spectrum utilization through the elimination of nonuseful or superfluous information. In light of current trends, preprocessing will probably not result in less bandwidth but rather more useful information.

REFERENCES

1. B. Dunbridge, "Adaptive Telemetry Study," IOC 9334.8-213, 29 June 1962.

2. "STL Research Report 1962," Adaptive Telemetry Section.

3. J. L. Markson, "Analysis of Data from Explorer VI and Pioneer V," 9334.8-340, 7 December 1962.

4. D. Kushner, "Data Processing for the Goddard Experiment," 1962 National Symposium on Space Electronics, Section 4.4, Kollsman Instrument Corp., Elmhurst, New York.

5. E. R. Carlson, "Study of Vibration Telemetry Using Statistical Approach," STL IOC to H. T. Hayes, 7240.4-923, 29 April 1960.

6. J. L. Sevy, "Errors Associated with the Measurement of Power Spectral Density," STL IOC to H. T. Hayes, 7240.4-908, 24 March 1960.

7. A Ratz, "Telemetry Bandwidth Compression Using Airborne Spectrum Analyzer," Proceedings of the IRE, April 1960, p 694.

8. C. Morrow, STL "Random Vibration," and "Averaging Time and Data-Reduction Time for Random Vibration Spectra," Journal of the Acoustical Society of America, May 1958 and June 1958. (STL Reprints No. 81 and No. 82).

9. C. T. Morrow, "Significance of Power Spectra and Probability Distributions in Connection with Vibration," reprinted from Noise Control, September 1960 and October 1960. (STL Reprint 263).

10. J. S. Bendat, "Principles and Applications of Random Noise Theory," J. Wiley, Chapter 2 (inc).

11. J. L. Markson, "Transmission of a Quantity's Amplitude Density Distribution," STL IOC, 9334.8-314, 9 October 1962.

12. M. Schwartz, Information Transmission, Modulation, and Noise, McGraw-Hill, Figure 6-9, page 289.

BIBLIOGRAPHY

1. J. R. Helme and R. A. Schomburg, "A Data Bandwidth Compressor for Space-Vehicle Telemetry," Lockheed Missile and Space Co., Proceedings of the 1962 National Telemetry Conference, Section 3-2, Washington, D. C.

2. W. K. Pratt, "Stop-Scan Edge Detection System for Interplanetary Television Transmission," Proceedings of 1962 National Symposium on Space Electronics and Telemetry, Section 4. 3, Miami Beach, Florida.

3. G. Rohrer, "Inertial Guidance Department Input on RIPS Telemetry," STL IOC 9331. 8-174, 13 December 1962.

4. A. Rosen, "Some Constraints Imposed on a Global Instrumentation Complex Resulting from Long-Range Space Experiment Requirements," STL IOC, 20 December 1962.

5. D. R. Weber and F. J. Synhoff, "The Concept of Self-Adaptive Data Compression," Proceedings of 1962 National Symposium on Space Electronics and Telemetry, Section 4. 1, Miami Beach, Florida.

Appendix XVII. ADAPTIVE TELEMETRY

Telemetry system design is conventionally based on a fixed sampling plan selected prior to a mission. The sampling rates are thus determined on the basis of worst-case environments (maximum frequency response); and, since average sampling rate requirements may be significantly lower than those of worst-case environments, inefficiency in terms of power and/or bandwidth usually results. In addition, even further inefficiency can accrue because no attempt is made to take advantage of the predictability of the data.

For some time past, a research program on advanced telemetry techniques has been conducted at Space Technology Laboratories, Inc. Since this program is believed to be typical of what is being done to investigate adaptive telemetry, it is described in the following pages.

The specific objective of the STL telemetry research program is the development of adaptive telemetry techniques to remove redundancy from data prior to transmission by employing more nearly optimum sampling plans as a function of changing requirements during a mission, and by removing predictable portions of the data. The redundancy reduction techniques that have been studied, analyzed, and developed could minimize the usual constraints on overall spacecraft weight and power, or alternately, could provide increased communication range or greater information return for fixed spacecraft weight and power. Although a shortage of bandwidth spectrum is not now a space telemetry problem, its advent will be another reason for employing redundancy reduction.

The program has included a study of the mechanisms which can cause redundancy, a study of format control, and a study of prediction techniques; additionally, an error analysis has been made of various forms of prediction. Equipment designed to verify various portions of the program includes a model predictor based on extrapolation, a probability generator that generates a serial bit stream (with conditional probabilities selectable up to the fourth order), and two types of format generators.

1. SUMMARY

In this research program, redundancy reduction techniques were developed and shown to have a definite capability for improving the link efficiency of space telemetry.

Adaptive format control refers to the dynamic control of experiment sampling rates. Redundancy reduction is secured by the mechanism of preventing the excessive sampling rates typical of present telemetry systems, and by the optimum allocation of the available samples among the experiments. The feasibility of efficient implementation of adaptive format control has been demonstrated by the design of format generators (References 1, 2). These format generators synthesize the appropriate multiplexer driving signals for a multitude of different sampling plans. The frequency spectrum of each experiment is matched to its chosen sampling rate by selecting one of the available format generator sampling plans either automatically or by ground command.

It is also possible to achieve redundancy reduction by the general method of prediction. This concept requires that a prediction of the forthcoming sampled data be made (on the basis of available past data), which, when subtracted from the actual data values, produces an error term. This error term can be coded and transmitted with the use of fewer bits than contained in the original data because of the partial elimination of the redundant portions. On the ground, an identical prediction is made which, when added to the received error term, reproduces exactly the original data samples. One type of predictor may be synthesized by the elementary approach of curve-fitting, whereby the sampled data is used to determine a smooth curve which is then extrapolated one sample-time to obtain a predicted value. In particular, a polynomial extrapolator was designed and analyzed which has the capability of eliminating data redundancy due to excessive sampling. An analysis of data return from Explorer VI and Pioneer V shows that a data compression of at least 10 db is easily possible using a simple polynomial extrapolator. A laboratory model was designed and fabricated to demonstrate the feasibility of the concept.

Prediction may also be based upon a probability measure of an experiment source. Work was initiated on the self-adaptive estimation of the joint probability distribution of a source when there is no a priori knowledge. Given the statistics of the source, a linear or nonlinear predictor can then be designed to efficiently compress its data samples. The purpose of prediction is to produce an error probability density whose entropy is minimized. An extensive analysis of prediction errors was undertaken to analyze the effectiveness of linear predictors for various classes of random and nonrandom sources. Theory was developed to derive the error distribution when the probability distribution of the source is given, and the mean-square prediction error when only the power spectrum of the source is known. Optimum linear predictors of various orders (the order refers to the number of past data samples operated upon) were derived. The prediction efficiency of polynomial extrapolation was compared to that of optimum linear predictors. The conditions under which higher-order linear predictors (including extrapolators) show an increase in efficiency were determined. The results were applied to gaussian random processes, and various types of deterministic (nonrandom) periodic source waveforms.

In addition to the more general techniques of format control, extrapolation, and prediction based on probability measure, special adaptive techniques were also investigated, such as special measurement design, limit checking, and sample-burst telemetering. These approaches can be used to supplement or even replace the general methods, depending upon the nature of the specific mission.

2. DISCUSSION OF PROBLEM

Prior to design of redundancy reduction techniques, the meaning of the term "redundancy" and the mechanisms responsible for its occurrence must be explored. Additionally, the application of a redundancy reduction technique generally creates some new requirements which need to be studied and understood. For instance, redundancy removal results in fewer symbols which often must be mapped into a new format requiring special coding before the samples can be correctly distinguished.

Even before discussing the above considerations, three points, which are considered axiomatic and which should be used as check points in any meaningful application of redundancy reduction, can be established.

> The weight, power, and reliability "cost" of a redundancy reduction concept (for a given mission) should be less than that required to achieve the same expected "gain" by increasing transmitter power, antenna size, etc.
>
> The redundancy reduction process should be implemented so that the original measurement can be recreated at the receiver. Thus, *a priori* knowledge, ground predictor output, or other information in connection with the received signal shall permit a recreation of f(t), or in more general case f(x) where x can be any parameter.
>
> The application of a redundancy reduction concept is no guarantee that the "expected" gain will be achieved. Indeed, under conditions of "unfavorable" statistics, the redundancy content may be significantly lower than expected. For the case where the system design is based on this expected value and the instantaneous information rate is larger than can be accommodated by the communication link, some means of priority control must be available. This may consist of decreasing accuracy, lowering sampling rates, etc.

Redundancy can be mathematically related to the basic measure of information, that is

$$R = \left[1 - \frac{H(x)}{H_E} \right] 100 \qquad (1)$$

where

R = redundancy in percent

$H(x)$ = measure of information from source x in bits/symbol

H_E = measure of information assuming all symbols equally likely

In the simplest case, with no symbol interdependence

$$H(x) = - \sum_{i=1}^{m} \rho(i) \log \rho(i) \qquad (2)$$

where

$\rho(i)$ = probability of ith symbol

m = number of symbols

Equation (2) is simply extended by use of joint or conditional probabilities to appropriately cover the more general case where there is symbol interdependence. For redundancy reduction processes which do not involve the determination of the probability distribution, Equations (1) and (2) primarily provide insight and establish limits on maximum possible gain. For instance, some evaluations of different probability distributions clearly show that a given distribution has to be particularly peaked if many db-equivalent gains are to be achieved. A simple example is the case where the amplitude distribution has a unity probability of existing in one-half of the total normalized range and, therefore, only one bit is saved. To save 3 db, the amplitude distribution must be confined (on the average) to the square root of the total number of quantization levels.

The mechanisms responsible for data redundancy are many: First, a designer may choose sampling rates far beyond the practical margins of the sampling theorem. This result may simply be an unintentional matter of poor prediction; but even if the prediction were perfect, the sampling rates would be based on peak frequency response requirements, while the average sampling rate requirements are generally significantly lower. Next, there are the limitations of the sampling theorem which makes no use of probability or prediction. Finally, there is the redundancy created as a result of the inefficient measurement technique. For example, some measurements are more efficiently characterized and transmitted in terms of their densities, moments, or time of occurrence rather than as a running amplitude function of time.

Although several sources have reported on the high redundancy in transmitted data and have quoted compression ratios up to 300, the foregoing discussion points up the difficulty of accurately assessing the

magnitude of the redundancy. Compression itself generally involves such new interface problems as coding and buffering. The net redundancy reduction must be determined after considering the additional coding information required to insure that the received data can be properly distinguished.

In a general sense, prediction is the basis for all redundancy reduction. For example, in either the fixed or adaptive sampling plan, a prediction is made that one format is better matched to actual requirements than another. Prediction in the vehicle and corresponding prediction at the receiver appears to offer the greatest potential for minimizing redundancy.

It could be correctly concluded that the problem of inefficient sampling would be of no consequence if an ideal prediction were possible. In an engineering sense, however, there is no ideal or 100-percent efficient system; consequently, the adoption of adaptive format control is necessary to establish a reasonably efficient sampling plan and must accompany the use of pure prediction to achieve a practical solution to the general redundancy reduction problem.

3. SPECIAL ADAPTIVE TECHNIQUES

In addition to the general approaches of format control and prediction by extrapolation or probability measure, there exist many special adaptive techniques that are capable of data compression. These special techniques are of limited applicability but, depending on the spacecraft mission, may be used to supplement or even replace the more general approaches. That is, they may be tailored to the particular experiments and environment of some special mission. A cross section of these special methods will be mentioned here.

The most obvious way to match the telemetry to the mission is by employing "special measurement design," such that only the most pertinent measurements from the experiments are telemetered. Most telemetry systems have been chosen to monitor some time function defined on each experiment. This does not necessarily represent the most efficient scheme, especially when the time of occurrence of the measurements is of insignificant value. Thus, it may be desirable to

transmit data in a form which is more directly usable by experimenters and scientists. For instance, it is possible (Reference 3) to transmit only data concerning the probability distribution of the amplitude of a physical quantity, such as the distribution of energies of particles. It may be appropriate to measure only the time of occurrence of peak data values or some other special event; time derivatives or other derived data characteristics may also be telemetered. The advantage of special measurement design is that only quantities of interest for each experiment are recorded, so that redundancy reduction is achieved by not transmitting irrelevant and redundant data. Of course the main disadvantage is that these special measurements may require added weight, power, and complexity, thus detracting from the objectives of an adaptive telemetry system.

Preprogrammed format control (Reference 4) is a special technique whereby sampling rates are automatically modified and redistributed at specific points of flight time or range. Mechanization of such control is quite feasible, but the applicability is only for those special missions where a priori information concerning the appropriate sampling rates, i.e., the expected activity of each experiment, is abundant.

Similarly, it is possible to employ a limit-checking technique (Reference 4) in which the data for each experiment are not transmitted when the samples are within certain preestablished amplitude limits. These limits represent the "normal" or the "expected" behavior of the experiment, so that only if the readings exceed these limits is the data of significant information value and worthy of transmission. Limit-checking is appropriate only for those classes of experiments in which the normal behavior is known beforehand.

In the way of special coding techniques, if it is expected that the physical quantities being measured have a highly peaked instantaneous amplitude distribution, then it will be appropriate to employ optimum coding procedures (Reference 5) for each data sample. This approach is related to that of limit-checking. It should be emphasized that the distribution must be considerably peaked with respect to the allowed voltage range of the telemetry in order that a significant data compression

be attained. For instance, a triangular distribution over the range yields only a 1-db compression.

Lastly, consider the special technique of sample-burst telemetry (Reference 6), whereby experiments are sampled at a high rate, on a duty cycle basis only. That is, in order to obtain information concerning the high frequency components of some telemetry source, a burst of samples is allocated to the source after which a longer period of no sampling ensues until the next burst, etc. One interpretation of this method is the scanning of each source in turn at the maximum sampling rate compatible with the available transmitter bandwidth:

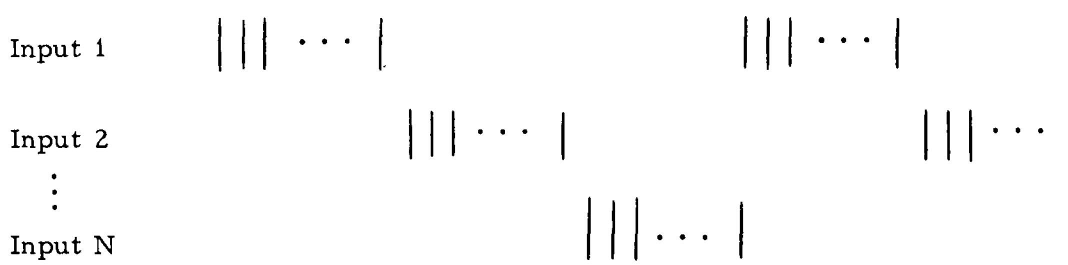

(Each line represents one sample)

This scan mode may also be used in conjunction with self-adaptive or command-adaptive format control for purposes of determining the optimum format. This is done by searching for high data activity in each source, and the signal conditioning bandwidths must also be altered in proportion to the change in sampling rates. Otherwise, the sample-burst approach offers a compromise to the situation in which the available spacecraft transmitter bandwidth is insufficient to permit sampling all sources at their appropriate (high) rates. Thus, information concerning all portions of the signal spectra is available only some of the time. However, it is also sometimes possible to regain the lost data by interpolation. For instance, if the source is statistically stationary, then burst sampling permits the fine grain as well as the coarse statistics to be detected and, during the periods of no sampling, it is expected that the source behaves in a manner similar to that observed during periods of burst sampling. In such cases, it can be shown that the sample-burst technique will provide a net redundancy reduction since it employs a

more efficient use of the available bandwidth. Finally, it should be noted that if it is desired to reconstruct exactly the continuous source waveform during the burst times, then there is a limitation as to the minimum number of samples which must be contained in a single burst (Reference 6).

4. FUTURE STUDY

Various techniques of adaptive telemetry have been devised which demonstrate a capability for the redundancy reduction or compression of telemetry data. Each method has its own merits and appropriate fields of application. However, the method of prediction based on probability measure offers promise as a more optimum general solution and, consequently, further detailed analytical and development effort should be applied in this direction.

Specifically, the technique of prediction based on probability measure warrants further effort on the adaptive estimation of statistical parameters. Also, optimum linear predictors should be studied in order that the upper bounds for all linear prediction techniques may be determined. Nonlinear predictors should be considered and their performance compared against that of optimum linear predictors. A prediction error analysis should be undertaken for various classes of random and nonrandom data sources. In connection with prediction, the general coding problem should be further studied.

In addition, there remain the tasks of optimization and practical mechanization of these predictive techniques, as well as the verification of their performance relative to that expected.

Prediction by polynomial extrapolation is presently a highly developed technique. Further effort should be devoted to the evaluation of other extrapolative methods, the comparison of extrapolation to optimum prediction, and the analysis of spacecraft data return from previous missions.

It is suggested that some of the more special adaptive techniques, such as sample-burst telemetering and special measurement design, be more closely scrutinized to determine their exact applicability and effectiveness.

REFERENCES

1. G. F. Marsh and R. E. Gottfried, "Adaptive Telemetry Format Generator," 1962 National Telemetering Conference.

2. B. Dunbridge, "Adaptive Telemetry Study: Format Generator," 9334.8-220, 9 July 1962.

3. J. L. Markson, "Transmission of a Quantity's Amplitude Density Function," 9334.8-314, 9 October 1962.

4. B. Dunbridge, "Adaptive Telemetry Study," 9334.8-213, 6 June 1962.

5. D. A. Huffman, "A Method for the Construction of Minimum Redundancy Codes," Proc. IRE, 40, 1952.

6. B. Dunbridge, "Sample-Burst Telemetry System," 9334.8-308, 27 September 1962.

BIBLIOGRAPHY

B. Dunbridge, "Prediction by Extrapolation of Equally-Spaced Data," 9334.8-296, 14 September 1962.

B. Dunbridge, "Synchronization Considerations for Adaptive Telemetry Systems," 9334.8-253, 8 August 1962.

B. Dunbridge, "Prediction Error Analysis and Predictive Coding," 9334.8-374, 26 December 1962.

B. Dunbridge, "Effect of Bandlimited Noise on Joint Probability Generator," 9334.8-303, 26 September 1962.

P. Elias, "Predictive Coding, Parts I and II," Transactions PGIT, March 1955.

J. R. Hulme and R. A. Schomberg, "A Data Bandwidth Compressor for Space Vehicle Telemetry," 1962 National Telemetering Conference.

J. L. Markson, "Joint Probability Generator," 9334.8-259, 5 September 1962.

J. L. Markson, "Analysis of Data from Explorer VI (Able-3) and Pioneer V," 9334., 8-340, 7 December 1962.

J. E. Medlin, "Buffer Requirements for a Telemetry Data Compressor," 1962 National Telemetering Conference.

E. Parzen, Modern Probability Theory and Its Applications, J. Wiley and Sons, 1960.

"Redundancy Reduction Memory Proposal," 9334.8-206, 22 June 1962.

M. Reza, Introduction to Information Theory, McGraw-Hill, 1961.

M. Schwartz, Information Transmission, Modulation, and Noise, McGraw-Hill, 1960.

D. R. Weber and F. J. Wynhoff, "The Concept of Self-Adaptive Data Compression," PGSET Record, 1962.

Appendix XVIII. COMMAND SYSTEM TECHNIQUES

A. INTRODUCTION

In many ways a command system is similar to a telemetry link except for the reversal in communication direction. Also the output of a command system always results in an action, as opposed to the output of a telemetry system which leads to an interpretation or an evaluation. This last factor introduces substantial differences in design philosophy. For a telemetry system the problem of whether or not data is being transmitted seldom intermingles with the problem of what the data being transmitted says. With the command system, not only must each possible command be distinguishable, but the state of no-command at all must be recognized. In other words, the analysis of a command system more closely parallels that of a radar system than that of a conventional communication or telemetry system. Thus the concept of a false alarm or the activation of a command mode when it was not initiated at the control center becomes extremely important.

There are two main problems concerned with the false alarm aspect of a command system. The first concerns false alarms arising from a natural, that is unintentional, background environment. The second class is concerned with those resulting from a deliberate action on the part of an unauthorized agency. In order to determine within which class any command problem lies, one must focus on both the consequences of a false alarm and the value to an unauthorized agency. (In this context, a false alarm consists of any command action taken by the vehicle which was not initiated from the proper control center.)

B. NATURAL BACKGROUND ENVIRONMENT

If it has been determined that the command system to be used for a specific mission falls into the category of operation in a natural background environment, the design process can proceed in a relatively straightforward manner. In essence, the problem consists of selecting waveforms for each command that are significantly unlike each other and whose probability of being duplicated in the existing natural environment is less than the desired probability of false alarm. Two factors contribute to the

selection of the waveforms. The first factor is the total energy of the waveform at the command receiver and the other is the distribution of this energy in time and frequency. There will always be a minimum total received energy required by the command system and this energy will be a function of the desired false-alarm rate, the number of commands, the rapidity with which commands can be sent, the statistical properties of the background noise environment, and the modulation efficiency of the communication technique employed. A lower bound for the amount of energy required can be determined by assuming a system consisting of a single command in a background of white gaussian noise of known spectral density, a modulation technique of perfect efficiency, and a combined transmission rate and frequency of tolerable false alarms which produce a specific probability of false alarm within one command interval.

This is accomplished by determining from a normal curve of error the number of standard deviations corresponding to the specified maximum accepted probability of false alarm. The minimum required command energy which must be received can then be determined by multiplying the variance by the noise spectral density at the corresponding point in the system. To refer this minimum value of received energy to that of transmitted energy one must make use of the range equation, remembering that power is energy per unit time and thus proportional to energy when comparing the two ends of the communication link. A knowledge of the available transmitter power can now be used with the required energy to determine the minimum command duration. As an example, consider a system operating in a background noise spectral density of -177 dbm per cps (double sided) and whose desired probability of false alarm per pulse is 10^{-8}. A normal curve of error says that 5.6 standard deviations will be exceeded this fraction of the time. Squaring this value and converting to db yields 15 db. Thus the required signal energy must be greater than 15 db above -177 db mw (-177 db relative to 1 mw/sec) or at least -162 db mw/sec. If the space loss for some particular application is 200 db, then the required transmitter energy will be 38 db mw/sec (that is, 38 db above a mw/sec or 8 db above a watt/sec). Thus 6.32 watt/sec of energy are required. This might consist of a 1-watt transmitter for 6.32 sec or a 1000-watt transmitter for 6.32 msec or any other compatible

combination. More commands will increase the required energy although not greatly because of the already large S/N ratio. Modulation inefficiencies, which consist of the use of transmitter energy for any purpose other than conveying the command itself, can require substantial increases in signal energy. As many as 20 db may have to be added in certain cases. This wasted power generally is used to overcome frequency instabilities, provide synchronization, overcome theoretically unneeded threshold, etc. Some of the best command systems in use today achieve overall modulation efficiencies of 12 db. (The modulation efficiency is the ratio of the power required for the system to operate with a specified performance to that required by an optimum system for the same level of performance.)

Having established the total energy required to prevent false alarms in the presence of thermal background noises, one must decide how this energy should be distributed throughout time and frequency so as to minimize its likelihood of generation by other nongaussian interferences such as radar signals, other command codes, television, voice, etc. There are several commonly accepted techniques for distributing the required energy throughout the time frequency domain. These include PCM (generally with error correcting and detecting pulses), PPM, and tone systems.

1. TONE SYSTEMS

For very simple command systems, the tone approach has received wide usage. By this technique one or more (usually more) of several possible tones must be simultaneously present to enact a specified command. The number of different commands (C) which are available can be quickly calculated in terms of the total number of tones available (N) and the number of tones which must simultaneously be present for validation (M). This is given by the formula $C = \frac{N!}{M!\,(N-M)!}$. The simple tone approach is generally not used where a large number of commands are required because of the unwieldy number of tones required. Hybrid tone systems employing sequences of tones are sometimes used. Thus a smaller number of tones can be used to generate an expanding number of command signals.

2. PCM SYSTEMS

Where a larger quantity of commands is required, the trend in command system design has universally been toward PCM. PCM consists of a series of zeros and ones which establish a predetermined acceptable pattern. The zeros and ones can be mechanized as any two distinguishable states of the transmitted signal. Synchronization is usually obtained by one or more pulses,at the beginning of the command sequence, which constitute a start symbol or by means of an auxiliary signal, usually a tone, which is continually transmitted. A parity check of one kind or another (that is, an error-detecting or-correcting code) is almost universally employed. One of the simplest forms of parity comparison consists of sending the command twice, generally inverted the second time (that is, a one replaced by a zero and a zero by a one), and requiring that the two portions of the command be identical (but inverted) before it is accepted. Sometimes a single parity bit is used in conjunction with a sequence of command pulses in the form of an error-detecting code. Also, it is possible to introduce redundant pulses in such a manner as to construct a system of orthogonal command codes. These codes have the property that half the bits in any command will be different from the corresponding bits in any other command. Two commands can never be confused unless at least half of the bits are in error. It is also possible to permit acceptance of commands, even though a single or small number of pulses is in error, without substantially risking the possibility of command misinterpretation.

3. PPM SYSTEM

PPM command systems have thus far not received wide usage. An equivalent application of PPM, however, has occurred in IFF equipment for a number of years. Generally speaking, PPM systems possess most of the properties of the orthogonal PCM system discussed previously, except that the ratio of peak-to-average power is substantially greater. PPM systems would find their greatest use in integrated tracking and command systems employing a pulsed radar ranging system. In this case, the large peak pulse powers required are inherently available in the

radar system and commands can then be conveyed by means of auxiliary pulses occupying specific delay relationships with respect to the periodically emitted ranging pulses.

C. HOSTILE ENVIRONMENT

When the environment, within which the command system is intended to operate, includes signals intentionally generated by an unauthorized agency to neutralize or take over a missile or spacecraft, considerably greater sophistication in the design of a command system is required. Although tone and PPM concepts might still be employed, ease of implementation almost invariably leads to the selection of PCM as a starting point. In designing a command system which requires a low false alarm rate in the presence of unauthorized counter action, it is not sufficient to utilize waveforms which are not likely to occur naturally because it can be anticipated that an intelligent agency will duplicate the class of signals used (such factors as modulation technique, carrier frequency, bit rates, etc. , cannot be concealed from such an agency indefinitely). As a minimum, what is required is that an extremely large class of possible codes exist from which only a relatively small number are valid at a time. This means that the unauthorized agency, even though he can quickly determine the properties of the large class of signals, has no rational means available to him to determine which of this large class are valid commands. He can, of course, begin a systematic procedure of generating all possible members of the class in the hope of stumbling upon a valid command. This is not, however, likely to provide him with success if the class of possible commands is sufficiently large and those within the class which are valid are changed sufficiently often. Typically a command system will be expanded by 40 pulses more than those actually required, to ensure security from unauthorized action. In addition, it is essential that the unauthorized agency not be able to reduce the class size substantially by examining the intercepted commands. This means, as a minimum, that no command code once transmitted can ever be used again.

There are several ways of implementing command security systems, the most secure of which requires the individual encoding of every command. Alternate techniques use a secure signal only to momentarily "unlock" the command encoder just prior to receipt of a "clear" command or to

cause execution of a command previously transmitted in the clear, stored in a command memory, and verified as to correctness through a telemetry link. Combinations of these techniques are also possible.

Because of the requirement for propagation between command station and spacecraft, commands must be modulated upon a carrier. Several techniques are available including AM, FM, and PM, both digital and analog. Each varies in its relative communications efficiency, that is the strength of the command signal required to produce an acceptable false alarm rate; and equipment capability including complexity, reliability, and ability to perform properly under all circumstances. Commands may be encoded directly on the carrier or they may be encoded on a subcarrier which is in turn modulated on a carrier. The latter approach is beneficial when an integrated CW tracking and command system is employed. This makes it particularly easy to separate tracking and command signals in the spacecraft receiver.

Appendix XIX. SUMMARY OF TELEMETRY, SPACE COMMUNICATIONS, AND SPACE COMMAND EQUIPMENT

This appendix contains tabulated estimates of all the telemetry, space communication, and space command equipment required at the instrumentation stations from 1965 to 1970 (Tables 1 through 6). This information is also included in Section IV, Recommended Network, together with additional information for each station. It is included here to show a condensed picture of the equipment distribution in the global network.

1965

TOTAL TELEMETRY, SPACE COMMUNICATIONS, AND SPACE COMMAND EQUIPMENT

Instrumentation Stations		Antennas		RF Receivers				Demultiplexers				PREDETECTION RECORDERS	LOCAL DISPLAY CHANNELS	FORWARDED DATA CHANNELS	VOICE COMMUNICATIONS	TELEVISION RECEIVER	COMMAND ENCODERS AND TRANSMITTERS	POSTDETECTION RECORDERS
						Other												
No.	Name	LOW GAIN	HIGH GAIN	VHF	UHF	TYPE	NO. TOTAL	PCM/FM	FM/FM	PAM/FM-PDM/FM	SS/FM							
A1	CCMTA	12	3	37	10	BC	3	15	28	20	18	3	100	-	5	2	RS/HK	16
A2. 1	Vero Beach	3	1	29	4	B	2	6	15	10	-	1	-	20	1	1	RS	10
A3	Grand Bahama	3	1	29	6	BC	3	6	15	10	1	1	8	20	2	1	RS/HK	10
A5	San Salvador	3	-	17	4	B	2	2	5	5	1	-	-	-	1	-	RS	6
A7	Grand Turk	3	-	9	4	B	2	2	5	5	1	-	-	-	1	-	RS	3
A9. 1	Antigua	3	1	18	6	B	2	6	15	10	3	1	20	50	2	1	RS/HK	6
A12	Ascension	6	1	19	6	A	2	6	12	4	3	1	10	20	2	1	HK	7
A13	Pretoria	6	1	10	6	-	-	6	12	2	-	1	20	10	2	1	HK	4
A14	Mahe, Seychelles	6	1	5	2	A	2	3	8	2	-	-	10	10	-	-	HK	2
A(B)	Bermuda	3	-	10	4	C	1	3	15	6	3	-	-	10	2	1	HK	4
D1	Mobile DSIF Sta.	3	-	-	-	B	2	2	-	-	-	1	20	20	-	-	HK	1
D2	Goldstone	3	4	-	-	B	2	2	-	-	-	1	20	20	1	1	HK	2
D4	Woomera	3	2	-	-	B	2	2	-	-	-	1	20	20	1	1	HK	2
D5	Johannesburg	3	2	-	-	B	2	2	-	-	-	1	20	20	1	1	HK	2
MR4	Grand Canary	2	1	4	2	-	-	2	-	-	-	-	-	20	2	1	HK	2
MR14	Guaymas	2	1	4	2	-	-	2	-	-	-	-	-	20	2	1	HK	2
MR16	Corpus Christi	5	2	8	2	-	-	6	1	1	-	-	20	10	2	-	HK	3
P1	Pt. Mugu	6	2	10	4	-	-	1	4	5	-	1	30	40	-	-	-	4
P2	Vandenberg	10	3	30	10	-	-	2	18	16	-	2	70	-	1	1	RS/HK	11
P3	San Nicholas	6	-	10	4	-	-	1	4	5	-	-	10	40	-	-	RS	4
P8	Pt. Pillar	6	-	5	2	-	-	1	4	2	-	-	10	40	-	-	-	2
P11	Kokee Park, Kauai	4	1	5	1	-	-	-	4	1	-	-	-	-	1	-	HK	2
P21	Kwajelein Atoll	4	-	5	1	-	-	1	4	1	-	1	10	20	-	-	HK	2
P23	Wake Island	3	1	2	3	C	1	1	10	1	-	-	-	10	1	-	HK	3
P24	Midway Island	3	-	2	2	C	1	1	10	1	-	-	-	10	1	-	HK	2
P25	Canton Island	4	-	5	1	-	-	1	4	1	-	1	10	20	-	-	HK	2
P41	Los Negros Island	4	-	5	2	-	-	1	4	1	-	1	10	20	1	-	HK	3
P(CA)	Carnarvon	6	1	5	1	E	2	2	4	1	-	-	10	20	-	-	HK	2

P2	Vandenberg	10	3	30	10	-	-	2	18	16	-	2	70	-	1	1	RS/HK	11
P3	San Nicholas	6	-	10	4	-	-	1	4	5	-	-	10	40	-	-	RS	4
P8	Pt. Pillar	6	-	5	2	-	-	1	4	2	-	-	10	40	-	-	-	2
P11	Kokee Park, Kauai	4	1	5	1	-	-	-	4	1	-	-	-	-	1	-	HK	2
P21	Kwajelein Atoll	4	-	5	1	-	-	1	4	1	-	1	10	20	-	-	HK	2
P23	Wake Island	3	1	2	3	C	1	1	10	1	-	-	-	10	1	-	HK	3
[illegible]	Midway Island	3	-	2	2	C	1	1	10	1	-	-	-	10	1	-	HK	2
[illegible]	Canton Island	4	-	5	1	-	-	1	4	1	-	1	10	20	-	-	HK	2
[illegible]	Los Negros Island	4	-	5	2	-	-	1	4	1	-	1	10	20	1	-	HK	3
[illegible]	Carnarvon	6	1	5	1	E	2	2	4	1	-	-	10	20	-	-	HK	2
[illegible]	Darwin	4	1	5	2	E	2	2	4	1	-	1	10	20	1	1	HK	3
P(JO)	Johnston Island	2	1	1	1	-	-	1	-	-	-	-	10	-	1	-	HK	2
EAFB	Edwards	10	1	5	1	C	1	1	4	1	-	-	50	20	1	1	HK	1
WSMR	White Sands	4	-	2	2	-	-	1	1	1	-	-	50	20	1	1	HK	2
APGC	Eglin	2	2	4	2	-	-	1	2	2	-	-	20	10	1	-	HK	2
SKTS	Kodiak	-	1	-	-	A	2	1	1	1	-	-	-	-	-	-	HK	1
SATS	Annette	-	1	-	-	A	2	1	1	1	-	-	-	-	-	-	HK	1
SFNS	Thule	-	1	-	-	A	2	1	1	1	-	-	-	-	-	-	HK	1
SNHS	New Hampshire	-	1	-	-	A	2	1	1	1	-	-	-	-	-	-	HK	1
SHTS	Kaena Point	-	1	-	-	A	2	1	1	1	-	-	-	-	-	-	HK	1
X1	Rosman, N. C.	2	1	2	1	E	2	1	-	-	-	-	-	-	-	-	HK	1
ARIS 1		6	1	15	6	C	1	2	2	1	1	1	20	-	1	-	HK	7
ARIS 2		6	1	15	6	C	1	2	2	1	1	1	20	-	1	-	-	7
AMRS 1	Twin Falls Victory	6	1	10	4	ABC	5	2	1	1	-	1	20	-	1	-	RS/HK	3
AMRS 2	Amer. Mariner	6	1	10	4	B	1	2	1	1	-	1	20	-	1	-	HK	3
PMRS 1	Range Tracker	6	1	10	4	C	1	2	1	1	-	1	20	-	1	-	HK	3
PMRS 4	Richfield	6	-	5	1	C	1	1	1	1	-	1	20	-	1	-	HK	2
PMRS 6	Watertown	6	-	5	1	-	-	1	1	1	-	1	20	-	-	-	-	2
PMRS 7	Huntsville	6	-	5	1	-	-	1	1	1	-	1	20	-	-	-	-	2
PMRS 8	T-AGM-8	2	-	5	1	C	1	1	1	1	-	1	-	-	1	-	HK	1
M006	Blossom Point	2	-	2	1	E	2	1	-	-	-	1	-	-	-	-	HK	1
M021	Ft. Myers	2	-	2	1	E	2	1	-	-	-	1	-	-	-	-	HK	1
M029	Grand Forks	2	-	2	1	E	2	1	-	-	-	1	-	-	-	-	HK	1
M030	Fairbanks	2	-	2	1	E	2	1	-	-	-	1	-	20	-	-	HK	1
M451	St. Johns	2	-	2	1	E	2	1	-	-	-	1	-	-	-	-	HK	1
M652	Winkfield	2	-	2	1	E	2	1	-	-	-	1	-	-	-	-	HK	1
M800	Quito	2	-	2	1	E	2	1	-	-	-	1	-	-	-	-	HK	1
M801	Lima	2	-	2	1	E	2	1	-	-	-	1	-	-	-	-	HK	1
M803	Antofagasta	2	-	2	1	E	2	1	-	-	-	1	-	-	-	-	HK	1
M802	Santiago	2	-	2	1	E	2	1	-	-	-	1	-	-	-	-	HK	1
WI	Wallops Island	2	-	2	2	-	-	1	-	-	-	-	-	-	-	-	HK	1

A = 400 mc B = DSIF C = SHF D = SGLS E = 136 mc

1966

TOTAL TELEMETRY, SPACE COMMUNICATIONS, AND SPACE COMMAND EQUIPMENT

Instrumentation Stations		Antennas		RF Receivers		Other		Demultiplexers										
No.	Name	LOW GAIN	HIGH GAIN	VHF	UHF	TYPE	NO. TOTAL	PCM/FM	FM/FM	PAM/FM-PDM/FM	SS/FM	PREDETECTION RECORDERS	LOCAL DISPLAY CHANNELS	FORWARDED DATA CHANNELS	VOICE COMMUNICATIONS	TELEVISION RECEIVER	COMMAND ENCODERS AND TRANSMITTERS	POSTDETECTION RECORDERS
A1	CCMTA	12	3	40	10	BC	3	15	28	20	18	3	100	-	5	3	RS/HK	16
A2. 1	Vero Beach	3	1	29	10	B	2	6	15	10	-	1	-	20	1	1	RS/HK	10
A3	Grand Bahama	3	1	29	10	BC	3	6	15	10	1	1	8	20	2	1	RS/HK	10
A5	San Salvador	3	-	17	10	B	2	2	5	5	1	-	-	-	1	-	RS	7
A7	Grand Turk	3	-	9	6	B	2	2	5	5	1	-	-	-	1	-	RS	4
A9. 1	Antigua	3	1	18	8	B	2	6	15	10	3	1	20	50	2	1	RS/HK	6
A12	Ascension	6	1	19	6	A	2	6	12	4	3	1	10	20	2	1	HK	7
A13	Pretoria	6	1	10	6	-	-	6	12	2	-	1	20	10	2	1	HK	4
A14	Mahe, Seychelles	6	1	5	2	A	2	3	8	2	-	-	10	10	-	-	HK	3
A(B)	Bermuda	6	-	8	4	C	1	3	15	6	3	-	-	10	2	-	HK	5
D1	Mobile DSIF Sta.	3	-	-	-	B	2	2	-	-	-	1	20	20	-	1	HK	1
D2	Goldstone	3	4	-	-	B	2	2	-	-	-	1	20	20	1	1	HK	2
D4	Woomera	3	2	-	-	B	2	2	-	-	-	1	20	20	1	1	HK	2
D5	Johannesburg	3	2	-	-	B	2	2	-	-	-	1	20	20	1	1	HK	2
MR4	Grand Canary	2	1	4	3	-	-	2	1	-	-	-	-	20	2	1	HK	2
MR14	Guaymas	2	1	4	3	-	-	2	-	-	-	-	-	20	2	1	HK	2
MR16	Corpus Christi	5	2	8	4	-	-	6	1	1	-	-	20	10	2	-	HK	3
P1	Pt. Mugu	6	2	10	4	-	-	1	4	5	-	1	30	40	-	-	-	4
P2	Vandenberg	10	3	30	10	A	2	2	18	16	-	2	70	-	1	1	RS/HK	11
P3	San Nicholas	6	-	10	4	-	-	1	4	5	-	-	10	40	1	-	RS	4
P8	Pt. Pillar	6	-	5	2	-	-	1	4	2	-	-	10	40	-	-	-	2
P11	Kokee Park, Kauai	4	1	5	2	-	-	-	4	1	-	-	-	-	1	-	HK	2
P21	Kwajelein Atoll	4	-	5	2	-	-	1	4	1	-	1	10	20	-	-	HK	2
P23	Wake Island	3	1	2	3	C	1	1	10	1	-	-	-	10	1	-	HK	3
P24	Midway Island	3	-	2	3	C	1	1	10	1	-	-	-	10	1	-	HK	2
P25	Canton Island	4	-	5	2	-	-	1	4	1	-	1	10	20	-	-	HK	2
P41	Los Negros Island	4	-	5	2	-	-	1	4	1	-	1	10	20	1	-	HK	3
P(CA)	Carnarvon	6	1	5	2	A	2	2	4	1	-	-	10	20	1	-	HK	2

P2	Vandenberg	10	3	30	10	A	2	2	18	16	-	2	70	-	1	1	RS/HK	11
P3	San Nicholas	6	-	10	4	-	-	1	4	5	-	-	10	40	1	-	RS	4
P8	Pt. Pillar	6	-	5	2	-	-	1	4	2	-	-	10	40	-	-	-	2
11	Kokee Park, Kauai	4	1	5	2	-	-	-	4	1	-	-	-	-	1	-	HK	2
21	Kwajalein Atoll	4	-	5	2	-	-	1	4	1	-	1	10	20	-	-	HK	2
23	Wake Island	3	1	2	3	C	1	1	10	1	-	-	-	10	1	-	HK	3
24	Midway Island	3	-	2	3	C	1	1	10	1	-	-	-	10	1	-	HK	2
P25	Canton Island	4	-	5	2	-	-	1	4	1	-	1	10	20	-	-	HK	2
P41	Los Negros Island	4	-	5	2	-	-	1	4	1	-	1	10	20	1	-	HK	3
P(CA)	Carnarvon	6	1	5	2	A	2	2	4	1	-	-	10	20	1	-	HK	2
P(D)	Darwin	4	1	5	2	A	2	2	4	1	-	1	10	20	1	1	HK	3
P(JO)	Johnston Island	2	1	1	2	C	-	1	-	-	-	-	10	-	1	-	HK	2
EAFB	Edwards	10	1	5	2	C	1	1	4	-	-	-	50	20	1	1	HK	2
WSMR	White Sands	4	-	2	2	-	-	1	1	1	-	-	50	20	1	1	HK	2
APGC	Eglin	2	2	4	3	-	-	1	2	2	-	-	20	10	1	-	HK	2
SKTS	Kodiak	-	1	-	-	A	2	1	1	1	-	-	-	-	-	-	HK	1
SATS	Annette	-	1	-	-	A	2	1	1	1	-	-	-	-	-	-	HK	1
SFNS	Thule	-	1	-	-	A	2	1	1	1	-	-	-	-	-	-	HK	1
SNHS	New Hampshire	-	1	-	-	A	2	1	1	1	-	-	-	-	-	-	HK	1
SHTS	Kaena Point	-	1	-	-	A	2	1	1	1	-	-	-	-	-	-	HK	1
X1	Rosman, N. C.	2	1	2	1	A	2	1	-	-	-	-	-	-	-	-	HK	-
ARIS 1		6	1	15	6	C	1	2	2	1	1	1	20	-	1	-	HK	7
ARIS 2		6	1	15	6	C	1	2	2	1	1	1	20	-	1	-	-	7
AMRS 1	Twin Falls Victory	6	1	10	4	ABC	5	2	1	1	-	1	20	-	1	-	RS/HK	3
AMRS 2	Amer. Mariner	6	1	10	4	B	1	2	1	1	-	1	20	-	1	-	HK	3
PMRS 1	Range Tracker	6	1	10	4	C	1	2	1	1	-	1	20	-	1	-	HK	3
PMRS 4	Richfield	6	-	5	2	C	1	1	1	1	-	1	20	-	1	-	HK	2
PMRS 6	Watertown	6	-	5	1	-	-	1	1	1	-	1	20	-	-	-	-	2
PMRS 7	Huntsville	6	1	5	1	-	-	1	1	1	-	1	20	-	-	-	-	2
PMRS 8	T-AGM-8	2	-	5	1	C	1	1	1	1	-	1	-	-	1	-	HK	-
M006	Blossom Point	2	-	2	2	E	2	1	-	-	-	1	-	-	-	-	HK	2
M021	Ft. Myers	2	-	2	2	E	2	1	-	-	-	1	-	-	-	-	HK	2
M029	Grand Forks	2	-	2	2	E	2	1	-	-	-	1	-	-	-	-	HK	2
M030	Fairbanks	2	-	2	2	AE	4	1	-	-	-	1	-	20	-	-	HK	2
M451	St. Johns	2	-	2	2	E	2	1	-	-	-	1	-	-	-	-	HK	2
M652	Winkfield	2	-	2	2	E	2	1	-	-	-	1	-	-	-	-	HK	2
M800	Quito	2	-	2	2	E	2	1	-	-	-	1	-	-	-	-	HK	2
M801	Lima	2	-	2	2	E	2	1	-	-	-	1	-	-	-	-	HK	2
M803	Antofagasta	2	-	2	2	E	2	1	-	-	-	1	-	-	-	-	HK	2
M802	Santiago	2	-	2	2	E	2	1	-	-	-	1	-	-	-	-	HK	2
WI	Wallops Island	2	-	2	-	-	-	-	-	-	-	-	-	-	-	-	HK	1

A = 400 mc B = DSIF C = SHF D = SGLS E = 136 mc

1967

TOTAL TELEMETRY, SPACE COMMUNICATIONS, AND SPACE COMMAND EQUIPMENT

Instrumentation Stations		Antennas		RF Receivers				Demultiplexers				PREDETECTION RECORDERS	LOCAL DISPLAY CHANNELS	FORWARDED DATA CHANNELS	VOICE COMMUNICATIONS	TELEVISION RECEIVER	COMMAND ENCODERS AND TRANSMITTERS	POSTDETECTION RECORDERS
						Other												
No.	Name	LOW GAIN	HIGH GAIN	VHF	UHF	TYPE	NO. TOTAL	PCM/FM	FM/FM	PAM/FM-PDM/FM	SS/FM							
A1	CCMTA	12	3	30	20	BC	3	15	28	20	18	3	100	-	7	4	RS/HK	18
A2.1	Vero Beach	3	1	25	15	B	2	6	15	10	-	1	-	20	2	1	RS/HK	12
A3	Grand Bahama	3	1	25	15	BC	3	6	15	10	1	1	8	20	2	1	RS/HK	12
A5	San Salvador	3	-	12	15	B	2	2	5	5	1	-	-	-	2	-	RS	8
A7	Grand Turk	3	-	7	8	B	2	2	5	5	1	-	-	-	2	-	RS	5
A9.1	Antigua	3	1	15	10	B	2	6	15	10	3	1	20	50	3	1	RS/HK	7
A12	Ascension	6	1	15	10	AD	3	6	12	4	3	1	10	20	2	1	HK	9
A13	Pretoria	6	1	7	10	-	-	6	12	2	-	1	20	10	2	1	HK	5
A14	Mahe, Seychelles	6	1	4	2	AD	3	3	8	2	-	-	10	10	-	-	HK	3
A(B)	Bermuda	3	-	6	4	C	1	3	15	6	3	-	-	10	2	-	HK	5
D1	Mobile DSIF Sta.	3	-	-	-	B	2	2	-	-	-	1	20	20	-	1	HK	1
D2	Goldstone	3	4	-	-	B	2	2	-	-	-	1	20	20	2	1	HK	3
D4	Woomera	3	2	-	-	B	2	2	-	-	-	1	20	20	2	1	HK	3
D5	Johannesburg	3	2	-	-	B	2	2	-	-	-	1	20	20	2	1	HK	3
MR4	Grand Canary	3	1	3	3	-	-	2	1	-	-	-	-	20	3	1	HK	3
MR14	Guaymas	3	1	3	3	-	-	2	-	-	-	-	-	20	3	1	HK	2
MR16	Corpus Christi	5	2	7	6	-	-	6	1	1	-	-	20	10	3	-	HK	3
P1	Pt. Mugu	6	2	8	6	-	-	1	4	5	-	1	30	40	-	-	-	4
P2	Vandenberg	10	3	25	15	AD	3	2	18	16	-	3	70	-	2	1	RS/HK	12
P3	San Nicholas	6	-	8	6	-	-	1	4	5	-	-	10	40	1	-	RS	5
P8	Pt. Pillar	6	-	5	3	-	-	1	4	2	-	-	10	40	-	-	-	3
P11	Kokee Park, Kauai	4	1	5	3	C	1	-	4	1	-	-	-	-	1	-	HK	2
P21	Kwajalein Atoll	4	-	5	3	-	-	1	4	1	-	1	10	20	-	-	HK	2
P23	Wake Island	4	1	2	4	-	-	1	10	1	-	-	-	10	2	-	HK	3
P24	Midway Island	3	1	2	3	-	-	1	10	1	-	-	-	10	2	-	-	2
P25	Canton Island	4	-	5	3	-	-	1	4	1	-	1	10	20	-	-	HK	3
P41	Los Negros Island	4	-	5	3	-	-	1	4	1	-	1	10	20	2	-	HK	3
P(CA)	Carnarvon	6	1	5	3	A	2	2	4	1	-	-	10	20	2	-	HK	2

P2	Vandenberg	10	3	25	15	AD	3	2	18	16	-	3	70	-	2	1	RS/HK	12
P3	San Nicholas	6	-	8	6	-	-	1	4	5	-	-	10	40	1	-	RS	5
P8	Pt. Pillar	6	-	5	3	-	-	1	4	2	-	-	10	40	-	-	-	3
P11	Kokee Park, Kauai	4	1	5	3	C	1	-	4	1	-	-	-	-	1	-	HK	2
P21	Kwajelein Atoll	4	-	5	3	-	-	1	4	1	-	1	10	20	-	-	HK	2
P23	Wake Island	4	1	2	4	-	-	1	10	1	-	-	-	10	2	-	HK	3
P24	Midway Island	3	1	2	3	-	-	1	10	1	-	-	-	10	2	-	-	2
[illegible]	Canton Island	4	-	5	3	-	-	1	4	1	-	1	10	20	-	-	HK	3
[illegible]	Los Negros Island	4	-	5	3	-	-	1	4	1	-	1	10	20	2	-	HK	3
[illegible]	Carnarvon	6	1	5	3	A	2	2	4	1	-	-	10	20	2	-	HK	2
[illegible]	Darwin	4	1	5	3	A	2	2	4	1	-	1	10	20	2	1	HK	4
[illegible]	Johnston Island	2	1	1	2	C	1	1	-	-	-	-	10	-	2	-	HK	2
EAFB	Edwards	10	1	5	3	C	1	1	4	-	-	-	50	20	2	1	HK	2
WSMR	White Sands	4	-	2	2	-	-	1	1	1	-	-	50	20	2	1	HK	2
APGC	Eglin	3	2	3	3	-	-	1	2	2	-	-	20	10	1	-	HK	3
SKTS	Kodiak	-	1	-	-	AD	3	1	1	1	-	-	-	-	-	-	HK	1
SATS	Annette	-	1	-	-	AD	3	1	1	1	-	-	-	-	-	-	HK	1
SFNS	Thule	-	1	-	-	AD	3	1	1	1	-	-	-	-	-	-	HK	1
SNHS	New Hampshire	-	1	-	-	AD	3	1	1	1	-	-	-	-	-	-	HK	1
SHTS	Kaena Point	-	1	-	-	AD	3	1	1	1	-	-	-	-	-	-	HK	1
X1	Rosman, N. C.	2	1	2	2	A	2	1	-	-	-	-	-	-	-	-	HK	1
ARIS 1		6	1	10	10	C	1	2	2	1	1	2	20	-	2	-	HK	7
ARIS 2		6	1	10	10	C	1	2	2	1	1	2	20	-	2	-	-	7
AMRS 1	Twin Falls Victory	6	1	8	6	ABC	5	2	1	1	-	2	20	-	2	-	RS/HK	3
AMRS 2	Amer. Mariner	6	1	8	6	B	1	2	1	1	-	2	20	-	2	-	HK	3
PMRS 1	Range Tracker	6	1	10	6	C	1	2	1	1	-	2	20	-	2	-	HK	3
PMRS 4	Richfield	6	-	5	3	C	1	1	1	1	-	1	20	-	1	-	HK	2
PMRS 6	Watertown	6	1	5	2	-	-	1	1	1	-	1	20	-	-	-	-	2
PMRS 7	Huntsville	6	1	5	2	-	-	1	1	1	-	1	20	-	-	-	-	2
PMRS 8	T-AGM-8	2	1	5	2	C	1	1	1	1	-	1	-	-	1	-	HK	-
M006	Blossom Point	2	-	2	2	E	2	1	-	-	-	1	-	-	-	-	HK	2
M021	Ft. Myers	2	-	2	2	E	2	1	-	-	-	1	-	-	-	-	HK	2
M029	Grand Forks	2	-	2	2	E	2	1	-	-	-	1	-	-	-	-	HK	2
M030	Fairbanks	2	-	2	2	AE	4	1	-	-	-	1	-	20	-	-	HK	2
M451	St. Johns	2	-	2	2	E	2	1	-	-	-	1	-	-	-	-	HK	2
M652	Winkfield	2	-	2	2	E	2	1	-	-	-	1	-	-	-	-	HK	2
M800	Quito	2	-	2	2	E	2	1	-	-	-	1	-	-	-	-	HK	2
M801	Lima	2	-	2	2	E	2	1	-	-	-	1	-	-	-	-	HK	2
M803	Antofagasta	2	-	2	2	E	2	1	-	-	-	1	-	-	-	-	HK	2
M802	Santiago	2	-	2	2	E	2	1	-	-	-	1	-	-	-	-	HK	2
WI	Wallops Island	2	-	2	-	-	-	-	-	-	-	-	-	-	-	-	HK	1

A = 400 mc B = DSIF C = SHF D = SGLS E = 136 mc

1968

TOTAL TELEMETRY, SPACE COMMUNICATIONS, AND SPACE COMMAND EQUIPMENT

Instrumentation Stations		Antennas		RF Receivers				Demultiplexers										
						Other												
No.	Name	LOW GAIN	HIGH GAIN	VHF	UHF	TYPE	NO. TOTAL	PCM/FM	FM/FM	PAM/FM-PDM/FM	SS/FM	PREDETECTION RECORDERS	LOCAL DISPLAY CHANNELS	FORWARDED DATA CHANNELS	VOICE COMMUNICATIONS	TELEVISION RECEIVER	COMMAND ENCODERS AND TRANSMITTERS	POSTDETECTION RECORDERS
A1	CCMTA	12	3	30	25	BC	3	15	28	20	18	3	100	-	.7	4	RS/HK	18
A2.1	Vero Beach	3	1	20	20	B	2	6	15	10	-	2	-	20	2	1	RS/HK	12
A3	Grand Bahama	3	1	20	20	BC	3	6	15	10	1	2	8	20	2	1	RS/HK	12
A5	San Salvador	3	-	10	15	B	2	2	5	5	1	1	-	-	2	-	RS	10
A7	Grand Turk	3	-	5	10	B	2	2	5	5	1	1	-	-	2	-	-	6
A9.1	Antigua	3	2	12	14	B	2	6	15	10	3	2	20	50	3	1	RS/HK	9
A12	Ascension	6	2	5	20	AD	3	6	12	4	3	1	10	20	2	1	HK	10
A13	Pretoria	6	2	4	15	-	-	6	12	2	-	2	20	10	2	1	RS/HK	5
A14	Mahe, Seychelles	6	2	3	4	AD	3	3	8	2	-	-	10	10	-	-	RS/HK	4
A(B)	Bermuda	3	1	4	6	C	1	3	15	6	3	-	-	10	2	-	HK	6
D1	Mobile DSIF Sta.	3	-	-	-	B	2	2	-	-	-	1	20	20	-	1	HK	2
D2	Goldstone	3	4	-	-	B	2	2	-	-	-	2	20	20	2	1	HK	3
D4	Woomera	3	2	-	-	B	2	2	-	-	-	2	20	20	2	1	HK	3
D5	Johannesburg	3	2	-	-	B	2	2	-	-	-	2	20	20	2	1	HK	3
MR4	Grand Canary	3	1	3	4	-	-	2	5	-	-	-	-	20	3	1	HK	3
MR14	Guaymas	3	1	3	4	-	-	2	4	-	-	-	-	20	3	1	HK	3
MR16	Corpus Christi	6	3	6	10	-	-	5	5	1	-	-	20	10	3	-	HK	4
P1	Pt. Mugu	6	2	6	8	-	-	1	4	5	-	2	30	40	-	-	RS	5
P2	Vandenberg	10	4	20	20	AD	3	2	18	16	-	3	70	-	2	1	RS/HK	12
P3	San Nicholas	6	-	6	8	-	-	1	4	5	-	-	10	40	1	-	RS	5
P8	Pt. Pillar	6	1	4	6	-	-	1	4	2	-	-	10	40	-	-	-	3
P11	Kokee Park, Kauai	4	1	4	5	C	1	-	4	1	-	1	-	-	1	-	HK	3
P21	Kwajelein Atoll	4	-	4	5	-	-	1	4	1	-	1	10	20	-	-	RS/HK	3
P23	Wake Island	4	1	2	4	-	-	2	10	1	-	-	10	20	2	-	HK	4
P24	Midway Island	4	1	1	3	-	-	1	10	1	-	-	-	10	2	-	-	3
P25	Canton Island	4	1	4	5	-	-	1	4	1	-	1	10	20	-	-	-	3
P41	Los Negros Island	4	1	4	5	-	-	1	4	1	-	1	10	20	2	-	HK	4
[illegible]	[illegible]	[illegible]	[illegible]	[illegible]	[illegible]			[illegible]	[illegible]	[illegible]		1	10	20	[illegible]		HK	3

P1	Pt. Mugu	6	2	6	8	-	-	1	4	5	-	2	30	40	-	-	RS	5
P2	Vandenberg	10	4	20	20	AD	3	2	18	16	-	3	70	-	2	1	RS/HK	12
P3	San Nicholas	6	-	6	8	-	-	1	4	5	-	-	10	40	1	-	RS	5
P8	Pt. Pillar	6	1	4	6	-	-	1	4	2	-	-	10	40	-	-	-	3
P11	Kokee Park, Kauai	4	1	4	5	C	1	-	4	1	-	1	-	-	1	-	HK	3
[illegible]	Kwajelein Atoll	4	-	4	5	-	-	1	4	1	-	1	10	20	-	-	RS/HK	3
[illegible]	Wake Island	4	1	2	4	-	-	2	10	1	-	-	10	20	2	-	HK	4
[illegible]	Midway Island	4	1	1	3	-	-	1	10	1	-	-	-	10	2	-	-	3
[illegible]	Canton Island	4	1	4	5	-	-	1	4	1	-	1	10	20	-	-	-	3
[illegible]	Los Negros Island	4	1	4	5	-	-	1	4	1	-	1	10	20	2	-	HK	4
P(CA)	Carnarvon	6	1	4	5	-	-	2	4	1	-	1	10	20	2	-	HK	3
P(D)	Darwin	4	2	4	5	-	-	2	4	1	-	1	10	20	2	1	-	4
P(JO)	Johnston Island	3	1	1	2	C	1	1	4	-	-	-	10	-	2	-	HK	2
EAFB	Edwards	10	1	4	5	C	1	1	4	-	-	1	50	20	2	1	HK	3
WSMR	White Sands	4	1	2	2	-	-	1	1	1	-	-	50	20	2	1	HK	3
APGC	Eglin	3	3	3	4	-	-	1	2	2	-	1	20	10	1	-	HK	3
SKTS	Kodiak	-	1	-	-	AD	3	1	1	1	-	-	-	-	-	-	HK	1
SATS	Annette	-	1	-	-	AD	3	1	1	1	-	-	-	-	-	-	HK	1
SFNS	Thule	-	1	-	-	AD	3	1	1	1	-	-	-	-	-	-	HK	1
SNHS	New Hampshire	-	1	-	-	AD	3	1	1	1	-	-	-	-	-	-	HK	1
SHTS	Kaena Point	-	1	-	-	AD	3	1	1	1	-	-	-	-	-	-	HK	1
X1	Rosman, N. C.	2	1	2	2	-	-	1	-	-	-	1	-	-	-	-	-	1
ARIS 1		6	1	8	12	C	1	2	2	1	1	2	20	-	2	1	HK	7
ARIS 2		6	1	8	12	C	1	2	2	1	1	2	20	-	2	1	HK	7
AMRS 1	Twin Falls Victory	6	1	6	8	ABC	5	2	1	1	-	2	20	-	2	-	RS/HK	3
AMRS 2	Amer. Mariner	6	1	6	8	B	1	2	1	1	-	2	20	-	2	-	HK	3
PMRS 1	Range Tracker	6	1	8	6	C	1	2	1	1	-	2	20	-	2	1	HK	3
PMRS 4	Richfield	6	1	4	5	C	1	1	1	1	-	1	20	-	1	-	HK	2
PMRS 6	Watertown	6	1	4	4	-	-	1	1	1	-	1	20	-	-	-	-	2
PMRS 7	Huntsville	6	1	4	4	-	-	1	1	1	-	1	20	-	-	-	-	2
PMRS 8	T-AGM-8	2	1	4	4	C	1	1	1	1	-	1	-	-	1	-	HK	-
M006	Blossom Point	2	-	1	3	E	2	1	1	1	-	1	20	-	-	-	HK	2
M021	Ft. Myers	2	-	1	3	E	2	1	1	1	-	1	20	-	-	-	HK	2
M029	Grand Forks	2	-	1	3	E	2	1	1	1	-	1	20	-	-	-	HK	2
M030	Fairbanks	2	-	1	3	E	4	1	1	1	-	1	20	20	-	-	HK	2
M451	St. Johns	2	-	1	3	E	2	1	1	1	-	1	20	-	-	-	HK	2
M652	Winkfield	2	-	1	3	E	2	1	1	1	-	1	20	-	-	-	HK	2
M800	Quito	2	-	1	3	E	2	1	1	1	-	1	20	-	-	-	HK	2
M801	Lima	2	-	1	3	E	2	1	1	1	-	1	20	-	-	-	HK	2
M803	Antofagasta	2	-	1	3	E	2	1	1	1	-	1	20	-	-	-	HK	2
M802	Santiago	2	-	1	3	E	2	1	1	1	-	1	20	-	-	-	HK	2
WI	Wallops Island	-	-	-	-	-	-	-	-	-	-	-	-	-	-	-	-	-

A = 400 mc   B = DSIF   C = SHF   D = SGLS   E = 136 mc

1969

TOTAL TELEMETRY, SPACE COMMUNICATIONS, AND SPACE COMMAND EQUIPMENT

Instrumentation Stations		Antennas		RF Receivers				Demultiplexers										
						Other												
No.	Name	LOW GAIN	HIGH GAIN	VHF	UHF	TYPE	NO. TOTAL	PCM/FM	FM/FM	PAM/FM-PDM/FM	SS/FM	PREDETECTION RECORDERS	LOCAL DISPLAY CHANNELS	FORWARDED DATA CHANNELS	VOICE COMMUNICATIONS	TELEVISION RECEIVER	COMMAND ENCODERS AND TRANSMITTERS	POSTDETECTION RECORDERS
A1	CCMTA	12	3	20	30	BC	3	15	28	20	18	3	100	-	7	5	RS/HK	22
A2.1	Vero Beach	3	1	15	20	B	2	6	15	10	-	2	-	20	2	1	RS	14
A3	Grand Bahama	3	1	15	20	BC	3	6	15	10	1	2	8	20	2	1	RS/HK	14
A5	San Salvador	3	-	10	15	B	2	2	5	5	1	1	-	-	2	-	RS	11
A7	Grand Turk	3	-	5	12	B	2	2	5	5	1	1	-	-	2	-	-	7
A9.1	Antigua	3	2	10	16	B	2	6	15	10	3	2	20	50	3	1	RS/HK	10
A12	Ascension	6	2	5	20	AD	3	6	12	4	3	1	10	20	2	1	HK	12
A13	Pretoria	6	2	4	15	-	-	6	12	2	-	2	20	10	2	1	RS/HK	6
A14	Mahe, Seychelles	6	2	3	4	AD	3	3	8	2	-	-	10	10	-	-	RS/HK	4
A(B)	Bermuda	3	1	2	8	C	1	3	15	6	3	-	-	10	2	-	HK	6
D1	Mobile DSIF Sta.	3	-	-	-	B	2	2	-	-	-	1	20	20	-	1	HK	2
D2	Goldstone	3	4	-	-	B	2	2	-	-	-	2	20	20	2	1	HK	4
D4	Woomera	3	2	-	-	B	2	2	-	-	-	2	20	20	2	1	HK	4
D5	Johannesburg	3	2	-	-	B	2	2	-	-	-	2	20	20	2	1	HK	4
MR4	Grand Canary	4	1	2	4	-	-	2	5	-	-	-	-	20	3	1	HK	4
MR14	Guaymas	7	1	2	4	-	-	2	4	-	-	-	-	20	3	1	HK	3
MR16	Corpus Christi	6	3	5	10	-	-	5	5	1	-	-	20	10	3	-	HK	4
P1	Pt. Mugu	6	2	6	10	-	-	1	4	5	-	2	30	40	-	-	RS	5
P2	Vandenberg	10	4	15	25	AD	3	2	18	16	-	4	70	-	2	1	RS/HK	13
P3	San Nicholas	6	-	6	10	-	-	1	4	5	-	-	10	40	-	-	RS	6
P8	Pt. Pillar	6	1	4	8	-	-	1	4	2	-	-	10	40	-	-	-	4
P11	Kokee Park, Kauai	4	1	2	5	C	1	-	4	1	-	1	-	-	1	-	HK	3
P21	Kwajelein Atoll	4	-	2	5	-	-	1	4	1	-	1	10	20	-	-	RS/HK	3
P23	Wake Island	4	1	2	4	-	-	2	10	1	-	-	10	20	2	-	HK	4
P24	Midway Island	4	1	1	3	-	-	1	10	1	-	-	-	10	2	-	-	3
P25	Canton Island	4	1	2	5	-	-	1	4	1	-	1	10	20	-	-	-	3
P41	Los Negros Island	4	1	2	5	-	-	1	4	1	-	1	10	20	2	-	HK	4
P(CA)	Carnarvon	6	1	2	5	-	-	2	4	1	-	1	10	20	2	-	HK	3

P2	Vandenberg	10	4	15	25	AD	3	2	18	16	-	4	70	-	2	1	RS/HK	13
P3	San Nicholas	6	-	6	10	-	-	1	4	5	-	-	10	40	-	-	RS	6
P8	Pt. Pillar	6	1	4	8	-	-	1	4	2	-	-	10	40	-	-	-	4
P11	Kokee Park, Kauai	4	1	2	5	C	1	-	4	1	-	1	-	-	1	-	HK	3
	Kwajelein Atoll	4	-	2	5	-	-	1	4	1	-	1	10	20	-	-	RS/HK	3
	Wake Island	4	1	2	4	-	-	2	10	1	-	-	10	20	2	-	HK	4
	Midway Island	4	1	1	3	-	-	1	10	1	-	-	-	10	2	-	-	3
	Canton Island	4	1	2	5	-	-	1	4	1	-	1	10	20	-	-	-	3
	Los Negros Island	4	1	2	5	-	-	1	4	1	-	1	10	20	2	-	HK	4
P(CA)	Carnarvon	6	1	2	5	-	-	2	4	1	-	1	10	20	2	-	HK	3
P(D)	Darwin	4	2	2	5	-	-	2	4	1	-	1	10	20	2	1	-	4
P(JO)	Johnston Island	3	1	1	2	C	1	1	4	-	-	-	10	-	2	-	HK	2
EAFB	Edwards	10	1	2	5	C	1	1	4	-	-	1	50	20	2	1	HK	3
WSMR	White Sands	4	1	1	2	-	-	1	1	1	-	-	50	20	2	1	HK	3
APGC	Eglin	4	3	3	4	-	-	1	2	2	-	1	20	10	1	-	HK	3
SKTS	Kodiak	-	1	-	-	AD	3	1	1	1	-	-	-	-	-	-	HK	1
SATS	Annette	-	1	-	-	AD	3	1	1	1	-	-	-	-	-	-	HK	1
SFNS	Thule	-	1	-	-	AD	3	1	1	1	-	-	-	-	-	-	HK	1
SNHS	New Hampshire	-	1	-	-	AD	3	1	1	1	-	-	-	-	-	-	HK	1
SHTS	Kaena Point	-	1	-	-	AD	3	1	1	1	-	-	-	-	-	-	HK	1
X1	Rosman, N. C.	2	1	2	2	-	-	1	-	-	-	1	-	-	-	-	-	1
ARIS 1		6	1	6	15	C	1	2	2	1	1	2	20	-	2	1	HK	7
ARIS 2		6	1	6	15	C	1	2	2	1	1	2	20	-	2	1	HK	7
AMRS 1	Twin Falls Victory	6	1	6	10	ABC	5	2	1	1	-	2	20	-	2	-	RS/HK	3
AMRS 2	Amer. Mariner	6	1	6	10	B	1	2	1	1	-	2	20	-	2	-	HK	3
PMRS 1	Range Tracker	6	1	4	10	C	1	2	1	1	-	2	20	-	2	1	HK	3
PMRS 4	Richfield	6	1	2	5	C	1	1	1	1	-	1	20	-	1	-	HK	2
PMRS 6	Watertown	6	1	2	5	-	-	1	1	1	-	1	20	-	-	-	-	2
PMRS 7	Huntsville	6	1	2	5	-	-	1	1	1	-	1	20	-	-	-	-	2
PMRS 8	T-AGM-8	2	1	2	5	C	1	1	1	1	-	1	-	-	1	-	HK	-
M006	Blossom Point	2	-	1	3	E	2	1	1	1	-	1	20	-	-	-	HK	2
M021	Ft. Myers	2	-	1	3	E	2	1	1	1	-	1	20	-	-	-	HK	2
M029	Grand Forks	2	-	1	3	E	2	1	1	1	-	1	20	-	-	-	HK	2
M030	Fairbanks	2	-	1	3	AE	4	1	1	1	-	1	20	20	-	-	HK	2
M451	St. Johns	2	-	1	3	E	2	1	1	1	-	1	20	-	-	-	HK	2
M652	Winkfield	2	-	1	3	E	2	1	1	1	-	1	20	-	-	-	HK	2
M800	Quito	2	-	1	3	E	2	1	1	1	-	1	20	-	-	-	HK	2
M801	Lima	2	-	1	3	E	2	1	1	1	-	1	20	-	-	-	HK	2
M803	Antofagasta	2	-	1	3	E	2	1	1	1	-	1	20	-	-	-	HK	2
M802	Santiago	2	-	1	3	E	2	1	1	1	-	1	20	-	-	-	HK	2
WI	Wallops Island	-	-	-	-	-	-	-	-	-	-	-	-	-	-	-	-	-

A = 400 mc B = DSIF C = SHF D = SGLS E = 136 mc

1970

TOTAL TELEMETRY, SPACE COMMUNICATIONS, AND SPACE COMMAND EQUIPMENT

Instrumentation Stations		Antennas		RF Receivers				Demultiplexers				PREDETECTION RECORDERS	LOCAL DISPLAY CHANNELS	FORWARDED DATA CHANNELS	VOICE COMMUNICATIONS	TELEVISION RECEIVER	COMMAND ENCODERS AND TRANSMITTERS	POSTDETECTION RECORDERS
						Other												
No.	Name	LOW GAIN	HIGH GAIN	VHF	UHF	TYPE	NO. TOTAL	PCM/FM	FM/FM	PAM/FM-PDM/FM	SS/FM							
A1	CCMTA	12	4	20	40	BC	3	15	28	20	18	3	100	-	7	5	RS/HK	22
A2.1	Vero Beach	3	1	15	20	B	2	6	15	10	-	2	-	20	2	1	RS	14
A3	Grand Bahama	3	1	15	20	BC	3	6	15	10	1	2	8	20	2	1	RS/HK	14
A5	San Salvador	3	-	10	15	B	2	2	5	5	1	1	-	-	2	-	RS	11
A7	Grand Turk	3	-	5	12	B	2	2	5	5	1	1	-	-	2	-	-	7
A9.1	Antigua	3	2	5	20	B	2	6	15	10	3	2	20	50	3	1	RS/HK	10
A12	Ascension	6	2	5	20	AD	3	6	12	4	3	1	10	20	2	1	HK	12
A13	Pretoria	6	2	2	15	-	-	6	12	2	-	2	20	10	2	1	RS/HK	6
A14	Mahe, Seychelles	6	2	2	5	AD	3	3	8	2	-	-	10	10	-	-	RS/HK	4
A(B)	Bermuda	3	1	2	10	C	1	3	15	6	3	-	-	10	2	-	HK	6
D1	Mobile DSIF Sta.	3	-	-	-	B	2	2	-	-	-	1	20	20	-	1	HK	2
D2	Goldstone	3	4	-	-	B	2	2	-	-	-	2	20	20	2	1	HK	4
D4	Woomera	3	2	-	-	B	2	2	-	-	-	2	20	20	2	1	HK	4
D5	Johannesburg	3	2	-	-	B	2	2	-	-	-	2	20	20	2	1	HK	4
MR4	Grand Canary	4	1	2	5	-	-	2	5	-	-	-	-	20	3	1	HK	4
MR14	Guaymas	4	1	2	5	-	-	2	4	-	-	-	-	20	3	1	HK	3
MR16	Corpus Christi	6	3	4	10	-	-	5	5	1	-	-	20	10	3	-	HK	4
P1	Pt. Mugu	6	2	4	10	-	-	1	4	5	-	2	30	40	-	-	RS	5
P2	Vandenberg	10	4	10	30	AD	3	2	18	16	-	4	70	-	2	1	RS/HK	13
P3	San Nicholas	6	-	4	10	-	-	1	4	5	-	-	10	40	-	-	RS	6
P8	Pt. Pillar	6	1	2	8	-	-	1	4	2	-	-	10	40	-	-	-	4
P11	Kokee Park, Kauai	4	1	2	6	C	1	-	4	1	-	1	-	-	1	-	HK	3
P21	Kwajelein Atoll	4	-	2	6	-	-	1	4	1	-	1	10	20	-	-	RS/HK	3
P23	Wake Island	4	1	2	4	-	-	2	10	1	-	-	10	20	2	-	HK	4
P24	Midway Island	4	1	1	3	-	-	1	10	1	-	-	-	10	2	-	-	3
P25	Canton Island	4	1	2	6	-	-	1	4	1	-	1	10	20	-	-	-	3
P41	Los Negros Island	4	1	2	6	-	-	1	4	1	-	1	10	20	2	-	HK	4
P(CA)	Carnarvon	6	1	2	6	-	-	2	4	1	-	1	10	20	2	-	HK	3

P2	Vandenberg	10	4	10	30	AD	3	2	18	16	-	4	70	-	2	1	RS/HK	13
P3	San Nicholas	6	-	4	10	-	-	1	4	5	-	-	10	40	-	-	RS	6
P8	Pt. Pillar	6	1	2	8	-	-	1	4	2	-	-	10	40	-	-	-	4
P11	Kokee Park, Kauai	4	1	2	6	C	1	-	4	1	-	1	-	-	1	-	HK	3
P21	Kwajelein Atoll	4	-	2	6	-	-	1	4	1	-	1	10	20	-	-	RS/HK	3
P23	Wake Island	4	1	2	4	-	-	2	10	1	-	-	10	20	2	-	HK	4
[illegible]	Midway Island	4	1	1	3	-	-	1	10	1	-	-	-	10	2	-	-	3
[illegible]	Canton Island	4	1	2	6	-	-	1	4	1	-	1	10	20	-	-	-	3
[illegible]	Los Negros Island	4	1	2	6	-	-	1	4	1	-	1	10	20	2	-	HK	4
[illegible]A)	Carnarvon	6	1	2	6	-	-	2	4	1	-	1	10	20	2	-	HK	3
P(D)	Darwin	4	2	2	6	-	-	2	4	1	-	1	10	20	2	1	-	4
P(JO)	Johnston Island	3	1	1	2	C	1	1	4	-	-	-	10	-	2	-	HK	2
EAFB	Edwards	10	1	1	5	C	1	1	4	-	-	1	50	20	2	1	HK	3
WSMR	White Sands	4	1	1	2	-	-	1	1	1	-	-	50	20	2	1	HK	3
APGC	Eglin	4	3	2	5	-	-	1	2	2	-	2	20	10	1	-	HK	3
SKTS	Kodiak	-	1	-	-	AD	3	1	1	1	-	-	-	-	-	-	HK	1
SATS	Annette	-	1	-	-	AD	3	1	1	1	-	-	-	-	-	-	HK	1
SFNS	Thule	-	1	-	-	AD	3	1	1	1	-	-	-	-	-	-	HK	1
SNHS	New Hampshire	-	1	-	-	AD	3	1	1	1	-	-	-	-	-	-	HK	1
SHTS	Kaena Point	-	1	-	-	AD	3	1	1	1	-	-	-	-	-	-	HK	1
X1	Rosman, N. C.	2	1	2	2	-	-	1	-	-	-	1	-	-	-	-	-	1
ARIS 1		6	1	4	15	C	1	2	2	1	1	2	20	-	2	1	HK	7
ARIS 2		6	1	4	15	C	1	2	2	1	1	2	20	-	2	1	HK	7
AMRS 1	Twin Falls Victory	6	1	4	10	ABC	5	2	1	1	-	2	20	-	2	-	RS/HK	3
AMRS 2	Amer. Mariner	6	1	4	10	B	1	2	1	1	-	2	20	-	2	-	HK	3
PMRS 1	Range Tracker	6	1	4	10	C	1	2	1	1	-	2	20	-	2	1	HK	3
PMRS 4	Richfield	6	1	1	5	C	1	1	1	1	-	1	20	-	1	-	HK	2
PMRS 6	Watertown	6	1	1	5	-	-	1	1	1	-	1	20	-	-	-	-	2
PMRS 7	Huntsville	6	1	1	5	-	-	1	1	1	-	1	20	-	-	-	-	2
PMRS 8	T-AGM-8	2	1	1	5	C	1	1	1	1	-	1	-	-	1	-	HK	-
M006	Blossom Point	2	-	1	3	E	2	1	1	1	-	1	20	-	-	-	HK	2
M021	Ft. Myers	[illegible]	-	1	3	E	2	1	1	1	-	1	20	-	-	-	HK	2
M029	Grand Forks	2	-	1	3	E	2	1	1	1	-	1	20	-	-	-	HK	2
M030	Fairbanks	2	-	1	3	AE	4	1	1	1	-	1	20	20	-	-	HK	2
M451	St. Johns	2	-	1	3	E	2	1	1	1	-	1	20	-	-	-	HK	2
M652	Winkfield	2	-	1	3	E	2	1	1	1	-	1	20	-	-	-	HK	2
M800	Quito	2	-	1	3	E	2	1	1	1	-	1	20	-	-	-	HK	2
M801	Lima	2	-	1	3	E	2	1	1	1	-	1	20	-	-	-	HK	2
M803	Antofagasta	2	-	1	3	E	2	1	1	1	-	1	20	-	-	-	HK	2
M802	Santiago	2	-	1	3	E	2	1	1	1	-	1	20	-	-	-	HK	2
WI	Wallops Island	-	-	-	-	-	-	-	-	-	-	-	-	-	-	-	-	-

A = 400 mc B = DSIF C = SHF D = SGLS E = 136 mc